Exploring Microbial Diversity

Extending the boundaries of biopolymer production using parallel cultivation

Stouten, G.R.

DOI
10.4233/uuid:1e63fd37-62af-4dcd-9650-6db0ebfa9ff5

Publication date
2021

Document Version
Final published version

Citation (APA)
Stouten, G. R. (2021). *Exploring Microbial Diversity: Extending the boundaries of biopolymer production using parallel cultivation*. [Dissertation (TU Delft), Delft University of Technology]. https://doi.org/10.4233/uuid:1e63fd37-62af-4dcd-9650-6db0ebfa9ff5

Important note
To cite this publication, please use the final published version (if applicable).
Please check the document version above.

Exploring Microbial Diversity

Extending the boundaries of biopolymer production using parallel cultivation

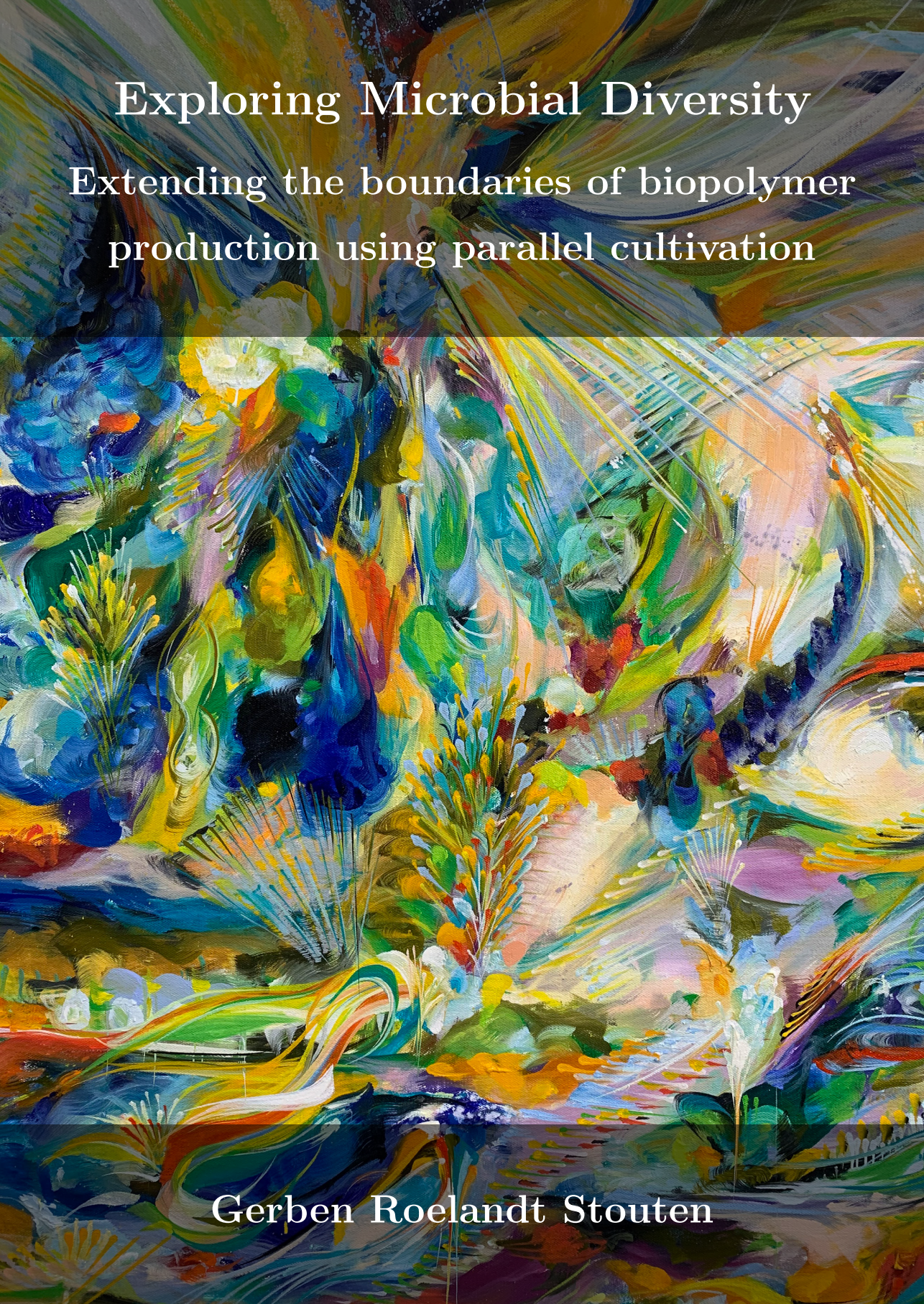

Gerben Roelandt Stouten

EXPLORING MICROBIAL DIVERSITY

EXTENDING THE BOUNDARIES OF BIOPOLYMER PRODUCTION USING PARALLEL CULTIVATION

Proefschrift

ter verkrijging van de graad van doctor
aan de Technische Universiteit Delft
op gezag van de Rector Magnificus Prof.dr.ir. T.H.J.J. van der Hagen,
voorzitter van het College voor Promoties,
in het openbaar te verdedigen op
vrijdag 1 oktober 2021 om 12:30 uur

door

Gerben Roelandt STOUTEN

Master of Science in Life Science & Technology,
Technische Universiteit Delft, Nederland,
geboren te 's-Gravenhage, Nederland.

Dit proefschrift is goedgekeurd door de

promotor: Dr.ir. R. Kleerebezem en
promotor: Prof.dr.dr.h.c.ir. M.C.M. van Loosdrecht

Samenstelling promotiecommissie:

Rector Magnificus,	voorzitter
Dr.ir. R. Kleerebezem	Technische Universiteit Delft
Prof.dr.dr.h.c.ir. M.C.M. van Loosdrecht	Technische Universiteit Delft

Onafhankelijke leden:

Prof.dr. W.T. Sloan	Universiteit van Glasgow, Verenigd Koninkrijk
Prof.dr. D.Z. Machado de Sousa	Wageningen Universiteit
Prof.dr. F.J. Bruggeman	Vrije Universiteit Amsterdam
Prof.dr.ir. J.B. van Lier	Technische Universiteit Delft
Prof.dr. F. Hollmann	Technische Universiteit Delft, reservelid

Overige leden:

Prof.dr. G. Muyzer	Universiteit van Amsterdam

This thesis was made possible by the Environmental Biotechnology department of the Delft University of Technology and the financial support from the Netherlands Organization for Scientific Research (NWO) funded UNLOCK project (NRGWI.obrug.2018.005) and the company Paques B.V. (Paques Partnership Program project 13002).

Keywords:	Microbial diversity, microbial cultivation, enrichment cultures, storage polymers, polyhydroxyalkanoates, dynamic system characterization.
Printed by:	24-drukwerk, 's Hertogenbosch
Cover art:	Excerpt of painting by Natalia Wróbel, "Breathing Underwater," 2020, oil paint on canvas, 152 cm x 122 cm

ISBN 978-94-91837-42-5

An electronic version of this dissertation is available at
http://repository.tudelft.nl/.

When day comes, we step out of the shade of flame and unafraid.

The new dawn balloons as we free it.
For there is always light,
if only we are brave enough to see it.

If only we are brave enough to be it.

Amanda Gorman

Namibia (2016)

CONTENTS

SUMMARY

QUICKLY, the show is about the start. Date: 3.5 thousand million years ago, location: planet Earth, event: life. Naturally, life is starting small, even microscopically tiny. Life in the form of microorganisms endures eons of time in which the world changes. They survived, failed, adapted, thrived, and they actually changed the world. They have seen humankind step into the light of day, and they will be there when we see no more.

Microorganisms are the link between the inanimate, mineral planet and the living world. They facilitate the natural cycle of the elements. The CO_2 we breathe out is transformed by phototropic algae to oxygen. The nitrogen in proteins that we eat finds its way to the nitrogen gas in the air, and back into the roots of plants through countless microorganisms. And central to our life: carbon, it is the food that we eat, the oil that we burn, and the plastics that will immortalize humans' existence.

We are life, we flourish, and like all living things, we are greedy. So greedy that we disrupted the circularity of nature. We are far from the first, nor the most successful, organism to change the face of the earth. Algae made the world aerobic, and the first trees covered the world in meters of indigestible wood for millions of years. And while nature seems to have found a new balance, those algae and trees now form the oil and coal that drive our manic existence.

What differentiates us from those earlier life forms is that we can appreciate that we are running on borrowed time, as we can see the world changing, fast. Over the past century, it has become clear that we are shaping a linear society, predominantly driven by fossil fuels. If we, by contrast, could manage to convert our waste streams back into resources at the same rate that we produce them, that would chime in a new era. And even more profound is that we are living in a world shaped and dominated by microorganisms. We need to start cooperating with them for our health and prosperity, which requires a better understanding of the microbial world. And although we are making significant progress; time is ticking and we could use all the help there is.

This thesis is on how we can explore and utilize 3.5 billion years of help. In the first chapter the vastness, complexity and wealth of the microbial world are introduced. It focusses on a fraction of that wealth, the specific topic of interest, which is the production of biopolymers by microbial communities. These biopolymers are important building blocks for a circular society, as they can serve as precursor to oil, plastics, food, and specialty materials. Of the many biopolymers in nature, the predominant one within this thesis are polyhydroxyalkanoates (PHA), which are produced by microorganisms as their equivalent to human fat, and can be used by us to produce bioplastics.

In the second chapter our key contribution to the scientific field of microbial community research is made. A key aspect that is holding back research on microbial communities is the lack of experimental freedom to bring nature to the lab. In this work, we attempt to bring cultivation research into the 21st century with a more flexible biodiscovery cultivation platform. This chapter describes a part of the hardware and soft-

ware that was developed to significantly assist parallel enrichment research in dynamic conditions, it elaborates on the bioreactor setups of 8 systems, the automatization, online data processing, and process modelling. We demonstrate a generalized respiration rate reconstruction tool for dynamic operated bioreactors. The setup and tools described here have facilitated over twenty research topics that were conducted during and alongside this Doctoral research.

The third chapter demonstrates how the setup can be used to increase the research intensity of enrichment studies. We investigated the influence of temperature on the enrichment of PHA accumulating microbial communities, which yielded several noteworthy findings. Besides an explanation for the global temperature optimum of 30°C, we identified other competitive strategies in feast-famine enrichment systems, that of fast-growth and decay, and subsequent growth on cell lysis. Furthermore, we were able to align shifts in microbial function with microbial community shifts, and addressed important issues of reproducibility in microbial community enrichments. The results demonstrate that a rigorous experimental approach involving parallel cultivation allows for unambiguous identification of competitive strategies in microbial communities. And a major improvement with this approach is that we can pinpoint where our knowledge is lacking.

The fourth chapter follows a systematic investigation of a specific surprising observation that was made possible by the close monitoring of the enrichment systems. During a study investigating the influence of pH on the enrichment of PHA accumulating microbial communities (analogous to the temperature study), we noticed markedly different microbial community structure and behavior between enrichments, that seemed solely based on the type of acid used for pH control. We demonstrated that the observed changes were not directly caused by the change in acid used for pH control, but resulted from the difference in corrosive strength of both acids and the related iron leaching from the bioreactor piping. Neither system was iron deficient, suggesting that the biological availability of iron is affected by the leaching process. Our results demonstrate that microbial competition and process development can be affected dramatically by secondary factors related to nutrient supply and bioavailability, and is way more complex than generally assumed in a single carbon substrate limited process.

In chapter five, we investigate a novel enrichment process for PHA accumulating microbial communities. The strict uncoupling in time of nutrient supply of two growth nutrients is investigated. The setup was used to optimize the process by investigating the influence of (i) nitrogen or phosphorous uncoupling from carbon, (ii) increased carbon to nutrient ratios, and (iii) increased exchange ratios. The uncoupling strategy resulted in stable enrichments, that achieved 89 wt% (gPHA/gDW) in eight hours, every operational cycle, making this the most PHA rich production system to date. The proposed strict uncoupling strategy yields stable microbial communities with an unprecedented combination of PHA storing capacity, productivity, product yield, and general applicability for feed streams without nitrogen or phosphate.

Chapter six looks forward on the future of microbial community research, it explores the collaborative efforts between Wageningen University and Delft University in the 24 million euro UNLOCK project, for which the work in this thesis laid a principal foundation.

SAMENVATTING

SNEL, de show begint zo. Datum: 3.5 duizend miljoen jaar geleden, locatie: planeet Aarde, gebeurtenis: leven. Natuurlijk begint het leven klein, zelfs microscopisch klein. Leven, in de hoedanigheid van micro-organismes, doorstaat alle tijd, alle wereldse veranderingen. Ze overleven, falen, passen zich aan, floreren, en juist zij veranderen de wereld. Ze zien de mensheid vormen, en zullen er zijn wanneer wij onze ogen sluiten.

Micro-organismes zijn de verbinding tussen de dode, ongedolven planeet, en de levende wereld. Zij voorzien de wereld van de natuurlijke cycli van de elementen. De CO_2 die wij uitademen wordt door algen omgezet in zuurstof. De stikstof in eiwitten die wij eten vindt haar weg naar de stikstof in de lucht, en terug in de wortels van de planten door talloze micro-organismes. En centraal in het leven staat koolstof, het is het voedsel dat we eten, de olie die we verbranden, en het plastic dat de mensheid zal vereeuwigen.

Wij zijn leven, we floreren, en net als alle andere levende dingen, zijn we gretig. Zo gretig dat we de circulariteit van de natuur hebben doorbroken. We zijn bij lange na niet het eerste, noch het meest succesvolle, organisme dat het aanzien van de aarde verandert. Algen maakten de wereld rijk aan zuurstof, en de eerste bomen zorgden ervoor dat de hele planeet voor miljoenen jaren was bedekt met meters, onverteerbaar, hout. En net wanneer de natuur alles weer redelijk in balans had gekregen, zijn het diezelfde algen en bomen die nu de olie en kolen zijn waarmee we ons manische bestaan voeden.

Hetgeen ons onderscheidt van de vroegere levensvormen is dat we inzien dat we op geleende tijd leven, aangezien we de wereld snel zien veranderen. Over de afgelopen eeuw is het duidelijk geworden dat we een lineaire maatschappij vormen, die voortdrijft op fossiele brandstoffen. Als het ons daarentegen zou lukken om onze afvalstromen om te zetten in nieuwe grondstoffen, met hetzelfde tempo waarmee we ze produceren, dan breekt een nieuw tijdperk aan. En nog fundamenteler is het feit dat we in een wereld leven die gevormd is en gedomineerd wordt door micro-organismes. We zullen met ze moeten samenwerken ten gunste van onze gezondheid en welvaart, en dat vereist dat we de microbiële wereld beter begrijpen. Op dat vlak maken we rasse schreden, er is echter nog een lange weg te gaan, de tijd tikt, en we kunnen alle hulp gebruiken.

Dit proefschrift gaat over hoe we 3.5 miljard jaar aan hulp kunnen verkennen en inzetten. In het eerste hoofdstuk wordt de weidsheid, complexiteit en rijkdom van de microbiële wereld geïntroduceerd. Een klein aspect daaruit lichten we op, de productie van biopolymeren door micro-organismes. Deze biopolymeren zijn bouwstenen voor de circulaire samenleving, omdat ze dienen als voorlopers voor brandstof, plastic, voedsel en speciale materialen. Van de vele natuurlijke biopolymeren, zijn de voornaamste in dit proefschrift de polyhydroxyalkanoaten (PHA), die door micro-organismes worden gemaakt als hun equivalent voor menselijk vet, en door ons gebruikt kunnen worden om bioplastics uit te vervaardigen.

In het tweede hoofdstuk wordt onze meest significante bijdrage gedaan aan het wetenschappelijke onderzoeksveld van microbiële culturen. Een belangrijk onderdeel dat

huidig onderzoek afremt is het gebrek aan experimentele vrijheid om de natuur het lab in te brengen. In dit werk hebben we getracht om cultivatie onderzoek naar de 21^{e} eeuw te brengen middels een flexibel bio-discovery cultivatie platform. Het hoofdstuk beschrijft een deel van de hardware en software die is ontwikkeld waarmee cultivaties in dynamische omstandigheden vereenvoudigd en in parallel kunnen worden uitgevoerd, het weidt uit over de bioreactor opstelling van 8 systemen, de automatisatie, de online dataverwerking, en over proces modelleren. We demonstreren een veralgemeende methode waarmee de respiratie snelheden kunnen worden gereconstrueerd in dynamische cultivaties. De opstelling en tools die we hier beschrijven zijn gebruikt in meer dan twintig onderzoekslijnen die zijn uitgevoerd tijdens en naast dit Doctorale onderzoek.

Het derde hoofdstuk demonstreert hoe de opstelling kan worden gebruikt om onderzoek te intensifiëren. We onderzochten de invloed van temperatuur op de verrijking van PHA-ophopingsculturen, hetgeen leidde tot een aantal noemenswaardige bevindingen. Naast een verklaring voor het globale temperatuur optimum van 30°C, identificeerden we andere competitieve strategieën van micro-organismes in de feast-famine verrijkingsstrategie. Te weten, snelle-groei en verval, gevolgd door groei op cel lysis. Daarnaast waren we in staat om de veranderingen in de samenstelling van de culturen te relateren aan veranderingen in functioneel gedrag, en adresseerden we het belangrijke thema omtrent reproduceerbaarheid. De resultaten demonstreren dat met een rigoureuze experimentele aanpak, middels parallelle cultivaties, competitieve strategieën ondubbelzinnig kunnen worden geïdentificeerd. En een belangrijke verbetering van deze aanpak is dat we kunnen lokaliseren waar onze kennis gebrekig is.

In hoofdstuk vier volgen we een systematische speurtocht waarin we een verklaring zoeken voor een verrassende observatie, die voortkwam uit het scherpe toezicht mogelijk gemaakt door de opstelling. Het was ons opgevallen dat er een aanzienlijk verschil ontstond in de samenstelling en functie van een microbiële cultuur, ogenschijnlijk alleen door het gebruik van een ander zuur om de pH te reguleren. We demonsteren dat de veranderingen niet het directe gevolg van het veranderde zuur waren, maar voortkwamen uit het verschil in corrosieve kracht van de zuren, en het gerelateerde extra ijzer van de reactor-invoer dat oploste. Nog opzienbarender was dat de culturen niet gelimiteerd waren in ijzer. Onze resultaten demonsteren dat microbiële competitie en procesontwikkeling dramatisch kan worden beïnvloed door secundaire factoren, gerelateerd aan nutriënt toevoer en biologische beschikbaarheid, en in het algemeen veel complexer is dan wordt aangenomen voor enkel koolstofbron gelimiteerde processen.

In hoofdstuk vijf bestuderen we een nieuwe verrijkingsstrategie voor PHA ophopingsculturen - de strikte ontkoppeling in tijd van de toevoer van twee verschillende groei nutriënten. We onderzochten verscheidene facetten van het proces met de opstelling: (i) stikstof of fosfaat ontkoppeling van koolstof, (ii) het vergroten van de verhouding tussen de hoeveelheid koolstof en nutriënten, (iii) het vergroten van het uitwisselingsvolume. De ontkoppelingsstrategie resulteerde in stabiele verrijkingen, die iedere cyclus 89 wt% (gPHA/gDW) behaalden in acht uur. Hetgeen dit de meest PHA rijke verrijkingsstrategie maakt tot nu toe, dat gekarakteriseerd wordt door stabiele cultivaties, met een ongekende combinatie van PHA-opslag capaciteit, productiviteit, product opbrengst, en algemene toepasbaarheid voor afvalstromen die of stikstof of fosfaat gelimiteerd zijn.

Hoofdstuk zes kijkt vooruit op de toekomst van onderzoek naar microbiële culturen,

het verkent de aankomende samenwerking tussen de Delftse en Wageningse universiteiten in het 24 miljoen euro UNLOCK-project, waarvoor het werk in dit proefschrift een fundamentele basis heeft gelegd.

PREFACE

STEW.[1] When you taste a stew, just after you have chopped up your ingredients and put them together in the pan, it tastes like old socks. But you do not meddle, and you do not add new ingredients, you wait and let time and fire work their magic. This thesis is like that stew, it tasted like socks, and required time and heat to become enjoyable – at least to its chef.

The long simmer has allowed me to experience the gems of academic life. Interactions with students, teaching, collaborations free from necessity, friends that savor facts for breakfast, people with whom to share and see the world, and foremost the endless void in which we can stare - the majestic void of science.

The heat came from the burning friction between what is and what could be. This thesis is not half as thick as it could be and not half as good as it should be. Science is an endless endeavour, and is therefore arduous to capture in a finite book. It required exceptional insight into my character from my close friend Peter Mooij to find the words that allowed me to finish this thesis. His words are paraphrased as proposition five of this thesis, and reflect what I love and loathe about the scientific world.

Science can be exciting, but is often communicated in a terse and amenable fashion. The stories within this thesis conform to the standard, but with a twinkle of the immense pleasure that this journey of discovery have brought me. The introduction and outlook chapters are employed as bridges, connecting my fascination with science, to the chapters on science, and forwards to the imagination that emanates from science.

Along the way – the cautious reader might find some relics of joy. It might not be for everybody, but now that it is done, it is available to everybody.

Gerben Roelandt Stouten
The Hague, January 2021

[1] Every story starts with a first word. " Words matter." – Prof.dr. Hanna Stouten

1

GENERAL INTRODUCTION

EXPLORING MICROBIAL DIVERSITY

Gerben Roelandt STOUTEN

1

1.1. IT ALL STARTED SOMETIME, SOMEWHERE, SOMEHOW

HUMANKIND entered a world inhabited, conquered, and shaped by microbes. And not only our world, also that of elephants, butterflies, and pistol shrimps depends on close interactions with microbes[1]. Even the tiniest insects are hosts to the tremendous microbial diversity that exists in nature. But how does the insect amass the microbes it needs, how do we for that matter? Why are there no plant-root bacteria thriving in our bellies, or no deep-sea-vent yeasts involved in the production of wine? To get even a glimpse of an idea of how the world is interconnected through the microbial world we have to go back, a bit. Some would say, go back for 3.5-4.2 billion years, that is when life could have started [1, 2]. And let us assume it did, and that it started small, possibly had to start over a couple of times, but at a certain point life got the hang of it and the show was on the road. Surprisingly, life thrived.

Life lives behind the eyes that read these words, and life also gives credence to *Corynebacterium mastitidis*, a microbe that resides on your eye, where it does its utmost to prevent pathogens from invading your vision [3]. It cannot be overstated how successful life is. And to give you an idea, we will crank some numbers. The fastest growing microbes can divide approximately every twenty minutes, the slower microbes divide possibly every month, so let us assume that when life started it replicated once, every day. That singular being has since passed over one trillion generations. Along the way every division was almost perfect. Almost. But 1 trillion times "almost perfect" will result in a tremendous amount of variation. This inability of life to make perfect replicas turned out to be its biggest success factor. Soon, the first living cell turned into thousands, into millions of living cells, each with some small variation, and all with a trillion more divisions on the horizon. Do some quick, big, calculations and get lost in the numbers. Think of this next time you walk on the beach. Each grain of sand harbors up to 100.000 microbes, each, grain, of, sand [4].

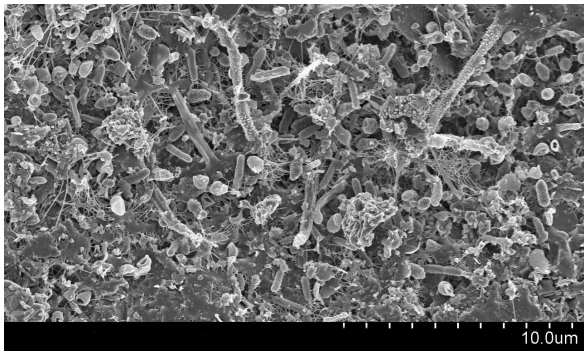

Figure 1.1: A natural community of bacteria growing on a single grain of sand. The sand was collected from intertidal sediment on a beach near Boston, MA in September 2008 and imaged using a Scanning Electron Microscope (SEM). Image courtesy of the Lewis Lab at Northeastern University. Image created by Anthony D'Onofrio, William H. Fowle, Eric J. Stewart and Kim Lewis.

[1] Semantics: "microbes", "micro-organisms", "bacteria", and "archaea" are in the context of this story all microscopic single-cell living things that are able to self-organize, replicate and interact with their environment.

Picture the beach, and now think of all the sand in the world, there, you had it, a small glimpse of the vastness of the microbial world. You lost it again, because you started to think of the Sahara and the oceans, and how much life could be there. It does not bode well to drown in big numbers, so we will accept their numerical superiority and take a closer look at the myriad of variations life has come up with, which, as a matter of fact, also includes you.

1.2. THROUGH THE EYES OF ANTONI VAN LEEUWENHOEK [5]

IT is not surprising that the whole microbial world went unnoticed for a very long time. And because microbes are, as one could say, microscopic, life had to await the first microscope before it could show its splendor. Liberation came by the name of Antoni van Leeuwenhoek[2]. This autodidact lived many interesting lives, but for this story we are specifically interested in his ability to make lenses, and what he could see through them. In the 1670-ies he corresponded a remarkable observation to the Royal Society in London: "I can see tiny animals."

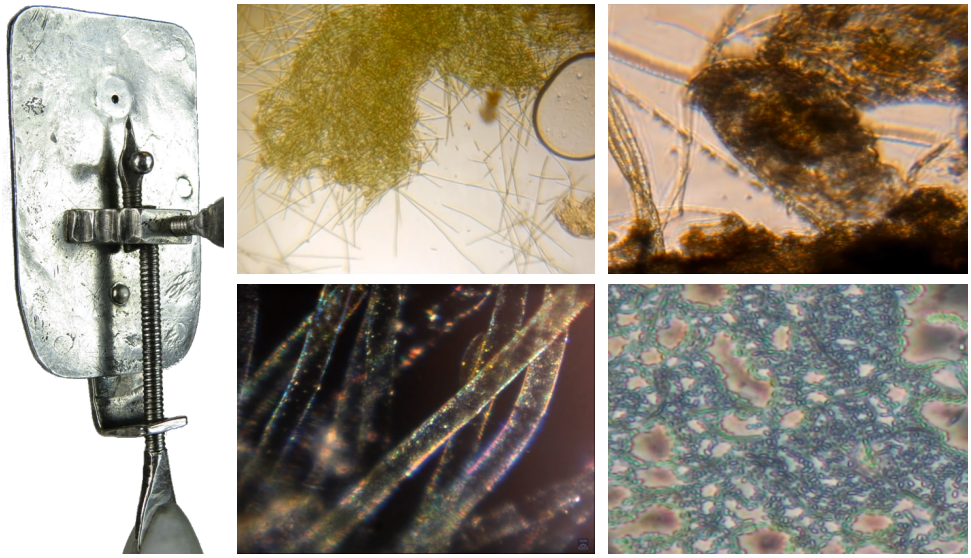

Figure 1.2: Antoni van Leeuwenhoek made his own microscope and lenses; the 1-millimeter glass lens was placed in the small opening at the top (left). This craftsmanship allowed him to observe various microscopic structures, under which living microbes. The four images on the right are still images taken through a replica of a van Leeuwenhoek microscope by Lesley Robertson [5]

[2] Constantijn Huygens wrote to Robert Hooke regarding van Leeuwenhoek on August 8, 1673: "a modest man, unlearned both in sciences and languages, but of his own nature exceedingly curious and industrious ... always modestly submitting his experiences and conceits about them to the censure and correction of the learned."

Van Leeuwenhoek's observations were classified as moderate trivialities; the microscopic fauna. Understandable, in a day and age where Isaac Newton diffracts light and describes the movement of stars and planets. For another 200 years, the tiny animals remained small in terms of the attention they received. Interest grew because we realized that bacteria can make us ill, therefore microbes got a bad reputation, and they still do. But that was all about to change.

1.3. TINY CHEMISTS

RUSSIA and The Netherlands, late 19th century. Sergei Winogradsky and Martinus Beijerinck, both botanists, start researching bacteria that are not related to human diseases. Their work transformed our understanding of the biological world. The key realization was that microbes are not animals, but that they are chemists. With painstaking rigor these men discovered new microbes that catalyzed all sorts of chemical conversions. They extrapolated that microbes are the link between the inanimate, mineral planet and the living world. Soon the insight formed that microbes carry the world on their shoulders. Seemingly, any compound could be converted by some microbe into something else. And all else could again be converted, everything is food for some microbe, from sugars to metals to dynamite [6]. The concept of waste is wasted on nature.

The microbial world operates an unremitting cycle in which chemicals are converted and exchanged between many different microbial species. But how many species? Only recently, thanks to the technical development of DNA sequencing, we have come to realize that microbes are not only abundant, they are also highly diverse. And the honest answer is, we do not know how many different species there are, because we do not know how to define a species. Where, in the animal kingdom, you can define species as different if they cannot produce offspring together[3], this does not hold for microbial cells that can divide of their own accord. The best tool we have is looking at the differences in the genetic code. Nowadays, organisms are generally defined as different species when the genetic code of the essential rRNA gene differs more than 1.5% from any other species[4] [7]. Based on that assumption, there are likely more than 1 billion different species of microbes [8, 9]. And even if you do not believe that number, it still underlines the tremendous variety present in nature.

Figure 1.3 shows the 'Tree of Life', where, based on the differences in the genetic code of the rRNA gene, branches emerge that group specific classes of organisms. You can find us, humans, grouped in one singular branch together with all other animals, from insects to whales, if that helps give some perspective. Except for the land plants and animals, practically all other branches consist of single cell organisms. And here comes the first philosophical question: why? Why are there so many different species?

[3] Whether biologically impossible, or geographically highly unlikely.

[4] This definition allows us to mathematically differentiate up to 10^{323} different species based on the variable regions in rRNA genes. In that perspective 10^9 is a small number.

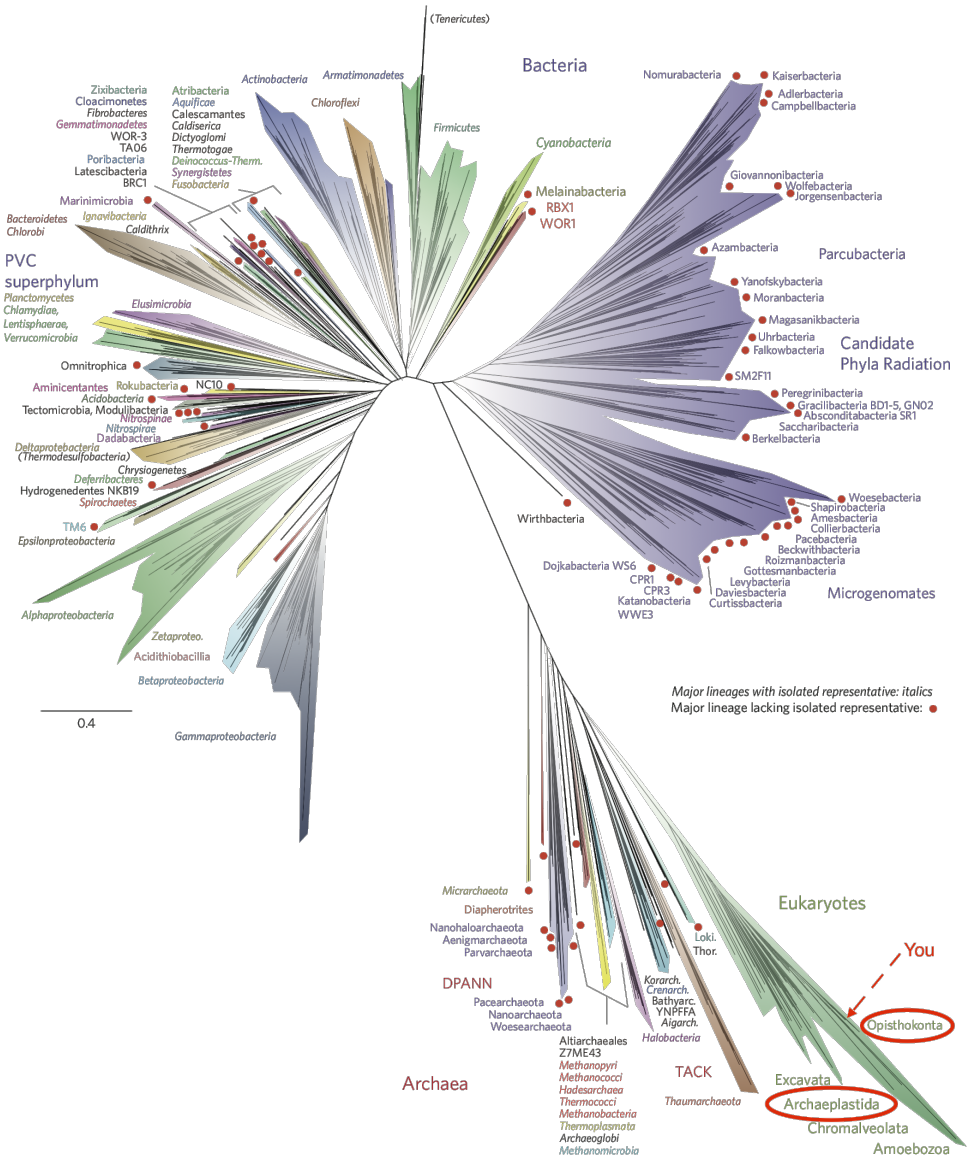

Figure 1.3: The tree of life, representing the living world. The two red circled divisions represent 99% of the visible world, the flora and fauna. All other branches represent the invisible world, where things can be more different from each other than a blade of grass and a giraffe. Image from Hug *et al.* [10]

.

1.4. WHY ARE THERE SO MANY DIFFERENT SPECIES?

THERE are many answers to why-questions. Let us start with what we know, all species that exist have found a niche which prevents them from being eliminated from the genetic pool. If that niche disappears, chances are that you as a species will also disappear. For example, humankind has been a very stringent selective force on the animal population. The rapidity by which the evolutionary landscape changed for all large land animals, from the moment that humans started throwing pointy rocks attached to sticks, completely evaporated their survival chances. And while we are responsible for mass extinctions, life itself really takes the cake regarding extermination. It is an inevitable consequence of imperfection.

Differentiation arises due to ongoing variations with each generation. Variants bloom up that devised novel tools that challenge the survival existence of previous generations. The interesting aspect is that as a response to these ongoing variations, evolution has brought forth an endless number of different organisms that compete, work together, and perish[5]. Life prods at all possibilities, slowly and unstructured, life does not discriminate. If you can survive, survive. The intricateness of microbial mechanisms of competition and cooperation is the result of 3.5 billion years of co-evolution that took place all over the world, under all possible environments. If we can already appreciate over thousands of different species of parasitoid wasps [11] that hijack other insects to host their developing larvae[6], then what bewildering magic awaits us in the invisible world?

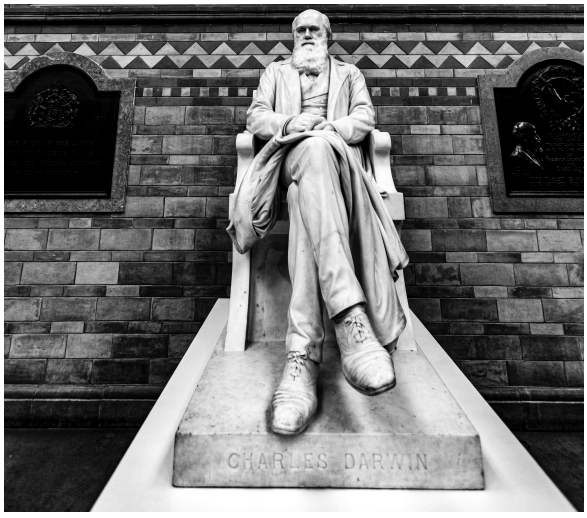

Figure 1.4: Darwin Sculpture. Natural History Museum. London, England. Image courtesy Hulki Okan Tabak

[5] Food for thought: Is it unthinkable that evolution could bring forth a single organism, an all potent being? Able to perform any chemical conversion possible, adapting to environmental changes, etc. What need would variation between generations still have? Can life evolve to make itself stop evolving?

[6] The parasitoid wasp is specifically what got Darwin to question a beneficent and omni-potent God. It pushed him to question whether it was necessary for things to have come about by design [12].

1.5. EVOLUTION, THERMODYNAMICS, AND MICROBIAL WARFARE

EVERY living organism needs energy. Due to the abundance and competitive greed of living things, freely utilizable energy is a scarcity. In order to harvest as much energy as possible from limited energy sources two distinct biological mechanisms drive the evolutionary processes. First, genetic variations that result in improved growth yield and metabolic rates, and second, variations that limit the survivability of competitors or increase protection from competitors and predators. Or in practical terms: "Being the best you can be, vs. beating the others."[7]

The second element, beating the others, describes microbial warfare, in which all is fair and allowed, it contains strategies like the production of antibiotics [13], nanoharpoons [14], shields [15], symbioses [16], toxins [17], microbial engines [18], communication and spreading of misinformation [19]. It is a rich and fascinating field of research in which the uke and shite[8] (Figure 1.5) harbor prodigious and resourceful techniques. These processes result from co-evolution, they are not driven by currently quantifiable laws, they always cost an organism energy, and as a result there is no evolutionary optimum to which microbial warfare develops. A highly efficient and fast growing microbe will easily be outcompeted by offspring that develop stabbing skills, yielding new selective pressures for thicker skin and a general distrust towards siblings, at the cost of some of that efficiency.

On the other hand, metabolic characteristics can be quantified, and they show general tendencies towards some form of optima. If you manage to gain more nutritional value out of the same food, harvest the food faster, find new food sources, or are able to perform equally well with a smaller body, chances are that over time you will be more prolific. The almost endless number of microbes combined with eons of time has allowed the microbial world to harvest energy from almost all energy sources, under almost any environmental condition. To appreciate this relationship between life and energy, we have to introduce ourselves to thermodynamics. But it will be worth it, as there is a profound beauty to the relationship between thermodynamics and the origin and evolution of life see (Box 1 - Thermodynamics and the origin of life).

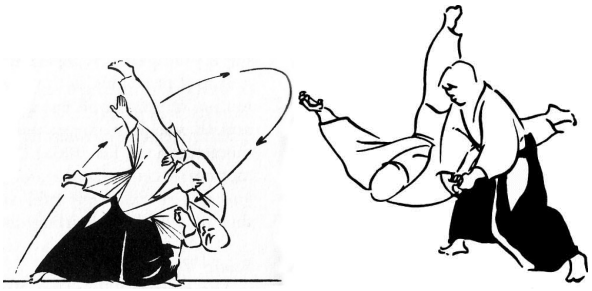

Figure 1.5: In most martial arts, there exists a harmony between both practitioners, where the performer and the receiver of a technique improve their respective skills over time. Images by Westbrook and Ratti [20]

[7] If there are no others, you compete with your siblings.

[8] (Japanese martial arts) Uke is the person who receives a technique, shite is the performer of the technique.

1

1.6. BOX 1 - THERMODYNAMICS AND THE ORIGIN OF LIFE

IT is time for the final lecture on thermodynamics for the first year cohort 2018 of Life Science and Technology. Thermodynamics is a notoriously difficult to grasp topic for which Robbert Kleerebezem, *my promotor - my friend and mentor - but in this case - my "lotgenoot"*,[9] and I employed all our considerable talents to bring the topic to life. And what best for a final lecture than an answer to the ultimate question of Life, the Universe and Everything [21]. What will follow is a two page synopsis of that lecture[10], which - out of all our lectures - managed to receive the least resistance from the students. But their reluctance to revolt could as easily have been due the monumental heat of the day.

Let us escape into the realm of thermodynamics. For here resides one of the most profound ideas on the origin and evolution of life. A theory that allows us to paint the bigger picture in terms of why life started and where it is heading. The short answer:

"Life is inevitable."

For us to arrive at this statement, we need two laws that describe the whole of the universe. Law one: energy cannot be created and it cannot be destroyed. Law two: chaos can be created but it cannot be destroyed, or visually:

Universal truths	Cannot be created	Can be created
Cannot be destroyed	**Energy**	**Chaos**

From these truths we have to accept that there always has been, and always will be, exactly the same amount of energy in the universe. When we say that we use energy, what happens is that energy is converted from one form to another. We can observe this with a light bulb that converts electrical energy to light and heat, but also when we go for a run, we are converting the chemical energy in food to work and heat. Energy is converted from one form into another. At the same time we recognize that these energy transitions have a direction. We do not expect that when we heat up a lamp that we get electricity from the other end, or that your car fills up with gasoline when you push it down the road. This seem logical, and it underlines our familiarity with the two laws from our personal experience, although it might still be difficult to wrap our minds around.

During all energy conversions some energy gets lost as heat energy, which on a molecular level is the increased jiggling of molecules. All energy eventually will end up as evenly distributed heat energy – in the aptly named heat-death of the universe [22]. At this point the whole universe is in equilibrium, the chaos is maximum, there is no possible way in which chaos can increase. And every day we are moving closer to that inevitable future.

Therefore, all processes that increase the total chaos in the universe are favorable, they lead to the inevitable. Let us compare two moments in time from an energy and

[9] fellow sufferer

[10] Thermodynamics of Living Systems: June 13th 2019 - Macromolecule assembly & A theory of life.

chaos point of view. We know from the first law that at both moments the total energy is the same, but from the second law we derive that one of these moments must have a larger total chaos. The moment with the highest chaos is the future moment. The second law therefore gives direction to time.

Regardless of life, physical phenomena take place, gravity pulls stuff together, stars shine their light, and the planets revolve. If we could observe one photon leaving our sun, we would see that it carries a specific amount of energy away from the sun. On its journey to Earth our specific photon did not interact with anything until it hits the Atlantic Ocean. Here it transfers its energy to the water molecule it collided with and consequently that molecule is jiggling just a tiny bit faster - it heated up and formed a tiny wave, the universe is a bit more chaotic.

LIFE STORES ENERGY AND CREATES CHAOS

Now, what is remarkable about life, is that it increases the rate by which chaos is created. Life fastens the chaotic ending. But you might think of yourself as a very well-structured system, few things out of place; You embody order. How is it possible that something so organized came about? It came about, because creating and sustaining all that local order, creates an unfathomable amount of universal chaos.

For any process to be favorable it needs to increase the total chaos (Law 2). The first and simplest building blocks of life, nucleic acids, could form because they are the most efficient, of all known molecules, at absorbing ultraviolet light from the sun and converting it into heat [23]. The property of nucleic acids to weakly attract each other allowed it to form collections (RNA). And given enough time, one of these structures became the ribosomal RNA (rRNA), which we already encountered as elemental to unraveling the tree of life. This rRNA is a true marvel as it is made up of genetic material (the order of nucleic acids result in a code), which - because molecules take up physical space - needs to fold in a 3D-structure. The emergent property of this specific code is that the 3D-structure is able to catalyze reactions that allow more complex molecules to be formed. And before you know it, life explodes into all that we see around us.

The whole of nature is driven by the energy that comes from the sun. Some photons no longer directly collide with rocks and water, their demise of electromagnetic energy (light) to heat is postponed as that little bit of energy is captured by an organic molecule, which increased jitter makes it more reactive and able to create more local order. The bloom of phototrophic life gave rise to predators that started to ignore the sun and focused their attention on digesting the energy residing as order in the phototrophs.

And here we have to realize that all structure, all order that is contained within life, within nature, is possible because as a whole it torrents the creation of chaos. And as humans we keep accelerating this trend, the caveman and the millennial both require equal amounts of food, but create orders of magnitude different amounts of chaos. Think of the amounts of rocks a caveman converted into spearheads, and think of the amount of rock that is crushed to yield ore for our electronics. Then think how long the sun needs to shine and waves need to crash to pulverize rock. It is an unremitting force that pulls humankind into the future. The origin and evolution of life can be understood as resulting from the natural thermodynamic imperative of increasing the chaos production of Earth in its interaction with the solar system.

1.7. PARADIGM SHIFTS

It is the beginning of the 20th century and the field of microbiology was officially born, and although the interest in nature's smallest members kept growing, two microbial contestants unlocked even greater fascination: a slum-dog and a rising star. Gut-bacteria and yeast. Discovering how life works required some model organisms to study. *Escherichia coli* and *Saccharomyces cerevisiae* turned out to be easy to cultivate in the lab, had prodigious resilience to scientific prodding and elucidated much of the internal workings of life. They became work-horses for industrial biotechnology and thousands of researchers have dedicated their lives to studying, using, and changing these microbes in a pursuit of knowledge and technological advancements. Several handfuls of microbial strains are currently used in industry for a bewildering number of processes, including the production of medicines, detergents, bulk-chemicals, bio-fuels, food, and beverages. And with much understanding still to be gained, the ubiquity of these (genetically modified) work-horses is stampeding on. Meanwhile, the exploration of the myriad of naturally occurring microbes remained modest, generally because there seemed no limit to the abilities of the work-horse microbes. But as time and insights progressed, it became more apparent how complex unicellular life can be. With so much effort invested in understanding these few microbes, the challenge of understanding the other countless species, complexed with their interactions seems truly unfathomable.

The idea of cultivating microbes as pure cultures stems from our desire to describe and study them purely. Because when everything is so small, how do we know who is responsible for what behavior? This problem does not exist in pure cultures, because we can be positive that a single species is responsible for the observations. But at the same time, we lose sight of all mechanisms and complexity that arise due to microbial interactions. It is proposed that less than currently 1% of all microbial species can be cultivated in the lab as pure cultures [24]. By studying isolated cultures, we are therefore limiting our insights in nature's diversity, abilities, and mechanisms.

BACK TO THE BASICS - PROBLEM AND SOLUTION

But from necessity a new wind started blowing through biotechnological research. The comprehension settles in that humankind needs to find a way to connect back into the circular process of nature to give itself a chance to keep growing, exploring, and discovering. We have run a short successful industrialization dash at the expense of growing devastations, and we can see that our boastful sprint cannot be sustained. Whether we are talking about climate change (Figure 1.6), world population [25], or air-, soil- and water-pollution [26], all of these are running on borrowed time and are testing Earth's amenability to sustain us. The microbial world has shown that it can survive and adapt to ice-ages, sweltering atmospheres and meteor-impacts; life itself will flourish; humankind needs help. We find ourselves in a strenuous spot, where it is difficult to change our way of living, but something has to change.

When in a pinch, it is smart to look at someone who has got it all figured out. So, naturally, our gaze has fallen back on the queen of sustainability: nature. We are looking at her to assist us in migrating away from petroleum as key economic driving factor, and to mitigate the fallout that we have caused along the way.

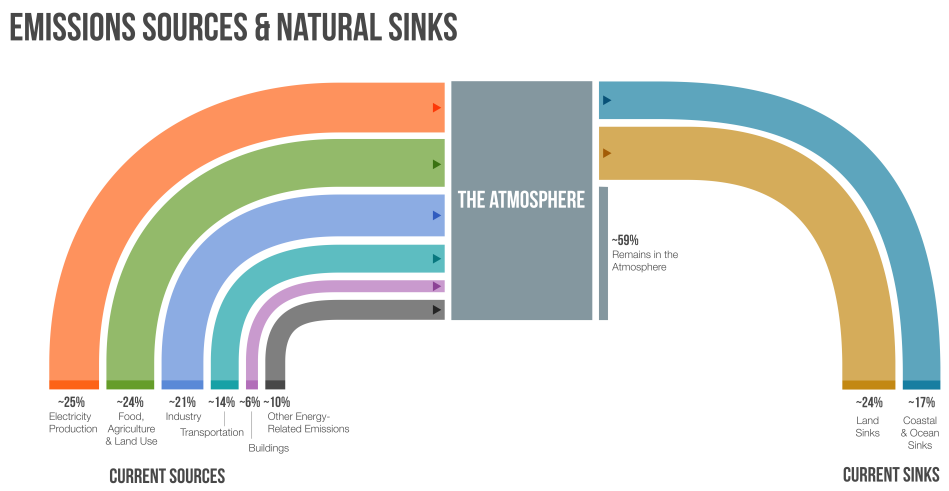

Figure 1.6: Drawdown is the future point in time when levels of greenhouse gases in the atmosphere stop climbing and start to steadily decline. This is the point when we begin the process of stopping further climate change and averting potentially catastrophic warming. It is a critical turning point for life on Earth. As becomes clear from the graphic there is still a tremendous gap between greenhouse gas emission and sequestration. Graphic from Project Drawdown.

In nature no species lives in isolation. And related, pure cultures perform bad in natural environments where they generally are easily outcompeted. The work horse microbes can be altered to yield almost any conversion, but what remains completely intangible, is altering them in such a way that they can thrive in specific natural environments. These work horse microbes need pampering, as those are also the conditions by which they were enriched. If we want to utilize natural processes to create a more sustainable society it therefore makes sense to focus on consortia of microorganisms working together. Compared to pure culture research, this approach might be more difficult to control and understand, but will likely yield highly sustainable processes. Applications from the field of environmental biotechnology such as waste-water treatment installations, show that we can achieve stable processes with undefined mixed cultures of microbes. The challenge now becomes, what can nature do for us, besides cleaning our mess? Is there a manner by which we can utilize microorganisms to produce resources?

Central to a mixed culture approach is the principle of microbial community engineering. It embraces the notion that 3.5 billion years of evolution resulted in a tremendous wealth of biological prowess. Now we are looking for ways to tap into this microbial treasure. By designing selective environments, we aim to let microbes with desired properties thrive in our biological processes. Laurens Baas-Becking stated it strikingly: “Everything is everywhere, but the environment selects.” [27] Everything – i.e. all diversity that nature has brought forth – is abundant and ubiquitous, but depending on the environment – i.e. selective conditions - some like a milieu better than others.

We set out to explore the vastness of microbial diversity by improving the experimental methods, allowing us to explore and utilize nature’s treasures to accelerate the production and reuse of resources; with a specific interest in bioplastics.

1.8. PLASTICS, BIOPOLYMERS, AND MICROBIAL FAT

The plastics that surround our daily life are exceptional. They come in a tremendous range of properties, are resilient, inert, and inexpensive. It is truly the invention of the 20th century [28]. The fact that they are cheap made them ubiquitous, which, combined with their durability, will allow future geologists to define the era of mankind by the presence of plastics in sediment layers. The use of oil-derived non-degradable plastics for single-use items is a major contributor to climate change and global pollution [29]. Its impact will grow exponentially with the rising prosperity of the world, and this stresses that alternatives are found and implemented.

On a molecular level, plastics are small molecules (monomers) chained together to form long strands or networks (polymers). The properties of a polymer arise from the type of monomers and how they are linked [30]. Broadly, two forms of polymers exist in nature: (i) those with unique make-up and properties, e.g.: RNA, DNA and proteins, and (ii) those with generalized make-up and properties, e.g.: cellulose, starch, and rubber. Where the first group contributes to the functional capabilities of the organism, the latter group is more related to its structure and to its eating habits.

Living things require a source of energy and nutrients to maintain themselves and form new biomass. Due to ongoing natural fluctuations, energy and nutrients are not continuously present. Evolution has brought forth a logical solution in the form of storage compounds, where cellular metabolism can direct energy and nutrients into polymers for later use. A specific group of these storage compounds is receiving tremendous attention, because they could form the chemical basis for bio-based and biodegradable plastics due to their thermoplastic and mechanical properties [31]. These bio-polymers are the research topic of this thesis and hold the hefty name *polyhydroxyalkanoates* (PHA).

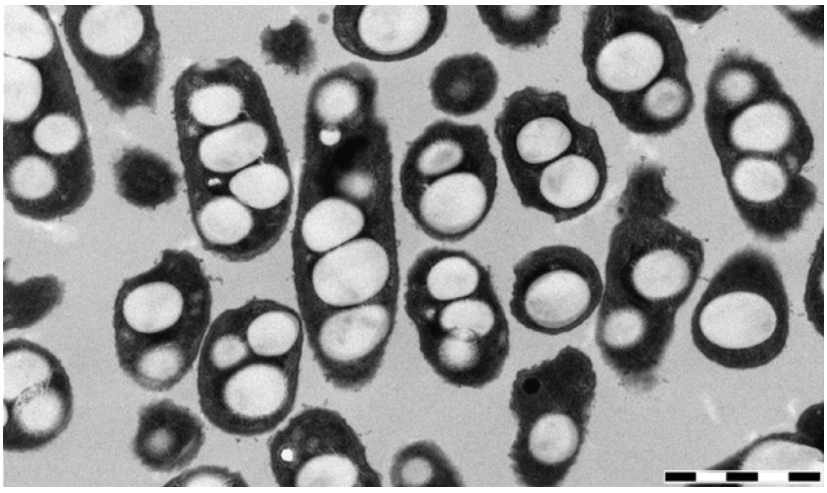

Figure 1.7: A Transmission Electron Microscopy (TEM) image of several microorganisms from the *C. nectar* H16 strain. A TEM allows for exceptional high magnifications (scale bar = 1 µm) and is therefore well suited for our first image of microorganisms with PHA granules. The dark outlines are the *C. nectar* cells, and the white inclusion bodies are the microbial equivalent of fat, i.e.: PHA granules. Image from Sedlacek *et al.* [32].

1.9. POLYHYDROXYALKANOATES - (PHA)

It is remarkable how we, as humans, can eat all kinds of different things, and it is converted into more human. Even more remarkable is that when you eat too much, whether it is a carrot, a candy bar, or berenklauw, that excess is stored as fat and not as small carrots. This funneling of different substrates into a narrow range of products also happens in micro-organisms. Microbes from all over the tree of life (Figure 1.3) can consume many different carbon substrates and produce PHA, signifying that the mechanisms for PHA production came about a long time ago.

If there is one resource that we have enough of, and often consists of a complex mix of substrates, it is waste streams. Waste streams are coined waste streams because they cannot be utilized economically in the process they originate from. Examples include wastewater from the food and paper industry, but also compost and municipal discharge fall within this category. The reason that these streams are waste, is that they have undesired consequences when directly discharged; think of water pollution, eutrophication, and streets filled with manure [33]. The deceptive beauty of these waste streams is that they are potent, they are not inert, they contain some chemical energy.

The idea of waste-to-resource research is to utilize this chemical energy, using waste as a heterogeneous feedstock from which interesting compounds can be produced, while also cleaning the discharge stream. One of those interesting compounds is PHA. In order to produce PHA from these complex feedstocks, a biological process is required that can be implemented in a wide range of environments, as waste streams all over the world can differ tremendously.

The ubiquity of PHA production in microbes means that the mechanics are there, the goal now becomes to find the conditions under which these mechanics thrive. Microbial community engineering utilizes ecological selection principles to enrich microbial communities with specific functional properties. The key question that drives this line of research is “Under which conditions does the desired characteristic help the microbial community?” Because, if we can intrinsically reward microorganisms for demonstrating a specific behavior, we can be sure that we can rely on selection and evolution to bring that characteristic to the forefront.

Figure 1.8: Visual representation of a real world implementation of the envisioned process. During the production of candy bars (1), a significant amount of waste water (2) is produced, by enriching for specific microorganisms (3), the waste water can be cleaned (4) and converted into PHA (5), from which ultimately biologically degradable wrappers (6) can be made. Image from TEDx Gerben Stouten - Candy becomes plastic (2014), photos by Olivier Huisman.

1.10. EXPLORING MICROBIAL DIVERSITY

Understandably, billions of years of evolution allows for a wealth of discoveries. In this introduction, we have glimpsed at the unfathomable number of microbes on Earth, we have touched ever so slightly on the span of microbial diversity, and we have an ephemeral idea of the complexity that resides within and between the microbes in the microbial world. But foremost, I hope that we can recognize that the microbial world holds the keys to a sustainable society. Nevertheless, due to the focus on mono-cultures, the potential of microbial communities is still far from adequately explored, nor known. To me, a key aspect that is holding back microbial community research is the lack of experimental freedom to mimic and characterize cultivations in dynamic conditions. In this work, we attempt to bring cultivation research into the 21st century with a more flexible bio-discovery cultivation platform.

Designing and studying selective environments and their effect on microbial communities is the central theme of this thesis. Specific effort was made to improve the manner in which enrichment research can be conducted, by means of automatization, parallelization, and increased operational freedom. The aim was to help advance the field of environmental biotechnology in such a way that research emphasis could shift from labor to thought. Naturally, we needed to focus our research, and the research topic throughout this work has been the role of storage polymers in microbial ecology, with the secondary objective the production of biopolymers from heterogeneous feedstocks. These biopolymers will be important building blocks for a circular society. This thesis therefore presents both noteworthy contributions to the waste-to-biopolymers research, as well as insights into optimizing enrichment research.

Chapter 2 describes the hardware and software that was developed to significantly assist parallel enrichment research in dynamic conditions, it elaborates on the bioreactor setups, the automatization, online data processing, and process modelling. In chapter 3 the setup is demonstrated and used to increase the research efforts of enrichment studies, making it possible to investigate the relationship between microbial community structure and microbial function throughout enrichments and during disturbances. Chapter 4 follows the systematic investigation of a specific surprising observation that was made possible by the close monitoring of the enrichment systems. It demonstrates the significant opportunities that can arise from increased research efforts. Chapter 5 takes the principles of microbial community engineering to heart and shows how microbes with superior biopolymer production characteristics can be enriched. We combined our insights in selection strategies to define an operational strategy that allows for enrichment of microorganisms with a superior storage polymer producing capacity.

Chapter 6 looks forward on the future of microbial community research, it explores the collaborative efforts between Wageningen University and Delft University in the 24 million euro Unlock project, for which the work in this thesis laid a principal foundation.

REFERENCES

[1] L. E. Orgel, *The Origin of Life on the Earth,* Scientific American , 9 (1994).

[2] W. Martin, J. Baross, D. Kelley, and M. J. Russell, *Hydrothermal vents and the origin of life,* Nature Reviews Microbiology **6**, 805 (2008).

[3] A. J. St. Leger, J. V. Desai, R. A. Drummond, A. Kugadas, F. Almaghrabi, P. Silver, K. Raychaudhuri, M. Gadjeva, Y. Iwakura, M. S. Lionakis, and R. R. Caspi, *An Ocular Commensal Protects against Corneal Infection by Driving an Interleukin-17 Response from Mucosal* Γδ *T Cells,* Immunity **47**, 148 (2017).

[4] D. Probandt, T. Eickhorst, A. Ellrott, R. Amann, and K. Knittel, *Microbial life on a sand grain: From bulk sediment to single grains,* The ISME Journal **12**, 623 (2018).

[5] L. Robertson, J. Backer, C. Biemans, J. van Door, K. Krab, W. Reijders, H. Smit, and P. Willemsen, *Antoni van Leeuwenhoek: Master of the Minuscule* (Brill, Leiden ; Boston, 2016).

[6] D. S. Blehert, K. Becker, and G. H. Chambliss, *Isolation and Characterization of Bacteria That Degrade Nitroglycerin,* , 9 (1996).

[7] E. Stackebrandt and J. Ebers, *Taxonomic parameters revisited: Tarnished gold standards,* Microbiology Today **33**, 152 (2006).

[8] D. E. Dykhuizen, *Santa Rosalia revisited: Why are there so many species of bacteria?* , 9 (1998).

[9] A. E. Magurran, *Measuring Biological Diversity* (Blackwell Pub, Malden, Ma, 2004).

[10] L. A. Hug, B. J. Baker, K. Anantharaman, C. T. Brown, A. J. Probst, C. J. Castelle, C. N. Butterfield, A. W. Hernsdorf, Y. Amano, K. Ise, Y. Suzuki, N. Dudek, D. A. Relman, K. M. Finstad, R. Amundson, B. C. Thomas, and J. F. Banfield, *A new view of the tree of life,* Nature Microbiology **1**, 16048 (2016).

[11] J. M. Heraty, R. A. Burks, A. Cruaud, G. A. P. Gibson, J. Liljeblad, J. Munro, J.-Y. Rasplus, G. Delvare, P. Janšta, A. Gumovsky, J. Huber, J. B. Woolley, L. Krogmann, S. Heydon, A. Polaszek, S. Schmidt, D. C. Darling, M. W. Gates, J. Mottern, E. Murray, A. Dal Molin, S. Triapitsyn, H. Baur, J. D. Pinto, S. van Noort, J. George, and M. Yoder, *A phylogenetic analysis of the megadiverse Chalcidoidea (Hymenoptera),* Cladistics **29**, 466 (2013).

[12] C. R. Darwin, *Darwin Correspondence Project, "Letter no. 2814," Darwin, C. R. to Gray, Asa,,* (1860).

[13] T. Baba and O. Schneewind, *Instruments of microbial warfare: Bacteriocin synthesis, toxicity and immunity,* Trends in Microbiology **6**, 66 (1998).

[14] M. Walden, J. M. Edwards, A. M. Dziewulska, R. Bergmann, G. Saalbach, S.-Y. Kan, O. K. Miller, M. Weckener, R. J. Jackson, S. L. Shirran, C. H. Botting, G. J. Florence, M. Rohde, M. J. Banfield, and U. Schwarz-Linek, *An internal thioester in a pathogen surface protein mediates covalent host binding,* eLife **4**, e06638 (2015).

[15] S. Lebeer, I. J. J. Claes, T. L. A. Verhoeven, J. Vanderleyden, and S. C. J. De Keersmaecker, *Exopolysaccharides of Lactobacillus rhamnosus GG form a protective shield against innate immune factors in the intestine: EPS as adaptation factor of L. rhamnosus GG,* Microbial Biotechnology **4**, 368 (2011).

[16] K. M. Oliver, A. H. Smith, and J. A. Russell, *Defensive symbiosis in the real world - advancing ecological studies of heritable, protective bacteria in aphids and beyond,* Functional Ecology **28**, 341 (2014).

[17] T. L. Czaran, R. F. Hoekstra, and L. Pagie, *Chemical warfare between microbes promotes biodiversity,* Proceedings of the National Academy of Sciences **99**, 786 (2002).
[18] G. H. Wadhams and J. P. Armitage, *Making sense of it all: Bacterial chemotaxis,* Nature Reviews Molecular Cell Biology **5**, 1024 (2004).
[19] B. L. Bassler and R. Losick, *Bacterially Speaking,* Cell **125**, 237 (2006).
[20] A. Westbrook and O. Ratti, *Aikido and the Dynamic Sphere: An Illustrated Introduction* (Tuttle Publishing, Tokyo, 1983).
[21] D. Adams and N. Gaiman, *The Ultimate Hitchhiker's Guide to the Galaxy: Five Novels in One Outrageous Volume* (Del Rey, 2010).
[22] T. M. Porter, C. Smith, and M. N. Wise, *Energy and Empire: A Biographical Study of Lord Kelvin,* Technology and Culture **32**, 145 (1991).
[23] K. Michaelian, *Thermodynamic dissipation theory for the origin of life,* Earth System Dynamics **2**, 37 (2011).
[24] E. J. Stewart, *Growing Unculturable Bacteria,* Journal of Bacteriology **194**, 4151 (2012).
[25] M. Bologna and G. Aquino, *Deforestation and world population sustainability: A quantitative analysis,* Scientific Reports **10**, 7631 (2020).
[26] F. R. Spellman, *The Science of Environmental Pollution* (CRC Press, 2017).
[27] L. G. M. Baas-Becking, *Geobiologie; of Inleiding Tot de Milieukunde.* (WP Van Stockum & Zoon NV, 1934).
[28] L. H. Baekeland, *Method of Making Insoluble Products of Phenol and Formaldehyde.* (1909).
[29] L. A. Hamilton and S. Feit, *Plastic & Climate: The hidden costs of a plastic planet,* (2019).
[30] J. Ferry, *Viscoelastic Properties of Polymers*, Viscoelastic Properties of Polymers (1980).
[31] M. Crank, O. Wolf, M. Patel, F. Marscheider-Weidemann, J. Schleich, B. Hüsing, and G. Angerer, *Techno-Economic Feasibility of Large-Scale Production of Bio-Based Polymers in Europe*, Tech. Rep. (European Commission, Brussels, 2005).
[32] P. Sedlacek, E. Slaninova, V. Enev, M. Koller, J. Nebesarova, I. Marova, K. Hrubanova, V. Krzyzanek, O. Samek, and S. Obruca, *What keeps polyhydroxyalkanoates in bacterial cells amorphous? A derivation from stress exposure experiments,* Applied Microbiology and Biotechnology **103**, 1905 (2019).
[33] E. Morris, *From Horse Power to Horsepower,* Access Magazine (2007).

2

PARALLEL BIOREACTOR SETUP & SYSTEM CHARACTERIZATION OF DYNAMIC BIOLOGICAL CULTIVATIONS THROUGH IMPROVED DATA ANALYSIS

Gerben Roelandt STOUTEN, Sieze DOUWENGA, Carmen HOGENDOORN, Robbert KLEEREBEZEM

Determining the functional development and dominant competitive strategy in a microbial community is complicated by the extensive measurement campaigns required for off-line system analysis. This study demonstrates that detailed system characterization of aerobic pulse fed enrichments can be established using on-line measurements combined with automated data analysis. By incorporating the physicochemical processes in on-line data processing with a Particle Filter and kinetic process model, an accurate reconstruction of the dominant biological rates can be made. We hereby can differentiate between storage compound production and biomass growth in sequencing batch bioreactors. The method proposed allows for close monitoring of changes in functional behavior of enrichment cultures, without the need for off-line samples, therewith enabling the identification of new insights in process dynamics with a minimal experimental effort. Even though a specific example application of the method proposed is described here, the approach can readily be extended to a wide range of dynamic experimental systems that can be characterized based on on-line measurements.

Parts of this chapter have been published as Stouten *et al.* [1].

This page is not entirely unlike a blank page.

2.1. INTRODUCTION

Enrichment studies are fundamental tools for understanding the microbial world. The earliest studies from Beijerinck and Winogradsky are based on restrictive growth media and gradients in space, which favor growth of particular microbes over others [2, 3]. They were used to elucidate the role of microorganisms in biogeochemical cycles, where carbon, nitrogen, oxygen, phosphorus and sulfur compounds are converted in a wide range of redox reactions. Later enrichments established by Grant and Brock focused on the use of environmental factors to enrich microbes that flourish at high temperatures and salinities for example [4, 5]. The countless combinations of selective media and environmental factors have unearthed a profound microbial richness [6]. Although many microbes have been enriched in a wide range of conditions, all of these enrichments are based on imposing a specific selective pressure in either a continuous or batch system.

Recent work has demonstrated that through imposing dynamic process conditions an additional wealth of microbial diversity is revealed, compared to traditional chemostat or batch cultivation [7–10]. Essentially all natural environments are subject to ever changing conditions, from scarce nutrient availability to its sudden abundance and more regular day-night cycles leading to fluctuations in temperature and substrate supply. An abundant portion of microbes evolved under dynamic conditions and as such developed different functional strategies to exploit a competitive edge. For example, the alternating absence and presence of light, electron acceptor, carbon substrate, and growth nutrients provides a competitive advantage for specific microorganisms that depend on the production and consumption of storage polymers. We propose that a large part of the microbial diversity and available functionality is overlooked by studying microorganisms in absence of dynamics.

The exploration of dynamic cultivation systems increases the experimental complexity but gives more information on the development over time as each operational cycle can be analyzed and compared [11]. The quantification of the variations between cycles requires data analysis which aims for identification of the time dependent stoichiometry and kinetics of the (biological) process in the bioreactor. The reconstruction of biological rates is complicated by two distinct dynamic properties. First, the change of environmental conditions, like cyclic nutrient pulses, result, by definition, in variable concentrations inside the bioreactor. The second dynamic is caused by the response time needed for measurable parameters to changes in the process, such as dissolved oxygen concentration or CO_2 in the off-gas.

Throughout an operational cycle, microbes will respond to the changing environmental conditions and can exhibit different functional properties depending on the actual conditions. Capturing these changes in functional properties requires frequent measurements at short intervals. Combined with the fact that enrichment studies take weeks to months, manual sample analysis becomes both cumbersome and non-scalable. On-line data from liquid probes and off-gas analysis is generally available but utilization of these measurements for on-line process identification beyond the observations of general trends is often limited, due to complicating physicochemical processes and measurements noise.

Here, we propose a method which allows high-definition system characterization, based solely on on-line measurements. This method combines a signal processing method

(Particle Filter) and a physicochemical model. We demonstrate this method by reconstructing the respiration rates in aerobic pulse fed bioreactors (Figure 2.1). The demonstration furthermore shows how the reconstructed respiration data can be used to ascribe microbial functionality to each cycle. Herewith we aim to show the added worth of standardizing data reconsolidation in dynamic cultivations. As such, the approach suggested is widely usable in microbial cultivation, and can help us unlock new insights in metabolism and regulation of microorganism.

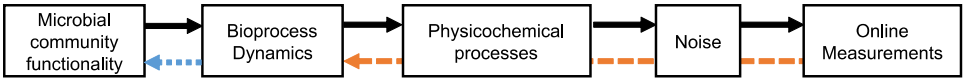

Figure 2.1: Schematic overview of the factors that influence on-line measurements. The goal of the Particle Filter (orange dashes) is to reconstruct the bioprocess rates as accurately as possible, taking into account the limitations resulting from system and measurement noise. Additional understanding of the metabolic processes is required (blue dots) to derive further biological information from the reconstructed bioprocess dynamics. In the example system, the reconstructed respiration rates are used to identify the dominant metabolic processes of the enrichment culture over time.

PARTICLE FILTER AND PHYSICOCHEMICAL MODEL FOR RESPIRATION RATE RECONSTRUCTION.

Mandenius and Gustavsson [12] reviewed several software sensor solutions that are used to derive new information from true sensors by combining them with software models. These models range from high mathematical signal processing complexity [13–15] to those with emphasis on biological system modeling that describe specific biological systems [16, 17]. A general downside of these models is that either their implementation is of such complexity that they are difficult to realize and verify or that they are not suited for a general solution. Especially the mass transfer limitations that occur in systems with imposed dynamics (e.g.: pulse fed systems) and the difference in measurement frequency and accuracy of sensors lead to implementation difficulties [18, 19]. Here we propose and demonstrate a model that is specifically suited for the reconstruction of respiration rates in dynamically operated bioreactors.

De Jonge and colleagues developed a physicochemical model that allows for the respiration rate reconstruction at per-second timescale of a chemostat culture perturbed by a single substrate pulse [20]. Their model is meant as a research tool to facilitate state estimation and requires significant calibration, parameter estimation, and understanding of the Extended Kalman Filter utilized. More recent advancements in state estimation come in the form of Particle Filters where the implementation of the system physics are more accessible [21], and the results are more accurate than the Extended Kalman Filter, but the implementation is computationally more expensive [22]. The Extended Kalman Filter and Particle Filter are used to estimate the internal states in dynamic systems based on partial observations in the presence of sensor noise. Both methods require a model of how the system changes in time as a response to changing inputs – in this case respiration rates. Here, the model incorporates the main physicochemical processes, which include inorganic carbon speciation, gas mixing in the bulk liquid and head space, delays and non-equilibrium phase transfer rates. While the Kalman Filter is

the optimal signal processor for linear models, and it has been adapted to support non-linear systems in the form of the Extended Kalman Filter, its application requires local linearization, which increases the mathematical complexity during model development and model expansion and makes the model error-prone during strong non-linear behavior. The Particle Filter overcomes those issues by introducing many alternative starting points (particles) for each prediction step, this increases the computational complexity but reduces mathematical complexity, and allows adaption to non-linearities.

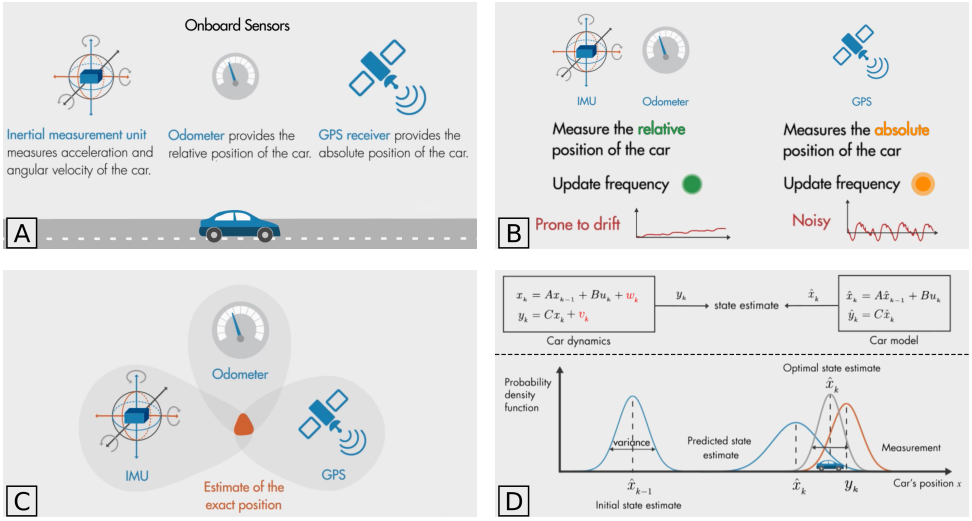

Figure 2.2: Schematic overview of the Kalman Filter when applied to tracking a car. (A) Multiple types of measurements are available (accelerometer, pedometer, and GPS). (B) these measurements can be high/low frequency, noisy, and susceptible to drift. (C) The Kalman Filter allows you to make the best estimate of the system state (in this example: position, direction, velocity, acceleration). (D) By making a model of how a car behaves with respect to the laws of physics we predict where it will end up in the next time step. This prediction has some uncertainty (blue bell shape), which increases with increasing time steps. When measurements are available, we take their uncertainty into account (red bell shape). The best estimate for the car state is than the statistical overlap of the two probabilities. **To complete the analogy, the problem that we are solving in our model is trying to get a good estimate of when and how far the gas paddle and brakes are pressed based only on GPS data.** Images adapted from *Understanding Kalman Filters* [23]

EXAMPLE SYSTEM: AEROBIC ORGANIC CARBON DEGRADATION IN A SEQUENCING BATCH PROCESS.

Microbial communities in pulse fed systems can exhibit at least two different metabolic functional strategies. Bacteria either grow on the pulsed substrate, or bacteria convert the pulsed substrate into an intracellular storage polymer. The latter type of hoarding bacteria can metabolize the stored polymers to catalytic biomass when the external substrate is depleted. Previous studies see a clear change in the community structure and functionality throughout the enrichment period of 30 to 100 days when pulse feeding is applied, resulting in a microbial community that is dominated by hoarding bacteria [24–27]. The main intracellular compound that is produced in these studies is polyhydroxybutyrate (PHB), which is gaining significant interest because its material properties

are similar to oil-derived plastics. These enrichment studies therefore predominantly focused on the final enriched community, reducing the interest in the development of the community functionality and structure throughout the enrichment. To allow more insights in the mechanisms behind microbial competition and succession in enrichment studies we aim to monitor and characterize the functional transitions of enrichment cultures in time based on on-line measurements. By reconstructing the respiration rates in the dynamic cultivation conditions important insight can be generated regarding the development of the dominant metabolic strategy.

2.2. MATERIAL & METHODS

This section is divided in (1) the materials and methods of a parallel cultivation system that allows continuous on-line measurements and characterization of enrichment cultures, (2) the description and implementation of the Particle Filter and physicochemical model for the reconstruction of respiration rates based on on-line measurements, and (3) the materials and methods of the example process of aerobic organic carbon degradation in a sequencing batch reactor on which we apply the proposed methodology.

2.2.1. CULTIVATION SETUP FOR ON-LINE CHARACTERIZATION OF ENRICHMENT CULTURES

In an effort to support high-resolution and reproducible enrichment studies a parallel bioreactor cultivation setup was designed and constructed (Figure 2.3). Considerable attention has been put in the flexibility of the hardware and software of the system to allow precise control over the cultivation conditions, which can be employed to impose a wide range of selective conditions on microbial cultivations.

The setup consists of eight identical 2.2L jacketed bioreactors (Applikon, the Netherlands), allowing temperature control through separate thermostats (RE630, Lauda, Germany). Each bioreactor is equipped with four feed/effluent pumps (WM120U, Watson Marlow, United Kingdom), and two acid/base pumps (MP8, DASGIP, Germany). Concentrated medium and water vessels are placed on balances (Mettler Toledo, The Netherlands). pH and dissolved oxygen probes for each reactor are connected to a measurement unit (PH8DO8, DASGIP, Germany). In-gas composition and gas flow for each individual bioreactor is delivered through a gas mixing manifold (MX44, DASGIP, Germany). Off-gas is led through a condenser, kept at 4 °C through a cryostat (Lauda, Germany), and connected to the gas mass spectrometer (Prima BT, Thermo Fisher, USA). System operational pressure (typically 50-100 mbar overpressure) is controlled through a manually adjustable pressure control valve placed in the off-gas line. Gas recirculation of the headspace to the gas-inlet is facilitated by an adjustable membrane pump (Buerkle, Germany). Two six-blade Rushton impellers are stirred by on overhead drive, which is controlled by a stirring unit (SC4D, DASGIP, Germany).

A central control unit was custom made (HAL, TU Delft, The Netherlands) for analog control of the 32 feed/effluent pumps, and for the digital communication with the DASGIP units, balances, thermostats and mass spectrometer. Custom logging and scheduling software (D2I) allowed for fine control over the dosing mechanism, gas profile switching, incorporation of off-gas and off-line measurements as system event triggers, and

general automatization of system variations and calibrations.

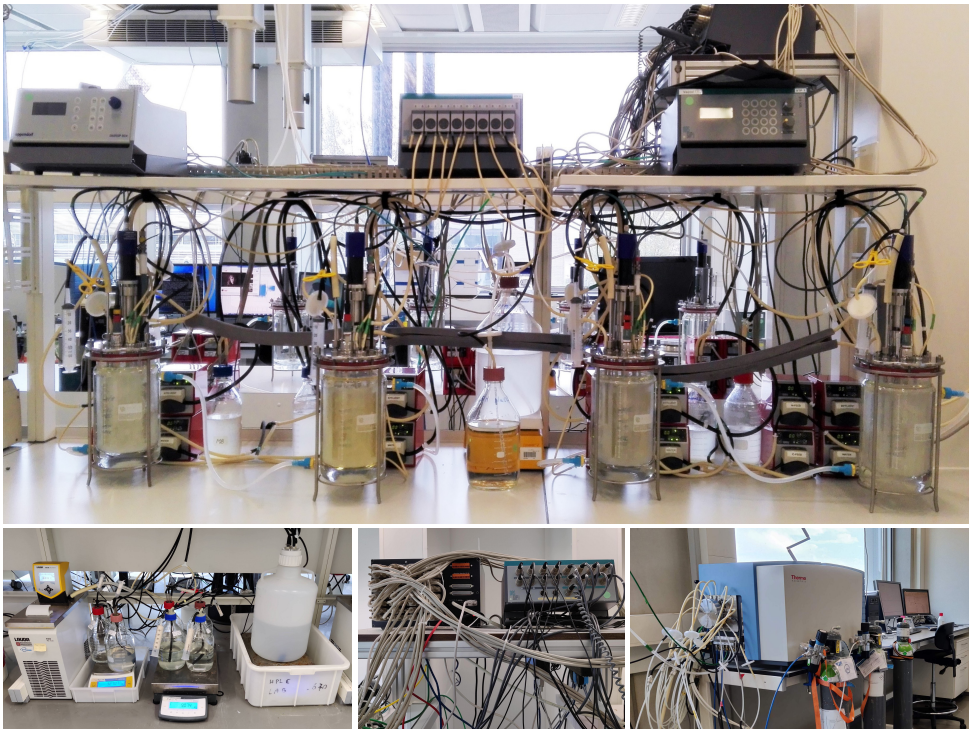

Figure 2.3: Photos of the parallel bioreactor setup. Shown are (top) four of the eight bioreactors, with their (bottom) balances and cultivation media, the custom central control system that connects all digital and analog equipment, and the off-gas mass-spectrometer with channel selector and calibration gasses. Images from personal archive G.R. Stouten.

MASS SPECTROMETER TUNING

Gas composition going in and coming out of the reactors was analyzed with on-line mass spectrometry (Prima BT, Thermo Fisher, USA). The fast switching of the mass spectrometer allowed for frequent gas composition monitoring, where the in-gas and the off-gas of eight reactors are measured every 3 minutes. The Prima BT mass spectrometer contains a small flow cell which is continuously analyzed at different m/z values. The composition of calibration gasses can be analyzed to ppm level because the gas composition remains constant. During dynamic bioreactor operation the off-gas composition changes continuously. As a result, the gas composition in the flow cell changes throughout the measurement window of the mass spectrometer. Therefore, a tradeoff has to be made between analysis time and accuracy. In the current configuration we use 10 seconds of stream flushing and 8 seconds of measurement per channel (2 seconds per m/z: 28, 32, 40, 44). This results in the expected errors in the gas composition measurements between 10-300 ppm depending on the gas compound mole fraction. With eight gas_{OUT} and one gas_{IN} channel, the total time between measurements for each system is less than three minutes.

ONLINE DATA PROCESSING PIPELINE

Online data is processed by filtering out erroneous measurements collected during operational disturbances (e.g.: bioreactor cleaning and maintenance), and correcting for the delayed off-gas composition measurement due to the off-gas plug-flow from the bioreactor to the mass spectrometer. Generally, filtering data and constructing datasets from raw measurement data is a manual task, due to many ambiguities that arise from differences in experimental setup and operation. Given that the parallel cultivation setup developed in this work spans eight analogue bioreactor setups that run highly comparable cultivations, this task could be largely automated. By processing the raw on-line measurement with a heuristic based, data filtering, and data pruning approach the task of data processing was significantly accelerated. Python3 code (filteredcycle.py) is included in the on-line code repository at: `https://github.com/GRS-TUD/d2i`, with examples of common disturbances, and their heuristics. From these filtered datasets the respiration rates (oxygen uptake rate and carbon evolution rate) are reconstructed throughout each cycle using the Particle Filter with the physicochemical model.

2.2.2. PARTICLE FILTER AND PHYSICOCHEMICAL MODEL FOR RECONSTRUCTING BIOPROCESS DYNAMICS

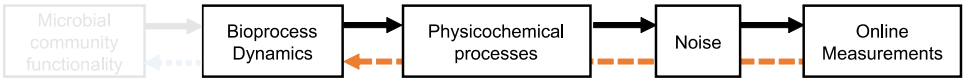

Figure 2.4: The goal of the Particle Filter (orange dashes) is to reconstruct the bioprocess rates as accurately as possible, taking into account the limitations resulting from system and measurement noise.

RECONSTRUCTING THE RESPIRATION RATES WITH A PARTICLE FILTER

The Particle Filter is a 3-step, prediction-update-resample, state estimation method that uses N samples from a distribution around the current (n) best estimate of the system state to predict the changes to the system state through an underlying model (detailed implementation in Supplementary Materials 2.6.1). With each calculation cycle a step (n+1) in time is made. Each particle represents a possible oxygen and carbon dioxide respiration rate (hidden state) which are used as input in the physicochemical model to predict the new compound concentrations and measurements. During the update step the uncertainty of N new state predictions and the uncertainties of the actual measurements (observation) are taken into account to make a weighted distribution of the most likely system state using Bayes' theorem. As N tends to infinity this method converges to a system state as expressed by a probability density function. During the resample step, new particles are chosen to prevent highly unlikely system states (particles) to take-up calculation time and to increase the resolution surrounding the current best state estimates. This resampling step requires a resampling algorithm, here we chose to implement the systematic resampling algorithm from Douc *et al.* [28].

The Particle Filter requires two additional inputs, (i) the covariance matrix of the process represents how fast the biological respiration rates can change, and (ii), the covariance matrix of the measurement captures correlations and noise of measurements. These matrices should be derived for each specific setup and experiment.

DETERMINING THE PARTICLE FILTER COVARIANCE MATRICES AND INITIAL STATE

The aim of the Particle Filter is to reconstruct the respiration rates of the biological community. During the prediction step each particle represents the rate of change of the current respiration uptake rates $\left(\frac{d\overrightarrow{UR}}{dt}\right)$, where the values are normally distributed around 0, and with a specific variance for both the oxygen uptake rate (OUR) and carbon dioxide uptake rate (CUR). Negative uptake rates equal positive production rates. The process variance for the OUR and CUR allows the model to emulate the development of the respiration rates and is chosen in such a way that the observed increase and decrease of the respiration rates on a substrate pulse can be achieved. If the values are too small, the model cannot respond quickly enough to changes in respiration rates, and if the values are too large a significant fraction of the particles will take on values that diverge far from the true mean.

In most aerobic biological systems a strong correlation exists between oxygen uptake and carbon dioxide production, incorporating this knowledge reduces the computational effort because fewer particles are required to reconstruct the respiration rates. To show the general applicability of the model, the results shown here assume no additional knowledge regarding the respiration covariance. Therefore, the initial estimates and covariance matrix are diagonal matrices. The modelled biological system does not involve nitrogen fixation or production (NUR = 0). The process covariance matrix ($mol^2\ s^{-2}$) for the system modelled here is given by:

$$U_k = \mathcal{N}\left(\begin{pmatrix}0\\0\\0\end{pmatrix}, \begin{pmatrix}1 & 0 & 0\\0 & 1 & a\\0 & a & 1\end{pmatrix}\begin{pmatrix}0\\7\cdot10^{-8}\\8\cdot10^{-8}\end{pmatrix}\right)$$

With U_k representing the covariance matrix for (nitrogen, oxygen and carbon dioxide uptake rates), where *a* is 0 if no correlation between OUR and CUR is assumed, and *a* is -1 assumes a perfect correlation.

All analyses contain some measurement uncertainty. This uncertainty is taken into account to make a weighted average between the predicted and measured values for the system state. The measurement noise covariance for the off-gas (N_2, O_2, CO_2) measurements (expressed as ppm^2) is based on the accuracy of the mass spectrometer:

$$R_k \sim \mathcal{N}\left(\begin{pmatrix}0\\0\\0\end{pmatrix}, \begin{pmatrix}30000 & 0 & 0\\0 & 25000 & 0\\0 & 0 & 300\end{pmatrix}\right)$$

With R_k representing the covariance of head space gas mole fraction (N_2(g), O_2(g), CO_2(g)).

The initial state of the system (gas concentrations and dissolved carbon species at t=0) is important for model predictions. The Particle Filter allows the initiation of N different initial states which converge to the most probable state. Simulation with the Particle Filter were performed with 10.000 particles, initially uniformly distributed between 0 and 10^{-6} $mol_{O2}\ s^{-1}$, and between -10^{-6} and 0 $mol_{CO2}\ s^{-1}$.

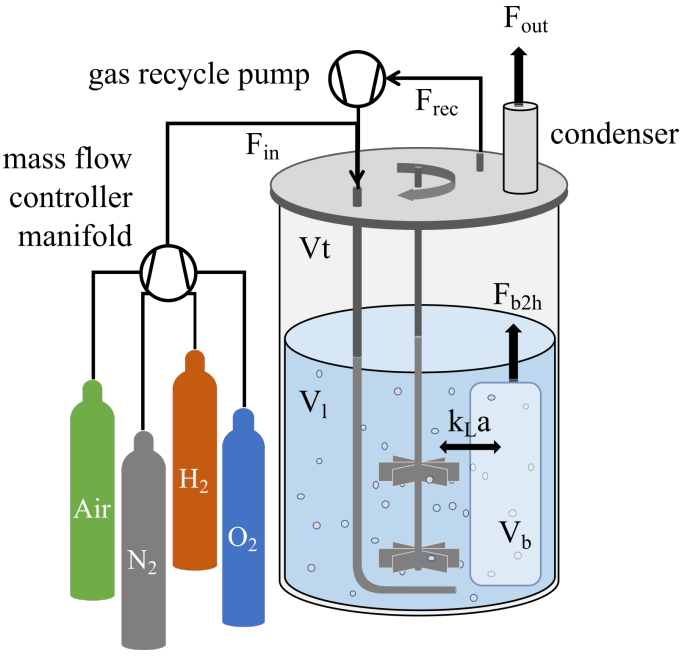

Figure 2.5: Schematic overview of the gas holdup and gas flow in a bioreactor. Dry gas (F_{in}) from the gas mixing manifold combines with wet gas from the headspace (F_{rec}), and is led into the bioreactor. The bubbles take up a specific volume (V_b) in the liquid (V_l), gas exchange takes place between the gas bubbles and the liquid through rate parameter (k_La). Gas in the bubbles saturates with water and a net flow of wet gas (F_{b2h}) takes place from the bubbles to the headspace (V_h). Wet gas is dried in the condenser and flows to the mass spectrometer (F_{out}).

PHYSICOCHEMICAL PROCESSES FOR GAS EXCHANGE

The mole fraction of gas species in the headspace (h) and in the bubbles (b) can be described in vector notation ($\vec{v}$ with $\odot$ as element wise multiplication operator). The change in the concentration of the dissolved gas species in the broth depends on the transfer to and from the gas phase ($\overrightarrow{\mathrm{TR}}$) and the uptake or production by micro-organisms ($\overrightarrow{\mathrm{UR}}$).

$$V_l \frac{d\vec{c_l}}{\mathrm{dt}} = \overrightarrow{\mathrm{TR}} + \overrightarrow{\mathrm{UR}} \tag{2.1}$$

The transfer rates ($\overrightarrow{\mathrm{TR}}$) depend on the partial pressure of the gasses in the bubbles ($P \cdot \vec{x_b}$), the concentration in the liquid ($\vec{c_l}$) and the mass transfer coefficients ($\vec{k_L a}$).

$$\overrightarrow{\mathrm{TR}} = V_l \cdot \vec{k_L a} \odot \left(P \cdot \vec{x_b} \odot \vec{H} - \vec{c_l} \right) \tag{2.2}$$

The transfer of gas to or from the bubbles changes the molar gas flow rate from the bubble to the headspace (F_n^{b2h}). It may practically be assumed that all gas in the reactor is saturated with water vapor (P_W). Headspace recycling (F_n^{rec}) bypasses the off-gas con-

denser to appropriate the drying capacity to off-gas flowing to the mass spectrometer (Figure 2.5).

$$F_n^{b2h} = F_n^{\text{rec}} + \frac{F_n^{\text{in}}}{1 - \frac{P_w}{P}} - \sum \frac{\overrightarrow{\text{TR}}}{1 - \frac{P_w}{P}} \tag{2.3}$$

The change in the composition of the gas in the bubbles depends on the gas composition flowing in (combining new in-gas with potential headspace recirculation).

$$\frac{V_b}{V_m} \frac{d\overrightarrow{x_b}}{\text{dt}} = F_n^{\text{in}} \cdot \overrightarrow{x_{\text{in}}} + F_n^{\text{rec}} \cdot \overrightarrow{x_h} - F_n^{b2h} \cdot \overrightarrow{x_b} - \overrightarrow{\text{TR}} \tag{2.4}$$

The change in the composition of gas in the head space depends on the molar gas flow rate and the composition of the bubble and headspace gasses.

$$\frac{V_h}{V_m} \frac{d\overrightarrow{x_h}}{\text{dt}} = F_n^{b2h} \cdot \left(\overrightarrow{x_b} - \overrightarrow{x_h}\right) \tag{2.5}$$

The equations above describe the change in concentrations and mole fractions of gasses in the liquid and gas phase. For carbon dioxide an additional factor needs to be taken into account, the speciation of inorganic carbon as CO_2(aq), H_2CO_3, HCO_3^-, and CO_3^{2-} (Figure 2.6). Speciation depends on forward and backward reaction rate constants (lowercase k) and equilibrium constants (uppercase K), their values have been adapted from the comprehensive studies by Harned and colleagues [29, 30], and Wang and colleagues [31][1].

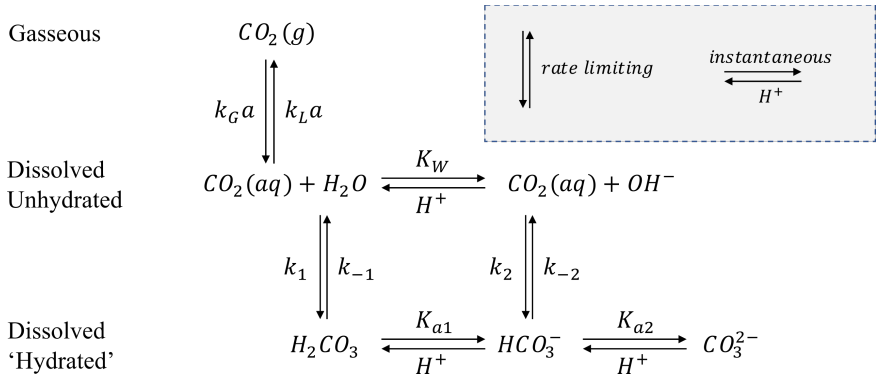

Figure 2.6: Reaction scheme of inorganic carbon in aqueous solution. Reactions that take place over the vertical axis are rate limiting, and reactions taking place over the horizontal axis are instantaneous protonation equilibria. In the gas-liquid exchange the $k_G a$ and $k_L a$ have the same physical meaning but are written from the perspective of the gas or liquid phase.

[1] Note that Wang and colleagues swapped the naming convention for the equilibrium constants Ka1, and Ka2, and inadvertently allowed some printing errors in the Parameters section of the Materials and Methods regarding the relationships between the equilibria.

The protonation equilibria are considered instantaneous with respect to the timescales of our experiments [32]. The hydrated carbonate species (carbonic acid, bicarbonate, and carbonate) can therefore all be expressed as a fraction (f_i) of the total hydrated inorganic carbon (CO_2^{hydr}), and depend on the pH.

$$f_{H_2CO_3} = \left(1 + \frac{K_{a1}}{c_{H^+}} + \frac{K_{a1} \cdot K_{a2}}{{c_{H^+}}^2}\right)^{-1} \tag{2.6}$$

$$f_{HCO_3^-} = \left(1 + \frac{c_{H^+}}{K_{a1}} + \frac{K_{a2}}{c_{H^+}}\right)^{-1} \tag{2.7}$$

$$f_{CO_3^{2-}} = \left(1 + \frac{c_{H^+}}{K_{a2}} + \frac{{c_{H^+}}^2}{K_{a1}}\right)^{-1} \tag{2.8}$$

$$f_{H_2CO_3} + f_{HCO_3^-} + f_{CO_3^{2-}} = 1 \tag{2.9}$$

The kinetics of inorganic carbon speciation can be seen as the net transfer of carbon between the hydrated (H_2CO_3 and HCO_3^-) and dehydrated (CO_2(aq)) species.

$$\frac{\mathrm{dc}^l_{CO_2^{hydr}}}{\mathrm{dt}} = c^l_{CO_2} \cdot \left(k_1 \cdot c^l_{H_2O} + k_2 \cdot c_{OH^-}\right) - c^l_{CO_2^{hydr}} \cdot \left(k_{-1} \cdot f_{H_2CO_3} + k_{-2} \cdot f_{HCO_3^-}\right) \tag{2.10}$$

The three processes that therefore contribute to the dissolved CO_2 concentration in the reactor broth are: the carbon dioxide evolution from microbial activity, the carbon dioxide transfer between the gas and liquid phase, and the (de)hydration reactions for carbon dioxide speciation. The initial two processes are already captured in equation (1), and therefore the (de)hydration rate has an additional (+=) effect on the concentration of dissolved CO_2.

$$\frac{dc^l_{CO_2}}{\mathrm{dt}} += \frac{-\,\mathrm{dc}^l_{CO_2^{hydr}}}{\mathrm{dt}} \tag{2.11}$$

Furthermore, the broth in a bioreactor is a non-ideal solution, therefore compound activity needs to be used instead of concentrations for charged species. The extended Debye-Hückel equation is used as approximation for the activity coefficients for solutions with an ionic strength (I) lower than 100 mmol L^{-1}:

$$\log_{10}\gamma_i = \frac{-Az_i^2\sqrt{I}}{1 + Ba_i\sqrt{I}} \tag{2.12}$$

Here, γ_i represents the activity coefficient and z_i is the charge of ion i (H^+, OH^-, HCO_3^-, CO_3^{2-}). A, and B are temperature dependent constants, and have values 0.496 ($kg^{0.5}$ $mol^{-0.5}$), and 0.325 ($Å^{-1}$ $kg^{0.5}$ $mol^{-0.5}$) at 30 °C. The value for a_i is the effective diameter of the ions (H^+ 9Å, OH^- 3.5Å, HCO_3^- 4Å, CO_3^{2-} 4.5Å [33]). The ionic strength of the medium is approximately 75 mmol L^{-1}, bringing the activity coefficients for protons, hydroxyl, bicarbonate, and carbonate to 0.84, 0.79, 0.8, and 0.41, respectively.

2.2.3. MATERIALS AND METHODS FOR APPLICATION OF PROPOSED METHODOLOGY ON ENRICHMENT OF PULSE FED AEROBIC SEQUENCING BATCH BIOREACTOR (EXAMPLE)

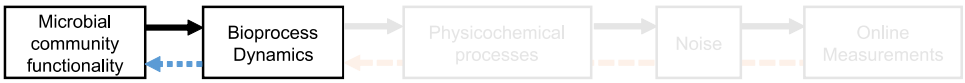

Figure 2.7: The Particle Filter reconstructs bioprocess dynamics in the form of respiration rates. These rates can be used to further characterize the microbial community functionality when additional information about the system is considered (blue arrow). This process is system specific, and here we describe how the Particle Filter can be used for the pulse fed aerobic bioreactor systems.

SEQUENCING BATCH BIOREACTOR

Throughout this manuscript the experimental data of a single enrichment study is used as example. The bioreactor was operated aerobically, for 200 cycles (100 days), with acetate as sole carbon source and electron donor (40 mCmol pulse per cycle). The working volume of the bioreactor was 1.4 L, and every 12 hours half of the bioreactor content was discharged and replaced by 0.7 L growth medium (7.1 mM NH_4Cl, 0.7 mM KH_2PO_4, 0.2 mM $MgSO_4.H_2O$, 0.2 mM KCl, and 1.5 mL L^{-1} trace solution [34]). pH was maintained at 7 ± 0.1 by use of 1 M HCl, and 0.5 M NaOH. Gas flow in the reactor was compressed air at a flow rate of 400 ± 2 mL min^{-1}. This enrichment was part of a study that investigated the influence of temperature on the development and performance of PHB enrichments by operating eight bioreactors in parallel [35].

CYCLE MEASUREMENTS.

Cycle measurements of SBR operations were performed to fully characterize the processes occurring in the system and verify system characterization efforts based on online data. Measurements are performed as described by [36]. Samples taken from the reactor for analysis of acetate and ammonium were immediately centrifuged and filtered with a 0.22 µm pore size filter (PVDF membrane, Millipore, Ireland). PHB and biomass dry weight measurements are performed on 15 mL bioreactor samples, after centrifuging at 5000 g and freeze-drying of the pellet.

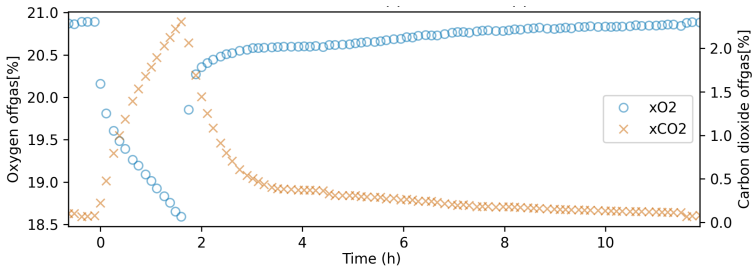

Figure 2.8: Example off-gas measurement of a single operational cycle. At t=0 a substrate pulse is given, which around t=2 h is completely consumed leading to a drop in respiration activity. The goal of the Particle Filter is to convert these measurements to the biological respiration rates.

KEY INDICATORS FOR CHARACTERIZATION OF FUNCTIONAL SYSTEM BEHAVIOR

In a pulse fed bioreactor, the extracellular carbon will be depleted at a certain time, this carbon period is defined as the feast-phase. The period in which no extracellular carbon is present is defined as the famine-phase. Three functional characteristic key indicators were derived that summarize the functional behavior in an aerobic pulse-fed sequencing batch bioreactor (Figure 2.9). All key indicators can be derived from the reconstructed respiration rates.

- The *feast-length* is derived as the inflection points of the OUR, CUR and dissolved oxygen (DO). By reducing the number of points in the respiration curves with the Ramer-Douglas-Peucker algorithm ($\varepsilon = 0.01$) the curve is simplified [37]. From this curve the slope was calculated for each segment, and the end of the feast-phase is positioned at the intersect of the most aggressive slope and the first prior segment with opposite sign. Offline measurement of acetate verified that this method closely predicts the true end of feast (Supplementary Materials 2.6.3).

- The $O_2feast\%$ is derived as the fraction of oxygen that is consumed in the feast-phase over the total oxygen consumed in the cycle. This value follows from the feast-length and OUR data, and is an indicator for the amount of respiration that takes place in the feast versus the famine phase. Where a lower $O_2feast\%$ indicates that significant respiration takes place in the famine phase, which is assumed to be due to respiring storage compounds.

- The OUR_{ratio} is derived as the ratio between the oxygen uptake rate at the beginning of the feast-phase (OUR_0) to the maximum observed oxygen uptake rate (OUR_{max}). A strong increase in the respiration activity throughout the feast phase indicates that the catalytic capacity of the system is increasing, which is likely caused by growth. While, if the respiration activity remains constant throughout the cycle, very limited growth can be expected and therefore the majority of the substrate is likely directed to storage polymers.

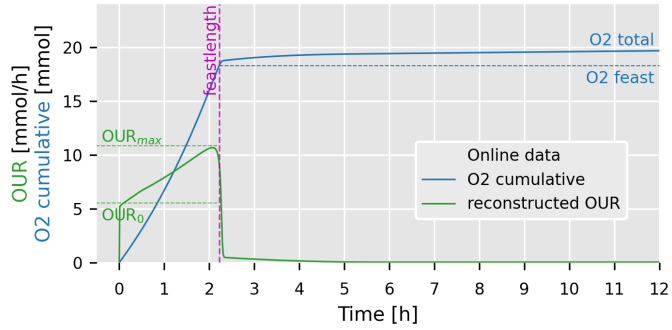

Figure 2.9: Schematic representation of how the reconstructed oxygen uptake rate (OUR in green) can be used to derive cycle specific key indicators. After the substrate pulse at t=0, a change in OUR is observed until the substrate is depleted at the end of the feast phase (feastlength in purple). By integrating the OUR over the cycle (O2 cumulative in blue), it is possible to estimate the fraction of total oxygen that is consumed during the feast phase.

IDENTIFICATION OF NON-GASEOUS COMPOUNDS

The Particle Filter is used to reconstruct the respiration rates of a biological system. These respiration rates reflect the changes in biological activity of the biomass in the system, but they represent only a limited number of compounds in the biological conversions of the system. To utilize the reconstructed respiration rates further, additional information on the cultivation and expected conversions is required. Here we will show, for this specific case, how the data can be used to reconstruct the dominant compound profiles in a sequencing batch bioreactor that is pulse fed with acetate.

The respiration profiles are used to perform carbon and electron recovery calculations throughout each cycle. The following assumptions are made with respect to the carbon and electron utilization. (i) Acetate is the only carbon and electron donor. (ii) All acetate is converted to either catalytic biomass ($CH_{1.8}O_{0.5}N_{0.2}$), storage polymers (PHB: n x $C_4H_6O_2$), or carbon dioxide. (iii) Storage polymers are transient, and are therefore consumed by the end of the cycle. (iv) Oxygen is the only electron acceptor. (v) The system operates in a pseudo steady state. (vi) PHB and biomass yields are taken from Johnson *et al.* [36]. Furthermore, the systems are only carbon substrate limited, pulsed with acetate at the start of the cycle (t=0h), and 50% of the reactor content is exchanged with new medium at the end of the cycle.

BIOMASS AND PHB PRODUCTION DURING THE FEAST PHASE

An approximation of the amounts of catalytic biomass and storage polymers that are produced during the feast phase can be made, based on the oxygen consumption and carbon dioxide production during the feast phase. The three biological processes involving acetate uptake during the feast phase are: biomass production, storage polymer production, and cellular respiration. The stoichiometries are taken from Johnson *et al.* [36] and given below.

$$Biomass: \quad -2.05Ac - O_2 + 1X + 1.05CO_2 \qquad [C-mol] \tag{2.13a}$$

$$PHB: \quad -3Ac - 0.75O_2 + 2PHB + 1CO_2 \qquad [C-mol] \tag{2.13b}$$

$$Respiration: \quad -1Ac - 1O_2 + 1CO_2 \qquad [C-mol] \tag{2.13c}$$

By combining these stoichiometries in the electron and carbon balance we can derive an analytical expression for the amounts of biomass and PHB that are produced during the feast phase. Simplified derivations are shown below, where the contribution of respiration is neglected during the short feast phase.

$$X_{new}: \quad \frac{M_{O_2,feast} - 0.25 \cdot M_{Ac,0}}{1 - 0.25 \cdot 2.05} \qquad [C-mol] \tag{2.14a}$$

$$PHB_{new}: \quad \frac{2}{3} \cdot \frac{M_{Ac,0} - 2.05 \cdot M_{O_2,feast}}{1 - 0.25 \cdot 2.05} \qquad [C-mol] \tag{2.14b}$$

These equations (2.14) demonstrate that the oxygen consumed in the feast phase can be used to give a direct insight in the prevalence of storage polymer production for each cycle. Analogues equations can be derived for total carbon dioxide. Here, the change in the respiration rate (e.g. OUR profile) is not yet taken into account, this is important because different profiles can yield similar total respirations. Therefore, more insights in biological functionalities could be derived by reconstructing the full compound profiles.

COMPOUND PROFILES

To reconstruct the compound profiles throughout the whole cycle we can make use of the biological process model of Johnson *et al.* [36]. This model takes as input off-line measurements of acetate, ammonium, biomass, and PHB, and combines them with on-line oxygen and carbon dioxide measurements. That model focuses on data reconciliation to derive kinetic parameters. We use the same model, but solely based on the on-line measurements to determine the acetate, ammonium, biomass, and PHB profiles. The frequency and resolution of our measurements do not allow for the determination of affinity constants, but do allow for the determination of dominant compound profiles. Additionally, it serves as a verification tool for off-line measurements.

The model requires initial estimates for the compound amounts, which are derived from the respiration measurements when combined with the principle assumptions described above. The initial amount of biomass in carbon-mol ($M_{X,0}$) can be estimated from the total carbon dioxide production, the dosed acetate ($M_{Ac,dosed}$), and applied exchange ratio (f_{ER}). This also gives an estimate for the initial amount of ammonium, by assuming a fixed catalytic biomass composition (Y_{NX} = 0.2 N-mol / C-mol), and known amount of dosed ammonium ($M_{NH4,dosed}$).

$$M_{Ac,0} = M_{Ac,dosed} \qquad [C-mol] \tag{2.15a}$$

$$M_{X,0} = (M_{Ac,0} - M_{CO2,out}) \cdot \left(\frac{1}{f_{ER}} - 1\right) \qquad [C-mol] \tag{2.15b}$$

$$M_{NH4,0} = \frac{M_{NH4,dosed}}{f_{ER}} - Y_{NX} \cdot M_{X,0} \qquad [N-mol] \tag{2.15c}$$

$$M_{PHB,0} = 0 \qquad [C-mol] \tag{2.15d}$$

With these initial estimates and the respiration profiles the compound profiles are constructed from which estimates for biomass specific rates follow in the kinetic and stoichiometric PHB model of Johnson *et al.* [36], but now solely based on on-line measurements.

2.3. RESULTS

A microbial enrichment was established from activated sludge in an aerobic sequencing batch reactor, characterized by the supply of the limiting carbon substrate (acetate) at the beginning of every 12-hour cycle [35]. Over a period of 200 cycles the functional performance of the bioreactor was characterized by on-line measurements. High frequency off-gas measurements were used to reconstruct the biological respiration rates through a physicochemical model and a particle filter. Reconstructions of two cycles with distinct functional performance are shown in Figure 2.10 and Figure 2.11.

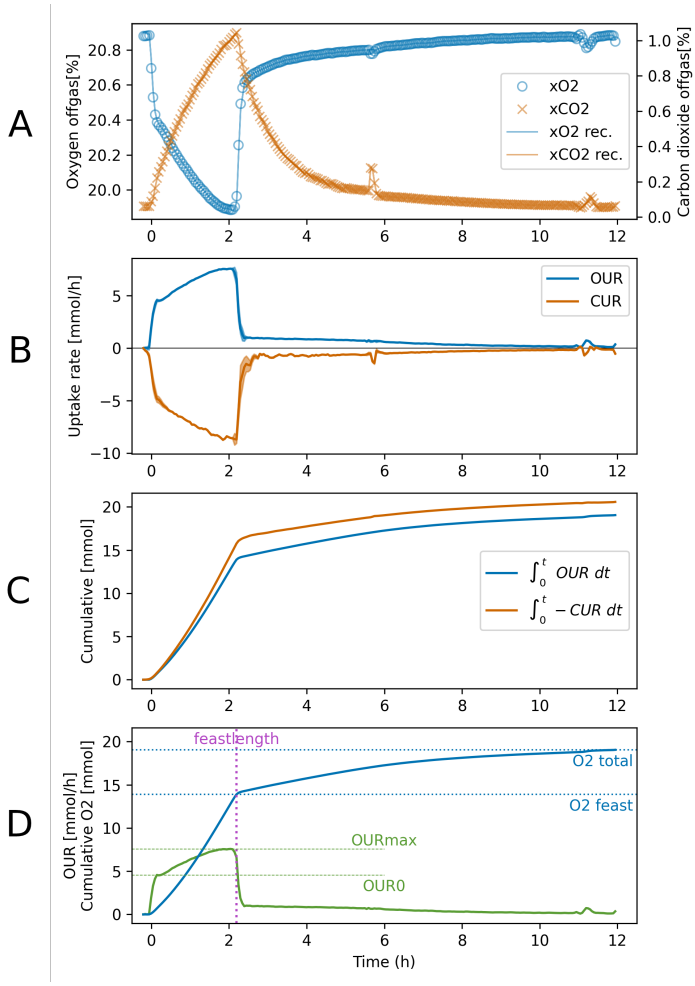

Figure 2.10: Reconstruction of microbial respiration rates from on-line measurements in a pulse-fed sequencing batch bioreactor exhibiting predominant growth and partial storage polymer production as response to the acetate pulse at t = 0 h. Figure A shows the off-gas measurements as symbols and the reconstructed off-gas profiles as continuous lines. Figure B shows the reconstructed respiration rates, where the line-widths represent the 95% confidence interval. Figure C shows the cumulative oxygen consumption and carbon dioxide production. Figure D shows the key indicators that were derived from the on-line data.

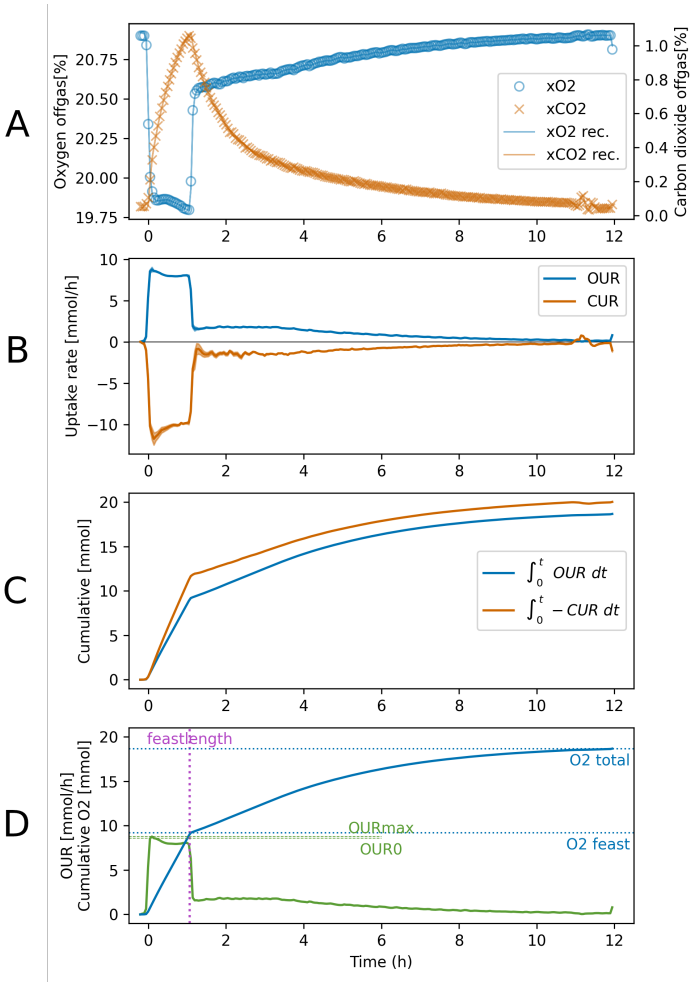

Figure 2.11: Reconstruction of microbial respiration rates from on-line measurements in a pulse-fed sequencing batch bioreactor exhibiting predominant storage polymer production as response to the acetate pulse at t = 0 h. Figure A shows the off-gas measurements as symbols and the reconstructed off-gas profiles as continuous lines. Figure B shows the reconstructed respiration rates, where the line-widths represent the 95% confidence interval. Figure C shows the cumulative oxygen consumption and carbon dioxide production. Figure D shows the key indicators that were derived from the on-line data.

2.3.1. FUNCTIONALITY DEVELOPMENT OVER TIME.

By processing the on-line data of 200 cycles and calculating the key functionality indicators for each cycle (sub-figures D in Figure 2.10 and Figure 2.11) it becomes possible to observe shifts in functionality over time (Figure 2.12). The observed shifts were verified with off-line measurements of PHB, microscopy, and microbial community composition through 16S rRNA gene sequencing. For an in depth analysis of the correlation between functionality and community developments and how they are influenced by temperature see chapter 3 and Stouten *et al.* [35].

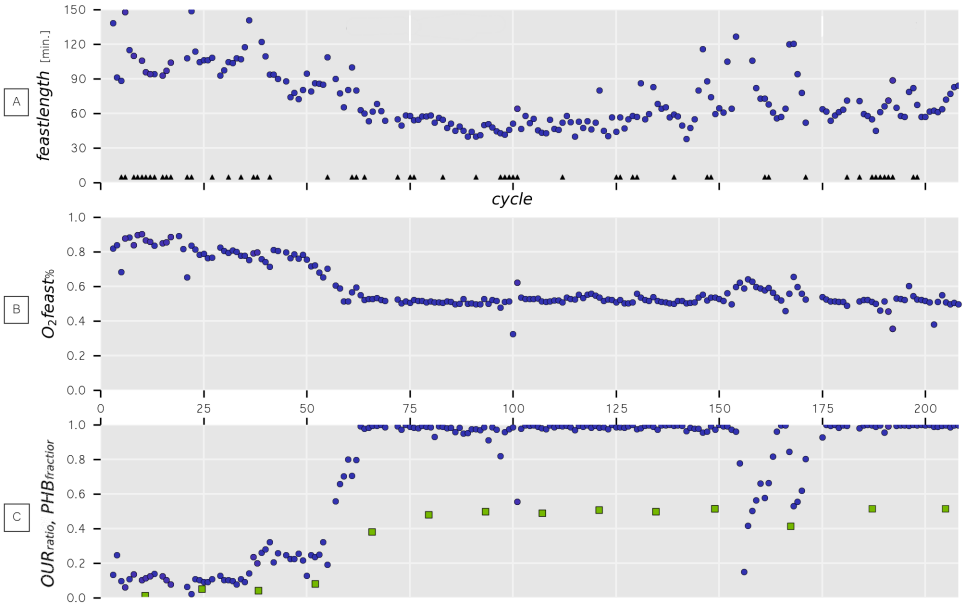

Figure 2.12: Overview of key functionality indicators over 208 enrichment cycles. Characteristic values (feast length, O_2feast%, and OUR_{ratio}). Also shown is the intermittently off-line measured PHB fraction (g_{PHB}/g_{VSS}) at the end of the feast phase (solid green squares). Clearly visible are the functional transition between cycle 50 and 62, the upsets between cycle 150 and 175, and the overall stability of the enrichment.

2.3.2. SYSTEM CHARACTERIZATION: COMPOUND PROFILES

The reconstructed respiration rates, combined with key indicators (Figure 2.10 and Figure 2.11) are used as input in the kinetic and stoichiometric biological model of Johnson *et al.* [36] to approximate the compound profiles of acetate, biomass, PHB, and ammonium. In Figure 2.13 the reconstructed profiles are shown and compared with off-line measurements. The reconstructed compound profiles during the feast phase closely match the off-line measurements. During the famine phase a distinct difference is shown for the predicted PHB and biomass profiles and measurements. The final modeled biomass at the end of the cycle does match the measurements. With the stoichiometric growth reaction on PHB present in the model, the PHB consumption profile from the off-line measurements cannot be achieved without a significant deviation from the reconstructed respiration profiles. In general, the model is able to clearly represent the compound profiles, and thereby also gives insights in biological rates. It should be noted that the biological rates as represented by the model (Figure 2.13C) reflect all biomass as if the community is composed of a single species that exhibits the same behavior.

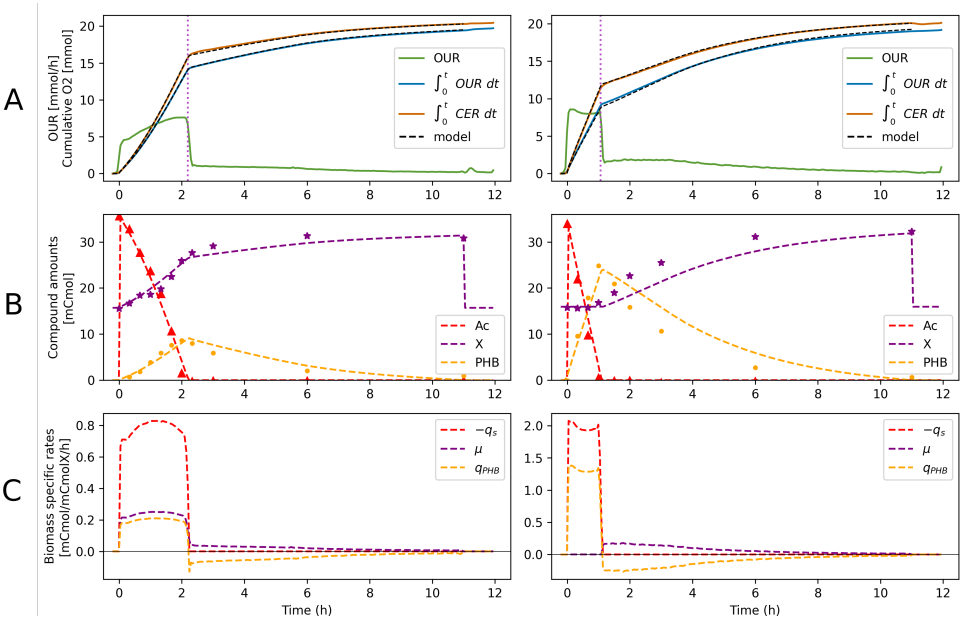

Figure 2.13: Reconstruction of compound profiles based on on-line data for two cycles during the enrichment of PHB producing microbial communities. On the left is shown the cycle from Figure 2.10 which reaches a maximum PHB content of 25 wt%, on the right the cycle from Figure 2.11 is shown, reaching a maximum PHB content of 55 wt%. Figure A shows the reconstructed oxygen uptake rate, cumulative oxygen consumption, and carbon dioxide production. The dashed lines overlapping the cumulative data indicate the modeled compound profiles for oxygen and carbon dioxide. Figure B shows the modeled compound profiles for acetate, biomass, and PHB - all based solely on on-line measurements. Also shown are off-line measurements as symbols. Figure C shows the on-line characterized biological rates for acetate uptake (q_s), biomass production (μ), and PHB production and consumption (q_{PHB}).

2.4. DISCUSSION

2.4.1. GENERAL APPLICABILITY.

The main objective of this study was to develop a parallel cultivation platform and the analytical tools to facilitate data processing during research with dynamically operated bioreactors. The eight identical bioreactor setups were equipped with a wide range of controls to allow mimicking and imposing exact environmental selection pressures. High-resolution off-gas measurements through mass spectrometry allow for non interfering monitoring of system dynamics. The off-gas signal is a convolution of the bioprocess gas uptake rates and several physicochemical processes. The developed Particle Filter model proved valuable in the reconstruction of actual respiration rates based solely on on-line off-gas measurements (Figure 2.10 and Figure 2.11). The purpose of the Particle Filter is demonstrated by reconstructing the respiration rates in an aerobic, pulse-fed bioreactor throughout a cultivation period of 100 days. The resulting reconstruction of the respiration rates made it possible to identify moments where the dominant metabolic functionality of the microbial community changed (Figure 2.12). These characterizations were used to correlate changes in community composition with changes in observed bioreactor performance (see chapter 3 and Stouten *et al.* [35]).

The Particle Filter implementation demonstrated here, was used to reconstruct the respiration rates in a wide range of dynamically operated bioreactors, varying from aerobic pulse-fed bioreactors [35], anaerobic bubble columns [38], anoxic N_2O respiration [39], aerobic/anaerobic fermentations [40], isotope labeled studies for identification of novel pathways [41], and in chain elongation studies [42]. The applicability of this reconstruction tool contributes to the identification of functional properties of biological processes in dynamic environments. It furthermore enables the identification of process instabilities (Figure 2.12) which are typically associated with operational irregularities, but in this case can directly be attributed to biological dynamics.

In future work, the tool can be used for improved experimental design of dynamically operated bioreactors, including periodic disturbance experiments, design of real-time system response as process triggers, and eventually enables improved process model calibration and identification of parameter values and their sensitivity.

2.4.2. PERFORMANCE OF THE SUGGESTED APPROACH IN PULSE-FED AEROBIC BIOREACTOR SYSTEM.

In the pulse-fed aerobic bioreactor system investigated in this work three performance indicators (feastlength, $O2_{feast}$%, and OUR_{ratio}) were identified that allow for monitoring of the system development in time. These identifications were based on minimal knowledge of the biological processes in the system. No process yields, nor reaction stoichiometries were required to identify periods where transitions in the dominant metabolic functionality occurred. The validity of the automated on-line performance indicators was assessed by manual off-line cycle measurements, where samples from the reactor broth were analyzed for biomass, acetate, ammonium, and PHB contents. The data from these cycle measurements shows high agreement with the identified respiration rates (Figure 2.13). These observed relationships allowed the indirect assessment of PHB productivity throughout the enrichment (Figure 2.12), solely based on on-line data.

For the pulse-fed system described here, a kinetic process model is available that determines affinity constants and biomass specific rates for acetate uptake, PHB production, biomass growth, and maintenance [36]. That model predominantly utilizes data collected off-line during cycle measurements, data from on-line off-gas measurements are assigned a low contributing weight (<10% relative to liquid measurements) during parameter fitting. This could be explained by the significant difficulty of incorporating on-line data of dynamic processes. Their less detailed physicochemical model of the bioreactor make it difficult to consolidate the on-line and off-line measurements, therefore the off-gas measurements were not in agreement with the modeled off-gas values. Furthermore, their kinetic process model describes the observed processes by a single set of stoichiometric and kinetic parameters. With the improved confidence in the reconstructed respiration data from the Particle Filter, new insights in the microbial functionality could be achieved. For example, the results in Figure 2.13 suggest that the biomass growth on PHB during the famine phase consists of at least two distinct processes, i.e.: the uptake of ammonium, and the cellular growth, including division. This distinction of PHB as carbon source (building block) and as energy source is shown in Figure 2.13, where the PHB consumption rate based on respiration data is lower than what is measured off-line. If both measurements are to be trusted, less PHB is respired in the early stage of the famine phase than is assumed to be necessary for growth, as described by the stoichiometries of the model. This increased confidence in reconstructed respiration profiles can thereby assist in our understanding of biological systems.

Off-line sampling strategies for the monitoring of enrichment systems and development of community characteristics over time are exceptionally laborious, even more so for dynamically operated systems. The Particle Filter combined with a process model allows for high resolution system characterization, but with a reduced parameter estimation compared to off-line measurements. The Particle Filter can be utilized for any biological system where the respiration data reflects the biological processes. In future work, the Particle Filter may be extended with detailed process models involving different microbial functionalities, and variable abundance of microorganisms, thereby attempting to model microbial ecosystem development, which in turn can be linked with molecular data on the development of the microbial community in the process [35].

2.4.3. LIMITATIONS AND EXTENSIONS OF THE PARTICLE FILTER AND PHYSICOCHEMICAL MODEL.

The Particle Filter will result in respiration profiles that best fit the measured off-gas concentrations and the dynamics as imposed by the process variance. Without any additional knowledge of the system this can result in periods where biologically unlikely uptake rates are modeled, for example carbon dioxide fixation and oxygen production in heterotrophic systems. Such behavior shows up in the Particle Filter when fast changes of the system are not covered by the process variance and number of particles, for example at the exact moment of the substrate pulse, or at the depletion of substrate. This behavior requires an adjustment to the process variance parameter (w_k). The predication uncertainty increases when the underlying biological process changes faster than is covered by the process variance and off-gas measurement frequency. The rapid change in carbon dioxide production and oxygen consumption at the start and end of the feast-

phase often falls between two measurements, this leads to an inherent uncertainty as shown in Figure 2.10B and Figure 2.11B.

By allowing a larger process variance, the Particle Filter can respond to these fast changes, but will also more closely follow the off-gas measurements, resulting in a more jagged prediction of the OUR and CUR during periods with smooth transitions, as more prediction emphasis will come from the measurement variance. This is seen in the initial period of the famine phase, where some oscillations are seen in the carbon dioxide production rates. Determining the appropriate variances requires understanding of the biological process and measurement equipment. More frequent off-gas measurements assist the model as less variance builds up between two consecutive measurements.

EXTENDING AND ADAPTING THE MODEL

Generally, the model predictions improve when additional independent measurements are available [43]. One on-line measurement that is often available in aerobic bioreactors, but was not used in this model, is the dissolved oxygen (DO) concentration, which yields fast-responding continuous measurements, but suffers from signal drift, nonlinear probe dynamics, and loss in linearity due to fouling [44]. de Jonge *et al.* [20] encountered DO related issues where, even in their experiments that lasted a couple of hours and involved rigorous calibrations, the DO probe data could not be used to improve the model performance. In the Supplementary Materials 2.6.2 a variance smoothing algorithm is described which allows the high frequency, but possibly inaccurate, DO measurement to improve the predictions by utilizing the first order derivative of the dissolved oxygen measurement as virtual measurement. This measurement is used to scale the process variance, allowing the system to respond quickly and timely in periods with fast dynamics. This approach is only viable for aerobic systems, or for analogous probes that measure concentrations in the reactor broth. This addition to the Particle Filter demonstrates a significant benefit of this approach, compared to the more math heavy solutions of for example Farza *et al.* [13] and Oliveira *et al.* [14]; i.e.: the relative ease by which the algorithm can be extended to new sensors, as well as adjusted to different bioreactor configurations and biological processes.

INITIAL STATE ESTIMATION

The initial state of the system is estimated by allowing N particles to assume uptake rates uniformly distributed around likely system states. By including more measurements before a system disturbance, the Particle Filter automatically converges towards the likely system state, and therefore the modeled uptake rates up to that point are prone to errors and should be discarded. The slowest convergence takes place for the hydrated carbon dioxide, especially at higher pH. Improved initial state predictions are produced by moving the start of state estimation backwards in time, if the dataset allows this, but it could also be derived mathematically by running the model backwards in time (not implemented here) [20]. Other issues with the Particle Filter arise when additional processes take place beside biological. For example the exchange of a significant fraction of the broth with new medium can run into reconstruction issues, due to the unknowns of the new medium like temperature, pH, and the dissolved gas concentrations before it is added to the reactor. This is especially pronounced when reactor broth with a high

carbonate concentration is exchanged for medium that is kept fully anaerobic by sparging it with nitrogen gas, and therefore has a low carbonate concentration. Wrongful or missing physical processes will translate in changes in off-gas measurements, which will erroneously be contributed to biological activity. Figure 2.11B shows this behavior to a minimal extent during the liquid exchange at t=11h. Generally, these events are easily spotted and corrected for by visual inspection of the reconstructed respiration rates.

IMPROVED EXPERIMENTAL DESIGN

The Particle Filter developed is a convenient tool for analyzing dynamically operated bioreactors and investigating the biological responses to the imposed dynamics, but it also allows optimizing the operational parameters of a cultivation to maximize the reconstruction resolution of the respiration rates. For example, by allowing the controlling system to adjust the gas flowrate of the cultivation it is possible to reconstruct respiration rates at high precision during phases with high and low respiration, without running into mass transfer limitations (examples are included in the Supplementary Materials 2.6.4). The resulting dataset can then only be processed with a model as proposed here as an additional convolution is added to the off-gas signal.

Overall, the Particle Filter allows biotechnology researchers that focus on microbial cultivations to extend their research tools by facilitating reconstruction and interpretation of biological respiration rates with little effort. Researchers with specific and detailed interest in dynamic cultivations should be able to adapt the proposed model with kinetic models and additional on-line analysis that are available to them.

2.5. CONCLUSION

A generalized respiration rate reconstruction tool is developed for dynamic operated bioreactors, based on the Particle Filter method. The reconstructed respiration rates are a direct reflection of biological activity in the bioreactor, and can be used to characterize the system developments over time. As a specific example, the functional characterization of a pulse fed bioreactor throughout an enrichment of 100 days was achieved solely based on on-line data. This allowed for the identification of shifts in the dominant metabolic processes without prior knowledge or additional off-line measurements of the system. Furthermore, the general model was able to reconstruct the respiration rates in many differently operated sequencing batch bioreactors. This tool increases the information density of on-line measurements as it enables the identification of specific process properties that define the development in time of the process. This paves the way for future implementations where the development in time of the microbial community structure and the functional performance can be linked at high resolution providing crucial insights in the factors that shape the microbial world

ACKNOWLEDGEMENTS

We gratefully acknowledge financial support from the Netherlands Organization for Scientific Research (NWO) funded UNLOCK project (NRGWI.obrug.2018.005) and the company Paques B.V. (Paques Partnership Program project 13002).

2.6. SUPPLEMENTARY MATERIALS

2.6.1. PARTICLE FILTER IMPLEMENTATION

The implementation of the Particle Filter, physicochemical model, and data pruning are included in the on-line code repository at: https://github.com/GRS-TUD/d2i, including data examples. What follows is a construction of the most important steps of the general implementation, which are useful for custom implementations and extensions. The reconstruction of the respiration rates occurs through the use of a Particle Filter. The idea behind the Particle Filter is to perform a set of Monte Carlo simulations in parallel, and then to perform Bayesian inference on the predicted system state and the available measurements. If the number of particles is large, and the model that describes the system is accurate, it becomes possible to identify hidden (non-measured / non-measurable) states. In most microbial cultivations one of those hidden states is the respiration rate of the microorganisms. The available measurement is relatively far removed from this state in the form of off-gas measurements (see section 2.2.2).

For example: oxygen is taken up by microorganism from the liquid broth at a specific rate (UR_{O_2} mol L^{-1} s^{-1}), this causes a decrease in total dissolved oxygen (c_{l,O_2}). The rate of gas exchange between the bubbles and the liquid depends on gas transfer coefficient ($k_L a_{O_2}$) and the difference of concentration in the liquid and partial pressure of oxygen in the bubbles (x_{b,O_2}), corrected for the Henry coefficient (H_{O_2}). The concentration in the gas bubbles depends on the inflow gas rate (F_{in}, dry air), the head space recycling gas rate (F_{rec}), and their relative compositions (x_{in,O_2} and x_{h,O_2}). The exchange of gas molecules between the bubbles and the liquid changes the molar gas flow from bubbles going in (F_{in} + F_{rec}) and coming out of the liquid (F_{b2h}). The gas coming from the bubbles mixes with the gas in the head space. The system is kept at operation pressure (P), which requires a net gas outflow from the reactor to the off-gas measurement equipment. To that end the gas is dried (P_w), and the gas composition is measured.

Comparable processes occur for all gaseous compounds that are consumed or produced in a bioreactor. And because all gasses affect the relative concentration of the other gasses, the reconstruction needs to take all gasses into account - including gasses that do no partake in biological processes in the system. Two additional significant complications arise due to carbon dioxide speciation, where a significant fraction of CO_2 is dissolved in the liquid as carbonates. The second complication is caused by the system dynamics, where either physical processes, like liquid exchange, environmental change (pH, temperature, pressure), gas change, or biological processes, like changing metabolisms, response to disturbances, or succession are causing rapid and slow changes in the measurements. If all physicochemical processes are taken into account, then all changes that remain can be ascribed to changes in biological rates. And such is the goal of the Particle Filter with physicochemical model as described in this work. Below follows the implementation of the Particle Filter, where the physicochemical aspect is covered in the main text.

(Particles) Let P = $[p_{ij}]$ be a matrix of size v × N (i.e., N represents the number of particles and v represents the number of states of the system and is equal to $(4 \cdot w + 1)$, with w the number of gas compounds of interest). For each gas the states include an uptake rate, concentration in the liquid, fraction in the bubbles, and fraction in the head space (i.e.,

total of 4 states per gas compound). One additional system state is required to describe all hydrated carbon dioxide species.

(Initial state) Let D = $[d_{pq}]$ be a matrix of size w × M (i.e., w represents the number of gas compounds measured by the off-gas analysis, and M the number of independent measurements. The initial state estimate assumes equilibria between the head space, bubbles, and liquid phase (equilibrium calculations based on environmental conditions and Henry coefficients), this populates P from p_{iw} onwards. All particles can start with identical state estimates, or an exception can be made for the uptake rates. The initial uptake rates p_{i0} till p_{iw}, then need to be picked uniformly between a ceiling and floor vectors of size w. This process improves the calculation time until a proper estimate of the uptake rates is achieved. The time t_k is set to the time of the initial measurement t_0.

(Uptake Rate covariance) Let U be a matrix of size w × w (i.e., often a diagonal matrix of the rate by which the uptake rates can change per time step). This covariance matrix determines the average variation that occurs each time step for the uptake rates. When elements are set to 0, the uptake rates will remain constant throughout the modeling, larger values allow for more disperse particles. If relationships exist between gas compounds (e.g. oxygen and carbon dioxide in heterotrophic systems, they can be included in de covariance matrix as it restrict the creation of unlikely system states). The determination of the covariance matrix values requires feeling for the system that is modelled.

$$p_{i,0..w} = p_{i,0..w} + \mathcal{N}(0, U_k)) \tag{2.16}$$

The uptake rates in the particle filter states are updated after each calculation step with a normally distributed random value based on the uptake rate covariance matrix U. The values of the covariance matrix can also be made dependent on time (k), as we will see in section 2.6.2. Additional checks can be included that limit the range of the uptake rates, e.g.: only positive or negative uptake rates for specific gas compounds. But particles that show biologically impossible behavior will easily be removed in the resampling step. Therefore no specific knowledge of the biological conversions is required at the expense of additional computational calculations.

(Predict) For each measurement m from 0...M we retrieve the time stamp and calculate the number of prediction cycles that have to be completed before a new measurement is available (i.e., from t_k till t_n). During each prediction step (of 1 second) one full iteration of the physicochemical model is made on P, which yields predictions for each particle, based on its current system state. After each model step, the uptake rate states in P are allowed to vary according to the Uptake Rate covariance matrix. This process is repeated until the next measurement is available, if measurements are sparse the predictions of the particles will vary significantly.

(Measurement covariance) Let R be a matrix of size w × w (i.e., a diagonal matrix of the variance of the standard error of the measurement equipment). This matrix is relatively easy to construct but might be subject to change if the equipment results in different errors depending on the relative or absolute nature of the error. Most off-gas analyzers cannot measure well at both low and high percentages of the same gas, given the same

calibration. Any knowledge on expected measurement variance is included in the model through the measurement covariance matrix R.

(Update) After all predictions between two measurements have been completed, the predicted state estimates are compared to the real measurements. The state estimates contain a prediction for the head space gas fraction, predictions that are close to the measured values are more likely to be correct. The distance between the measured and predicted values is expressed as the likelihood that the predication occurred given the uncertainty of the measurement covariance matrix R. To this end the probability density function (PDF) for a normal continuous random variable is used.

$$f(x) = \frac{e^{-x^2/2}}{\sqrt{2\pi}} \tag{2.17}$$

If many prediction steps exist between to measurement, and multiple gas compounds need to be modeled, it is likely that a large fraction or all of the predictions are very far removed from the measurements. From a computational point of view we therefore make use of the logarithmic PDF, as it allows for a wider coverage in uncertain areas (300 orders of magnitude). Each particle has a weight attributed to it (W of size N), which represents how likely this particle is to be the real representation of system state. The weights are updated with the new PDF and the total is normalized to 1.

$$W_{k+1} = \frac{W_k \cdot PDF_{k+1}}{\sum W_k \cdot PDF_{k+1}} \tag{2.18}$$

(Estimate) The updated weights are used to make an estimate of the current system state by taking a weighted average of the particles. Also the weighted variance of the estimate can be calculated in an analogous fashion. These estimates represent the mathematically best prediction of the system states.

(Resample) Importantly, an ever increasing fraction of the particles is assuming system states that are far removed from the likely states. Resampling is required to stop needless calculations and to improve next predictions by utilizing the unlikely particles as copies of more likely particles. The resampling threshold and resampling method allow for control on this process. Here we chose to implement the systematic resampling algorithm which yields new particles proportional to their weight. After the resampling step several copies of a particle exist, but after the prediction step they are all updated with a different variance in their uptake rate estimates, which allows for a finer scanning around the current best system state estimates.

(Environmental triggers) The physicochemical model needs to take into account all imposed changes that occur throughout a cycle, as they are likely to affect the measurements. If these imposed changes are not modelled well they will skew the reconstruction of the respiration rates. To this end, several (time) triggers can be included in the model that allow for changes in environmental parameters (e.g., reactor volumes, liquid exchange (including dissolved gasses), gas flows, in-gas composition, ionic strength). Parameters depending on temperature, pressure, and ionic strength are automatically adjusted (e.g.: Henry coefficients, kLa, and activity coefficients). These time triggers can

also be used to dynamically change the Uptake Rate covariance matrix U, or measurement covariance matrix R, based on system specific knowledge.

2.6.2. ADDING DO MEASUREMENT TO PARTICLE FILTER

A straightforward implementation of the DO probe in the Particle Filter would be to use it as measurement of c_{l,O_2}. The DO measurement is available at each prediction step, and could therefore yield significant improvements to the estimates of the particles, as they can be steered over 100 times more often than only based on off-gas measurements. The downside of the DO probe is that it is susceptible to signal drift and loss in linearity, especially in longer cultivations and under dynamic conditions. Therefore, if the DO measurements are included, even with significant large error margins in the measurement covariance matrix R, it will have a tendency to pull the particles towards its erroneous representation of c_{l,O_2}. This behavior is observed in state estimation filters when precise measurements, with variable accuracy, are included.

Alternatively the precision and frequency of the DO measurements can be used as environmental input to dictate the Uptake Rate covariance matrix U for each time point. In periods where the DO measurements do not change ($dDO/dt \approx 0$), it is also more likely that the respiration rates change little. And during periods with strong changes in DO, the direction of the change can be used to indicate an proportional increase or decrease in oxygen respiration rates. By combining the Ramer-Douglas-Peucker algorithm (Supplementary Materials 2.6.3), or a general signal smoothing algorithm, the DO data can be used to improve the respiration rate reconstructions to dynamics occurring at 5 to 10 second resolution. Investigations where cultivations are exposed to stronger dynamics are required to verify the reconstructed rates.

The relationship between U_k and the rate of change in the dissolved oxygen concentration is mechanistically linear. Yet, with respect to the Particle Filter it is always preferable to allow some variance in the uptake rate kinetics.

$$U_k = U \cdot \frac{a \cdot b + \left|\frac{dDO}{dt_k}\right|}{a + \left|\frac{dDO}{dt_k}\right|} \tag{2.19}$$

Saturation curve with half saturation parameter a and offset parameter b, which prevents U_k from becoming 0.

2.6.3. DETERMINATION OF THE FEAST-LENGTH

We determined the end of the feast phase based on the inflection points of the OUR, CER, and the on-line measured dissolved oxygen (DO) profile. In several rapid sampling experiments we measured the acetate profiles of different reactors. Interestingly, the DO plots, and off-gas profiles during intense sampling look significantly different from undisturbed cycles. This is likely caused by the interference from sampling, and the decreasing reactor volume.

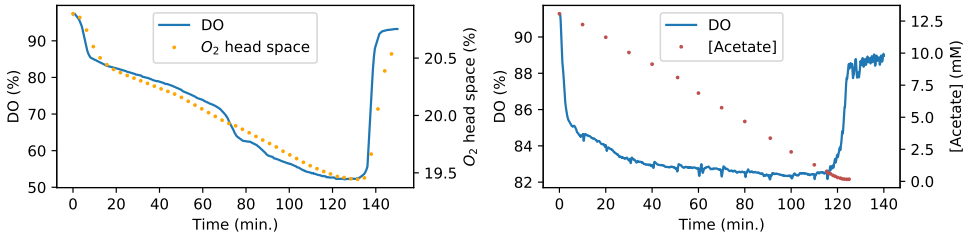

Figure 2.14: DO and O_2 concentration in the head space of an undisturbed feast famine reactor after a pulse at t=0 (left), and the acetate and DO profiles during the following operation cycle. Difference in DO profiles between the two cycles likely results from sampling, and decreasing reactor volume, as the following (undisturbed) cycle more closely represents the left figure (not shown).

Figure 2.14 left, shows a typical oxygen and DO profile associated with a growing culture. A clear deflection point is visible around t=140 where the respiration peaks and quickly decreases. This point is correlated with low extracellular acetate concentrations (right), followed by complete consumption of acetate. Comparable graphs and data were collected for reactors that exhibited the typical hoarding strategy, and of cultures exhibiting partial growth and hoarding characteristics. From these measurements we could derive and verify a mathematical definition for the feast phase length.

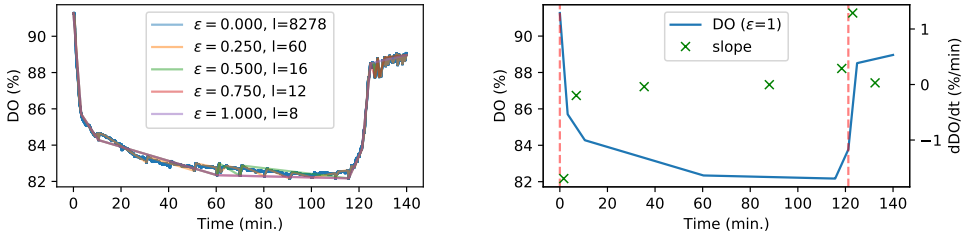

Figure 2.15: Identification of significant time points from the original DO dataset with the Ramer-Douglas-Peucker algorithm. It allows for a close estimate of the beginning and end of the feast phase (dashed red lines) by selecting the fragments with the minimum and maximum slope (green x).

The DO dataset contains a measurement every second, these 8400 data points (140 min.) together describe the right DO curve in Figure 2.14. The Ramer-Douglas-Peucker algorithm [37] can be used to reduce the number of points while still capturing the shape of the curve. The algorithm requires one fitting parameter ϵ which is the maximum distance any data point can have from the approximated curve. In Figure 2.15 left, the over-

lapping RDP curves are plotted with 5 different values for ϵ. In this manner, it becomes possible to identify important points; the original curve can for example be approximated by 8 data points, given that all other points are within 1 DO %. And alternatively, an ϵ of 0.25 allows for easy identification of all sampling points. In either case, the end of the feast phase most closely correlates with the section with the steepest slope (Figure 2.15 right).

Analogue calculations can be made for the reconstructed OUR and CER, which are based on less frequent, but independent, off-gas measurements. And in most dynamic systems, the same approach can be used for acid or base titration data, or gradual shifts in pH within the dead band of pH controlled reactors.

2.6.4. INCREASE OFF-GAS MEASUREMENT RESOLUTION

To improve the reconstruction accuracy a significant change in gas composition of in-gas and off-gas is beneficial. A lower gas inflow rate results in a stronger change, but also comes at the cost of a stronger delay and convolution of respiration dynamics. Additionally, a different gas inflow rate also changes the partial pressures of the gasses, which can lead to significant changes in the speciation of compounds, and even to limitations. The conflicting requirements regarding improved off-gas signal and capturing of process dynamics, preferably without disturbing the system must be considered during experimental design.

By allowing for changing gas inflow rates, the resulting off-gas signal becomes exceptionally more difficult to interpret without a physicochemical model. The proposed model in this work allows for experimental design with changing flow rates, and changing in-gas compositions. In Figure 2.16 an example is shown where during the famine phase of a feast-famine system little respiration activity is taking place compared to during the feast phase. This results in a strong limitation on the ability to reconstruct the biological respiration rates as the off-gas signal comes within the measurement uncertainty of the equipment. By reducing the gas inflow rate instantaneous after 5 hours of cultivation, the signal is 'amplified' and reconstruction is possible with higher fidelity. Naturally, more complex and more autonomous changes are possible regarding the in-gas flow and composition.

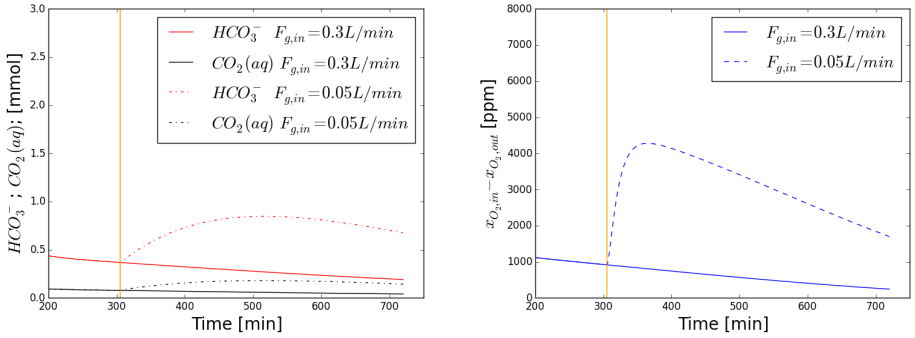

Figure 2.16: Simulation of the liquid CO_2 and HCO_3^-, and the gas phase O_2 profiles; with constant and adapted gas inflow rates. The orange line indicates where the flow rate is changed from 300 to 50 mL min^{-1}.

REFERENCES

[1] G. R. Stouten, S. Douwenga, C. Hogendoorn, and R. Kleerebezem, *System characterization of dynamic biological cultivations through improved data analysis,* bioRxiv (2021), 10.1101/2021.05.14.442977.

[2] M. W. Beijerinck, *Fixation of free atmospheric nitrogen by Azotobacter in pure culture. Distribution of this bacterium,* Koninklijke Nederlandse Academie van Wetenschappen Proceedings **11**, p.67 (1908).

[3] S. N. Winogradsky, *über Schwefelbakterien,* Botanische Zeitung **45**, p.489 (1887).

[4] W. Grant and B. Tindall, *The isolation of alkalophilic bacteria.* in *Microbial Growth and Survival in Extremes of Environments.* (New York: Academic Press, London, 1980) pp. 27–36.

[5] T. D. Brock, *Life at High Temperatures: Evolutionary, ecological, and biochemical significance of organisms living in hot springs is discussed,* Science **158**, 1012 (1967).

[6] D. J. Brenner, N. R. Krieg, J. T. Staley, and G. M. Garrity, eds., *Bergey's Manual® of Systematic Bacteriology* (Springer US, Boston, MA, 2005).

[7] M. van Loosdrecht, G. Smolders, T. Kuba, and J. Heijnen, *Metabolism of microorganisms responsible for enhanced biological phosphorus removal from wastewater, Use of dynamic enrichment cultures,* Antonie van Leeuwenhoek **71**, 109 (1997).

[8] F. Carta, J. Beun, M. van Loosdrecht, and J. Heijnen, *Simultaneous storage and degradation of phb and glycogen in activated sludge cultures,* Water Research **35**, 2693 (2001).

[9] P. Van den Abbeele, C. Grootaert, M. Marzorati, S. Possemiers, W. Verstraete, P. Gerard, S. Rabot, A. Bruneau, S. El Aidy, M. Derrien, E. Zoetendal, M. Kleerebezem, H. Smidt, and T. Van de Wiele, *Microbial Community Development in a Dynamic Gut Model Is Reproducible, Colon Region Specific, and Selective for Bacteroidetes and Clostridium Cluster IX,* Applied and Environmental Microbiology **76**, 5237 (2010).

[10] P. R. Mooij, G. R. Stouten, J. Tamis, M. C. M. van Loosdrecht, and R. Kleerebezem, *Survival of the fattest,* Energy & Environmental Science **6**, 3404 (2013).

[11] M. Strous, J. J. Heijnen, J. G. Kuenen, and M. S. M. Jetten, *The sequencing batch reactor as a powerful tool for the study of slowly growing anaerobic ammonium-oxidizing microorganisms,* Applied Microbiology and Biotechnology **50**, 589 (1998).

[12] C.-F. Mandenius and R. Gustavsson, *Mini-review: Soft sensors as means for PAT in the manufacture of bio-therapeutics,* Journal of Chemical Technology & Biotechnology **90**, 215 (2015).

[13] M. Farza, H. Hammouri, C. Jallut, and J. Lieto, *State observation of a nonlinear system: Application to (bio)chemical processes,* AIChE Journal **45**, 93 (1999).

[14] R. Oliveira, E. C. Ferreira, and S. Feyo de Azevedo, *Stability, dynamics of convergence and tuning of observer-based kinetics estimators,* Journal of Process Control **12**, 311 (2002).

[15] J. Robles-Magdaleno, A. Rodríguez-Mata, M. Farza, and M. M'Saad, *A filtered high gain observer for a class of non uniformly observable systems – Application to a phytoplanktonic growth model,* Journal of Process Control **87**, 68 (2020).

[16] M. U. Estler, *Recursive on-line estimation of the specific growth rate from off-gas analysis for the adaptive control of fed-batch processes,* Bioprocess Engineering **12**, 205 (1995).

[17] S. Winckler, R. Krueger, T. Schnitzler, W. Zang, R. Fischer, and M. Biselli, *A sensitive monitoring system for mammalian cell cultivation processes: A PAT approach,* Bioprocess and Biosystems Engineering **37**, 901 (2014).

[18] I. Bouraoui, M. Farza, T. Ménard, R. Ben Abdennour, M. M'Saad, and H. Mosrati, *Observer design for a class of uncertain nonlinear systems with sampled outputs—Application to the estimation of kinetic rates in bioreactors,* Automatica **55**, 78 (2015).

[19] C. Tréangle, M. Farza, and M. M'Saad, *Observer design for a class of disturbed nonlinear systems with time-varying delayed outputs using mixed time-continuous and sampled measurements,* Automatica **107**, 231 (2019).

[20] L. de Jonge, J. Heijnen, and W. van Gulik, *Reconstruction of the oxygen uptake and carbon dioxide evolution rates of microbial cultures at near-neutral pH during highly dynamic conditions,* Biochemical Engineering Journal **83**, 42 (2014).

[21] J. Kager, C. Herwig, and I. V. Stelzer, *State estimation for a penicillin fed-batch process combining particle filtering methods with online and time delayed offline measurements,* Chemical Engineering Science **177**, 234 (2018).

[22] I. V. Stelzer, J. Kager, and C. Herwig, *Comparison of Particle Filter and Extended Kalman Filter Algorithms for Monitoring of Bioprocesses,* in *Computer Aided Chemical Engineering*, Vol. 40 (Elsevier, 2017) pp. 1483–1488.

[23] M. Ulusoy, *Understanding Kalman Filters,* https://mathworks.com/videos/series-/understanding-kalman-filters.html (2017).

[24] K. Johnson, Y. Jiang, R. Kleerebezem, G. Muyzer, and M. C. M. van Loosdrecht, *Enrichment of a Mixed Bacterial Culture with a High Polyhydroxyalkanoate Storage Capacity,* Biomacromolecules **10**, 670 (2009).

[25] Y. Jiang, D. Y. Sorokin, R. Kleerebezem, G. Muyzer, and M. van Loosdrecht, *Plasticicumulans acidivorans gen. nov., sp. nov., a polyhydroxyalkanoate-accumulating gammaproteobacterium from a sequencing-batch bioreactor,* International Journal of Systematic and Evolutionary Microbiology **61**, 2314 (2011).

[26] J. Tamis, K. Lužkov, Y. Jiang, M. C. van Loosdrecht, and R. Kleerebezem, *Enrichment of Plasticicumulans acidivorans at pilot-scale for PHA production on industrial wastewater,* Journal of Biotechnology **192**, 161 (2014).

[27] L. Marang, M. C. van Loosdrecht, and R. Kleerebezem, *Combining the enrichment and accumulation step in non-axenic PHA production: Cultivation of Plasticicumulans acidivorans at high volume exchange ratios,* Journal of Biotechnology **231**, 260 (2016).

[28] R. Douc, O. Cappé, and E. Moulines, *Comparison of Resampling Schemes for Particle Filtering,* arXiv:cs/0507025 (2005), arXiv:cs/0507025 .

[29] H. S. Harned and R. Davis, *The Ionization Constant of Carbonic Acid in Water and the Solubility of Carbon Dioxide in Water and Aqueous Salt Solutions from 0 to 50°,* Journal of the American Chemical Society **65**, 2030 (1943).

[30] H. S. Harned and S. R. Scholes, *The Ionization Constant of HCO3- from 0 to 50°,* Journal of the American Chemical Society **63**, 1706 (1941).

[31] X. Wang, W. Conway, R. Burns, N. McCann, and M. Maeder, *Comprehensive Study of the Hydration and Dehydration Reactions of Carbon Dioxide in Aqueous Solution,* The Journal of Physical Chemistry A **114**, 1734 (2010).

[32] I. Tinoco, *Diffusion-Controlled Reactions,* in *Physical Chemistry: Principles and Applications in Biological Sciences* (Pearson, Boston, MA., 2014) pp. 354–355.

[33] J. Kielland, *Individual Activity Coefficients of Ions in Aqueous Solutions,* Journal of the American Chemical Society **59**, 1675 (1937).

[34] W. V. Vishniac and M. Santer, *The thiobacilli,* Bacteriological reviews **21**, 195 (1957).

[35] G. R. Stouten, C. Hogendoorn, S. Douwenga, E. S. Kilias, G. Muyzer, and R. Kleerebezem, *Temperature as competitive strategy determining factor in pulse-fed aerobic bioreactors,* The ISME Journal (2019), 10.1038/s41396-019-0495-8.

[36] K. Johnson, R. Kleerebezem, and M. C. van Loosdrecht, *Model-based data evaluation of polyhydroxybutyrate producing mixed microbial cultures in aerobic sequencing batch and fed-batch reactors,* Biotechnology and Bioengineering **104**, 50 (2009).

[37] D. H. Douglas and T. K. Peucker, *Algorithms for the reduction of the number of points required to represent a digitiezed line or its caricature,* Cartographica: The International Journal for Geographic Information and Geovisualization **10**, 112 (1973).

[38] M. Mulders, A. Estevez-Alonso, G. R. Stouten, J. Tamis, M. Pronk, and R. Kleerebezem, *Volatile Fatty Acid Product Spectrum as a Function of the Solids Retention Time in an Anaerobic Granular Sludge Process,* Journal of Environmental Engineering **146**, 04020091 (2020).

[39] M. Conthe, C. Parchen, G. R. Stouten, R. Kleerebezem, and M. C. M. van Loosdrecht, *O2 versus N2O respiration in a continuous microbial enrichment,* Applied Microbiology and Biotechnology **102**, 8943 (2018).

[40] L. G. da Silva, S. Tomás-Martínez, M. C. van Loosdrecht, and S. A. Wahl, *The Environment Selects: Modeling Energy Allocation in Microbial Communities under Dynamic Environments*, Preprint (Systems Biology, 2019).

[41] L. C. Valk, M. Diender, G. R. Stouten, J. F. Petersen, P. H. Nielsen, M. S. Dueholm, J. T. Pronk, and M. C. M. van Loosdrecht, *"Candidatus Galacturonibacter soehngenii" Shows Acetogenic Catabolism of Galacturonic Acid but Lacks a Canonical Carbon Monoxide Dehydrogenase/Acetyl-CoA Synthase Complex,* Frontiers in Microbiology **11** (2020), 10.3389/fmicb.2020.00063.

[42] M. T. Allaart, G. R. Stouten, D. Z. Sousa, and R. Kleerebezem, *Product inhibition and pH affect stoichiometry and kinetics of chain elongating microbial communities in sequencing batch bioreactors.* Frontiers in Bioengineering and Biotechnology (2021 under review).

[43] T. Bayes and n. Price, *LII. An essay towards solving a problem in the doctrine of chances. By the late Rev. Mr. Bayes, F. R. S. communicated by Mr. Price, in a letter to John Canton, A. M. F. R. S,* Philosophical Transactions of the Royal Society of London **53**, 370 (1763).

[44] O. Samuelsson, A. Björk, J. Zambrano, and B. Carlsson, *Fault signatures and bias progression in dissolved oxygen sensors,* Water Science and Technology **78**, 1034 (2018).

3

TEMPERATURE AS COMPETITIVE STRATEGY DETERMINING FACTOR IN PULSE FED AEROBIC BIOREACTORS

Gerben Roelandt STOUTEN, Carmen HOGENDOORN, Sieze DOUWENGA, Estelle Silvia KILLIAS, Gerard MUYZER, Robbert KLEEREBEZEM

Exposing a microbial community to alternating absence and presence of carbon-substrate in aerobic conditions is an effective strategy for enrichment of storage polymers (polyhydroxybutyrate, PHB) producing microorganisms. In this work we investigate to which extent intermediate storage polymer production is a temperature independent microbial competition determining factor. Eight parallel bioreactors were operated in the temperature range of 20-40°C, but intermediate storage polymer production was only obtained at 25-35°C. Besides PHB production and consumption, cell decay and subsequent cryptic growth on lysis products was found to determine process properties and the microbial community structure at all operational temperatures. At 40°C decay processes cannot be overcome with additional energy from storage polymers, and fast-growing microorganisms dominate the system. At 20°C, highly competitive communities with ambiguous storage properties were enriched. The results described here demonstrate that a rigorous experimental approach could aid in the understanding of competitive strategies in microbial communities.

Parts of this chapter have been published as Stouten *et al.* [1].

3.1. INTRODUCTION

Natural microbial communities are complex biological matrices, that typically contain thousands of different types of microorganisms [2]. Understanding the ecological and evolutionary implications of this diversity is one of the central topics in Biology [3]. With the arrival of Next Generation Sequencing techniques, a wealth of genomic information is now available on the composition of microbial communities in both natural and man-made ecosystems. While the genotypical makeup of microbial communities can be well described, our knowledge of phenotypical aspects like biochemical functionality and interspecies dependencies is still wanting [4–7]. The changes in the microbial community composition is a key research topic in fields like environmental biotechnology, gut microbiology, and agricultural microbiology [8–10]. By using well-controlled bioreactors, the development of microbial community structure and functional properties can be investigated with more accurateness then by studying natural habitats. A profound limitation remains in the resolution of functional characterization, mostly due to the required sampling and analysis effort and its possible interference with bioreactor operation. Therefore, infrequent or limited description of the functional development often restricts the linking of community structure dynamics to changes in functionality, and is thereby a bottleneck in our understanding of microbial community development and succession in ecosystems upon exposure to different environmental conditions.

The ever-present microbial diversity is of specific importance in environmental biotechnological processes, such as resource recovery facilities, that rely on selective conditions to maintain stable process operations. Microbial ecology research in many cases aims for identifying the mechanisms driving changes in functionality [11, 12]. Functional changes are eventually reflected in the microbial community structure that establishes. An increased understanding of the relationship between the functional performance and microbial community structure will lead to improved microbial ecosystem understanding and enables improved process design and operation, and facilitate the development of novel microbial community-based processes. A significant contribution to this understanding will come from observation-based research where a single process condition is changed in a selective environment. By operating multiple parallel systems, microbial community related questions regarding inoculum, medium composition, reproducibility, and bioreactor operation can be addressed properly. While attempts to combine datasets from different studies to obtain a comprehensive understanding of the influence of process parameters on process performance are hampered by the fact that almost all studies are performed in a dissimilar way. The limitations in our understanding of microbial competition and coexistence should therefore benefit from more rigorous efforts to compare the structure and function development of a microbial community at specific selective conditions.

To enable this research intensification, a high-resolution system characterization platform has been developed. In a separate manuscript, system characterization by high resolution online data consolidation in dynamic systems is further expanded upon [13]. The study presented here shows an implementation of research intensification to investigate the influence of temperature on pulse-fed enrichments of bacteria in sequencing batch reactors (SBR). The experimental setup of this study is analogous to previous studies [14–17], but now encompasses a temperature range from 20°C to 40°C in eight biore-

actors. As is well documented in earlier studies, pulse-fed SBR, operated with a single nutrient limitation establish a feast-famine enrichment. Microorganisms can compete for the limiting nutrient with at least two distinct ecological strategies. 'Growers' directly produce catalytic biomass from the substrate supplied, while 'hoarders' store the substrate as internal storage compounds and metabolize them later to catalytic biomass. The relative biochemical simplicity of storage polymer production compared to catalytic biomass production as well as the lower energy requirements have been proposed to provide a kinetic competitive advantage to hoarders compared to fast-growing microorganisms. This possibility of feast-famine systems to enrich for microorganisms that produce storage polymers has sizeable industrial potential, especially in the field of resource recovery from waste streams [18]. The type of storage polymer that is formed depends on the available substrate. Waste streams are generally rich in volatile fatty acids, which are consumed to produce polyhydroxyalkanoates (PHA), which can serve as a renewable resource for the production of bioplastics and biochemicals [19]. Polyhydroxybutyrate (PHB) is the most common type of PHA that is produced by a variety of bacteria.

This work aims to identify the role of storage polymers in microbial competition at different operational temperatures. The use of parallel-operated reactors combined with online data collection with community structure analysis, this study furthermore strives to align the structural and functional development in time of the microbial community as a function of temperature. The methodology used in this work provides insight in microbial community structure development and contributes to future advancements in microbial community-based bioprocess development, of which PHB production by mixed microbial cultures is a prime example. This manuscript focuses on the implementation of high-resolution system characterization, and specifically on the comparative results that can be discussed due to the parallel nature of this work.

3.2. MATERIAL & METHODS

3.2.1. SEQUENCING BATCH REACTORS

Eight bioreactors (glass, double-jacket, 1.4L working volume) (Applikon, the Netherlands) were operated in parallel, under non-sterile conditions for 208 cycles, following the operating strategy as outlined in Table 3.1. Stirring was set to 700 rpm (SC4, DASGIP, Germany), air gas flow was controlled by mass flow controllers (MX44, DASGIP, Germany) at 400±2 mlN/min. Reactors were temperature controlled by means of a water jacket and thermostat bath (Lauda, Germany) at different operational temperatures (20A,B, 25, 30A,B, 35 and 40A,B ±0.5 °C, duplicates are indicated with a superscript), pH was maintained at 7.0±0.1 using 1M HCl and 0.5M NaOH. The 48 pumps for feeding, effluent removal and pH control were controlled by a hardware abstraction layer (HAL, TU Delft, Netherlands). The HAL in turn was controlled by a PC using custom scheduling software (D2I, TU Delft, Netherlands). D2I was also used for data acquisition of the online measurements, i.e., dissolved oxygen, pH, acid/base dosage, feed-balance, in-gas/off-gas composition).

The removal of 50% of the reactor volume at the end of each cycle resulted in a solid and hydraulic retention time of 1 day (SRT and HRT respectively). The reactors were cleaned twice per week to reduce the influence of wall growth. The reactors were inoc-

ulated at the same time with a mixture (Supplementary Materials 3.6.7) of aerobic activated sludge from the municipal wastewater treatment plant Harnaschpolder in Delft, the Netherlands, (operational temperature 10-20°C), and process water from a papermill from Hoogezand, the Netherlands, (operated at 35-45°C). The medium was prepared on molality (moles/kg [m]) as dosing is performed through a balance. Each cycle a total of 680 g nutrients were dosed: 20 g acetate feed stock (1 m), 20 g nutrient feed stock (250 mm NH_4Cl, 25 mm KH_2PO_4, 6.25 mm $MgSO_4.7H_2O$, 7.5 mm KCl and 50 g/L trace element solution [20]) and 640 g distilled water. With a working volume of 1.4 L the peak concentration of acetate at the start of each cycle is 28.5 mCmol/L. Throughout the cycle, pH correction results in the addition of approximately 20 g of 1 M HCl to the bioreactor.

SEQUENCING BATCH REACTOR RECIPE

The sequencing batch bioreactors were operated in 12-hour cycles (720 minutes), which consisted of five operational phases. During the first two minutes the carbon source, Acetate, is fed. During the following 11 hours the reactor was normally operated. After which two exchange phases followed, a withdraw of 50% of the reactor content, and its replacement by water and a concentrated nutrient feed solution. The remaining time in the last hour is used for temperature stabilization. The newly fed water was led through a tubing coil in the thermostat baths of each specific bioreactor to limit the temperature disturbance. The maximum temperature difference throughout the feeding phase was 4°C (R40A and R40B) and lasted less than ten minutes.

Table 3.1: Operational phases of the aerobic sequencing batch bioreactors.

Time (min.)	Phase	Liquid amounts
0-2	Carbon Feed Pulse (40 mCmol)	20 g
0-660	Normal cycle operation, pH control	20 g
660-670	Withdraw 50% of reactor volume	700 g
675-683	Water & Nutrient Feed	640g and 20 g
683-720	Temperature stabilization	-

CYCLE AND FED BATCH MEASUREMENTS

Cycle measurements of normal SBR operations were performed to fully characterize the bioreactor and verify online measurements. Measurements are performed as described by Johnson *et al.* [14]. After 146 enrichment cycles the bioreactors were exposed to a fed batch experiment in order to determine the maximum PHB production capacity of the biomass. After collecting the effluent of cycle 145 and storing it at 4°C, a fed-batch experiment was performed by adding 660 g acetate and ammonium-free medium to the remaining biomass. After one hour, a 28.5 mCmol/L sodium acetate pulse was given. For pH control, 1 M acetic acid and 0.5 M NaOH were used, thereby constructing a feed on demand strategy. Fed batch experiments ran for 12 hours, after which the total reactor content was replaced by the stored biomass.

TEMPERATURE DISTURBANCE

From cycle 150 till cycle 200 several temperature disturbance experiments were performed with the enriched biomass. The bioreactors continued their normal SBR operations, with the exception that the bioreactor temperature was increased or decreased by 5°C after extracting the effluent. Within one hour, the desired temperature in the bioreactor was reached and the 28.5 mCmol/L acetate pulse was given. The disturbance ran for 2 cycles, after which the temperature was restored to normal. The reactors were allowed to stabilize for 10 cycles before another disturbance experiment was performed.

ANALYTICAL METHODS

Online measurements consisted of pH, dissolved oxygen (Mettler Toledo, USA), acid and base dosage through integrated revolution counter (MP8, DASGIP, Germany), feed balance (LE34001S, Sartorius, Germany) and high frequency in-gas and off-gas composition analysis through mass spectrometry (PRIMA BT Benchtop, Thermo Scientific, UK). Offline measurements were performed for acetate, ammonia, PHB, total suspended solids (TSS) and volatile suspended solids (VSS) as described by Johnson *et al.* [14]. Catalytic biomass is determined by subtracting PHB from VSS measurement. Catalytic biomass is assumed to have a composition of $CH_{1.8}O_{0.5}N_{0.2}$ [21].

3.2.2. FUNCTIONALITY CHARACTERIZATION FROM ONLINE DATA

Identification of functional changes is performed by observing dynamics in key indicators, which are calculated for each cycle. Indicators were derived from principle system characterization of online measurements. Online measurements can, under well-defined conditions, be used for a full system characterization [13].

An important indicator in feast-famine systems is the end of the feast phase, where external substrate is depleted. The feast length is indicative of the substrate uptake rate and allows for further characterization of the behavior of the biomass in the feast and famine phase. The feast length is derived from the inflection point of the oxygen transfer rate, which is a strong indicator for the depletion of extracellular substrate [22].

The proposed key functionality indicators are specific to the aerobic feast-famine system. The indicators are normalized values, making it possible to compare bioreactors with different process parameters. $O2_{feast}$%: the fraction of oxygen consumed in the feast phase ($O_{2,feast}/(O_{2,feast}+O_{2,famine})$). R_{ratio}: the ratio of the initial to the maximum oxygen transfer rate (OTR) in the feast phase ($OTR_{start\text{-}feast}/OTR_{max}$). The sharp transition of the feast to the famine phase suggest that the biomass has a high substrate affinity as expressed by a low K_m value. How $O2_{feast}$% and R_{ratio} are related to different functionalities is illustrated in Figure 3.1. Shifts in functionality are identified by observing changes throughout the enrichments of these characteristic indicators.

PARAMETER IDENTIFICATION

Cycle experiments were used to identify biomass specific parameters according to the approach proposed by Johnson *et al.* [22]. After sampling and physicochemical corrections, the carbon and electron balances closed for 95% (±5). The corrected data was evaluated in a metabolic model to determine the biomass specific reaction rates and other kinetic parameters, as described by Marang *et al.* [23]. A biomass viability parameter (k_d

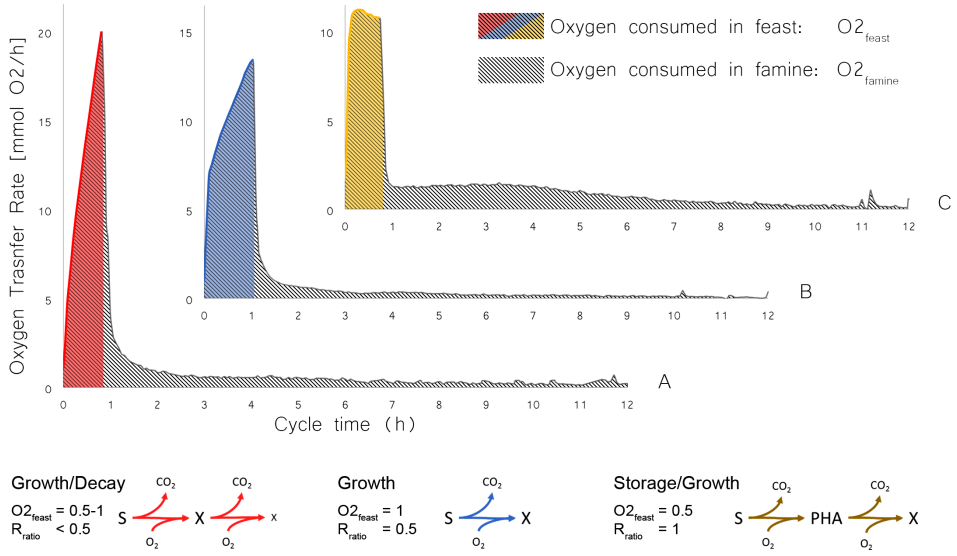

Figure 3.1: Overview of three distinct functional responses of different microbial communities to a new feed pulse at t=0 after half of the biomass is removed. The colored regions indicate the feast period in which external substrate is available, all systems have a comparable feast length of 1 hour, but different functional responses. Response A (red) shows a significant increase in respiration activity, indicating that either inactive biomass takes time to reactivate, or a relative large fraction of biomass has decayed and needs to be replenished. Response B (blue) shows a doubling in respiration activity, which is associated with high cell viability and production of new catalytic biomass. Response C (yellow) shows a constant respiration activity, indicating that no new catalytic biomass is produced in the feast phase. The change in oxygen transfer rate throughout the feast is referred to as R_{ratio}. The area under the graphs represents the total oxygen consumption, which can be divided in oxygen consumption in the feast $O_{2,feast}$ and famine $O_{2,famine}$. Oxygen is consumed in the famine phase for growth on storage polymers and cell maintenance. Substrate (S) is either directly converted to biomass (X) or first to PHB, and consequently to biomass.

[h^{-1}]) was added to the model to allow for biomass decay [24]. Weighing factors in the squared errors were made proportional to measurement errors [25]. Adaptations to the model of Johnson can be found in Supplementary Materials 3.6.3.

3.2.3. COMMUNITY STRUCTURE ANALYSIS BY 16S RRNA AMPLICON SEQUENCING.

Microbial community composition analysis was performed by taking a 15 ml sample from the bioreactor at the end of a cycle and centrifuging it for 10 minutes at 5000 g. The pellet was transferred to a 2 ml Eppendorf tube and stored at -80°C, awaiting further treatment. Genomic DNA of 146 samples (18 time points for eight bioreactors + two replicates of the inoculum) was extracted with the PowerSoil DNA Isolation Kit (Mo Bio Laboratories, Inc., Carlsbad, CA, USA) according to the protocol as described by the manufacturer. The extracted DNA was quantified using absorption spectrophotometry at 280 nm. 16S rRNA gene amplicon sequencing was performed on an Illumina Miseq sequencer by the company MR DNA. The sequences have been stored in GenBank under project number PRJNA448046.

FOCUS OF SEQUENCING DATA FOR THIS STUDY

This study aims at comparing the developments in microbial community structure and functional behavior of the reactors upon exposure to a selective environment. To that end the 16S rRNA gene amplicon sequencing data is processed by the following pipeline.

The merged 16S Illumina reads file (.fastq) together with the mapping file (.txt) were processed and sorted using a phred threshold of 29 and read length between 398 and 450 base pairs on QIIME version 1.9.1 (split_libraries_fastq.py) [26]. Chimera identification was performed with USEARCH [27] and the GOLD reference database. Quality filtered reads were clustered to OTUs at 97% similarity (pick_otus.py) [28], singletons were dropped. Sequence alignment is performed with the MUSCLE [29] aligner, and taxonomy was assigned with the RDP classifier with a confidence of 0.9.

Brooks [30] and Sinha [31] showed that biases in 16S studies due to sample handling, DNA extraction and PCR amplification strongly restricts the quantitative interpretation of sequencing results. The processing steps affect different bacteria in different ways, resulting in amplified and suppressed observed proportions of a community. The high technical reproducibility does allow visualization of relative community dynamics in time throughout enrichments. Plotting the natural logarithm of the relative abundance of species allows for a clearer interpretation of community shifts. The sequencing results yielded between 48.000 and 117.000 paired-end reads per sample. Community dynamics that occur below 1000 reads cannot be represented in a classical stacked barplot as these dynamics occur within 1% of the relative abundance. Logarithmic representations utilize the whole measurement range of the 16S sample reads, leading to deeper visualizations of community dynamics, and thereby capture the gradual dynamics that can occur in communities (Supplementary Materials 3.6.6).

Correlations between community composition and functionality were performed using Pearson's method (Supplementary Materials 3.6.9). The relative abundance of each OTU for each bioreactor is correlated against the feast length, $O2_{feast}$% and R_{ratio} for that bioreactor at the 18 sampling timepoints.

3.3. RESULTS

3.3.1. FUNCTIONAL CHARACTERIZATION FROM ONLINE DATA

Eight bioreactors, pulse-fed with acetate and operated under aerobic conditions for 100 days, were seeded with activated sludge and operated identically, except for the operational temperature. Bioreactors were operated at 20, 25, 30, 35, and 40°C. Duplicate reactors were operated at 20, 30 and 40°C. The development of the functional properties of the microbial communities in the bioreactors was determined by online measurements during the enrichments. Online measured variables were O_2 and CO_2 off gas, base and acid dose, bioreactor temperature, dissolved oxygen (DO) and pH. O_2 off gas measurements were used to functionally characterize the process, whereas DO measurements were used to verify O_2 off gas data. CO2-offgas measurements were used for solving the carbon balance over each operational cycle, where acid and base dose were used for identifying the stoichiometric factor for protons in the metabolic stoichiometry.

Two variables calculated from O_2 off gas data were found to correlate well with offline functionality characterizations: the fraction of oxygen consumed in the feast phase

($O2_{feast}$%), and the normalized change in oxygen transfer rate (OTR) throughout the feast phase, expressed as the ratio of maximum and initial OTR (R_{ratio}). These process variables correlate with the growth and hoarding strategies as follows:

The growing strategy is characterized by the production of catalytic biomass during the feast phase, and relatively little respiratory activity in the famine phase. The biomass in bioreactor A operated at 20°C (R20A) exhibited a characteristic growing strategy as shown in Figure 3.2. The growth strategy was identified by online measurements (Figure 3.2A) and confirmed by offline cycle measurements (Figure 3.2B). In line with the growth strategy, oxygen uptake in the cycle occurs mainly in the feast phase, and the $O2_{feast}$% is high (87%). Minor amounts of respiration occurring in the famine phase can be attributed to completion of the growth cycle, maintenance and/or endogenous respiration. The growth strategy is confirmed by the increase in respiration rate during the feast phase. In absence of storage compounds, the doubling of the biomass during the feast phase as imposed by the exchange ratio of 50% corresponds to an R_{ratio} of 0.5, as is observed for R20A and shown in Figure 3.2A.

The hoarding strategy is characterized by the production of PHB during the feast phase, and growth on PHB throughout the famine phase. The biomass in bioreactor A operated at 30°C (R30A) developed into a characteristic hoarding strategy within 30 days of operation as shown in Figure 3.2. This hoarding strategy can directly be observed from online measurements (Figure 3.2C) and was confirmed by offline cycle measurements (Figure 3.2D). Respiration in the famine phase is dominated by the oxidation of PHB, coupled to biomass production as confirmed by off-line measurement of PHB degradation and biomass production. Carbon and electron balances close within 95%. The cycle of R30A shown in Figure 3.2C has an $O2_{feast}$% of 50%, signifying that more than 95% of the catalytic biomass is produced in the famine phase (see Supplementary Materials 3.6.5). Furthermore, the absence of growth during the feast phase is confirmed by the constant OTR in the feast phase as reflected by an R_{ratio} of 1.0.

The online determined feast length, R_{ratio} and the $O2_{feast}$% were found to correlate well with the functionalities identified from offline cycle measurements as shown in Figure 3.2. It was concluded that online characterization could effectively be used as identifier of the dominant competitive strategy as well as the process development and stability in time.

3.3.2. COMPARING STRUCTURAL AND FUNCTIONAL DEVELOPMENT

Eight reactors were operated for 208 cycles. For brevity, only a detailed overview of the development of the feast length, $O2_{feast}$%, R_{ratio}, and microbial community structure, for bioreactor R30A is presented here (Figure 3.3). The full datasets for the bioreactors are available in Supplementary Materials 3.6.8.

The competition on the limiting, pulsed, substrate is reflected by a downward trend of the feast length throughout the enrichment (Figure 3.3A). The reduction of the feast-length in time does not elude which competitive strategy dominates or when a functionality shift occurs. The plot of the $O2_{feast}$% shows a clear decrease from 80% to 50% from cycle 50 to 65 approximately (Figure 3.3B). The plot of the R_{ratio} shows a shift towards a value of 1 in the same period (Figure 3.3C). This demonstrates a clear shift from the growth to hoarding competitive strategy, as confirmed by the PHB fraction measured at

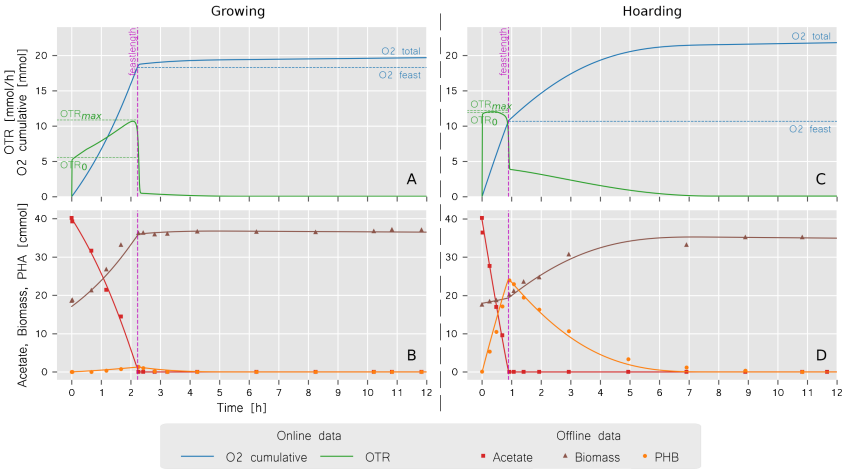

Figure 3.2: Online and offline data of R20A (A, B) and R30A (C, D). System characterizations by online measurements is based on key indicators, represented by text labels and dashed lines in the online data (A, C): Oxygen Transfer Rate (OTR) and oxygen consumption in the feast and famine (O2). These characterizations align with off-line (B, D) measurements. Clear differences are observed between growing bioreactors (R20A – A&B) and hoarding bioreactors (R30A – B&D) allowing for online characterization of functional behavior without offline measurements. Solid lines in offline data represent the fitted model based on [22, 23], where ammonium measurements are used to determine the biomass production.

the end of the feast phase (green squares in Figure 3.3C representing g_{PHB}/g_{VSS}).

Eighteen biomass samples were collected from each bioreactor for microbial community composition analysis. The relative abundance of eight bacterial populations are displayed in Figure 3.3D. The bar plot representation allows for identification of community dynamics and stability of relative abundant OTUs. The natural logarithm plot of the relative abundance (Figure 3.3E) gives a clearer interpretation of time-dependent community shifts by visualizing the whole measurement range of 16S Amplicon sequencing as described in the material and methods section.

Comparison of the $O2_{feast}$% and R_{ratio} data with the natural relative abundance plot shows that the upcoming of *Plasticicumulans acidivorans* in bioreactor R30A is correlated with a shift in functionality from growth to hoarding (Pearson r=0.920, p<<0.001, n=18, see Supplementary Materials 3.6.9). The culture that established within the first 50 cycles was starting to be washed out from the moment that *P. acidivorans* became dominant. The rate of exponential washing-out or growing-in results in trends in Figure 3.3E. The slopes reflect the difference in substrate uptake rate compared to its competitors. *P. acidivorans* increased its relative abundance approximately with 30% each cycle, during its in-growing period. *Acinetobacter sp.* slowly washed out at less than 5% every cycle (see Supplementary Materials 3.6.6, and 3.6.8).

MICROBIAL COMMUNITY MEMBER FUNCTIONALITIES

A family of *Flavobacteriaceae* that is not commonly associated with fast growth or the production of storage polymers, but is abundantly present in all bioreactors. This family is well known for the degradative abilities of macromolecules such as proteins and

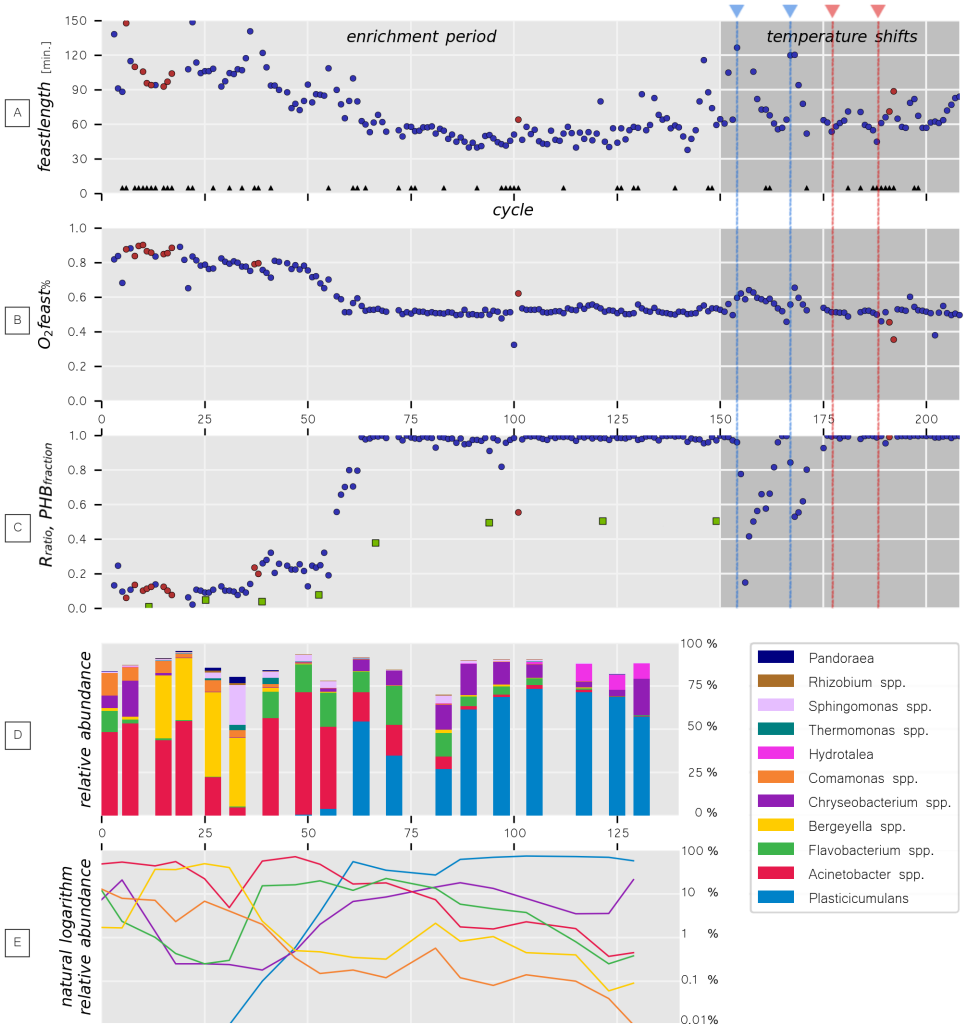

Figure 3.3: 208 enrichment cycles of R30A: Overview of characteristic values (A: feast length, B: $O2_{feast}$%, C: R_{ratio} and $PHB_{fraction}$) and community structure (D: relative abundance, E: natural logarithm of relative abundance of selected species). Upward triangles in A indicate cycles where the reactor was cleaned. Red circles indicate cycles where reactor operation was disturbed by excessive foaming, pH disturbance or other manual interventions. The greyed-out region indicates the time period in which temperature shift experiments were performed. Dashed vertical lines indicate specific temperature disturbance experiments (blue: decrease, red: increase). In C, the intermittently measured PHB fraction (g_{PHB}/g_{VSS}) at the end of the feast phase is plotted as solid green squares. The relative abundance plots show the eleven most abundant OTUs that makeup over 90% of all reads, other species are not plotted and are reflected as the missing fractions in D.

polysaccharides [32]. Most other relatively abundant bacteria are associated with acetate metabolism, e.g.: *Acinetobacter* [33], *Comamonas* [34], *Sphingomonas* [35], *Plasticicumulans* [36], and *Zoogloea* [8]. A literature-supported overview of the functional capabilities of abundant genera is included in Supplementary Materials 3.6.10. This in-

formation is indicative of the roles that microbes can play in the restrictive environment.

CATEGORIZING ENRICHMENTS BASED ON DISPLAYED FUNCTIONALITY

The kinetic performance of the enriched biomass in all eight systems was evaluated in detail by cycle measurements at the end of the enrichment when a functionally steady process was established. An overview of the observed and model-derived parameters is given in Table 3.2. The eight bioreactors can be divided in three groups, based on the functionality displayed at the end of the enrichment: Growers; R20A, R40A, R40B, Hoarders; R25, R30A, R30B, R35; and Mixed; R20B. The results of representative feast-famine cycles for growers and hoarders are shown in Figure 3.2. For full experimental data on all bioreactors the reader is referred to the Supplementary Materials 3.6.8.

Table 3.2: Overview of observed variables, model-derived yields and biomass-specific rates, and characteristic values derived from online measurements during normal SBR operation (averages and standard deviation of 10 consecutive cycles). Dominant microorganisms based on 16S sequencing results. PHB content results from normal cycle operation ($PHB_{end\text{-}feast}$) and accumulation experiments (PHB_{max}).

bioreactor		R20A	R20B	R25	R30A	R30B	R35	R40A	R40B
SBR cycles									
Observed									
feast length	[min]	140±3	143±8	77±4	50±4	54±4	46±3	53±1	65±4
$PHB_{end\text{-}feast}$	[wt%]	4±2	30±3	51±1	52±1	51±1	48±1	0±0	0±0
Model									
$q_{s,max}$	[cmol/cmol/h]	0.7	0.8	1.9	2.3	2.3	2.8	3.5	1.9
$q_{phb,max}$	[cmol/cmol/h]	0.0	0.2	1.1	1.6	1.5	1.7	0.0	0.0
μ_{feast}	[cmol/cmol/h]	0.37	0.16	0.07	0.08	0.09	0.14	1.54	0.65
k_d	[cmol/cmol/h]	0.01	0.00	0.00	0.01	0.01	0.02	0.06	0.02
Y_{sx}	[cmol/cmol]	0.51	0.47	0.50	0.48	0.47	0.45	0.41	0.40
Characterization									
$Group_{functionality}$		Grow	Mixed	Hoard	Hoard	Hoard	Hoard	Grow	Grow
R_{ratio}	[-]	0.52	0.71	1.0	1.0	1.0	0.95	0.19	0.35
$O2_{feast}$%	[mol/mol]	80	61	53	50	51	55	80	76
dominant m.o.¤									
Growing		*a.spp.*	*a.spp.*				*a.spp.*	*a.spp.*	*a.spp.*
Hoarding			*z.sp.*	*p.a.*	*p.a.*	*p.a.*	*2 sp.**		
$Cryptic_{potential}$		*f.spp.*	*f.spp.*	*cl. sp.*	*ch.spp.*	*ch.spp.*	*2 sp.**	*b.spp.*	*b.spp.*
Thermophilic									*m.sp.*
Accumulation									
PHB_{max}	[wt%]	53±2	75±2	86±1	91±1	90±1	90±1	55±2	46±3
PHB:X	[gPHB:1gX]	1.1	3.1	6.1	10.5	9.4	9.4	1.2	0.9

¤ Dominant microorganisms as derived from relative abundance. *Acinetobacter (a.spp.), Zoogloea (z.sp.), Plasticicumulans acidivorans (p.a.), Flavobacterium (f.spp.), Cloacibacterium (cl.sp.), Chryseobacterium (ch.spp.), Bergeyella (b.spp.), Meiothermus (m.sp.).* * Hoarding: *Plasticicumulans acidivorans* & *Nesiotobacter,* potentially cryptic growth*: Chryseobacterium* & *Alicycliphilus.*

3.3.3. OVERVIEW OF STRUCTURAL AND FUNCTIONAL DEVELOPMENT OF THE MICROBIAL COMMUNITIES

Figure 3.4 shows an overview of the development of the respiration ratio (R_{ratio}) for all bioreactors. The respiration ratio correlates well with the observed functionality (distinguishing growing and hoarding strategies), thereby also serving as a process stability indicator. R25 and R30B show very comparable dynamics and community structure as is described for R30A, with a clear shift towards the hoarding strategy in *P. acidivorans* dominated systems that furthermore are functionally and microbially very stable systems (Pearson r=0.908 and r=0.800 respectively, with p«0.001 and n=18). R35 has a slower transition towards the hoarding strategy. The gradual increase in the hoarding strategy aligns with the appearance of *Nesiobacter* and *Alicyclipilus* (Pearson r=0.637 and r=0.611 respectively, with p<0.01 and n=18). The rapid shift towards the hoarding strategy after 120 cycles was unfortunately not covered by the 16S amplicon sequencing.

The bioreactors operated at 40°C show a stable and comparable community structure from cycle 10 onward. A gradual functional shift takes place over 150 cycles, in which the feast length decreases and the respiration ratio increases, but no change in the $O2_{feast}$% is observed. Throughout the enrichment, no PHB is detected at the end of the feast phase in both bioreactors. Despite the absence of PHB, R40A consumes more oxygen in the famine phase (20-32%) than a community with a typical growth strategy. Furthermore, a significant amount of ammonium is released (30-55% of ammonia taken up in the feast phase) and the low R_{ratio} indicates a low cell viability at the beginning of the operational cycle. The data suggest abundance of a third competitive strategy characterized by an important role of cell decay and endogenous respiration.

Minor amounts of PHB were observed in the bioreactors operated at 20°C. The increase in the R_{ratio} after 100 cycles indicates a shift towards the hoarding strategy for both bioreactors. From cycle 120 onwards, the two bioreactors diverge into different functional states; R20A transitions back to the growth strategy and R20B reaches a pseudo-steady state where the hoarding and growing strategy co-occur. The observed feast length for the cultures at 20°C are highly comparable. Community data analyses (Supplementary Materials 3.6.8) suggest that both bioreactors demonstrate a strongly variable microbial community structure throughout the first 100 cycles. No clear enrichment of a limited number of species is observed, as opposed to most other operational temperatures. The observed functional shift after 100 cycles is associated with the appearance of *Zoogloea* in both bioreactors (Pearson r=0.659 and r=0.816 respectively, with p<0.01 and p<<0.001 and n=18). Whereas *Zoogloea* remained abundant in R20B, a decrease in *Zoogloea* abundance in R20A after 20 cycles was observed and aligns with the drop in R_{ratio}. The eventual community composition of R20B seems stable and is composed of multiple members, resulting in a combined growing and hoarding functionality.

MAXIMUM PHB STORAGE CAPACITY

To assess the maximum PHB production capacity of the cultures, ammonia-limited fed-batch experiments were performed at the end of the enrichment. The limitation of growth due to ammonia limitation constrains the metabolism of cells to non-growth-related pathways, such as PHB production. All eight enrichments yielded biomass that produces the storage compound PHB (Table 3.2 and Figure 3.5). The four highest per-

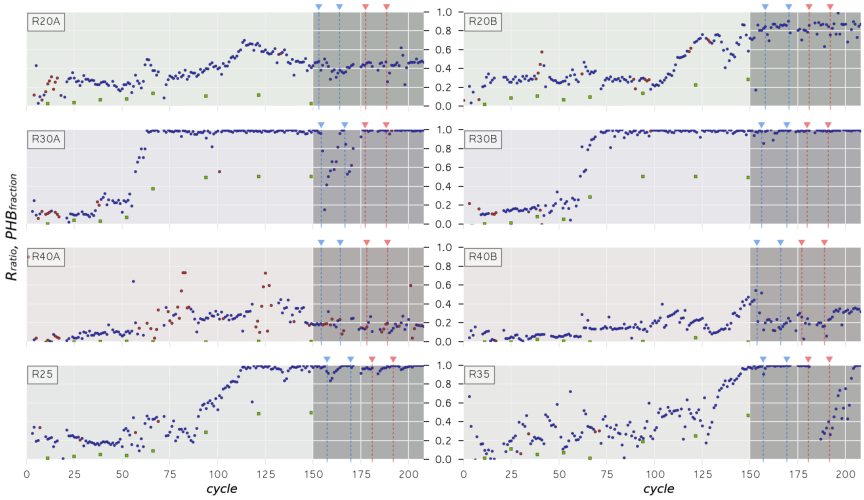

Figure 3.4: Characteristic normalized change in oxygen transfer rate throughout the feast phase (R_{ratio}) for eight bioreactors over 150 cycles of enrichment (light) and 58 cycles of temperature disturbance experiments (dark). R_{ratios} below 0.5 indicate cell decay, R_{ratios} close to 1 indicate PHB production. The intermittently measured PHB fraction (g_{PHB}/g_{VSS}) at the end of the feast phase is plotted as solid green squares.

forming bioreactors, R25, R30A,B and R35, reached 86-91±1 wt% (g_{PHB}/g_{VSS}). This is in the range of previously highest reported PHB storage capacities [15, 37]. The three lowest performing bioreactors, R20A, R40A and R40B reached 46-53±2 wt%. For reference: a 90% PHB accumulation is 9 times more PHB per cell than a 50% PHB accumulation (PHB:X = 9:1 vs 1:1). The two biological replicates operated at 20°C, R20A and R20B, reach a PHB content of 53±2wt% and 75±1wt%, respectively. R20B produces three times as much PHB as its biological replicate, while the replicates at 30 and 40°C do not differ significantly, and show very comparable production capacities.

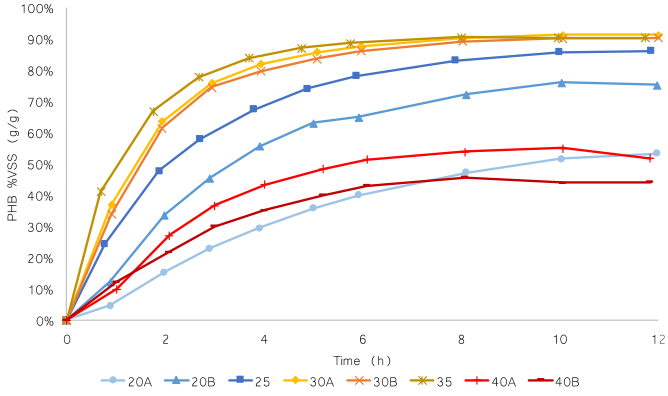

Figure 3.5: PHB accumulation dynamics during the nutrient limited fed batch experiment of eight reactors at different operating temperatures. The three cultures that show low PHB production kinetics (R20A, R40A and R40B) show limited to no PHB production during the normal cycles. The other five bioreactors show increasing kinetics with increasing temperature.

RESPONSE TO TEMPERATURE SHIFTS

Short-term temperature shift experiments were carried out to investigate the temperature dependency of the processes observed. During the experiments, the temperature was either increased or decreased by 5°C for two cycles, indicated with red and blue triangles in Figure 3.4. Biomass in bioreactors R30A and R35 was strongly affected by the temperature disturbance during the second cycle, and required approximately ten cycles to recover. No change of functional strategy was observed during the first feast phase of the temperature shift experiments, but kinetic changes could readily be identified from online measurements.

The biomass specific substrate uptake rates (q_s) changed during the temperature shift experiments (Table 3.3). Generally, all biomass specific rates increased at higher temperatures and decreased at lower temperatures [38]. The only exception was the decrease (up to 40%) in biomass specific conversion rates when the temperature of the bioreactors operated at 35 and 40°C was increased to 40 and 45°C respectively

The biomass in R25, when shifted to 20°C achieved a biomass specific substrate uptake rate 80% higher than the highest rate observed with biomass enriched at 20°C. The same occurred for the shifts from 30 to 35°C, achieving a 70% higher biomass specific substrate uptake rate than the enrichment at 35°C.

Table 3.3: Short-term temperature change experiment. The middle column represents the biomass specific substrate uptake rate of the biomass culture that is obtained at the end of the enrichment (average of ten consecutive cycles, standard deviation in parenthesis). The left and right column represent the biomass specific uptake rates derived for the temperature shifts experiments (-5 and +5°C) (average and standard deviation of two cycles). The cells in red did not follow the general Arrhenius relationship. Cells in green did, with the different shades representing how competitive the culture is with respect to long-term enrichments.

T	-5	T_0	+5
20	0.4 (0.2)	0.7 (0.2)	1.2 (0.5)
20	0.5 (0.2)	0.8 (0.2)	1.5 (0.6)
25	1.5 (0.2)	1.9 (0.4)	2.2 (0.2)
30	1.5 (0.1)	2.3 (0.2)	4.9 (0.2)
30	1.7 (0.1)	2.3 (0.2)	4.8 (0.2)
35	2.2 (0.1)	2.8 (0.2)	2.6 (0.1)
40	2.7 (0.1)	3.5 (0.3)	2.0 (0.1)
40	1.4 (0.1)	1.9 (0.2)	1.1 (0.1)

3.4. DISCUSSION

3.4.1. CULTURE ENRICHMENTS AND BIOREACTOR OPERATION

All bioreactors established a feast-famine regime within two operational cycles. As is shown in the overview plots, the competition for the limiting carbon substrate leads to a decreasing feast length demonstrating the enrichment of a faster community (Figure 3.3 and Supplementary Materials 3.6.8). There are two strategies for effective competition for acetate: the growing strategy and the hoarding strategy. Two on-line data derived functional indicators - R_{ratio} and $O2_{feast}$% - allow for a direct interpretation whether PHB is produced as intermediate storage polymer, and differentiation between the growing and hoarding strategy. In time, microbial communities grown at temperatures from 25 to 35°C changed towards the hoarding strategy (Table 3.2). In general, higher biomass specific rates and decreased overall biomass yield values were identified at increasing temperatures, in line with the generalizations proposed by Heijnen and Kleerebezem [39]. The temperature shift experiments resulted in a typical increase and decrease of the biomass specific rates, except above 35°C, where a temperature increase of 5°C resulted in decreased biomass specific rates (Table 3.3). Additionally, the hoarding biomass enriched at 25°C, when incubated to 20°C, had a biomass specific substrate uptake rate two times higher than biomass enriched at 20°C. This suggests that the reactors operated at 20°C could also have enriched the faster hoarding microbial community as obtained at 25 °C. This observation, and the surprising absence of the hoarding strategy at 40°C, and only intermittently at 20°C form the basis of further discussion.

3.4.2. HOARDING VERSUS GROWTH AS DOMINANT COMPETITIVE STRATEGY

Enrichments with a short biomass retention time, based on one carbon source and electron donor, such as acetate, and oxygen as electron acceptor are highly selective and therefore one may expect a low biological diversity if one strain is outcompeting other microorganisms. Furthermore, the feast-famine strategy enriches microorganisms with the highest overall substrate uptake rate, which is directly reflected in the length of the feast phase. From a reductionist point of view, we may argue that producing catalytic biomass from acetate involves more complex metabolic machinery and therefore has a larger chance of being rate limiting than the relative short pathway from acetate to the storage polymer PHB. Theoretically this results in a tradeoff between a high biomass specific substrate uptake rate (q_s) with PHB production (hoarding strategy) versus a lower q_s with an increasing number of catalysts (growing strategy). As far as we can see there is no intrinsic reason why this tradeoff would be temperature dependent. Though, for the inoculum that was used in this study, the hoarding strategy was only dominant in the temperature range of 25-35°C. Surprisingly, no PHB hoarding species were able to dominate at 20 and 40°C, where the growth strategy prevailed. Although the enrichments were operated for more than 75 generations and the inoculum contained a highly diverse microbial community (Supplementary Materials 3.6.7), it is possible that the observations are inoculum specific. Nevertheless, all enriched communities were able to produce PHB when exposed to ammonium limitation, demonstrating the widespread abundance of the PHB production and degradation pathway in prokaryotes (Table 3.2 and Figure 3.5). Evidently, the dominance of the hoarding versus growing strategy re-

sults from different kinetic properties and/or different pathway regulation in the different communities enriched at different temperatures. In other words, the competitive strength of both strategies apparently is not homogeneously distributed in all temperature domains. This means that no single competitive strategy consistently leads to dominance in feast-famine systems.

3.4.3. FUNCTIONALITY AND ABUNDANCE

The high number of sequence reads were successfully used to analyze the dynamics within the microbial communities throughout the enrichments. Logarithmic presentation of the data allows a visual alignment of a change in time of functional properties and populations within the reactors (Figure 3.3E and Supplementary Materials 3.6.8). The resulting data suggest that much of the microbial community dynamics cannot be explained only by differences in kinetic and stoichiometric parameters. The general absence of clear successions of dominant community members and the persistent cooccurrence of microbial species and their oscillating relative abundance, suggests that processes like mutualism, adaptation, decay, and predation may play a significant role in the enrichment process [40, 41].

Even though changes in time can effectively be analyzed with NGS based methods, a major limitation of the NGS methodology used in this study remains that no reliable quantitative distribution of OTU's in time is possible. Herewith we cannot distinguish between enrichment of one strain with satellite populations, versus two or more dominant strains, and the origin of functional interdependencies remain unclear.

The strong correlation of the online data with population shifts allows for better sampling and 16S rRNA gene analysis strategies in future experiments (see Supplementary Material 3.6.9 for Pearson correlations). For example, the functionality shift from cycle 120 to 150 in bioreactor R35 is currently not captured due to the predetermined 16S sampling strategy. With the online parameter identification, it is possible to collect frequent samples and analyze them at a high resolution in order to capture the specific regions of interest where functional shifts are identified with online measurements.

With the current sampling strategy, the community dynamics that occur within one cycle can also not be distinguished. More complex microbial community dynamics could involve a combination of growth on acetate, hoarding, decay, and cryptic growth. Analyzing multiple samples throughout one cycle could help to distinguish and identify the activity and abundance of specific populations by their change in relative abundance throughout one cycle.

3.4.4. CRYPTIC GROWTH AS A THIRD COMPETITIVE STRATEGY

Although the majority of the functional responses of the bioreactors can be attributed to the presence of growers and hoarders, there are three observations that suggest that cell viability is a key biological factor that complicates the interpretation of the results in terms of microbial competition in sequencing batch bioreactors.

First, all bioreactors show a decreased respiration ratio (R_{ratio} in Figure 3.4) during the initial cycles, and the higher temperature bioreactors maintain these low respiration ratios throughout the cultivation period. R_{ratio} values lower than 0.5 indicate that biological activity more than doubles throughout the feast phase, while only half of the

biomass is removed. This suggests that some form of biomass inactivation, decay and/or endogenous respiration takes place during the famine phase, resulting in a lower respiration rate at the beginning of the cycle than expected based on exchange ratios.

Second, the ammonia that is released during the famine phases of bioreactors R40A and R40B, and to a lesser extent in R35, is likely coming from respired proteins and cell material. The biomass in bioreactor R40A, for example, releases more than half of the ammonium consumed in the feast phase, which suggests a viability of less than 40% at the end of the cycle.

Third, the relatively high abundance of microbial species, under which those from the family of *Flavobactiriaceae*, that are associated with growth on macromolecules such as proteins and polysaccharides, suggest that cell lysis and cryptic growth occur in many bioreactor systems [42]. Further differentiation of the abundance and strategies of the observed microbial species and their role in the microbial community remains unclear and would require a combination of metagenomic and metatranscriptomic analyses or an analysis of the community development during the cycle.

From these observations, we hypothesize that a third competitive strategy emerges as a result of biomass decay, lysis and growth on the cellular constituents released in the famine phase, i.e.: cryptic growth. (Table 3.2). This could explain the persistent microbial diversity that is observed in very selective microbial ecosystems, as described in this work, and the relatively high respiration rate in the famine phase in R40A and R40B in the absence of PHB. The low R_{ratio} observed in the initial cycles of all systems suggests that cell viability and cryptic growth could play a significant role in the biodiversity of pulse fed bioreactors, even at moderate temperatures. As mentioned before, future research could specifically be aimed to elucidate this behavior by, for example, utilizing whole genome sequencing techniques. Additionally, the low cell viability of biomass at higher temperatures allows for a mechanistic explanation as to why hoarding is no preferred strategy at higher temperatures in pulse fed systems.

3.4.5. HOARDING: A NON-SUCCESSFUL STRATEGY AT HIGHER TEMPERATURES

Substrate consumption for maintenance purposes and cell viability related processes affect hoarders and growers differently. At low maintenance and decay rates, hoarders outcompete growers when their biomass specific substrate uptake rate (q_s) exceed that of growers at a 50% exchange ratio in a pulse fed bioreactor by at least a factor 1.4 (see Figure 3.6 and Supplementary Materials 3.6.2). At higher temperatures, the energy requirements for maintenance purposes become more pronounced [43], as can be seen from the decreased biomass yield in Table 3.2. In absence of external or stored substrate, cell maintenance requirements result in a decrease of the viable biomass concentration due to decay even though the concentration of VSS is hardly affected. This influences the competition between growers and hoarders significantly. Reduced viability of growers favors the hoarding strategy to a point where hoarding becomes the preferred survival strategy, regardless of q_s. At increasing temperatures, the increased maintenance requirements should benefit the hoarding strategy. Nevertheless, no PHB production is observed in the bioreactors operated at 40°C, suggesting that other factors than only maintenance affect the cell viability or cultivability [44, 45].

Biomass viability also seems to play an important role at 35 °C. The biomass in bioreactor R35 displays the hoarding strategy, but 10-20wt% PHB is not degraded at the end of the famine phase. Furthermore, biomass in both bioreactors at 30°C, when shifted to 35°C, achieved significantly higher q_s than the hoarding biomass that was enriched at 35°C (Table 3.2). The lower q_s observed for biomass from R35 is likely due to a significant lower fraction of active biomass in R35. This indicates that significant biomass decay occurs, despite the presence of significant cellular PHB. Apparently, decay occurs despite the presence of an energy source for maintenance purposes. We propose that temperature induced cell decay is independent of the cellular PHB content and therewith affects growers and hoarders equally (Figure 3.6). In such a case, the hoarding strategy will only become favorable if the bacteria achieve an even higher q_s. It is possible that at high temperatures the effects of temperature induced cell decay outweigh the benefits of reduced overall maintenance costs in hoarding microorganisms. Microbial community data support the mechanistic explanation described here.

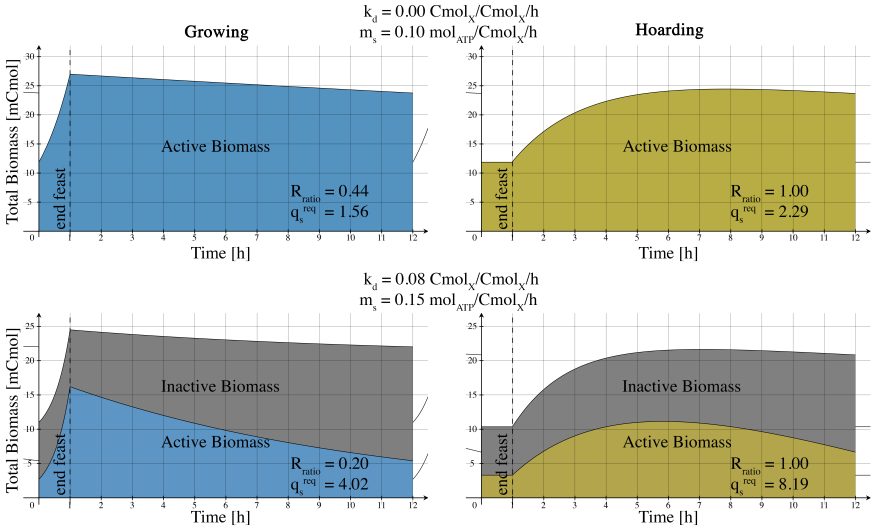

Figure 3.6: Overview of the proposed influence of increased maintenance and cell inactivation on the competition between growing (blue and left) and hoarding (yellow and right) biomass. Absence of biomass decay (k_d =0) on the top shows that the hoarding bacteria require a 1.5 (2.29/1.56) times higher biomass specific substrate uptake rate (q_s^{req}) to outcompete growing bacteria (same feast length). With an increased biomass decay (k_d=0.08) the hoarding biomass requires a 2.0 times higher q-rate. The inactive biomass (grey) does not contribute to biological activity but is present in dry weight measurements. The sum of the active and inactive fraction of the biomass in the bottom figures closely resembles the biomass profile in a system without decay (top). The respiration ratio (R_{ratio}) gives a good indication that biomass decay occurs in systems that exhibit the growing strategy, an R_{ratio} below 0.4 indicates significant biomass decay. For hoarding biomass, the respiration ratio does not change during the feast and therefore no indication of biomass decay can be derived from online measurements for systems that exhibit the hoarding strategy.

3.4.6. REPRODUCIBILITY OF ENRICHMENTS

The three pairs of biological replicates developed differently throughout the enrichment, but reached comparable functional outcomes after 150 cycles, with some notable differences, as will be discussed below. During the cycle measurements of R40A and R40B, two different growing functionalities are observed: the shorter feast length and lower cell viability of bioreactor R40A versus the longer feast length and higher cell viability of bioreactor R40B. Throughout the enrichments, both functionalities are observed in both systems at varying times resulting in a relatively stable length of the feast phase at variable R_{ratio} values. The 16S rRNA gene analysis indicates that both mesophilic and thermophilic bacteria are present in both bioreactors (Supplementary Materials 3.6.8), which may indicate that community members are competitive by either having a fast biomass specific uptake rate, or high cell viability.

The biological replicates at 30°C developed in a very similar fashion, both functionally as well as structurally. Both bioreactors shift at approximately the same time after inoculation and take approximately 10 cycles to shift from growth to storage as main competitive strategy. The high synchronicity of these bioreactors is likely due to the parallel enrichment of *P. acidivorans* in both bioreactors, as its dominance is associated with a feast length reduction of approximately 30%. *P. acidivorans* is well-known for its superior PHB-producing capabilities resulting in a maximum PHB content of up to 90wt% under nutrient (i.e. ammonium) limiting conditions (Table 3.2 and Figure 3.5) [46].

The enrichments performed at 20°C resulted in a mixed characteristic of growth and hoarding after 150 cycles of enrichment, with emphasis on growth for bioreactor R20A and hoarding for bioreactor R20B. Both bioreactors also show ongoing community dynamics throughout the experimental period, indicating highly competitive conditions. This is reflected in the highly comparable length of the feast phase of bioreactors R20A and R20B. Jiang *et al.* [15] managed to achieve a functionally stable enrichment at 20°C within 50 operational cycles. Their microbial community was dominated by *Zoogloea*, as visually verified with FISH, but no 16S rRNA gene analysis is available to compare their findings with our community structure. Their setup was highly comparable to ours, but was augmented with enriched hoarding biomass, which may explain the longer period required for *Zoogloea* to become dominant in our bioreactor, but it does not explain why *Zoogloea* did not become dominant from cycle 100 onwards.

In general, we observe significant variations in bioreactor functionality and diversity in some temperature domains, while other temperatures yield highly reproducible results. This indicates that there are still many factors left ununderstood, already in these relatively simple systems. A major improvement with this rigorous approach is that we can pinpoint specific circumstances where our knowledge is lacking.

3.5. CONCLUSION

Parallel cultivation from the same starting point (inoculum) allows for effective investigation of the functional development of microbial communities grown in variable environmental conditions. By combining functional system analysis based on online data with frequent community structure analysis by 16S rRNA gene amplicon sequencing, comparative system development upon variation of a single variable can be studied in an effective way. Here we investigated pulse-fed selective conditions at five different temperatures in eight bioreactors. Exploration of competitive strategies benefit from the rigorous approach described here and will greatly contribute to our understanding of microbial ecosystem development and functioning, and subsequent development of bioprocesses.

The competitive strategies identified in pulse-fed bioreactors can be divided in three types: (i) Direct growth on the primary substrate, (ii) hoarding of primary substrate and subsequent growth on storage polymers, and (iii) growth on the primary substrate combined with subsequent decay and cryptic growth. These three functional properties can, to a large extent, be directly identified from online data.

All communities were able to produce PHB to at least 50% dry weight when incubated in excess of carbon-substrate and ammonium limitation demonstrating the ubiquity of bacterial PHB production. Still, the microbial communities established in some bioreactors did not show any PHB production during the enrichment and therefore their PHB production mechanism played no role in the competition. Communities that produced PHB during the cycles, were also able to reach the highest PHB content during the accumulation experiments. The utilization of the PHB machinery as functional strategy to outcompete other microorganisms appears to have a temperature optimum at 30°C in pulse fed bioreactors. Dominance of the hoarding strategy is correlated with a high relative abundance of *Plasticicumulans acidivorans*.

The different developments of biological replicates from the same inoculum indicate that stochastic processes dominate the initial enrichment period. Replicates generally achieve comparable functional and microbial characteristics.

ACKNOWLEDGEMENTS

We gratefully acknowledge financial support from Netherlands Organization for Scientific Research (NWO) which is funded by the Ministry of Economic Affairs and the company Paques B.V. (Paques Partnership Program project 13002).

DATA AVAILABILITY

Sequence data collected for this study have been deposited in GenBank with BioProject ID PRJNA448046 and SRA Study SRP137048. Datasets of online measurements of 1824 cycles (8x228) are available as HDF5 dataset [47]. All other data generated or analyzed during this study are included in this published article and its supplementary materials files.

3.6. SUPPLEMENTARY MATERIALS

3.6.1. INFLUENCE OF MAINTENANCE, ENDOGENOUS RESPIRATION, AND CELL DECAY ON THE COMPETITION BETWEEN GROWTH, HOARDING, AND CRYPTIC GROWTH STRATEGIES

Biomass maintenance is expressed as energy requirements per unit of biomass per hour ($mol_{ATP}/Cmol_X/h$) [48] . In continuous culture systems, these energy requirements are met by oxidation of extracellular substrate. In the feast famine system, during the famine phase, no extracellular substrate is available. Therefore, each cell needs to supply its own resources for survival, oxidizing storage compounds and biomass, which yields ATP, CO2, and ammonia. This endogenous respiration was proposed by Herbert [49], in the context of continuous culture systems. The mechanism of endogenous respiration in dynamic systems could have significant influence on functionality and structure of the microbial community.

Here, we propose that cell decay is independent from maintenance and endogenous respiration and results in the production of inactive biomass. Different mechanisms may contribute to cell decay, such as prolonged endogenous respiration leading to respiration of vital cell components, virus activity, predation, programmed cell death in microbial communities, and other stochastic processes like temperature related protein instability. After cell lysis, decayed cells are available to other microorganisms as complex substrate. If the rate of hydrolysis exceeds the rate of decay in a system, no inactive biomass will be present. If the decay rate exceeds the rate of hydrolysis a net fraction of inactive biomass will be present in the bioreactor. The extent to which maintenance and cell decay affect the competitive strategies depends on the relative contributions of each.

In feast famine systems, where 50% of the reactor volume is exchanged at the end of the cycle, each active cell present at the start of the cycle needs to result in two active cells at the end of the cycle to maintain a steady state. In steady state, the three competing strategies have different active biomass profiles throughout a cycle. The biomass that grows on decaying cell matter (cryptic growth) does not have to compete for the pulsed substrate. Therefore, this cryptic biomass grows throughout the whole cycle as long as hydrolyzed cell matter is available. The diversity in compounds resulting from decaying cell matter could allow for a rich microbial diversity. Therefore, the mechanism of cryptic growth could be a key contributor to the microbial diversity observed in feast famine systems. The abundance of cryptic growing biomass depends on the decay and hydrolysis rates, both of which are not readily characterized. More quantitative microbial community abundance tools are required for further elucidations.

3.6.2. HOARDING STRATEGY REQUIRES HIGH BIOMASS SPECIFIC SUBSTRATE UPTAKE RATE (Q_S)

The two strategies that rely on the primary pulsed substrate, growing and hoarding, have highly distinguishable biomass profiles (Figure 3.2). The two strategies are competitive if the bacteria can deplete the pulsed substrate (S [$Cmol_S$]) within the same time (feast length [h], *fl*). The factors that influence the substrate uptake rate are the total active biomass ($M_{X,act}$ [$Cmol_X$]) and the biomass specific substrate uptake rate (q_S $Cmol_S/Cmol_X/h$).

$$\int_{t=0}^{t=fl} M_x(t) \cdot q_s(t) \cdot dt = S$$

Due to the relative high substrate concentration during the pulse, the influence of substrate affinity is relatively minor for a large fraction of the feast phase. The growing biomass increases its total biomass (M_X) throughout the feast phase, therefore its overall substrate uptake rate increases. Hoarding biomass, on the other hand, does not increase its total active biomass throughout the feast phase, therefore, to remain competitive with growers they need either a higher $M_{X,0}$ or a higher q_S.

The active biomass concentration depends on the biomass growth yield on substrate (Y_{SX}), the maintenance costs per biomass per hour (m_s), the biomass decay rate (k_d) and the fraction of biomass that is retained at the end of the cycle (f_{retain}). The retained biomass fraction is an operational parameter, which in all systems is set to 50%. The aerobic biomass yield for direct growth on acetate is approximately 0.5 $Cmol_X/Cmol_S$, while the biomass yield of hoarders via the PHA intermediate is intrinsically lower at 0.44 $Cmol_X/Cmol_S$. Hoarding biomass is therefore limited by their limited growth during the feast phase and their lower biomass growth yield.

At negligible maintenance costs and decay rates, and an arbitrary feast length of one hour, the substrate uptake rate of growing biomass is approximately 1.39 $Cmol_S/Cmol_X/h$. For hoarding biomass to remain competitive, the q_S has to reach 2.25 $Cmol_S/Cmol_X/h$. The hoarding strategy therefore relies on a significant higher q_S.

Increased maintenance costs favor the hoarding strategy somewhat, due to the more efficient respiration of PHA for energy than the relative expensive biomass in terms of growth yield. Stochastic biomass inactivation is analogue to a lower retained biomass fraction. In such a case the growing strategy even further benefits, due to its ability to increase in active biomass throughout the feast phase. The only case in which hoarding biomass is further aided by maintenance processes is when biomass inactivation is dominated by prolonged endogenous respiration. As this mechanism likely affects fast growing biomass significantly more than slow growing biomass. This principle can be used to further explore environmental factors that could favor hoarding bacteria over growing bacteria.

3.6.3. INCORPORATION OF BIOMASS VIABILITY IN THE PARAMETER IDENTIFICATION MODEL

Biomass viability was added to the parameter identification model [22] as a distinguishable property from cell maintenance (m_s). The principle differences between the two processes are described in the sections above. Maintenance is expressed as energy requirements per unit of biomass per hour ($mol_{ATP}/cmol_X h$). If external substrate or internal storage polymers are available, they will be oxidized for energy generation. Otherwise, biomass will be oxidized to yield ATP, CO2, and ammonia.

$$X + \frac{\gamma_X}{\gamma_{O2}} O_2 = CO_2 + Y^{stoi}_{NH3/X} NH_3 + aH_2O + Y^{stoi}_{ATP/X} ATP$$

The degree of reduction of a compound (γ_i), represents the number of electrons per C-mol of compound upon complete oxidation [43]. a depends on the stoichiometric composition of biomass. For a general biomass composition $CH_{1.8}O_{0.5}N_{0.2}$ [21], and oxidation yield of $2 mol_{ATP}/cmol_X$ the oxidation results in:

$$CH_{1.8}O_{0.5}N_{0.2} + 1.05\ O_2 = CO_2 + 0.2NH_3 + 0.6H_2O + 2ATP$$

BIOMASS VIABILITY

Biomass viability is described independently of maintenance by allowing a fraction of the catalytic biomass to become deactivated. This is of specific importance to systems at higher temperatures, where a biomass inactivation of more than 50% is observed, but also in cycles throughout the enrichments where the increase in respiration activity throughout the feast phase more than doubles. The biomass decay is modeled as a first order reaction rate k_d [h^{-1}] to simulate this deactivation.

$$\frac{dX_{\text{inact}}}{\text{dt}} = X_{\text{act}} \cdot k_d \tag{3.1a}$$

$$\frac{dX_{\text{act}}}{\text{dt}} = X_{\text{act}} \cdot -k_d \tag{3.1b}$$

3.6.4. WEIGHING AND MEASUREMENT ERROR

In previous models, arbitrary weights are attributed to different compounds and no correction for compound concentration offset is introduced, but an error relative to the current value (SSqRE). This means that compound concentrations between 0 and 4 mmol would have a disproportionate large calculated error compared to concentration that would lay between 20 and 24 mmol, especially when concentrations get close to the lower bound. Here we re-introduce weighing according to the measurement error proportionality and independent of offset [25]. Measurements with large errors will contribute less to the sum of errors.

$$SSE(c_i) = \sum_0^t \left(\frac{c_i^{\text{meas}}(t) - c_i^{\text{model}}(t)}{\sigma_i^{\text{meas}}} \right)^2$$

3.6.5. THEORETICAL $O2_{FEAST}$% HOARDING BIOMASS

The electron yield (Γ) for the conversion of substrate to product is derived from the theoretical carbon yield and degrees of reduction of substrate (γ_{Ac}=4) and product (γ_{PHB}=4.5). Carbon yields are taken from [21], $Y_{PHB,S} = \frac{2}{3}$ Cmol/Cmol and $Y_{X,PHB} = \frac{2}{3}$ Cmol/Cmol.

$$\Gamma_{PHB,S} = \frac{\gamma_{\text{PHB}}}{\gamma_S} \cdot Y_{PHB,S} = 0.75 \frac{e^-}{e^-}$$

$$\Gamma_{X,PHB} = \frac{\gamma_X}{\gamma_{\text{PHB}}} \cdot Y_{X,PHB} = 0.62 \frac{e^-}{e^-}$$

The electrons that are not converted to product are taken up by oxygen to produce energy. The electron loss is equal to the amount of oxygen required. If no cell maintenance occurs and all substrate is converted to PHB the fraction of electrons that are lost during the feast phase equals: $1 - \Gamma_{PHB,S} = 0.25$. The total fraction of electrons of the substrate that ends up in biomass is $\Gamma_{PHB,S} \cdot \Gamma_{X,PHB}$. Therefore, the fraction of electrons lost throughout the whole cycle is $1 - \Gamma_{PHB,S} \cdot \Gamma_{X,PHB}$. The ratio between electrons lost in the feast and the total electrons in the cycle equals the fraction of oxygen consumed in the feast phase.

$$O2_{\text{feast}}\% = \frac{O_{2,feast}}{O_{2,\ total}} = \frac{e^-_{\ oxi,feast} \cdot \gamma_{O2}}{e^-_{\ oxi,\ total} \cdot \gamma_{O2}} = \frac{1 - \Gamma_{PHB,S}}{1 - \Gamma_{PHB,S} \cdot \Gamma_{X,PHB}} = 0.54$$

In non-ideal systems, cell maintenance requires some respiration. Given that the famine phase is significantly longer than the feast phase, the fraction of oxygen consumed in the famine phase will slightly increase, reducing the $O2_{\text{feast}}$% towards 50%.

3.6.6. COMPETITIVE GROWTH RATES AND SUCCESSION

Every cycle (n), competitive species (i) multiplies (d) times, after which 50% is removed at the end of the cycle. This should be reflected in the change in number of reads (R) of that species in the 16S data Figure 3.3E and subsection 3.6.8.

$$R_i(n) = (d_i \cdot 0.5)^n \cdot R_{i,0}$$

$$\ln(R_i(n)) = n \cdot ln(d_i \cdot 0.5) + ln(R_{i,0})$$

Which takes the form of a linear equation: $y = ax + b$. And reversely, when solved for d we can estimate the doubling rate of an organism during a time period with a linear trend. Based on the difference in ln(relative abundance) (Δy) and number of cycles over which the trend takes place (Δn).

$$d = 2 \cdot e^{\frac{\Delta y}{\Delta n}}$$

Example: The linear growing in of *Plasticicumulans acidivorans* in R30A is observed from cycle 30 to cycle 60, ranging from a ln(relative abundance) of -4.7 to 4. The doubling rate d is approximately 2.6 during the ingrowing period. 1 cell becomes 2.6 cells during the cycle, 50% is exchanged, so the species abundance increases with 30% every cycle.

The linear washing out of *Acinetobacter species* in R30A is observed from cycle 64 to cycle 128, ranging from a ln(relative abundance) of 4.3 to -0.8. The doubling rate d is approximately 1.9. Species abundance decreases with approximately 5% every cycle.

3.6.7. INOCULUM - COMMUNITY STRUCTURE ON PHYLUM AND FAMILY LEVEL

The reactors were inoculated, at the same time, with a mixture of aerobic activated sludge from the municipal wastewater treatment plant Harnaschpolder in Delft, the Netherlands, (operational temperature 10-20°C), and process water from a papermill from Hoogezand, the Netherlands, (operated at 35-45°C). Questions surrounding the inoculum will always arise in microbial community enrichment research. And it is possible that the results obtained in this study do depend on this specific inoculum. Nevertheless of all microbial species that became relatively abundant throughout the enrichments, none were present in a high relative abundance in the inoculum. This again signifies that enrichment studies are able to bring to the forefront microorganisms that make up only a tiny fraction of the inoculum.

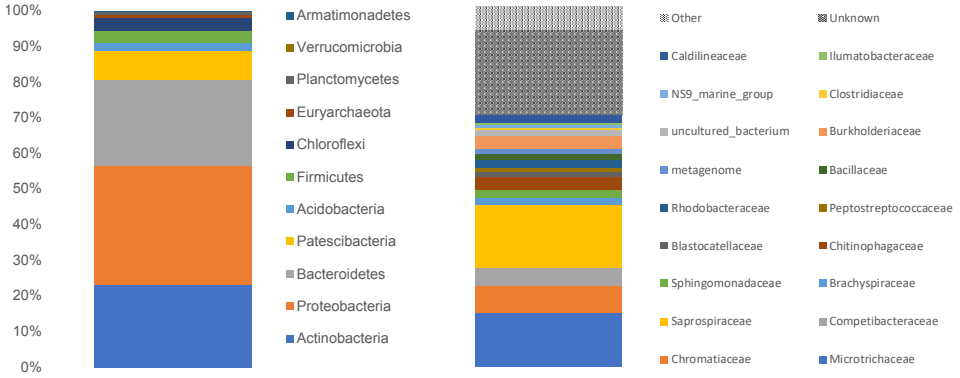

Figure 3.7: Community structure of the inoculum of all eight bioreactors. The inoculum consists of a mixture of biomass from a waste water treatment plant and a paper mill (see main text). The diversity is too large at genus level for a visual representation, therefore a grouping is displayed on phylum (left) and family (right).

3.6.8. FUNCTIONAL AND STRUCTURAL DEVELOPMENT IN 8 BIOREACTORS

208 enrichment cycles of eight bioreactors (R20A, R20B, R30A, R30B, R40A, R40B, R25 and R35). Each figure shows an overview of characteristic values (A: feast length, B: $O2_{feast}$%, C: R_{ratio}) and community structure (D: relative abundance, E: natural logarithm of relative abundance of selected species). Upward triangles in subfigure A indicate cycles where the reactor was cleaned. Red circles indicate cycles where reactor operation was disturbed by excessive foaming, pH disturbance or other manual interventions. The greyed-out region indicates the time period in which temperature shift experiments were performed. The online data for all cycles of all eight bioreactors are available at Stouten [47]. The eight figures follow on the next pages.

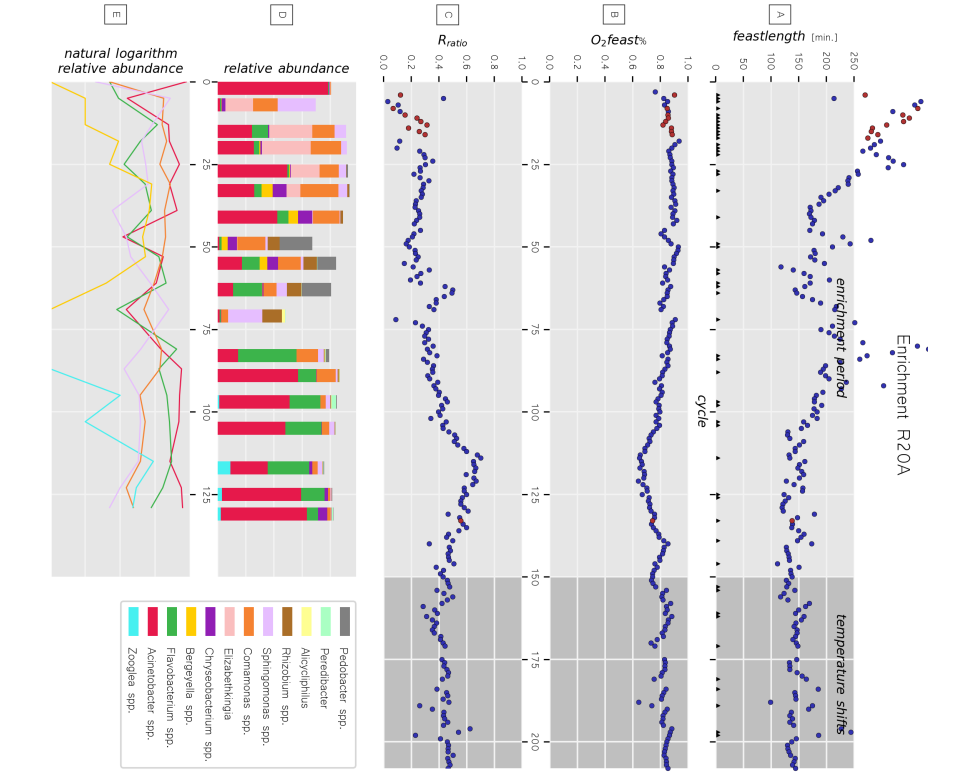
Enrichment R20A
A
feastlength [min.]
enrichment period
cycle
temperature shifts
B
O2feast%
C
Rratio
D
relative abundance
E
natural logarithm
relative abundance
Pedobacter spp.
Pseudoxanthomonas spp.
Paracoccus spp.
Alicycliphilus spp.
Rhizobium spp.
Sphingomonas spp.
Comamonas spp.
Elizabethkingia spp.
Chryseobacterium spp.
Bergeyella spp.
Flavobacterium spp.
Acinetobacter spp.
Zoogloea spp.

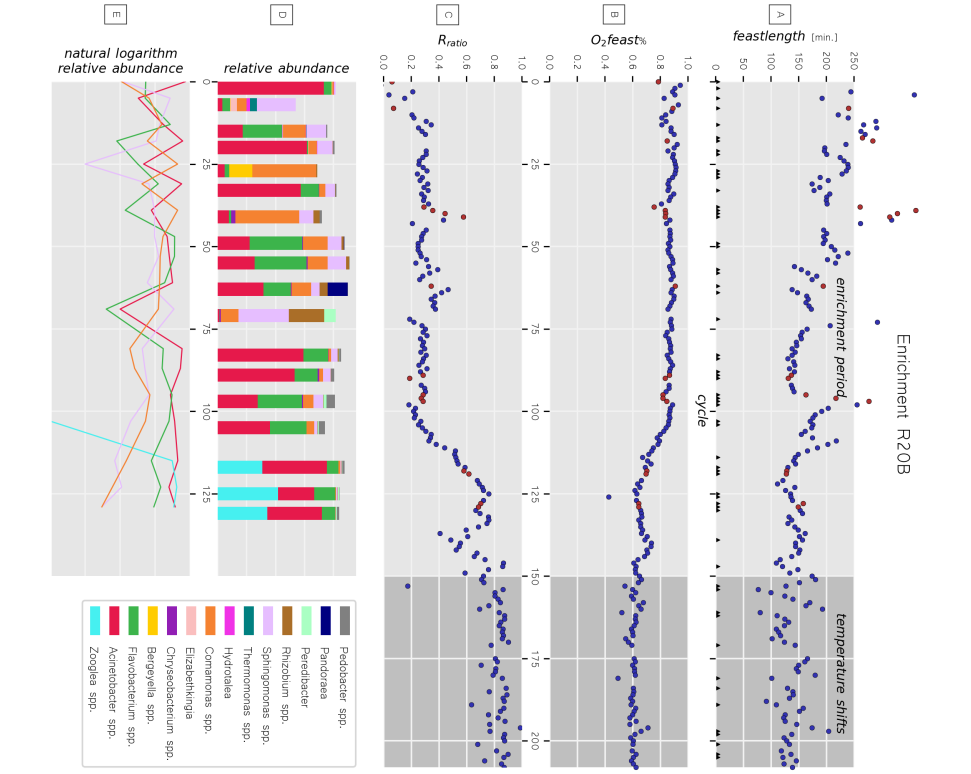
Enrichment R20B
A
feastlength [min.]
enrichment period
cycle
temperature shifts
B
O2feast%
C
Rratio
D
relative abundance
E
natural logarithm
relative abundance
Pedobacter spp.
Pandoraea spp.
Paracoccus spp.
Rhizobium spp.
Sphingomonas spp.
Thermomonas spp.
Hydrotalea spp.
Comamonas spp.
Elizabethkingia spp.
Chryseobacterium spp.
Bergeyella spp.
Flavobacterium spp.
Acinetobacter spp.
Zoogloea spp.

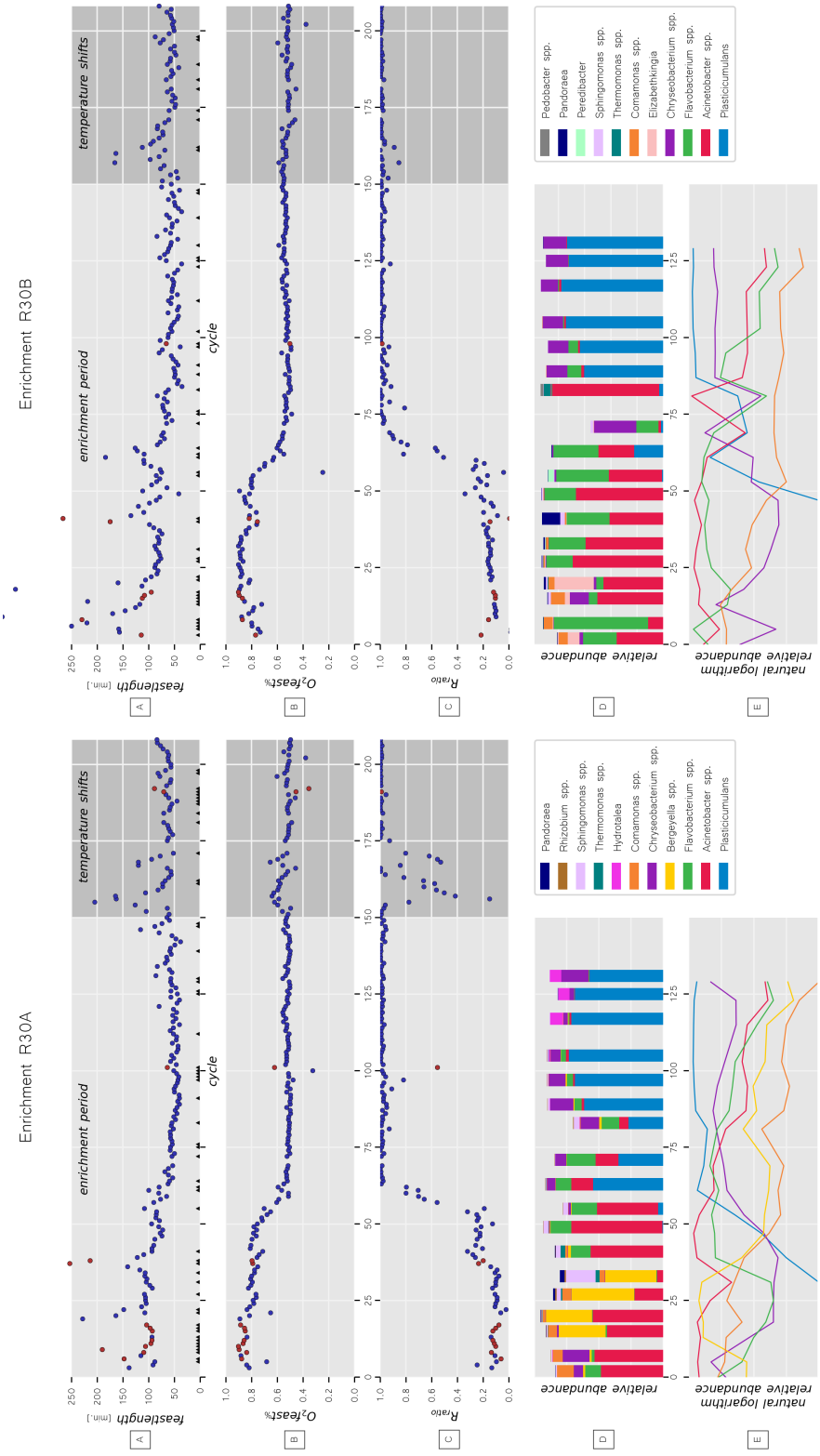
Enrichment R30B
Enrichment R30A
temperature shifts
enrichment period
cycle
feastength [min.]
O2feast%
Rratio
relative abundance
natural logarithm relative abundance
Pedobacter spp.
Pandoraea
Peredibacter
Sphingomonas spp.
Thermomonas spp.
Comamonas spp.
Elizabethkingia
Chryseobacterium spp.
Flavobacterium spp.
Acinetobacter spp.
Plasticicumulans
Rhizobium spp.
Hydrotalea
Bergeyella spp.

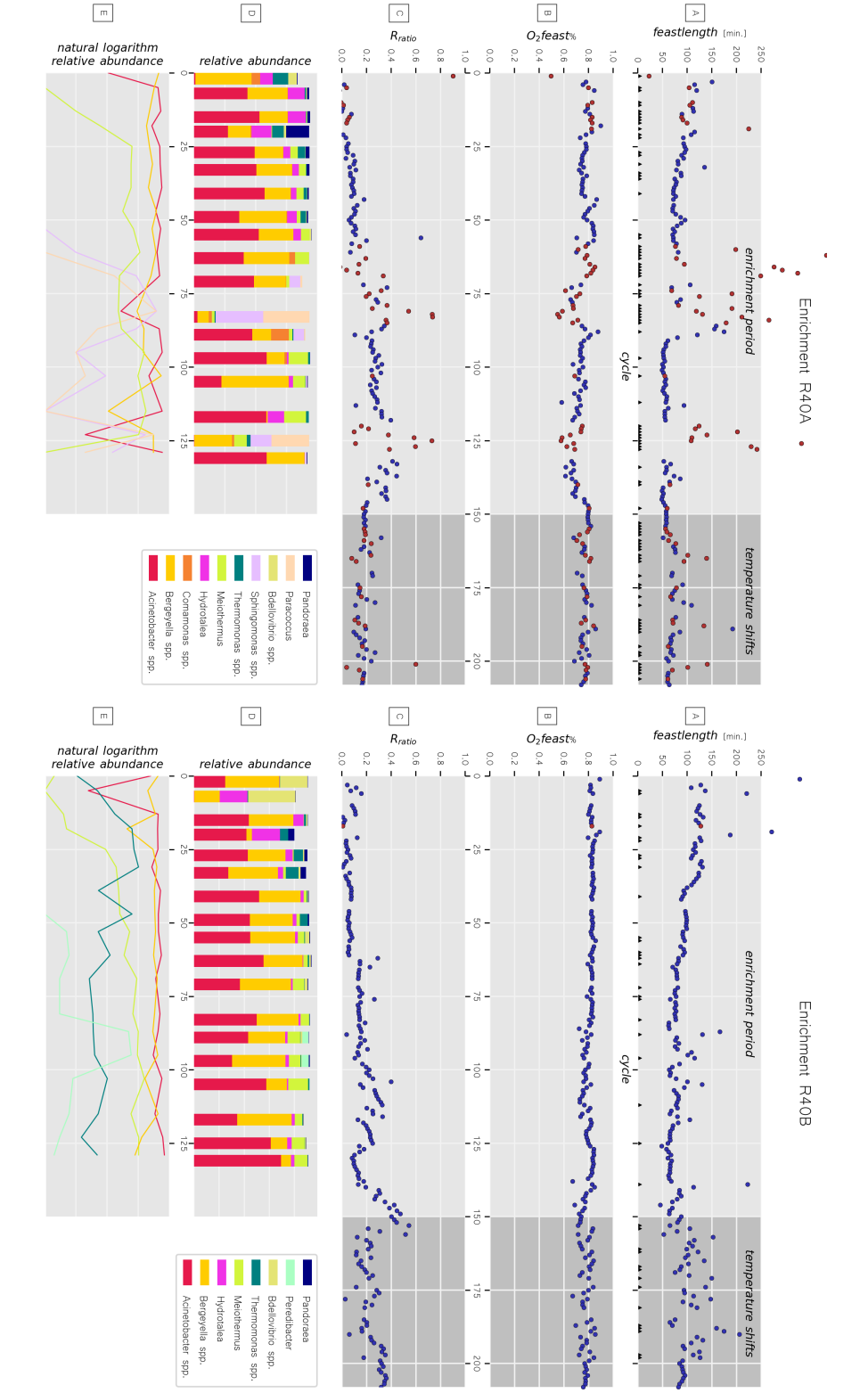
Enrichment R40A
Enrichment R40B
A
B
C
D
E
feastlength [min.]
O_2feast%
R_{ratio}
relative abundance
natural logarithm relative abundance
cycle
enrichment period
temperature shifts
Pandoraea
Paracoccus
Bdellovibrio spp.
Sphingomonas spp.
Thermomonas spp.
Meiothermus
Hydrotalea
Comamonas spp.
Bergeyella spp.
Acinetobacter spp.
Pandoraea
Peredibacter
Bdellovibrio spp.
Thermomonas spp.
Meiothermus
Hydrotalea
Bergeyella spp.
Acinetobacter spp.

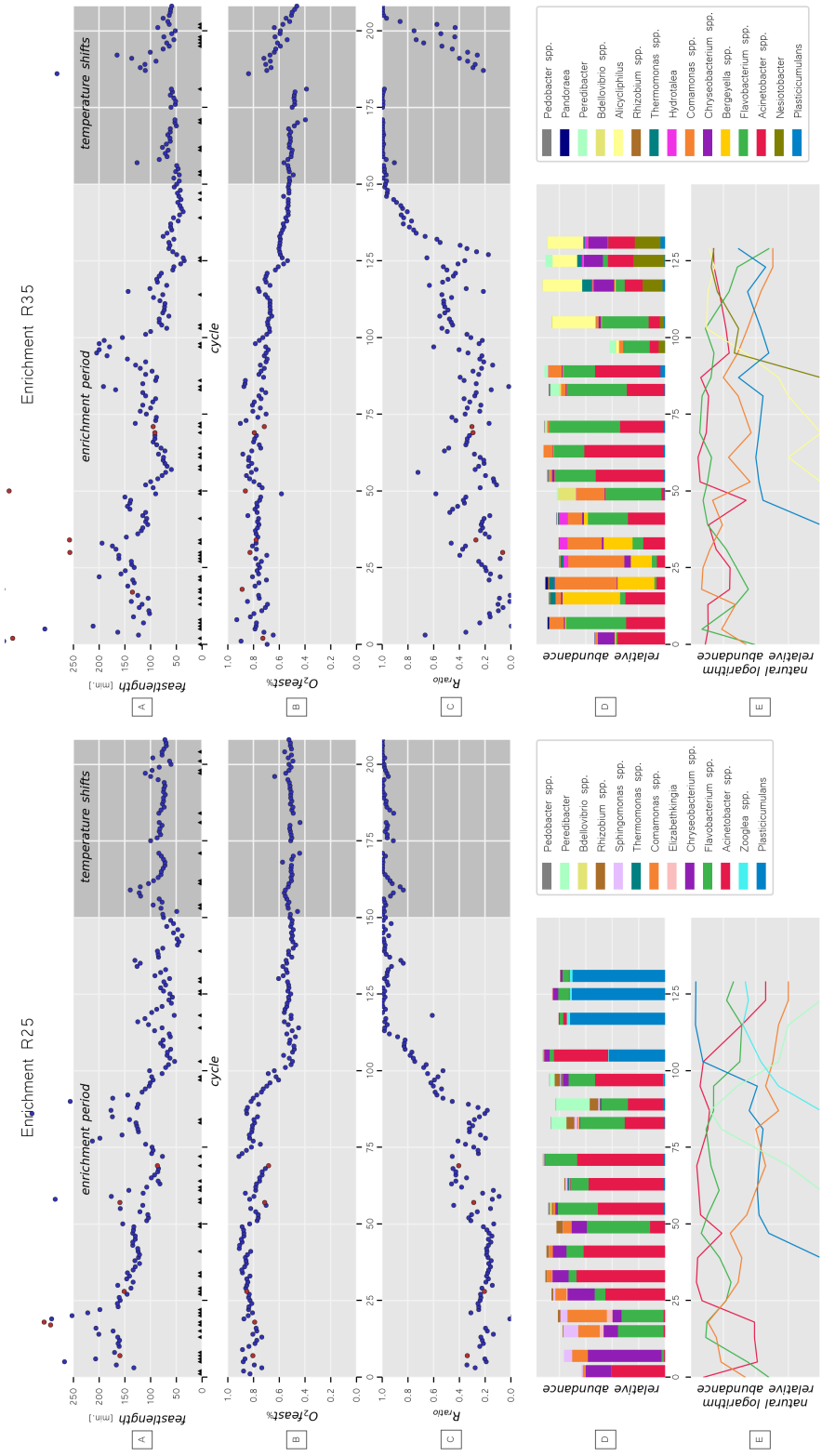
Enrichment R35
Enrichment R25
temperature shifts
enrichment period
cycle
feastength [min.]
O2feast%
Rratio
relative abundance
natural logarithm relative abundance
Pedobacter spp.
Pandoraea
Peredibacter
Bdellovibrio spp.
Alicycliphilus
Rhizobium spp.
Thermomonas spp.
Hydrotalea
Comamonas spp.
Chryseobacterium spp.
Bergeyella spp.
Flavobacterium spp.
Acinetobacter spp.
Nesiotobacter
Plasticicumulans
Sphingomonas spp.
Elizabethkingia
Zoogloea spp.
A
B
C
D
E

3.6.9. PEARSON CORRELATIONS OF FUNCTIONALITY AND ABUNDANCE

Overview of the positive (green) and negative (orange) correlations between the microbial relative abundance and functional characteristics of eight bioreactors: feast length, oxygen consumption in the feast phase ($O2_{feast}$%), and respiration ratio (R_{ratio}). Pearson correlation values (r-values) fall between -1 and +1. The table shows all OTUs that have a significant correlation ($p < 0.01$, $n = 18$) with at least one of the three characteristics. Greyed values score above a p-value of 0.01.

[a] Negative correlation in the feast length indicates an OTU that contributes to a shorter feast length.
[b] Negative correlation in the O2feast% indicates an OTU that consumes less oxygen (of total oxygen) in the feast phase.
[c] Postive correlation in the Rratio indicates an OTU that does not grow significantly during the feast phase.

3.6.10. DOCUMENTED FUNCTIONALITIES OF COMMUNITY MEMBERS

Acinetobacter [20,25,30,35,40]
The genus *Acinetobacter* is well known for its fast-growing behavior, but is also associated with PHA production under nutrient limited conditions [33]. This genus is most likely associated with fast growth on acetate and only with PHB production during the fed-batch experiments.

Plasticicumulans acidivorans [25,30,35]
Plasticicumulans acidivorans is well known for its tremendous PHB producing capabilities of up to 90 wt% and its high biomass specific substrate uptake rate [36].

Zoogloea [20,25]
Zoogloea is a well know hoarding genus able to store up to 75wt% PHB and is often found in colder environments [15].

Chryseombacterium, Flavobacterium [20, 25, 30, 35]
Bergeyella [30, 35, 40], *Elizabethkingia* [20, 25, 35], *Cloacibacterium* [25, 30]
These genera are members of the family of *Flavobacteriaceae,* which is well known for the degradative abilities of macromolecules such as proteins and polysaccharides [32]. These community members are therefore likely associated with degradative abilities and cryptic growth.

Comamonas [20, 25, 30, 35, 40]
The *Comamonas* genus is well known for its PHB degradation capabilities [50] and acetate metabolism. This species might therefore be involved in consuming released PHB. Especially interesting is its presence in R40A, where it increases in relative abundance after *Paracoccus* comes up, which is the only genus in R40A that is directly associated with PHB production.

Sphingomonas [20,25,30,40]
Sphingomonas is associated acetate metabolism [34] and the production of gellan exopolysaccharide, a potential storage polymer [51]. This polymer is only produced during cell growth and at low relative amounts. It is therefore unlikely to be a competitive storage product to PHB but could explain additional respiration in the famine phase.

Paracoccus [40]
Paracoccus is associated with the production of PHB [52]. This is the only genus in the 40°C environment that is positively linked to PHB production. Its short upcoming around cycle 80 and 120 of R40A are reflected by a strong increase in feast length. Indicating that this genus might have a low substrate uptake rate. Its upcoming is followed by a strong increase in *Comamonas,* well known for its PHB degradation capabilities.

Nesiotobacter [35]
Nesiotobacter has been associated with PHB production [53].

Alicyclipilus [35]
Alicyclipilus is generally associated with degradation of cyclic compound polyesters [54]. No studies were found that indicate PHB production by *Alicyclipilus.*

Hydrotalea [30,35,40]
The *Hydrotalea* that comes up at the end of the enrichment in R30A is relatively unknown but is possibly not able to assimilate acetate [35]. It is more likely to grow on cell lysis products.

Meiothermus [40]
The *Meiothermus* genus is associated with the production of high levels of 3-hydroxy fatty acids during growth [55]. These compounds can be used for energy requirements later in the cycle, analogue to *Sphingomanas*' behavior.

Thermomonas [40]
This genus is regularly found in sludge and biofilm systems, but no PHB producing characteristics have been attributed [56].

Bdellovibrio [40]
This genus is strongly associated with parasitizing other Gram-negative bacteria. [57].

REFERENCES

[1] G. R. Stouten, C. Hogendoorn, S. Douwenga, E. S. Kilias, G. Muyzer, and R. Kleerebezem, *Temperature as competitive strategy determining factor in pulse-fed aerobic bioreactors,* The ISME Journal (2019), 10.1038/s41396-019-0495-8.

[2] V. Torsvik, L. Øvreås, and T. F. Thingstad, *Prokaryotic Diversity–Magnitude, Dynamics, and Controlling Factors,* Science **296**, 1064 (2002).

[3] O. X. Cordero and M. F. Polz, *Explaining microbial genomic diversity in light of evolutionary ecology,* Nature Reviews Microbiology **12**, 263 (2014).

[4] S. Mitri and K. Richard Foster, *The Genotypic View of Social Interactions in Microbial Communities,* Annual Review of Genetics **47**, 247 (2013).

[5] M. Carballa, L. Regueiro, and J. M. Lema, *Microbial management of anaerobic digestion: Exploiting the microbiome-functionality nexus,* Current Opinion in Biotechnology **33**, 103 (2015).

[6] A. Briones and L. Raskin, *Diversity and dynamics of microbial communities in engineered environments and their implications for process stability,* Current Opinion in Biotechnology **14**, 270 (2003).

[7] O. Perez-Garcia, G. Lear, and N. Singhal, *Metabolic Network Modeling of Microbial Interactions in Natural and Engineered Environmental Systems,* Frontiers in Microbiology **7** (2016), 10.3389/fmicb.2016.00673.

[8] Y. K. Shin, A. Hiraishi, and J. Sugiyama, *Molecular Systematics of the Genus Zoogloea and Emendation of the Genus,* International Journal of Systematic Bacteriology **43**, 826 (1993).

[9] S. F. Bender, C. Wagg, and M. G. van der Heijden, *An Underground Revolution: Biodiversity and Soil Ecological Engineering for Agricultural Sustainability,* Trends in Ecology & Evolution **31**, 440 (2016).

[10] M. Wagner, A. Loy, R. Nogueira, U. Purkhold, and N. Lee, *Microbial community composition and function in wastewater treatment plants,* Antonie van Leeuwenhoek **81**, 665 (2002).

[11] J. J. Barr, F. R. Slater, T. Fukushima, and P. L. Bond, *Evidence for bacteriophage activity causing community and performance changes in a phosphorus-removal activated sludge: Effects of bacteriophage on activated sludge,* FEMS Microbiology Ecology **74**, 631 (2010).

[12] Y. Chen, J. J. Cheng, and K. S. Creamer, *Inhibition of anaerobic digestion process: A review,* Bioresource Technology **99**, 4044 (2008).

[13] G. R. Stouten, S. Douwenga, C. Hogendoorn, and R. Kleerebezem, *System characterization of dynamic biological cultivations through improved data analysis,* bioRxiv (2021), 10.1101/2021.05.14.442977.

[14] K. Johnson, Y. Jiang, R. Kleerebezem, G. Muyzer, and M. C. M. van Loosdrecht, *Enrichment of a Mixed Bacterial Culture with a High Polyhydroxyalkanoate Storage Capacity,* Biomacromolecules **10**, 670 (2009).

[15] Y. Jiang, L. Marang, R. Kleerebezem, G. Muyzer, and M. C. M. van Loosdrecht, *Effect of temperature and cycle length on microbial competition in PHB-producing sequencing batch reactor,* The ISME Journal **5**, 896 (2011).

[16] Y. Jiang, L. Marang, J. Tamis, M. C. van Loosdrecht, H. Dijkman, and R. Kleerebezem, *Waste to resource: Converting paper mill wastewater to bioplastic,* Water Research **46**, 5517 (2012).

[17] J. Tamis, K. Lužkov, Y. Jiang, M. C. van Loosdrecht, and R. Kleerebezem, *Enrichment of Plasticicumulans acidivorans at pilot-scale for PHA production on industrial wastewater,* Journal of Biotechnology **192**, 161 (2014).

[18] R. Kleerebezem and M. C. van Loosdrecht, *Mixed culture biotechnology for bioenergy production,* Current Opinion in Biotechnology Energy Biotechnology / Environmental Biotechnology, **18**, 207 (2007).

[19] G.-Q. Chen, *A microbial polyhydroxyalkanoates (PHA) based bio- and materials industry,* Chemical Society Reviews **38**, 2434 (2009).

[20] W. V. Vishniac and M. Santer, *The thiobacilli,* Bacteriological reviews **21**, 195 (1957).

[21] J. J. Beun and K. Dircks, *Poly-b-hydroxybutyrate metabolism in dynamically fed mixed microbial cultures,* Water Research , 14 (2002).

[22] K. Johnson, R. Kleerebezem, and M. C. van Loosdrecht, *Model-based data evaluation of polyhydroxybutyrate producing mixed microbial cultures in aerobic sequencing batch and fed-batch reactors,* Biotechnology and Bioengineering **104**, 50 (2009).

[23] L. Marang, M. C. van Loosdrecht, and R. Kleerebezem, *Combining the enrichment and accumulation step in non-axenic PHA production: Cultivation of Plasticicumulans acidivorans at high volume exchange ratios,* Journal of Biotechnology **231**, 260 (2016).

[24] H. J. Kuhn, S. Cometta, and A. Fiechter, *Effects of Growth Temperature on Maximal Specific Growth Rate, Yield, Maintenance,and Death Rate in Glucose-LimitedContinuous Culture of the Thermophilic Bacillus ca/dotenax,* Applied Microbiology and Biotechnology , 13 (1980).

[25] P. Verheijen, *Data Reconciliation and Error Detection,* in *The Metabolic Pathway Engineering Handbook*, edited by C. Smolke (CRC Press, 2009).

[26] J. G. Caporaso, C. L. Lauber, W. A. Walters, D. Berg-Lyons, J. Huntley, N. Fierer, S. M. Owens, J. Betley, L. Fraser, M. Bauer, N. Gormley, J. A. Gilbert, G. Smith, and R. Knight, *Ultra-high-throughput microbial community analysis on the Illumina HiSeq and MiSeq platforms,* The ISME Journal **6**, 1621 (2012).

[27] R. C. Edgar, *Search and clustering orders of magnitude faster than BLAST,* Bioinformatics **26**, 2460 (2010).

[28] J. G. Caporaso, J. Kuczynski, J. Stombaugh, K. Bittinger, F. D. Bushman, E. K. Costello, N. Fierer, A. G. Peña, J. K. Goodrich, J. I. Gordon, G. A. Huttley, S. T. Kelley, D. Knights, J. E. Koenig, R. E. Ley, C. A. Lozupone, D. McDonald, B. D. Muegge, M. Pirrung, J. Reeder, J. R. Sevinsky, P. J. Turnbaugh, W. A. Walters, J. Widmann, T. Yatsunenko, J. Zaneveld, and R. Knight, *QIIME allows analysis of high-throughput community sequencing data,* Nature methods **7**, 335 (2010).

[29] R. C. Edgar, *MUSCLE: Multiple sequence alignment with high accuracy and high throughput,* Nucleic Acids Research **32**, 1792 (2004).

[30] J. P. Brooks, D. J. Edwards, M. D. Harwich, M. C. Rivera, J. M. Fettweis, M. G. Serrano, R. A. Reris, N. U. Sheth, B. Huang, P. Girerd, J. F. Strauss, K. K. Jefferson, and G. A. Buck, *The truth about metagenomics: Quantifying and counteracting bias in 16S rRNA studies,* BMC Microbiology **15** (2015), 10.1186/s12866-015-0351-6.

[31] R. Sinha, G. Abu-Ali, E. Vogtmann, A. A. Fodor, B. Ren, A. Amir, E. Schwager, J. Crabtree, S. Ma, C. C. Abnet, R. Knight, O. White, and C. Huttenhower, *Assessment of variation in microbial community amplicon sequencing by the Microbiome Quality Control (MBQC) project consortium,* Nature Biotechnology (2017), 10.1038/nbt.3981.

[32] M. J. McBride, *The Family Flavobacteriaceae,* in *The Prokaryotes: Other Major Lineages of Bacteria and The Archaea*, edited by E. Rosenberg, E. F. DeLong, S. Lory, E. Stackebrandt, and F. Thompson (Springer, Berlin, Heidelberg, 2014) pp. 643–676.

[33] K. J. Towner, E. Bergogne-Bérézin, and C. A. Fewson, *Acinetobacter: Portrait of a Genus,* in *The Biology of Acinetobacter: Taxonomy, Clinical Importance, Molecular Biology, Physiology, Industrial Relevance*, Federation of European Microbiological Societies Symposium Series, edited by K. J. Towner, E. Bergogne-Bérézin, and C. A. Fewson (Springer US, Boston, MA, 1991) pp. 1–24.

[34] J. Tamaoka, D. Ha, and K. Komagata, *Reclassification of Pseudomonas acidovorans den Dooren de Jong 1926 and Pseudomonas testosteroni Marcus and Talalay 1956 as Comamonas acidovorans comb. nov. and Comamonas testosteroni comb. nov., with an Emended Description of the Genus Comamonas,* (1987), 10.1099/00207713-37-1-52.

[35] P. Kämpfer, N. Lodders, and E. Falsen, *Hydrotalea flava gen. nov., sp. nov., a new member of the phylum Bacteroidetes and allocation of the genera Chitinophaga, Sediminibacterium, Lacibacter, Flavihumibacter, Flavisolibacter, Niabella, Niastella, Segetibacter, Parasegetibacter, Terrimonas, Ferruginibacter, Filimonas and Hydrotalea to the family Chitinophagaceae fam. nov.* International Journal of Systematic and Evolutionary Microbiology **61**, 518 (2011).

[36] Y. Jiang, D. Y. Sorokin, R. Kleerebezem, G. Muyzer, and M. van Loosdrecht, *Plasticicumulans acidivorans gen. nov., sp. nov., a polyhydroxyalkanoate-accumulating gammaproteobacterium from a sequencing-batch bioreactor,* International Journal of Systematic and Evolutionary Microbiology **61**, 2314 (2011).

[37] K. Johnson, J. van Geest, R. Kleerebezem, and M. C. M. van Loosdrecht, *Short- and long-term temperature effects on aerobic polyhydroxybutyrate producing mixed cultures,* Water Research **44**, 1689 (2010).

[38] S. Arrhenius, *über die Reaktionsgeschwindigkeit bei der Inversion von Rohrzucker durch Säuren,* Zeitschrift für Physikalische Chemie **4U** (1889), 10.1515/zpch-1889-0416.

[39] J. J. Heijnen and R. Kleerebezem, *Bioenergetics of Microbial Growth,* in *Encyclopedia of Industrial Biotechnology* (John Wiley & Sons, Inc., Hoboken, NJ, USA, 2010) p. eib084.

[40] J. M. Chacón and W. R. Harcombe, *Antimicrobials: Constraints on microbial warfare,* Nature Microbiology **1**, 16225 (2016).

[41] T. Baba and O. Schneewind, *Instruments of microbial warfare: Bacteriocin synthesis, toxicity and immunity,* Trends in Microbiology **6**, 66 (1998).

[42] A. Aertsen and C. W. Michiels, *Stress and How Bacteria Cope with Death and Survival,* Critical Reviews in Microbiology **30**, 263 (2004).

[43] L. Tijhuis, M. C. M. Van Loosdrecht, and J. J. Heijnen, *A thermodynamically based correlation for maintenance gibbs energy requirements in aerobic and anaerobic chemotrophic growth,* Biotechnology and Bioengineering **42**, 509 (1993).

[44] M. C. M. Van Loosdrecht and M. Henze, *Maintenance, endogeneous respiration, lysis, decay and predation,* Water Science and Technology Modelling and Microbiology of Activated Sludge Processes, **39**, 107 (1999).

[45] J. D. Oliver, *Recent findings on the viable but nonculturable state in pathogenic bacteria,* FEMS Microbiology Reviews **34**, 415 (2010).

[46] Y. Jiang, L. Marang, R. Kleerebezem, G. Muyzer, and M. C. van Loosdrecht, *Polyhydroxybutyrate production from lactate using a mixed microbial culture,* Biotechnology and Bioengineering **108**, 2022 (2011).

[47] G. R. Stouten, *ExploDiv - Temperature Dataset (200 cycles, 8 reactors),* (2018).

[48] S. J. Pirt and C. N. Hinshelwood, *The maintenance energy of bacteria in growing cultures,* Proceedings of the Royal Society of London. Series B. Biological Sciences **163**, 224 (1965).

[49] D. Herbert, *Some principles of continuous culture,* in *Recent Progress in Microbiology, VII International Congress for Microbiology* (1958) pp. 381–396.

[50] D. Jendrossek and R. Handrick, *Microbial Degradation of Polyhydroxyalkanoates,* Annual Review of Microbiology **56**, 403 (2002).

[51] D. Lobas, S. Schumpe, and W. D. Deckwer, *The production of gellan exopolysaccharide with Sphingomonas paucimobilis E2 (DSM 6314),* Applied Microbiology and Biotechnology **37**, 411 (1992).

[52] M. A. van Aalst-van Leeuwen, M. A. Pot, M. C. van Loosdrecht, and J. J. Heijnen, *Kinetic modeling of poly(beta-hydroxybutyrate) production and consumption by Paracoccus pantotrophus under dynamic substrate supply,* Biotechnology and Bioengineering **55**, 773 (1997).

[53] L. Villanueva, J. Del Campo, and R. Guerrero, *Diversity and physiology of polyhydroxyalkanoate-producing and -degrading strains in microbial mats,* FEMS Microbiology Ecology **74**, 42 (2010).

[54] L. F. Pérez-Lara, M. Vargas-Suárez, N. N. López-Castillo, M. J. Cruz-Gómez, and H. Loza-Tavera, *Preliminary study on the biodegradation of adipate/phthalate polyester polyurethanes of commercial-type by* Alicycliphilus *sp. BQ8,* Journal of Applied Polymer Science **133**, n/a (2016).

[55] A. P. Chung, F. Rainey, M. F. Nobre, J. Burghardt, and M. S. D. Costa, *Meiothermus cerbereus sp. nov., a New Slightly Thermophilic Species with High Levels of 3-Hydroxy Fatty Acids,* International Journal of Systematic Bacteriology **47**, 1225 (1997).

[56] J. Mergaert, *Thermomonas fusca sp. nov. and Thermomonas brevis sp. nov., two mesophilic species isolated from a denitrification reactor with poly(-caprolactone) plastic granules as fixed bed, and emended description of the genus Thermomonas,* International Journal of Systematic and Evolutionary Microbiology **53**, 1961 (2003).

[57] J. J. Germida, *Isolation of Bdellovibrio spp. that prey on Azospirillum brasilense in soil,* Canadian Journal of Microbiology (2011), 10.1139/m87-076.

4

SEEMINGLY TRIVIAL SECONDARY FACTORS MAY DETERMINE MICROBIAL COMPETITION:

A CAUTIONARY TALE ON THE IMPACT OF IRON SUPPLEMENTATION THROUGH CORROSION.

Gerben Roelandt STOUTEN, Kelly HAMERS, Rinke Johanna VAN TATENHOVE-PEL, Eline VAN DER KNAAP, Robbert KLEEREBEZEM

Microbial community engineering aims for enrichment of a specific microbial trait by imposing specific cultivation conditions. This work demonstrates that things may be more complicated than typically presumed and that microbial competition can be affected by seemingly insignificant variables, like in this case the type of acid used for pH control. Aerobic bioreactors pulse fed with acetate operated with hydrochloric acid resulted in the enrichment of Plasticicumulans acidivorans*, and changing the pH controlling agent to sulfuric acid shifted the community towards* Zoogloea sp. *Further research demonstrated that the change in community structure was not directly caused by the change in acid used for pH control, but resulted from the difference in corrosive strength of both acids and the related iron leaching from the bioreactor piping. Neither system was iron deficient, suggesting that the biological availability of iron is affected by the leaching process. Our results demonstrate that microbial competition and process development can be affected dramatically by secondary factors related to nutrient supply and bioavailability, and is way more complex than generally assumed in a single carbon substrate limited process.*

Parts of this chapter have been published as Stouten *et al.* [1].

4.1. INTRODUCTION

Microbial community engineering (MCE) utilizes ecological selection principles to enrich microbial communities with specific functional properties, e.g. the production of chemicals and bioenergy [2]. MCE finds its roots in the work of Baas Becking: "Everything is everywhere, but the environment selects" [3]. By using selective environments, we aim to enrich and maintain microbial communities with desired functionalities under non-axenic, i.e. open, conditions. MCE can contribute to the circular economy and valorize non-sterilized mixed substrate streams, thereby unlocking the tremendous carbon and energy resources originating from heterogeneous feedstocks currently regarded as waste streams.

In general, laboratory enrichment studies are designed with the idea in mind that one substrate is present in the influent in a rate determining concentration. Typically, in selective conditions favoring heterotrophic growth, the limiting substrate is the carbon and energy source. All other essential growth nutrients are supplied in excess with the objective to characterize the process as a function of a single substrate limitation. In this way, microbial competition is assumed to be investigated as a function of a single variable, and conclusions can be drawn in terms of the dependency of system development on this variable. For example, the competition in chemostat enrichment experiments generally is assumed to be determined by the affinity for one limiting substrate. To which extent this assumption holds true is rarely verified due to the large number of medium constituents that would need to be tested. Nevertheless, it remains largely unclear if microbial ecosystem development depends on the concentration and bioavailability of secondary substrates such as trace elements.

In this work we describe our analysis of an unanticipated secondary limitation encountered in experiments aiming for enrichment of a polyhydroxyalkanoates (PHA) producing microbial community. PHA is a polymer with chemical properties that make it an interesting bioplastic that is fully biodegradable [4, 5]. Enrichment of PHA producing microorganisms can be established by aerobic cultivation in alternating presence and absence of the carbon substrate. Over the past 10 years, this strategy was shown repeatedly to enable the effective enrichment of the superior PHA-producer *Plasticicumulans acidivorans* from sewage sludge, and it has been elemental to mixed culture PHA research [6–10]. Typically, the enrichment of *P. acidivorans* from activated sludge can be established within 30 generations [10]. In a new attempt to enrich for *P. acidivorans* we operated a Sequencing Batch Bioreactor (SBR) for more than 60 generations. Although conditions known to enable effective enrichment of *P. acidivorans* were applied, no enrichment of *P. acidivorans* was established and the functional performance in terms of substrate conversion rates was markedly different. The sole operational difference with previous systems was the choice of acid used for pH control; Previous enrichments were conducted with HCl, while in this enrichment H_2SO_4 was used. Based on this observation we decided to investigate in more detail the role of the type of acid used for pH control in the process, with the objective to identify the secondary factors that determine enrichment and functional process development.

4.2. MATERIALS AND METHODS

4.2.1. SEQUENCING BATCH BIOREACTOR OPERATION

Two microbial enrichments using acetate as carbon source and electron donor, and oxygen as electron acceptor, were established in sequencing batch bioreactors (SBR) under a feast-famine regime at 30 °C, pH 7, cycle length 12 hours, and exchange ratio of 50%. This operation results in a solid retention time (SRT) of approximately 24 hours. The reactor set-up and operation are described in detail by Johnson *et al.* [6]. Bioreactors were inoculated with activated sludge from a sewage treatment facility (Harnaschpolder, Delft, the Netherlands), and were operated at a working volume of 1.4 L (Applikon the Netherlands), where each cycle started with 5 minutes of discharging 700 mL of mixed reactor content, feeding 640 mL of demineralized water, 20 mL of nutrient medium (250 mM NH_4Cl, 25 mM KH_2PO_4 , 6.25 mM $MgSO_4{\cdot}7H_2O$, 7.50 mM KCl, 50 mL L^{-1} trace elements solution [11]), and after one hour a 20 mL carbon pulse (1 M sodium acetate) is dosed in 1 minute. Throughout the cycle approximately 20 mL of acid and base is dosed for pH control, resulting in the final volume of 1.4 L. The stability of the cultures in terms of conversion rates and microbial community composition was monitored by regular sampling and via online monitoring of off-gas composition and acid and base (0.5 M NaOH) dosage. The two main enrichment bioreactor systems were operated in an identical fashion with the exception of acid source for pH control. SBR_{HCl} and $SBR_{H_2SO_4}$ were operated with 1 M HCl, and 0.5 M H_2SO_4 as acid dosing agent respectively.

4.2.2. SHIFT EXPERIMENTS

During the effluent phase of each operational cycle, half of the reactor content is discharged. This broth was used as the starting culture (inoculum) for shift experiments in three separate bioreactors without disturbing the enrichments. Transfer of half of the biomass to a new bioreactor was verified to result in highly comparable performance in both bioreactors. Shift experiments are operated as identical replicates of the main enrichments, except for a single change in medium composition. Eight types of shift experiments were performed where the acid dosing agent was changed or different salts were added to the medium (Table 4.1). Shift experiments were operated for at least twenty operational cycles, after the initial change in medium composition.

In some of the shift experiments specific trace metals were dosed throughout the cycle from three stock solutions: 1.5 mM $CrK(SO_4)_2.2H_2O$, 1 mM $NiSO_4.H_2O$, and 5 mM $Fe(II)Cl_2$. Titration was conducted through continuous dosing at 0.42 mL h^{-1} (5 mL per cycle). If no response was observed within 5 cycles, the flow rate was gradually increased to 1.67 mL h^{-1}.

4.2.3. ANALYTICAL PROCEDURES

Samples from the reactor for analysis of acetate, ammonium, iron, chromium, and nickel were immediately centrifuged (2 min. 10.000g) and filtered after sampling (0.45 µm pore size poly-vinylidene difluoride membrane, Merck Millipore, Carrigtohill, Ireland). The acetate concentration was measured by HPLC (BioRad Aminex HPX-87H column, Waters 2489 UV/RI detector, 1.5mM H_3PO_4 mobile phase with a flow rate of 0.6 mL min^{-1} and a temperature of 60 °C). Ammonium, iron (II/III), chromium and nickel concentra-

Table 4.1: Operational changes in acid, salt, and metal added during shift experiments

Shift	Origin	Acid	Salt
1[a]	SBR_{HCl}	H_2SO_4	
2[a]	$SBR_{H_2SO_4}$	HCl	
3[b]	SBR_{HCl}	HCl	Na_2SO_4
4[b]	$SBR_{H_2SO_4}$	H_2SO_4	NaCl
5[b]	SBR_{HCl}	H_2SO_4	NaCl
6[c]	SBR_{HCl}	H_2SO_4	$Ni(II)SO_4.H_2O$
7[c]	SBR_{HCl}	H_2SO_4	$Cr(III)K(SO_4)_2.2H_2O$
8[c]	SBR_{HCl}	H_2SO_4	$Fe(II)Cl_2$

[a] Acid shift experiment where HCl and H_2SO_4 are interchanged
[b] Anion change experiment with chloride and sulfate
[c] Metal leaching experiment with artificial leaching substrates

tions were determined spectrophotometrically using cuvette test kits (Hach Lange, Düsseldorf, Germany). The chromium, nickel, and iron concentrations were determined after digestion at a pH of 2, for 60 minutes at 100 °C. PHA content was measured as described by Johnson, Yang et al. 2009. Concentrations of N_2, O_2, Argon and CO_2 in the off-gas of the reactor were measured online using mass spectrometry (Prima BT, Thermo Scientific).

4.2.4. CALCULATIONS

Characterization of biological functioning of the microbial community is performed by reconstructing the oxygen uptake rate and carbon evolution rate profiles in each cycle based on online gas measurements as described in Stouten *et al.* [12]. Online characterization allows discerning the extent of growth and PHA production in a cycle by correlating an increase in respiration activity with growth, and respiration in absence of extracellular substrate with metabolism of PHA. For all calculations the carbon mass balance and electron balance close within 95%.

4.2.5. MICROBIAL COMMUNITY STRUCTURE AND MICROSCOPY

The taxa-based microbial community composition of the enriched cultures was determined by amplicon sequencing of the 16S rRNA gene following the procedure described in Stouten *et al.* [10] and the sequences are available at NCBI under BioProject accession number [PRJNA577272].

Microscopy pictures were taken using a Leica DM500B light microscope (Leica Microsystems, Wetzlar, Germany) equipped with fluorescence filtercube A. 1 µl BODIPY 505/515 (Invitrogen D3921, Life Technologies, Grand Island, USA) in DMSO (1 mg ml^{-1}) was used to stain PHA inclusion bodies in bacterial cells in 1 mL bioreactor sample.

4.3. RESULTS

4.3.1. PRELIMINARY RESULTS GIVING RISE TO THE RESEARCH DESCRIBED IN THIS PAPER

In an attempt to establish a PHA producing microbial community dominated by *P. acidivorans*, an SBR was inoculated with activated sludge and operated at 30 °C, pH 7, and a cycle length of 12 h. This strategy had repeatedly been demonstrated to enable *P. acidivorans* enrichment. However, in this case *P. acidivorans* was not observed as dominant community member and the functional behavior of the community as reflected in the dissolved oxygen patterns throughout the cycle was markedly different from *P. acidivorans* dominated enrichments, despite prolonged enrichment (Figure 4.1). The only operational difference we could identify from previous enrichment efforts was the acid used for pH control: H_2SO_4 was used in this study to minimize corrosion of the bioreactor-inlet, whereas we used HCl in the past. To investigate if the used acid determined the community structure and function, two new enrichments were started with HCl and H_2SO_4 as pH controlling agent.

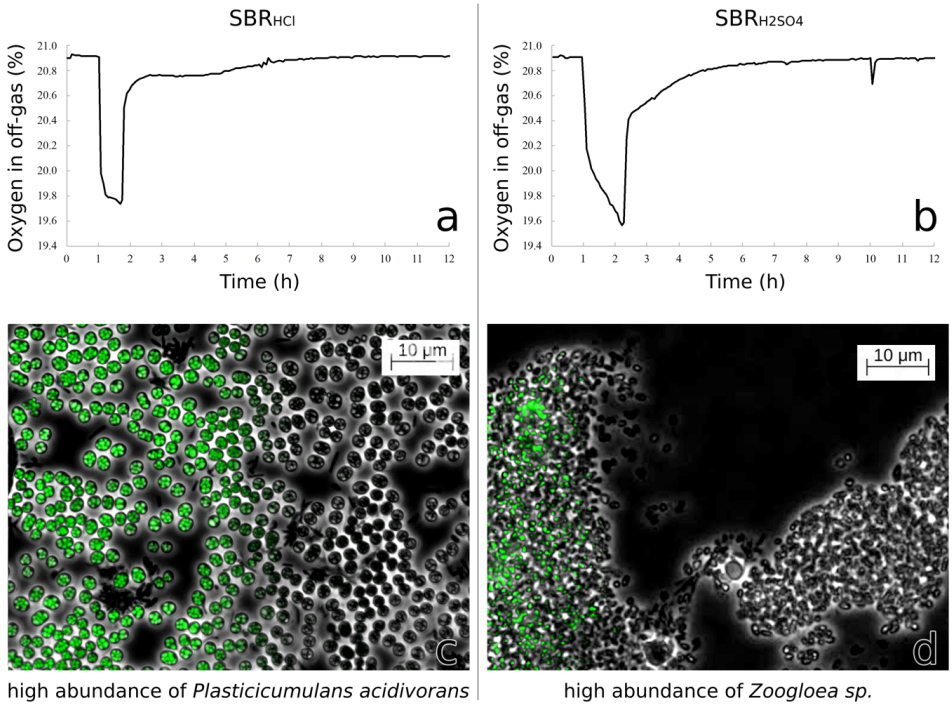

Figure 4.1: Respiration profiles and microbial morphological differences between the enrichment of SBR_{HCl} (left) and $SBR_{H_2SO_4}$ (right). The oxygen off-gas profiles during steady state cycles are shown at the top (a,b). Microscopic images of the microbial cultures at the end of the feast phase in dark field and fluorescent BODIPY 505/515 PHA staining are shown half overlapping to clearly show the PHA granules (green) and the cellular morphology differences between the enriched microbial cultures (c, d).

4.3.2. DIFFERENCES BETWEEN STEADY STATE ENRICHMENTS WITH HCL AND H_2SO_4 AS ACID USED FOR PH CONTROL

Two microbial communities were enriched from activated sludge using acetate as carbon source and electron donor, and oxygen as electron acceptor. The sequencing batch reactors (SBR) were operated for 90 days resulting in the development of a feast-famine regime. Operationally, the only difference between system SBR_{HCl} and $SBR_{H_2SO_4}$ was the choice of acid for pH control, hydrochloric acid and sulfuric acid respectively. Both enrichments achieved a pseudo steady state characterized by constant conversion rates and yields (within 5% variation) (Table 4.2). Sequencing of the 16S rRNA genes of the microbial community demonstrated enrichment of stable communities dominated by *Plasticicumulans acidivorans* in SBR_{HCl} and *Zoogloea sp.* in $SBR_{H_2SO_4}$ (Figure 4.2). Morphological differences between the two genera were clearly observed through microscopy (Figure 4.1).

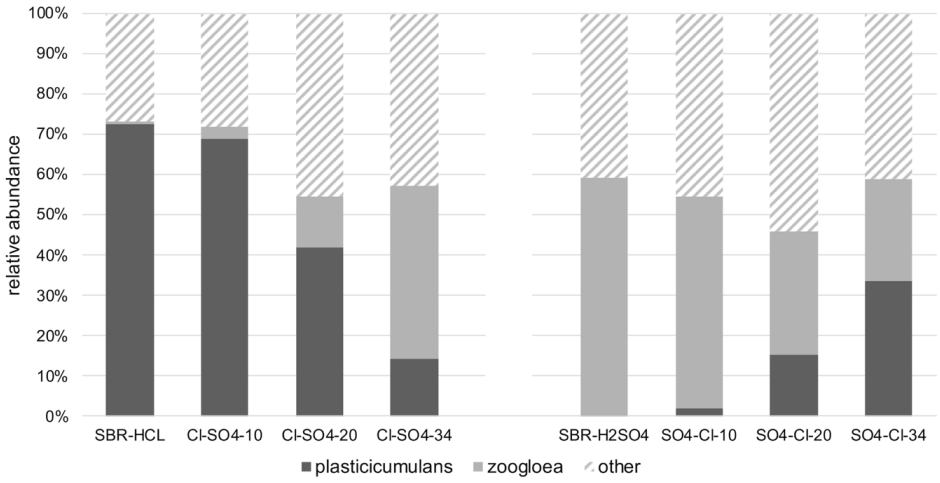

Figure 4.2: Relative abundance of 16S rRNA genes of *Plasticicumulans* and *Zoogloea* genera at several timepoints. SBR_{HCl} and $SBR_{H_2SO_4}$ represent the relative community structure at the end of the enrichment period. The three following samples indicate samples at 10, 20, and 34 cycles after switching the relative acids for pH control. For graphing purposes, all other genera are combined under *other*, a more detailed overview of the relative community structure is given in Supplementary Materials Figure 4.10 and Figure 4.11.

Functionally, SBR_{HCl} showed the typical hoarding strategy (Stouten et al. 2019). During the feast phase, carbon was converted into PHA within 40 minutes, and negligible growth occurred during substrate uptake as reflected in negligible ammonium uptake and a constant respiration rate (Figure 4.2). New catalytic biomass was produced in the famine phase, where storage polymers were converted into new biomass in the absence of an extracellular carbon source.

$SBR_{H_2SO_4}$ showed a mixed behavior, where storage polymers and catalytic biomass were produced during the 80 minutes feast phase, significant ammonium was taken up and the respiration rate increased (Figure 4.1 and Table 4.2). In the famine phase the stored polymers were converted into catalytic biomass.

Table 4.2: Overview of the characteristic differences between the enrichment of SBR_{HCl} and $SBR_{H_2SO_4}$. Standard deviations of 8 cycles in parenthesis.

	unit	SBR_{HCl}	$SBR_{H_2SO_4}$
Dominant species	-	*P. acidivorans*	*Zoogloea sp.*
Length of feast phase	min.	40 (4)	80 (6)
Respiration ratio [a]	%	90 (3)	60 (5)
Ammonium consumed in feast [b]	%	5 (1)	38 (6)
Oxygen consumption in feast [b]	%	47 (4)	60 (5)
PHA end feast [c]	%	52 (3)	30 (7)
Maximum PHA accumulation [c]	%	89	78

[a] Ratio of oxygen transfer rate at the start of the feast-phase to the end of the feast-phase

[b] Percentage of the total ammonium or oxygen consumed throughout the cycle

[c] Weight percentage (g g_{DW}^{-1}) of PHA of volatile suspended solids (VSS) [13]

4

4.3.3. INVERTING THE ACIDS USED FOR PH CONTROL

Biomass from SBR_{HCl} and $SBR_{H_2SO_4}$ was used as inoculum for two additional bioreactors switching HCl with H_2SO_4 and vice versa. The microbial community structure in both systems shifted, demonstrating that the acid used for pH control determined the microbial community structure established, in a comparable timeframe (Figure 4.2). Also, a shift in functionality of both systems was observed in response to the change in acid used for pH control (Table 4.1), but in a different timeframe (Figure 4.3). $SBR_{H_2SO_4 \rightarrow HCl}$ showed a gradual shift in functionality as reflected by the decrease in the length of the feast phase, which was accompanied by a corresponding increase in relative abundance of *P. acidivorans*. $SBR_{HCl \rightarrow H_2SO_4}$ showed a rapid increase in length of the feast phase (within 5 cycles comparable to $SBR_{H_2SO_4}$), but the microbial community remained dominated by *P. acidivorans* for at least 20 cycles after the switch from HCl to H_2SO_4. After 20 cycles, microscopy showed a decrease in community dominance of *P. acidivorans*, and after 34 cycles a shift towards a *Zoogloea sp.* dominated culture had occurred as supported by 16S rRNA gene sequencing (Figure 4.2).

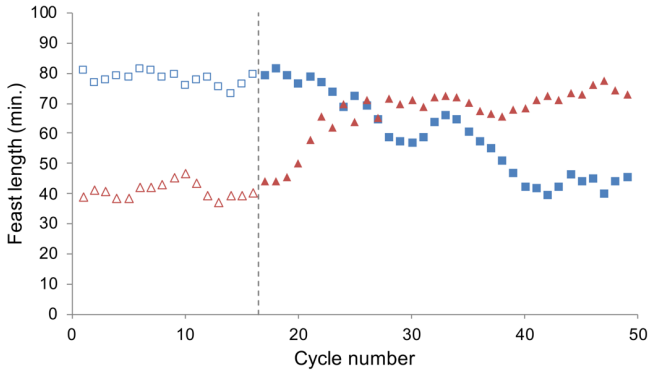

Figure 4.3: Change in feast length of SBR_{HCl} (red triangles) and $SBR_{H_2SO_4}$ (blue squares) when switching their respective acids for pH control. Open figures represent the steady state feast length of fifteen cycles prior to the acid shift, the dashed line at cycle 16 indicates the moment where the acids were changed.

Switching within 20 cycles the acid agent in $SBR_{HCl \rightarrow H_2SO_4}$ back to HCl reduced the length of the feast phase to the original values of SBR_{HCl} within two operational cycles (Figure 4.4). This nearly instantaneous change in functionality occurred even though a shift in the microbial community was only observed after 10 generations. This response was achieved repeatedly with biomass from SBR_{HCl} when the acid used for pH control was changed to H_2SO_4. We define this period as the transition state; a state in which the microbial community of SBR_{HCl} was not perceived to have changed, but the functionality did change as a result of the switch in acid agent.

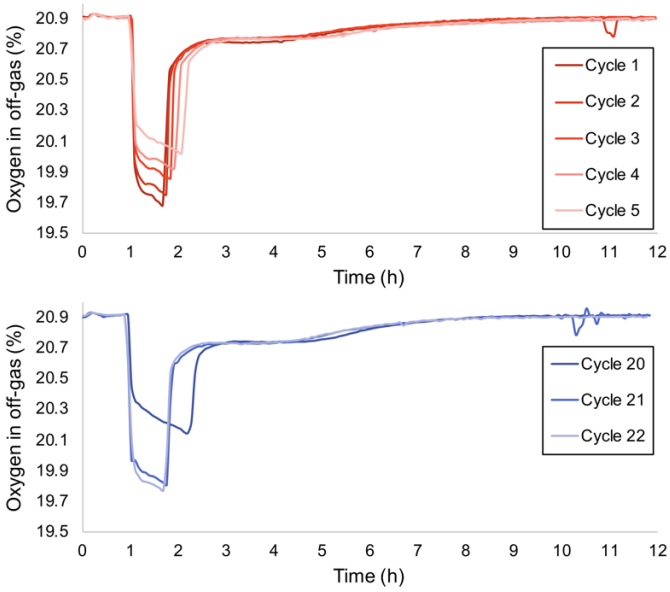

Figure 4.4: Overlay of oxygen off-gas profiles of SBR_{HCl} after switching from HCl to H_2SO_4 for acid control (top - red) and switching back to HCl (bottom - blue) after 20 cycles of operation with H_2SO_4. Color gradient from dark to light indicates sequential cycles. In the HCl controlled system the feast length initially takes around 40 minutes, but increases to 80 minutes over 5 cycles when switching to H_2SO_4. The longer feast length, lower initial respiration rate, and increasing respiration activity during the feast phase indicate a functional shift from solely PHA production to mixed PHA production and catalytic biomass production as detailed in Figure 4.1.

4.3.4. CHLORIDE AND SULFATE IONS

Switching the acid agent for pH control between HCl and H_2SO_4 results in a change in anions concentration in the reactor broth. Additionally, the divalent sulfate ions result in a slightly lower ionic strength compared to monovalent chlorine. To investigate the impact of the dominant anions in the system, sulfate and chloride sodium-salts were added to the medium of SBR_{HCl} and $SBR_{H_2SO_4}$ respectively. By these means the eventual salt composition and concentration were identical in both systems. The process performance and microbial community structure in SBR_{HCl} was not affected by supplementing the medium with Na_2SO_4 during 50 operational cycles (data not shown). The enrichment performance of the $SBR_{H_2SO_4}$ changed slightly with the addition of 20 mM NaCl as reflected in a feast length reduction from 80 to 75 min after 15 cycles. Overall,

only a minor functional effect of the salt composition and concentration was observed. From these experiments it was concluded that the dominant anion in the process could not explain the differences in microbial community structure and operational properties between SBR_{HCl} and $SBR_{H_2SO_4}$.

4.3.5. ABIOTIC METAL PITTING CORROSION

The reason for switching from HCl to H_2SO_4 during cultivation was to reduce the corrosive effect of HCl on the stainless-steel inlet feed triplet of the bioreactors (SAE 316L stainless steel, Applikon, Delft, The Netherlands) (Kovach 2002). The triplets needed to be replaced every 6-8 months when operated with 1 M HCl due to corrosion induced leakage (Figure 4.5 left). A secondary effect of the corrosion is the leaching of trace metals in the fermentation broth. To investigate how much trace metals are added over time, small parts from a leaking inlet triplet were cut off using electrical pliers and immersed in the acids that were used for pH control, 1 M HCl and 0.5 M H_2SO_4. Over a period of 30 days an obvious change due to corrosion of steel was observed in the HCl bottle: the clear acid solution became blue and the metal part turned black. The liquid and metal in the bottle with H_2SO_4 remained visually unaffected (Figure 4.5 right).

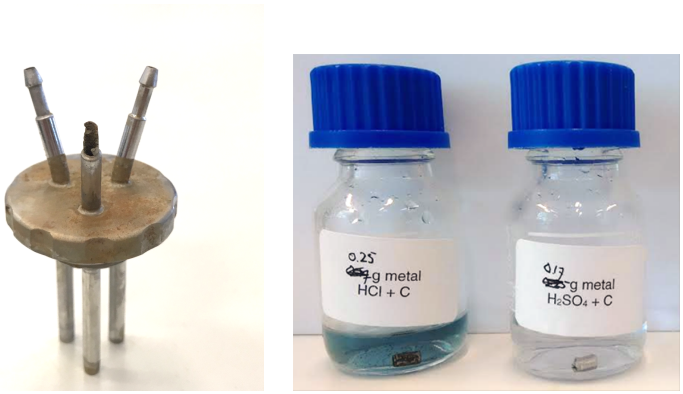

Figure 4.5: Photographs of an inlet triplet (left) of which the acid inlet is significantly corroded, and two acid bottles (right) with 5 mL 1 M HCl, and 5 mL 0.5 M H_2SO_4 with a small piece of 316L reactor metal after 30 days.

From the chemical composition of 316L stainless steel (Supplementary Materials Table 4.3), iron, chromium, and nickel are present in significant quantities (>10 wt%) and are therefore the most likely candidates to have an impact on the microbial cultures [14]. The concentrations in the HCl bottle after 30 days were determined to be 4.6 mM Fe, 1.4 mM Cr, and 0.8 mM Ni. Concentrations in the H_2SO_4 bottle were below the detection limit (chromium <0.5 µM, nickel <1.6 µM), except for iron which was determined to be 50 µM. Approximate calculations suggest that operation of the SBR with 1M HCl can result in a leaking inlet within 500-1000 operational cycles (Supplementary Materials Table 4.5) which agrees with the observed failure rate of these inlets. The additionally titrated iron is within the same order of magnitude as iron dosed in the nutrient medium, chromium and nickel are not present in the nutrient medium.

4.3.6. TITRATION OF NICKEL AND CHROMIUM

Chromium and nickel are not included in the medium and may therefore affect the microbial community when leached in the fermentation broth due to pH control with HCl. In two transition experiments, biomass from $SBR_{HCl}$was transferred to a separate bioreactor and HCl was replaced with H_2SO_4 as pH controlling agent. In both bioreactors, the functional behavior changed towards the transition state within 10 cycles. Starting 10 cycles after the acid switch, increasing amounts of chromium or nickel were continuously titrated to the bioreactor to final concentrations of 40 µM and 30 µM respectively. These final concentrations were estimated from the leaching experiments described previously. As shown in Figure 4.6, no change in functional performance was observed in either bioreactor. Microscopy observations suggest that the transition away from a *Plasticicumulans* dominated microbial community may have been faster in presence of chromium (Supplementary Materials Figure 4.8).

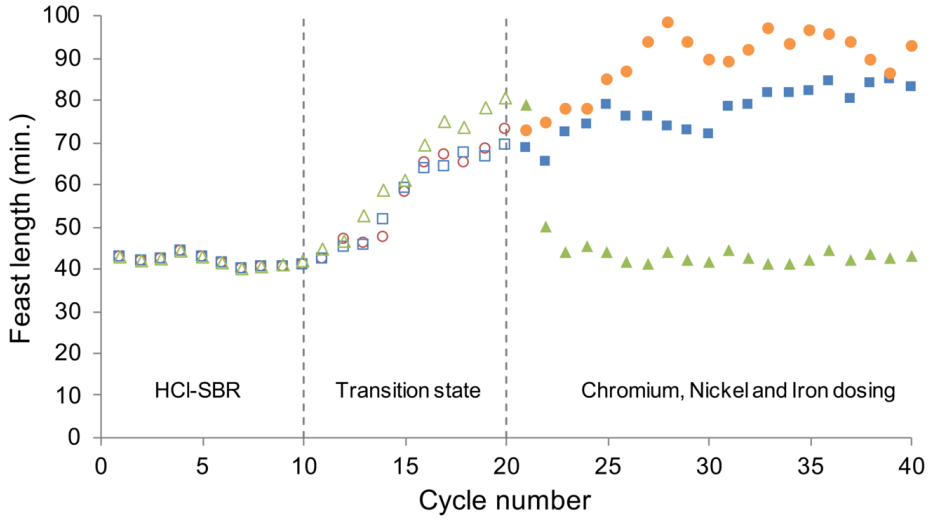

Figure 4.6: Feast length of *P. acidivorans* dominated enrichments, cultivated with continuous dosage of chromium (orange circles), nickel (blue squares), or iron (green triangles). Biomass from a stable enrichment in SBR_{HCl} (cycles 1-10) was cultivated for ten cycles by replacing HCl with H_2SO_4 as acid source (cycles 10-20). From cycle 20 on, the bioreactors were supplemented with increasing amounts of chromium, nickel, or iron, up to final concentrations of 40 µM, 30 µM, and 35 µM respectively.

4.3.7. TITRATION OF ADDITIONAL IRON

Iron measurements in filtered reactor effluent from $SBR_{H_2SO_4}$ and SBR_{HCl} demonstrated that at least 50% of the influent iron (16 µM Fe) was detected in filtered reactor effluent samples. Even though considerable iron concentrations were found in both bioreactors, titration experiments analogue to the experiments with chromium and nickel were conducted with iron. The continuous addition of iron had a pronounced effect on the feast length as is displayed in Figure 4.6. The functional response showed a remarkable similarity to the response observed when switching H_2SO_4 back to HCl (Figure 4.4).

4.4. DISCUSSION

4.4.1. MICROBIAL COMPETITION IS AFFECTED BY THE TYPE OF ACID USED FOR PH CONTROL

In this work we have demonstrated that in a pulse fed aerobic bioreactor fed with acetate as sole carbon and energy source, the type of acid ($SBR_{H_2SO_4}$ and SBR_{HCl}) used as pH controlling agent has a paramount impact on the functional properties of the process and the microbial community established in steady state (Figure 4.1). Switching the pH controlling agent resulted in the functional and microbial transition to the alternating state: $SBR_{H_2SO_4 \rightarrow HCl}$ became equivalent to SBR_{HCl} and vice versa. The reproducibility of these remarkable transitions was verified over twenty times with biomass from both SBR_{HCl} and $SBR_{H_2SO_4}$. The changes in functional performance of the microbial communities throughout all transition experiments were highly comparable, which further emphasizes the dependency of the process on the acid used for pH control.

4.4.2. MICROBIAL COMPETITION IS DIRECTLY AFFECTED BY IRON LEACHING DUE TO CORRODING REACTOR INLETS

Additional experiments demonstrated that the type of anion supplied with the acid used for pH control only had a minor impact on the enrichment. Apparently, the differences observed were an indirect effect of the type of acid used for pH control. Abiotic experiments demonstrated that steel from the bioreactor corroded in HCl, and not in H_2SO_4 resulting in increased concentrations of iron, chromium and nickel (Figure 4.5). Independent titration experiments with these main constituents of 316L steel, demonstrated that supplementing $SBR_{H_2SO_4}$ with chromium and nickel did not enable the establishment of a process equivalent to SBR_{HCl}, nor the functional enrichment of *P. acidivorans* (Figure 4.6). The presence of chromium was correlated with minor shifts in functionality and morphology and could therefore be a contributing factor to the microbial competition as observed in the cultivations [15]. The titration of iron did result in a steady state operational performance of $SBR_{H_2SO_4}$ fully equivalent to SBR_{HCl} and enrichment of *P. acidivorans*. This led to the remarkable conclusion that some form of iron limitation was preventing the enrichment of *P. acidivorans* even though less than 50% of iron in the original medium was consumed.

4.4.3. IRON BIOAVAILABILITY AND ITS ROLE IN MICROBIAL COMPETITION

From the results in this research it was not apparent which factors affect the biological availability of iron for *P. acidivorans*. Iron is the most important micro nutrient for almost all microorganisms, and due to iron's complex speciation and precipitation properties microorganisms have evolved to scavenge iron at very low concentrations [16]. Natural ecosystems show dissolved iron concentrations below 1 nM [17]. Neilands [18] describes how microbes with high iron affinity due to siderophores and cognate transport apparatus still grow optimal at iron concentrations below 0.1 µM. The genome of *P. acidivorans* contains several high-affinity iron transporters (e.g.: catecholate siderophore receptor: PWV65540.1, iron ABC transporter: PWV65654.1, ferrous iron transporter: PWV63195.1), making it unlikely that the measured iron Fe(III) concentrations (>9 µM) are limiting its growth rate [19].

Although iron was added to the medium as Fe(II), it oxidizes to Fe(III) in aerobic conditions, resulting in complex speciation [20]. EDTA was added as chelating agent to the medium to prevent precipitation of iron salts and oxides. The high binding strength of the EDTA-Fe(III) complex ($k_{f\_Fe(III)} \approx 25$) reduces the free iron concentration to the order of 10^{-29} M Fe(III) in the bioreactors, possibly affecting the iron uptake rate [21]. Additionally, the method of trace metal dosing was shown to influence microbial functionality in anaerobic digestion, where continuous titration at low concentrations achieved higher rates than pulse dosing excessive amounts [22]. The oxidation state of iron, its complexation with chelating agents, and the manner in which iron is added to the medium, i.e. through pulse or titration, was demonstrated to play a key role in microbial competition and enrichment in this work.

4.4.4. TRANSITION STATE – ALTERED FUNCTIONAL PERFORMANCE OF THE MICROBIAL COMMUNITY.

SBR_{HCl} enrichments dominated by *P. acidivorans* showed an almost instantaneous change in functional performance when the acid agent was switched to H_2SO_4 (Figure 4.4). Despite the change in functional performance within 1 to 2 generations, the change in abundance of the dominant microbial community members seemed to take at least 10 generations as shown through 16S rRNA gene sequencing and microscopy (Figure 4.2). The perceived change in function is related to microbial abundance and activity, here it is likely that the activity of the dominant community members changed. During the first cycles after the acid switch, the functional performance of *P. acidivorans* dominated enrichments showed high similarity to enrichments dominated by *Zoogloea sp.* The apparent decrease in the biomass specific substrate uptake rate upon the transition from HCl to H_2SO_4 as pH controlling agent diminishes the competitive advantage of *P. acidivorans* in the experiments described in this work, allowing the minor community members to increase in abundance during the consecutive cycles. Pure culture cultivations with *P. acidivorans* and *Zoogloea sp.* might aid in unraveling the specific mechanisms behind the current observation by looking at transcriptomics and proteomic changes under different iron limitations. These observations evidently raise the question to what extent we may overlook other limitations and corresponding differences in functional distinct behavior due to choices in bioreactor operation and medium composition.

4.4.5. SECONDARY LIMITATION MAY HAVE AN IMPORTANT IMPACT ON MICROBIAL COMMUNITY STRUCTURE AND FUNCTIONING - THE ENVIRONMENT SELECTS

From these experiments it becomes apparent that seemingly negligible operational differences may impact enrichment results. The results as observed in this study raise the question to which extent our assumption of single limiting factors in enrichment studies can be supported. Starting from the hypothesis of Baas Becking “everything is everywhere; but the environment selects” [3], the question arises how much diversity and alternative functionalities can be unlocked and are currently overlooked by the nuances of enrichment studies. Many microbiologists have anecdotal evidence where their tricks of the trade allowed them to cultivate and isolate specific microbial species. In most mi-

crobiology literature, minute differences often go unnoticed or undocumented, possibly hampering the elucidation of novel biological mechanisms. Some noteworthy exceptions include the works of Zeikus and Thauer in their respective labs on *Methanobacterium thermoautotrophicum* [23, 24]. Eventually the difference in growth rate measured in both laboratories was related to the nickel in the needles in Zeikus' lab [24]. And a more recent publication from the group of Op den Camp explains the growth dependencies of *Methylacidiphilum fumariolicum* on rare earth metals, which were present in medium supplemented with mudpot water from Solfatara ([25]).

The above-mentioned findings resulted from close observation and critical analysis of operational practices. In order to facilitate the discovery and understanding of secondary factors affecting enrichment studies, more systematic and comparative research is required.

4.5. CONCLUSIONS

Aerobic, pulse fed sequencing batch bioreactors allow efficient enrichment of microbial communities with superior PHA storing capacity. This work has demonstrated that minute differences in medium composition may strongly affect microbial competition and therewith affect the PHA producing capacity significantly. Here we elucidated that the type of acid used for pH-control affected the bioavailability of iron and therewith determined the microbial community structure and the PHA producing capacity: Even though no iron limitation was observed in any of the systems, the titration of additional iron through corrosion of reactor inlets facilitated the enrichment of the well-known PHA producer *Plasticicumulans acidivorans*. By changing the hydrochloric acid for sulfuric acid as pH controlling agent, the corrosion of acid inlet points of the reactor halted and an immediate change in functional response was observed, followed by a change in microbial community towards a *Zoogloea sp.* dominated culture. The results described in this work demonstrate that apparently insignificant variations in medium composition can induce secondary nutrient limitations and have a major impact on the functional and structural development of microbial enrichments.

ACKNOWLEDGEMENTS

We gratefully acknowledge financial support from Netherlands Organization for Scientific Research (NWO) which is funded by the Dutch Ministry of Economic Affairs, and the company Paques B.V. (NWO-Paques Partnership Program project 13002).

4.6. SUPPLEMENTARY MATERIALS

4.6.1. COMPOSITION OF MEDIUM, AND TYPE 316L STAINLESS STEEL

Table 4.3: Composition of 316L stainless steel from which the reactor inlets are made.

Compound	316L steel [%[a]]
Carbon	0.03 max.
Sulfur	0.03 max.
Phosphorus	0.045 max.
Nitrogen	0.1 max.
Silicon [b]	0.75 max.
Manganese	2.00 max.
Molybdenum	2.00 - 3.00
Chromium [b]	**16.00 - 18.00**
Nickel [b]	**10.00-14.00**
Iron	**Balance**

[a] Weight percentage (g/g)
[b] Element not present in media (Table 4.4)

Table 4.4: Composition of the trace elements solution, and relative contribution of leaching on reactor medium.

Compound	MW	Concentration		Reactor feed	Inlet leaching
	g/mol	(g/L)	(mmol/L)	µmol/L	µmol/L
EDTA Titriplex III [a]	372	63.69	171	256	
$ZnSO_4.7H2O$	288	22.00	77	116	
$CaCl_2.H_2O$	147	7.34	50	75	
$MnCl_2.4H_2O$	198	5.06	26	39	
$FeSO_4.7H_2O$	278	2.99	11	16.5	35 - 140
$CoCl_2.6H_2O$	238	1.61	7	10.5	
$CuSO_4.5H_2O$	250	1.51	6	9	
$(NH_4)_6Mo_7O_{24}.4H_2O$	1164	1.10	1	1.5	
$NiSO_4.H_2O$				-	7 - 30
$CrK(SO_4)_2.H_2O$				-	10- 40

[a] EDTA chelator is added in equal molar ratio to trace metals

4.6.2. CALCULATION OF CORROSION AND TITRATION OF ACID INLET

Table 4.5: Rough estimation of reactor triplet corrosion

Measurements leaching experiment HCl			30 **days in acid**		
Mass:	250	mg			
Volume HCl	5	ml			
Measurement dilution	100	x			
Measured concentration	2.54	mg Fe/L			
Implied corrosion from steel composition:			~ Composition 316L		MW
Fe	254	mg Fe/L	Fe	62%	56
Cr	74	mg Cr/L	Cr	18%	52
Ni	57	mg Ni/L	Ni	14%	59
Mo	8	mg Mo/L	Mo	2%	96
Mn	8	mg Mn/L	Mn	2%	55
Total metal leached	2.048	mg			
	0.82%	of pipe corroded in 30 days			
Estimation of number of days until leakage at continuous exposure to (fresh) acid					
Breakpoint occurs when	10%	of pipe has corroded (Assumption)			
	366	days until breakpoint			
Estimation of additional supplemental iron due to leaching					
Dosed	27	ml acid / cycle			
Concentration Fe in acid	51	mg Fe / L	(low estimate)		
	254	mg Fe / L	(high estimate)		
Dosed iron per cycle	0.025	mmol Fe / cycle	(low estimate)		
	0.123	mmol Fe / cycle	(high estimate)		
Stock solutions (derived from leaching experiment)					
Iron	5.0	mM Fe			
Chromium	1.5	mM Cr			
Nickel	1.0	mM Ni			
Titration experiment ranging from low to high estimate					
Flow rate titration	5	ml/12 hour	(low estimate)		
	20	ml/12 hour	(high estimate)		
Supplemented metals	low	high			
	0.025	0.100	mmol Fe / cycle		
	0.008	0.030	mmol Cr / cycle		
	0.005	0.020	mmol Ni / cycle		

4.6.3. INFLUENCE OF HIGHER SALT CONCENTRATIONS

SLIGHT EFFECT OF SODIUM CHLORIDE ON FUNCTIONALITY

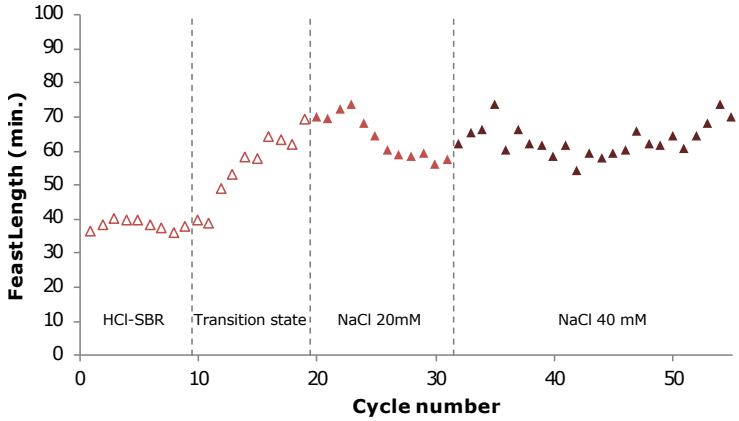

Figure 4.7: Feast length of $SBR_{HCl \rightarrow H_2SO_4}$ after switching the acid to H_2SO_4 (from cycle 10) during cultivation with increased NaCl (from cycle 20), 20mM in light triangles and 40mM in dark triangles. *P. acidivorans* remained the most abundant species in $SBR_{HCl \rightarrow H_2SO_4}$ for 30 cycles with the NaCl supplemented medium, but eventually the community shifted towards a community dominated by *Zoogloea sp.* after 40 cycles (Figure 4.9).

POSSIBLE EFFECT OF CHROMIUM ON CELL VIABILITY

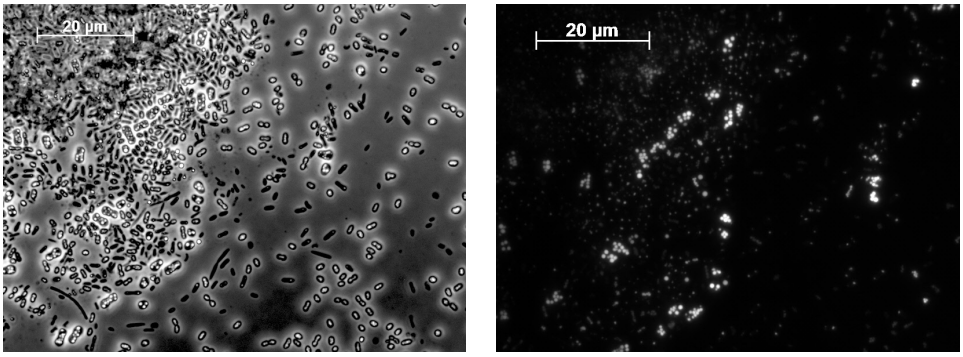

Figure 4.8: Microscopic images of the microbial culture in $SBR_{HCl \rightarrow H_2SO_4}$ with additional chromium at the end of the feast phase in dark field (left) and BODIPY 505/515 PHA staining (right). This image is taken after ten operational cycles at a chromium concentration of approximately 20µM in the bioreactor. The morphology of the microbial cells is distinct from those in stable HCl and H_2SO_4 enrichments, and from biomass in the transition state.

The presence of chromium is an additional factor that could contribute to microbial competition as observed in the cultivations [15].

4.6.4. 16S RELATIVE ABUNDANCE

16S RELATIVE ABUNDANCE HCL TRANSITION INCREASED NACL

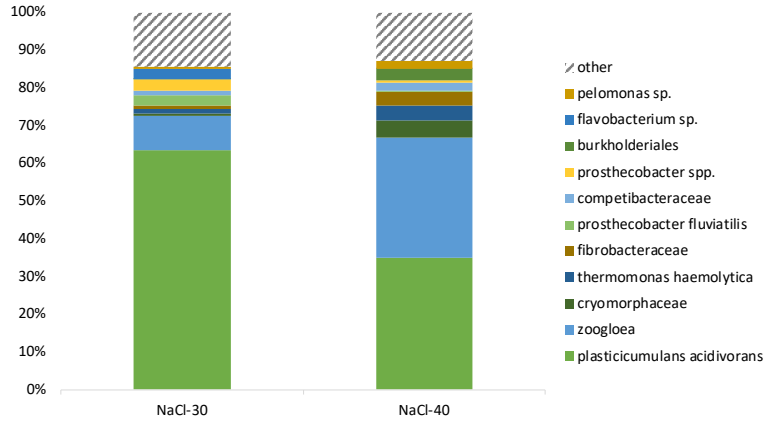

Figure 4.9: Relative abundance of microbial community structure based on 16S rRNA-gene Amplicon sequencing for bioreactor $SBR_{HCl \rightarrow H_2SO_4}$ at two timepoints, 30 and 40 cycles after the start of the titration of NaCl.

16S RELATIVE ABUNDANCE HCL TRANSITION

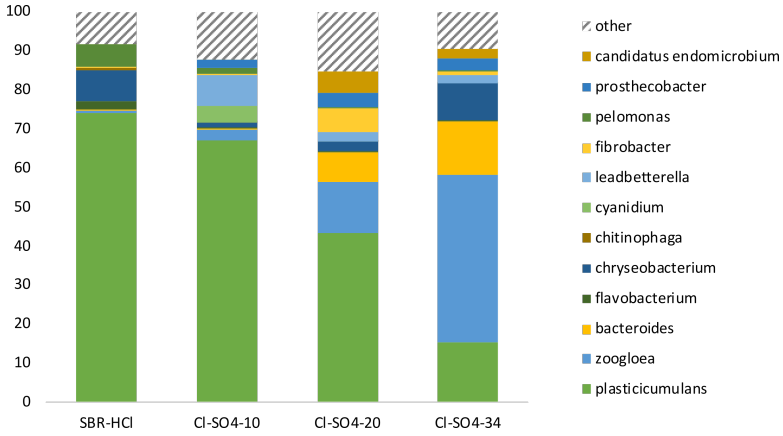

Figure 4.10: Relative abundance of microbial community structure based on 16S rRNA-gene Amplicon sequencing for bioreactor SBR_{HCl} at four timepoints. SBR-HCl indicates the community composition before a shift in acid for pH control to H_2SO_4, and 10, 20, and 34 cycles after the shift.

During the transition from a *P. acidivorans* dominated culture to *Zoogloea sp.* no specific transient micro-organisms are detected with 16S rRNA-gene Amplicon sequencing. The running theory proposed in this manuscript is that some form of iron limitation occurs during cultivation with H_2SO_4, which suggests that increased abundance is expected of microbes with a higher iron affinity, or iron uptake mechanism. Secondly,

species with a decreased iron affinity that are initially present (e.g: *P. acidivorans*) could suffer from decreased viability and decay. This would also allow microbes that grow on complex substrates to transiently proliferate. This mechanism if elaborated in Stouten *et al.* [10].

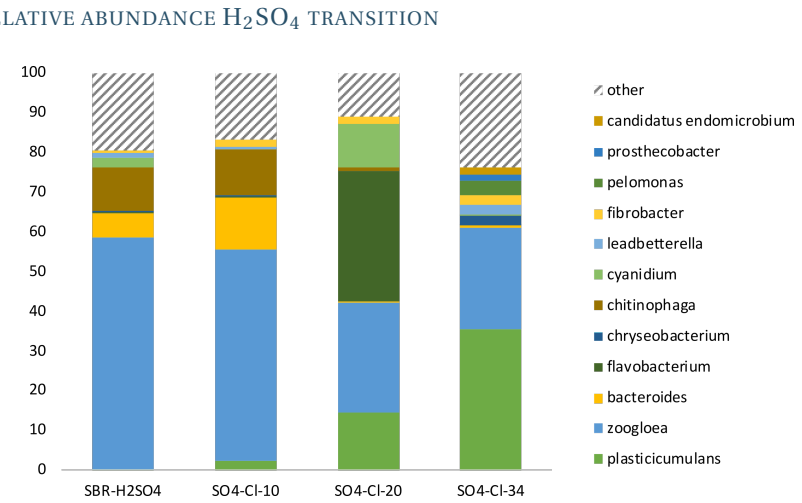

Figure 4.11: Relative abundance of microbial community structure based on 16S rRNA-gene Amplicon sequencing for bioreactor SBR$_{text H_2SO_4}$ at four timepoints. SBR-H_2SO_4 indicates the community composition before a shift in acid for pH control to HCl, and 10, 20, and 34 cycles after the shift.

Contrary to the shift describe above (Figure 4.10), during the transition from a *Zoogloea sp.* dominated culture to *P. acidivorans* specific transient micro-organisms are detected with 16S rRNA-gene Amplicon sequencing. In this system the bioavailability of iron likely increases, allowing a transient high abundance of the *Flavobacterium*. Its abundance aligns with an increase in the feast length (Figure 4.3), signifying that its competitiveness might not be related to carbon substrate uptake rate. Possible competitive factors include opportunistic growth on decaying cell matter by hydrolysis of complex substrates [26], and alternative complex III (ACIII) used in the respiration chain which is more iron dependent [27]. The transient nature could be explained by the superior carbon substrate uptake rates of *P. acidivorans*, and its maintained cell viability [10].

REFERENCES

[1] G. R. Stouten, K. Hamers, R. J. van Tatenhove-Pel, E. van der Knaap, and R. Kleerebezem, *Seemingly trivial secondary factors may determine microbial competition: A cautionary tale on the impact of iron supplementation through corrosion,* FEMS Microbiology Ecology **97** (2021), 10.1093/femsec/fiab002.

[2] R. Kleerebezem and M. C. van Loosdrecht, *Mixed culture biotechnology for bioenergy production,* Current Opinion in Biotechnology Energy Biotechnology / Environmental Biotechnology, **18**, 207 (2007).

[3] L. G. M. Baas-Becking, *Geobiologie; of Inleiding Tot de Milieukunde.* (WP Van Stockum & Zoon NV, 1934).

[4] G.-Q. Chen, *A microbial polyhydroxyalkanoates (PHA) based bio- and materials industry,* Chemical Society Reviews **38**, 2434 (2009).

[5] J. Tamis, M. Mulders, H. Dijkman, R. Rozendal, M. C. M. van Loosdrecht, and R. Kleerebezem, *Pilot-Scale Polyhydroxyalkanoate Production from Paper Mill Wastewater: Process Characteristics and Identification of Bottlenecks for Full-Scale Implementation,* Journal of Environmental Engineering **144**, 04018107 (2018).

[6] K. Johnson, Y. Jiang, R. Kleerebezem, G. Muyzer, and M. C. M. van Loosdrecht, *Enrichment of a Mixed Bacterial Culture with a High Polyhydroxyalkanoate Storage Capacity,* Biomacromolecules **10**, 670 (2009).

[7] Y. Jiang, L. Marang, R. Kleerebezem, G. Muyzer, and M. C. van Loosdrecht, *Polyhydroxybutyrate production from lactate using a mixed microbial culture,* Biotechnology and Bioengineering **108**, 2022 (2011).

[8] J. Tamis, K. Lužkov, Y. Jiang, M. C. van Loosdrecht, and R. Kleerebezem, *Enrichment of Plasticicumulans acidivorans at pilot-scale for PHA production on industrial wastewater,* Journal of Biotechnology **192**, 161 (2014).

[9] L. Marang, M. C. van Loosdrecht, and R. Kleerebezem, *Combining the enrichment and accumulation step in non-axenic PHA production: Cultivation of Plasticicumulans acidivorans at high volume exchange ratios,* Journal of Biotechnology **231**, 260 (2016).

[10] G. R. Stouten, C. Hogendoorn, S. Douwenga, E. S. Kilias, G. Muyzer, and R. Kleerebezem, *Temperature as competitive strategy determining factor in pulse-fed aerobic bioreactors,* The ISME Journal (2019), 10.1038/s41396-019-0495-8.

[11] W. V. Vishniac and M. Santer, *The thiobacilli,* Bacteriological reviews **21**, 195 (1957).

[12] G. R. Stouten, S. Douwenga, C. Hogendoorn, and R. Kleerebezem, *System characterization of dynamic biological cultivations through improved data analysis,* bioRxiv (2021), 10.1101/2021.05.14.442977.

[13] Y. Jiang, L. Marang, R. Kleerebezem, G. Muyzer, and M. C. M. van Loosdrecht, *Effect of temperature and cycle length on microbial competition in PHB-producing sequencing batch reactor,* The ISME Journal **5**, 896 (2011).

[14] E. Oberg and F. D. Jones, *Machinery's Handbook.*, (28th ed.) ed. (Industrial Press Inc., p. 406, 1916).

[15] J. A. Lemire, J. J. Harrison, and R. J. Turner, *Antimicrobial activity of metals: Mechanisms, molecular targets and applications,* Nature Reviews Microbiology **11**, 371 (2013).

[16] C. E. Lankford and B. R. Byers, *Bacterial Assimilation of iron,* CRC Critical Reviews in Microbiology **2**, 273 (1973).

[17] P. G. Falkowski, *Biogeochemical Controls and Feedbacks on Ocean Primary Production,* Science **281**, 200 (1998).

[18] J. B. Neilands, *Iron Absorption and Transport in Microorganisms,* Annual Review of Nutrition **1**, 27 (1981).

[19] M. Göker, *Genomic Encyclopedia of Type Strains, Phase IV (KMG-IV): Sequencing the most valuable type-strain genomes for metagenomic binning, comparative biology and taxonomic classification,* (2017).

[20] W. Davison and G. Seed, *The kinetics of the oxidation of ferrous iron in synthetic and natural waters,* Geochimica et Cosmochimica Acta **47**, 67 (1983).

[21] G. Anderegg, *Critical Survey of Stability Constants of EDTA Complexes* (Elsevier, 1977).

[22] G. Gonzalez-Gil, R. Kleerebezem, and G. Lettinga, *Effects of Nickel and Cobalt on Kinetics of Methanol Conversion by Methanogenic Sludge as Assessed by On-Line CH4 Monitoring,* Applied and Environmental Microbiology **65**, 5 (1999).

[23] J. G. Zeikus and R. S. Wolfe, *Methanobacterium thermoautotrophicus sp. n., an Anaerobic, Autotrophic, Extreme Thermophile,* Journal of Bacteriology **109**, 7 (1972).

[24] P. Schönheit, J. Moll, and R. K. Thauer, *Nickel, cobalt, and molybdenum requirement for growth of Methanobacterium thermoautotrophicum,* Archives of Microbiology **123**, 105 (1979).

[25] A. Pol, T. R. M. Barends, A. Dietl, A. F. Khadem, J. Eygensteyn, M. S. M. Jetten, and H. J. M. Op den Camp, *Rare earth metals are essential for methanotrophic life in volcanic mudpots: Rare earth metals essential for methanotrophic life,* Environmental Microbiology **16**, 255 (2014).

[26] J. F. Bernardet, *Proposed minimal standards for describing new taxa of the family Flavobacteriaceae and emended description of the family,* International Journal of Systematic and Evolutionary Microbiology **52**, 1049 (2002).

[27] C. Sun, S. Benlekbir, P. Venkatakrishnan, Y. Wang, S. Hong, J. Hosler, E. Tajkhorshid, J. Rubinstein, and R. Gennis, *Structure of the alternative complex III in a supercomplex with cytochrome oxidase,* Nature **557**, 123 (2018).

5

UNCOUPLING OF NUTRIENT SUPPLY FOR ENRICHMENT OF POLYHYDROXYALKANOATES ACCUMULATING BACTERIA

Gerben Roelandt STOUTEN, Francesca CECCONI, Rinke Johanna VAN TATENHOVE-PEL, Michel MULDERS, Peter Rudolf MOOIJ, Henk DIJKMAN, Robbert KLEEREBEZEM

A circular society necessitates the production of commodities from renewable resources. Some of these commodities can be produced cost-effectively from low-value feedstocks by specialized microbial communities. For example, the production of specific biopolymers (such as polyhydroxyalkanoates, PHA) can be achieved using microbial enrichments as alternative to oil-derived plastics and polymers. To this end, enrichment strategies are employed to select for microbial communities where biopolymer production is favored over biomass growth. Here we describe a novel enrichment strategy for PHA producing microorganisms based on strict uncoupling in time of the supply of two growth nutrients, i.e. organic carbon and nitrogen or phosphorous. Optimization of the PHA production was achieved through increasing the exchange ratios in the sequencing batch process and optimizing the carbon to nutrient ratios. The uncoupling strategy resulted in stable enrichments, that achieved 89 wt% (gPHA/gDW) in eight hours, every operational cycle, making this the most PHA rich production system to date. Specific benefits of the approach described here include (i) stable productivity and PHA-content, (ii) combination of enrichment and production in one process step, (iii) the use of ammonia or phosphate as the secondary limiting growth nutrient, and (iv) a more balanced oxygen consumption throughout the cycle.

Parts of this chapter have been published as Stouten *et al.* [1].

5.1. INTRODUCTION

Advancing into a circular society requires the sustainable production of bulk commodities. To replace oil-derived plastics, researchers are looking into the production of biopolymers like polyhydroxyalkonaotes (PHA) as a basis for biodegradable and bio-based plastics.

PHAs are produced by many microorganisms as an intermediate store of energy and carbon, allowing them to endure periods of limited substrate availability. PHA production from heterogeneous feedstocks can be achieved if a microbial community can be established that consists of microorganisms with strong PHA production characteristics. The establishment of microbial communities with desired properties is achieved through enrichment strategies, where the ecological role of PHA is used to select for PHA producing microbial communities.

Two enrichment strategies that are currently most promising for PHA production are phosphate limitation during cultivation in a chemostat process [2] and pulse-fed sequencing batch systems [3]. A limitation of these enrichment strategies is that ecological niches exist where competing non-PHA producing microorganisms can flourish. For the phosphate limited system phosphate accumulating organisms may effectively compete with PHA producers [4], whereas fast growers can effectively compete with PHA storing microorganisms in the pulse-fed sequencing batch systems [5]. Maintaining a productive PHA producing enrichment can therefore be challenging.

In principle, enrichment strategies are criteria that are imposed on an environment. Microbial communities that are able to maintain the highest viability in an environment will flourish. Depending on the ingenuity of nature, some criteria can be met by different functional strategies. For example, pulse-fed environments, in which the nutrient source is available for a limited time at a relatively high concentration, select for a high substrate uptake rate. This substrate can be either channeled into new biomass, increasing the catalytic capacity; or into storage polymers, requiring a less complex metabolic pathway. During the subsequent period, in which extracellular substrate is absent, if storage polymers are produced, they can be used as growth substrate. The competition between fast growing and hoarding microorganisms can be tilted by additional environmental factors, like the time period in between pulses, maintenance related processes, oxygen availability, etc. Compounding several criteria, results in the design of a selective environment, which aims to enrich microbial communities with the desired functionalities.

The tremendous functional diversity that is observed in microbial ecology makes some criteria hard selectors and others soft selectors for specific characteristics. For example, the pulse-fed criterion used in “feast-famine” enrichment strategies is a soft selector for storage polymer production, as it is based on the difference in kinetic properties of competing strategies. Undesired functional characteristics (growers) can emerge that offer a competitive advantage over the desired characteristic (hoarders). It is therefore suggested to look for hard selection criteria that, by understanding the ecological role of desired characteristics, can be used to design robust and productive selection strategies [6].

Examples of hard selection criteria in other microbial enrichment systems include the anaerobic uptake of substrate by phosphate and glycogen accumulating organisms,

in systems where the electron acceptor supply is uncoupled from the electron donor supply [7, 8]. The uncoupling of essential growth factors (light+CO_2 and ammonium) at different times also results in a hard criterion for storage polymer production in algae [9]. In both cases the uncoupling of essential growth factors in time restricts the direct formation of new catalytic biomass. It is therefore a prerequisite in these systems that storage polymers are produced from the carbon source, provided that the desired catalytic capacity is available in nature. After the carbon uptake phase, supply of the missing growth factor, e.g.: a nutrient pulse or electron acceptor, can be utilized by microorganisms with storage polymers. Plasticity in this criterion may result from adaptive cellular C:N and C:P ratios of catalytic biomass.

The work described in this paper aims for enrichment of PHA producing microorganisms through uncoupling of the supply of carbon substrate and essential growth nutrients in time, in a sequencing batch process. Three express process variables of the proposed uncoupling strategy were investigated: (i) the secondary limiting nutrient, ammonium or phosphate (N/P), (ii) the carbon to N/P ratio of the feed pulses, and (iii) the exchange ratio, which is the fraction of biomass removed after each operational cycle.

5.2. MATERIALS AND METHODS

5.2.1. SEQUENCING BATCH BIOREACTOR OPERATION

Seven aerobic sequencing batch bioreactors with a working volume of 1.4 L were operated in such a way that the carbon substrate (acetate) and a secondary growth nutrient, either ammonium or phosphate (N/P), were never present at the same time (Figure 5.1 and Table 5.1). The reactors were operated without oxygen limitations, at 30 °C, pH 7.0±0.1, and were inoculated at the same time with activated sludge from a sewage treatment plant (Harnaschpolder, Delft, operational temperature 10-20 °C) and operated for 180 cycles. The stability of the cultures in terms of conversion rates was monitored by regular sampling and via online monitoring of off-gas composition and acid (1M HCl) and base (0.5 M NaOH) dosage.

Figure 5.1 shows the anticipated response of the process in different limiting regimes: (a) process performance at the perfect C:N-ratio (mol/mol) for biomass production, (b) at increased C:N-ratio, and (c) at an increased exchange ratio. Clearly visible are the carbon phase, and the nutrient phase, each ending when the pulsed substrate is depleted. For the P-uncoupled systems, the secondary limiting nutrient is phosphate instead of ammonium. The time between the carbon feed pulse and the N/P pulse is referred to as the carbon phase (τ, minutes). The length of the carbon phase was set manually to the time needed for carbon uptake plus approximately 30-60 minutes. Within 10 operational cycles after an operational change, no adjustments to τ were made and it was kept constant. At the end of the cycle a fraction of the mixed bioreactor content is replaced with medium without carbon, nitrogen and phosphorus (137 mg L^{-1} EDTA Titriplex III; 47 mg L^{-1} $ZnSO_4 \cdot 7H_2O$; 36 mg L^{-1} MgSO4·7H_2O, 16 mg L^{-1} $CaCl_2 \cdot H_2O$; 14 mg L^{-1} KCl, 11 mg L^{-1} $MnCl_2 \cdot 4H_2O$; 7 mg L^{-1} $FeSO_4 \cdot 7H_2O$; 3 mg L^{-1} $CoCl_2 \cdot 6H_2O$; 3 mg L^{-1} $CuSO_4 \cdot 5H_2O$; and 2 mg L^{-1} $(NH_4)_6Mo_7O_{24} \cdot 4H_2O$ [10]). A system that achieves a pseudo steady state implies that all removed biomass grows back throughout the cycle.

Table 5.1: Overview of sequencing batch bioreactor operational parameters. R1-R4 investigated the influence of ammonium and phosphate limitation at two carbon to N/P ratios. R5-R7 investigated the influence of an increased exchange ratio (ER). The cycle length (CL) and exchange ratio (ER) result in an average solid retention time (SRT) of the biomass in the bioreactor.

Reactor name	Limiting nutrient	ratio C:N/P	ER [%]	τ [h]	CL [h]	SRT [h]	Carbon [mCmol]	Ammonium [mNmol]	Phosphate [mPmol]
R1-CN12	Ammonium	12	50%	2.5	12	24	40	3.33	0.6
R2-CN20	Ammonium	20	50%	3.0	12	24	40	2	1.6
R3-CP200	Phosphate	200	50%	2.5	12	24	40	5	0.2
R4-CP300	Phosphate	300	50%	3.0	12	24	40	5	0.133
R5-CN14	Ammonium	14	75%	5.0	30	40	120	8.57	2.4
R6-CP200	Phosphate	200	75%	10	30	40	120	15	0.6
R7-CN14	Ammonium	14	83%	14	40	50	132	9.43	2.64

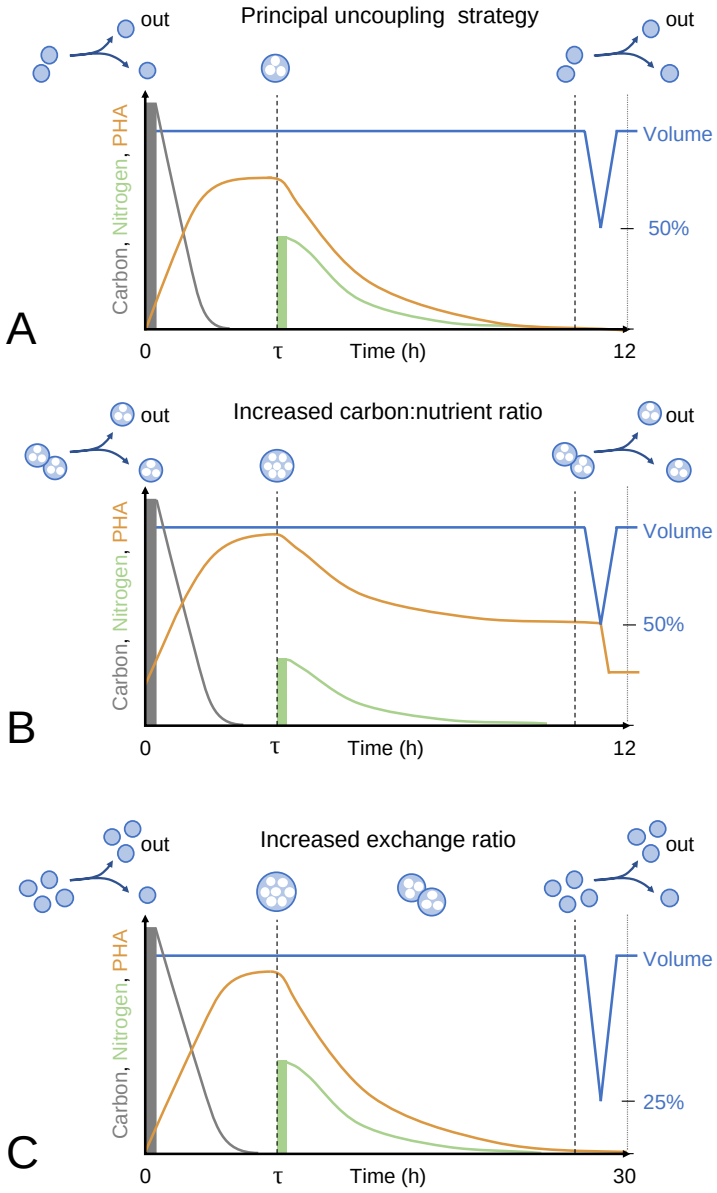

Figure 5.1: Overview of the experimental parameters for strict uncoupled enrichments and their anticipated influence on the concentration profiles of substrates and product during pseudo steady state cycles. The carbon pulse (grey) at t=0 is depleted before the secondary limiting nutrient pulse, e.g. nitrogen (green), is given at t=τ. Carbon is converted into PHA (orange) and consumed after the N/P pulse to form new catalytic biomass. Figure (A) shows the anticipated profiles for a 50% exchange ratio at a C:N-ratio of 12 (mol_C/mol_N) that was estimated to enable full uptake of C and N in the corresponding period. Figure (B) shows the anticipated profiles at an increased C:N ratio of 20, while maintaining a 50% exchange ratio; less catalytic biomass can be formed and excess carbon ends up as residual PHA at the end of the cycle. Figure (C) shows the anticipated profiles at an increased exchange ratio (blue) from 50% to 75% while maintaining the C:N ratio of 12; the starting biomass has to accumulate more PHA per unit of biomass in order to take up all carbon substrate supplied. The proposed cell division and PHA content are depicted above each graph with PHA as white granules.

5.2.2. ANALYTICAL PROCEDURES

Liquid broth samples from the reactors for analysis of acetate, ammonium and phosphate were immediately centrifuged (2 min. 15.000g) and filtered after sampling (0.22 µm pore size poly-vinylidene difluoride membrane, Merck Millipore, Carrigtohill, Ireland). The acetate concentration was measured by HPLC (BioRad Aminex HPX-87H column, Waters 2489 UV/RI detector, 1.5mM H_3PO_4 mobile phase with a flow rate of 0.6 mL min^{-1} and a temperature of 60 °C). Ammonium and phosphate were determined spectrophotometrically using a Discrete Analyzer (Gallery TM Plus, Thermo Scientific). PHA content was measured as described by Johnson *et al.* [3]. Concentrations of N_2, O_2, Ar and CO_2 in the off-gas of the reactor were measured online using mass spectrometry (Prima BT, Thermo Scientific).

5.2.3. KINETIC METABOLIC MODEL OF SEQUENCING BATCH BIOREACTOR

A metabolic model was designed to determine key kinetic properties of the enrichment cultures. This model adds uncoupling of carbon and N/P supply to previous work by Johnson *et al.* [11], Tamis *et al.* [12], and Korkakaki *et al.* [4]. A full model description is included in Supplementary Materials 5.6.1. Key implementations include the expression of biomass specific rates in terms of phosphate content of the biomass, ammonium limitation for growth on acetate and PHA, and limiting the PHA degradation rate to the maximum biomass growth rate. Furthermore, a single set of expressions was used to describe the behavior of all enrichment cultures, for both ammonium and phosphate limitations. All systems could be described based on 4 biomass specific variables: (i) maximum growth rate, (ii) maximum substrate uptake rate, (iii) maximum phosphate uptake rate, and (iv) the poly-phosphate accumulation potential. The Python3 code is available online at GitHub: `https://github.com/GRS-TUD/uncoupled-model`.

5.2.4. PREDICTION OF ENRICHMENT PERFORMANCE AND OPERATIONAL PARAMETER JUSTIFICATION

The goal of PHA enrichment cultures is to optimize the amount of PHA that is produced from the substrate stream. Therefore, high intracellular PHA contents need to be achieved. In the strict uncoupled system two parameters contribute to the PHA content, the carbon to N/P ratio in the influent pulses, and the exchange ratio. In both cases the biomass has to take up a significant amount of carbon before the N/P pulse is dosed (Figure 5.1). The additional operational parameter that influences the strict uncoupled bioreactors is the type of secondary nutrient, either ammonium or phosphate. In order to design the uncoupled experiments, the following assumptions were used concerning the catalytic biomass (X): (i) it has a fixed molar composition ($CH_{1.8}O_{0.5}N_{0.2}P_{0.0125}$, C:N:P of 80:16:1), (ii) all catalytic biomass is produced from storage polymers, (iii) all conversions are stoichiometric, and (iv) the system is in pseudo steady state, indicating that the amount of biomass throughout a cycle is identical to the previous cycle.

From the theoretical process stoichiometries described by Johnson *et al.* [11], a carbon to nitrogen ratio of 11.2 (C:N), or carbon to phosphorus ratio of 180 (C:P) is needed in the feed to achieve full conversion of carbon and N/P to biomass. In order to prevent the leaking of nutrients into the carbon phase, R1-CN12, and R3-CP200, are operated at slightly higher carbon to N/P ratios. When even more carbon is dosed than is required to

consume all N/P, then the biomass can contain residual storage polymers at the end of the cycle (Figure 5.1B). The carbon to N/P ratio in the feed thereby affects the maximum PHA fraction of the biomass without the need for additional nutrients. We derived an equation (Supplementary Materials 5.6.2) that enables the estimation of the PHA fraction at the end of the carbon phase (Equation 5.1 %PHA Cmol/Cmol). This equals the PHA fraction that needs to be achieved by the biomass to achieve uncoupled growth on carbon and nitrogen, an analog equation can be derived for uncoupled growth with phosphorus with $C{:}P_{feed}$ and $C{:}P_X$, instead of $C{:}N_{feed}$ and $C{:}N_X$.

$$\%PHA(ER,\ C:N_{\text{feed}}) = \frac{C:N_{\text{feed}} \cdot Y_{\text{PHA}/S} - C:N_X \cdot Y_{X/\text{PHA}}^{-1} \cdot (1-ER)}{C:N_{\text{feed}} \cdot Y_{\text{PHA}/S} + C:N_X \cdot (1-ER) \cdot \left(1 - Y_{X/\text{PHA}}^{-1}\right)} \tag{5.1}$$

%PHA expressed in Cmol% with $Y_{\text{PHA/S}} = 0.67\ \frac{\text{Cmol}_{\text{PHA}}}{\text{Cmol}_{\text{S}}}$, $Y_{\text{X/PHA}} = 0.67\ \frac{\text{Cmol}_{\text{X}}}{\text{Cmol}_{\text{PHA}}}$, $C{:}N_X = 5$

For general application, the PHA fraction is often given as gram PHA per gram dry weight, which can be calculated from the molecular weights of PHA (MW_{PHA} = 21.5 g $Cmol^{-1}$) and catalytic biomass (MW_X = 24.6 g $Cmol^{-1}$).

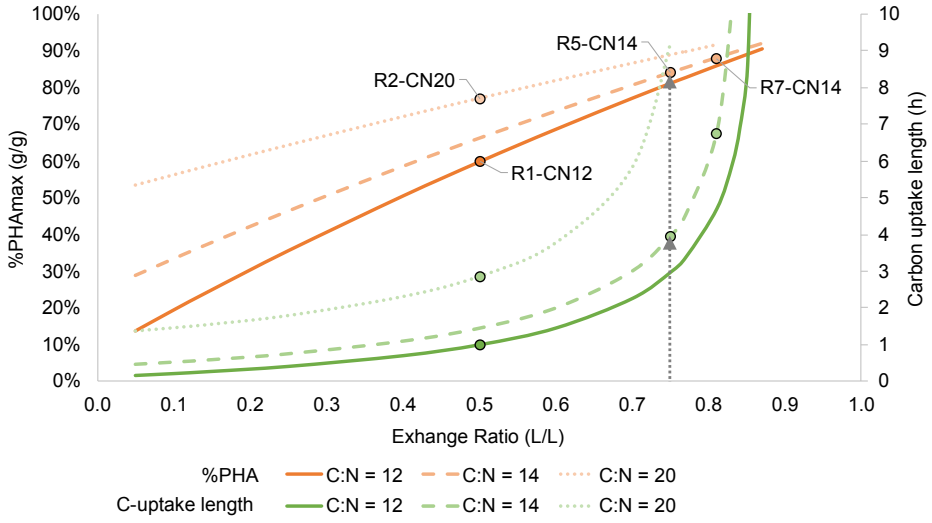

Figure 5.2: Predicted PHA cell dry weight (orange) and carbon substrate uptake length (green) as a function of the exchange ratio. Predications of the four carbon/nitrogen uncoupled systems are indicated in the figure. Example for R5-CN14: in dashed lines the predictions for $C{:}N_{feed}$ = 14 are plotted, and by following the operational exchange ratio of 0.75 (grey arrow), the predicted carbon uptake length of 4 hours, and the PHA cell dry weight of 84% are found. The other C:N uncoupled systems are shown (R1-CN12, R2-CN20, and R7-CN14) on their respective C:N ratio curves.

5.2.5. MICROBIAL COMMUNITY STRUCTURE AND MICROSCOPY

The taxa-based microbial community composition of the enriched cultures was determined by amplicon sequencing of the V3-V4 (341F, 785R) region of the 16S rRNA gene after DNA extraction with the DNeasy PowerSoil Pro kit (Qiagen GmbH, Germany). After

sequencing, the reads were quality filtered and analyzed using FASTQC and NG-Tax 2.0 using the common workflow language in a Kubernetes deployment pipeline developed within the UNLOCK initiative [13–15]. The sequence data are available at NCBI under BioProject accession number PRJNA674007.

Microscopy pictures were taken using a Leica DM500B light microscope (Leica Microsystems, Wetzlar, Germany) equipped with fluorescence filtercube A. 1 µl BODIPY 505/515 (Invitrogen D3921, Life Technologies, Grand Island, USA) in DMSO (1 mg ml^{-1}) was used to stain PHA inclusion bodies in bacterial cells in 1 mL bioreactor sample.

5.3. RESULTS

Microbial enrichments were established from activated sludge in aerobic sequencing batch reactors, characterized by the supply of carbon substrate (acetate) and a specific growth nutrient (ammonium or phosphate) at different moments in the cycle. The uncoupling in time of the supply of carbon substrate and growth nutrients (N/P) limits the direct production of catalytic biomass on the carbon source, as either ammonia or phosphate is only supplied when all carbon has been depleted. All enrichments reached a functional steady state within 40 cycles of operation exhibiting the proposed functional characteristic (Figure 5.1): After carbon substrate supply, initial PHA is produced, and when full carbon uptake is achieved, ammonium and phosphate nutrients are supplied and catalytic biomass is produced from PHA (Figure 5.3).

5.3.1. UNCOUPLING OF CARBON DOSING WITH AMMONIUM OR PHOSPHATE

The principal uncoupled systems (R1-CN12 and R3-CP200) performed in essence close to the prediction shown in Figure 5.1A (Figure 5.3). Detailed analysis of the data revealed clear differences between the functionally equivalent systems limited by N and P. The N-uncoupled systems show no increase in catalytic capacity (growth) during the carbon period (Figure 5.3 left) and perform close to the modeled predictions (Figure 5.2). Phosphate-uncoupled systems show a different response during the carbon period. The biomass takes up ammonia during the carbon period indicating the formation of catalytic biomass (Figure 5.3: PHA degradation and nitrogen uptake in R3-CP200). After the phosphate pulse, phosphate is assimilated within 5 minutes and the conversion rates of PHA degradation, ammonium uptake, and biomass growth rate (μ) approximately double, indicated by the change in slope of the compound profiles. In the kinetic model, this behavior is implemented by expressing the biomass specific rates as first-order related to phosphate content of the biomass [4] (Supplementary Materials 5.6.1).

5.3.2. INCREASING THE CELLULAR PHA CONTENT BY INCREASING THE CARBON TO NUTRIENT RATIO

A first operational change that was proposed to result in an increased cellular PHA content, is increasing the overall C:N or C:P ratio in the feed (Figure 5.1B and Equation 5.1: $C:N_{feed}$). At an increased carbon to nutrient ratio not all organic carbon in the feed can be converted to catalytic biomass (R2-CN20 and R4-CP300 in Figure 5.3). Consequently, the theoretical analysis suggested that at the end of the nutrient period significant cellular PHA-contents should remain (Figure 5.1B). Figure 5.3 (R2-CN20 and R4-CP300) demonstrates that indeed the carbon supplied was stoichiometrically converted into PHA (and carbon dioxide) in the carbon supply period, but more PHA was consumed during the nutrient phase than stoichiometrically needed for N/P uptake. Cell dry weight measurements of biomass from R2-CN20 indicate that other organic solids are produced besides catalytic biomass and PHA (Figure 5.3 after t = 7h). The excess PHA was converted in nitrogen-poor (non-catalytic) biomass, like secondary storage compounds. These secondary storage compounds formed could not be identified (Table 5.2: Gap in elemental balances). In the P limited system, R4-CP300, almost no residual PHA was detected at the end of the cycle. Instead, nitrogen rich biomass was produced from the excess PHA,

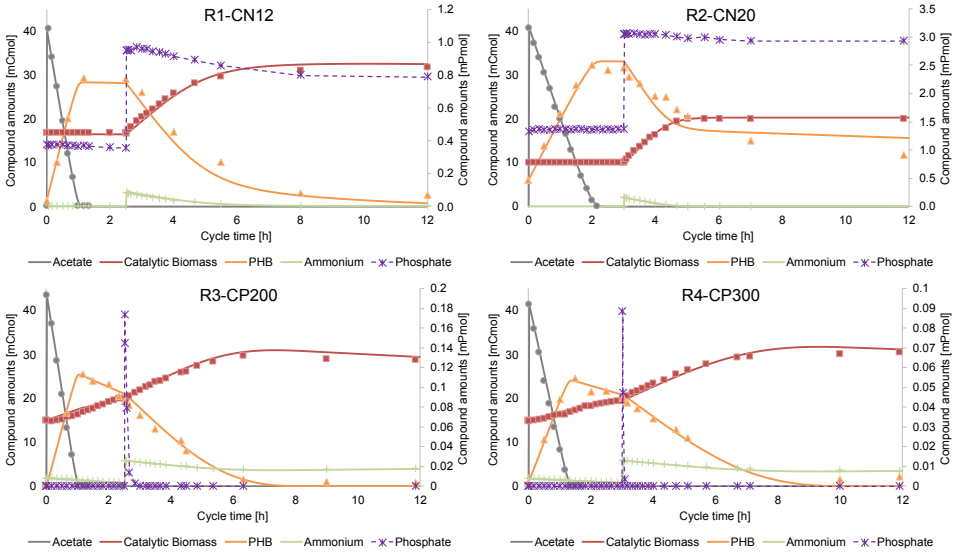

Figure 5.3: Cycle measurements of R1-CN12, R2-CN20, R3-CP200, and R4-CP300 during pseudo steady state. Symbols represent the experimental data and continuous lines indicate the kinetic model. Acetate (grey ●), PHA (orange ▲), catalytic biomass (red ■), phosphate (purple ∗), ammonia (green +). The catalytic biomass is based on the organic nitrogen measurements and general biomass composition.

thereby diluting the cellular phosphate content. The conversion of excess PHA to non-catalytic biomass was not included in Equation 5.1 and therefore some discrepancies are observed between predicted and measured PHA contents for systems with excess carbon (Table 5.2: predicted- and maximum observed PHA content).

5.3.3. INCREASING THE CELLULAR PHA-CONTENT BY INCREASING THE EXCHANGE RATIO

A second approach to increase the cellular PHA content is to increase the exchange ratio (Figure 5.1C and Equation 5.1: ER). In systems R5-CN14 and R6-CP200 the exchange ratio was increased from 50% to 75%, and R7-CN14, the exchange ratio was increased to 83% (Figure 5.4 and Table 5.2). Increasing the exchange ratio results in lower biomass concentrations in the carbon phase, and a larger carbon pulse, resulting in a higher PHA content after substrate depletion. A side effect of the lower catalytic biomass concentration in the carbon phase is that the length of carbon uptake period needs to be increased significantly (Figure 5.2 and Supplementary Materials 5.6.3). This strategy proved successful and in all three systems the anticipated functional properties as predicted in Figure 5.1C were observed.

In R6-CP200, the biomass continued taking up ammonia in the carbon phase, although phosphate was limited. This resulted in both phosphate and ammonium limitation, and thereby skewed the interpretation of the uncoupling data as the system became dually limited. The phosphate limited system was furthermore characterized by very high biomass specific phosphate uptake rates (Table 5.2: q_P). After rapid phosphate

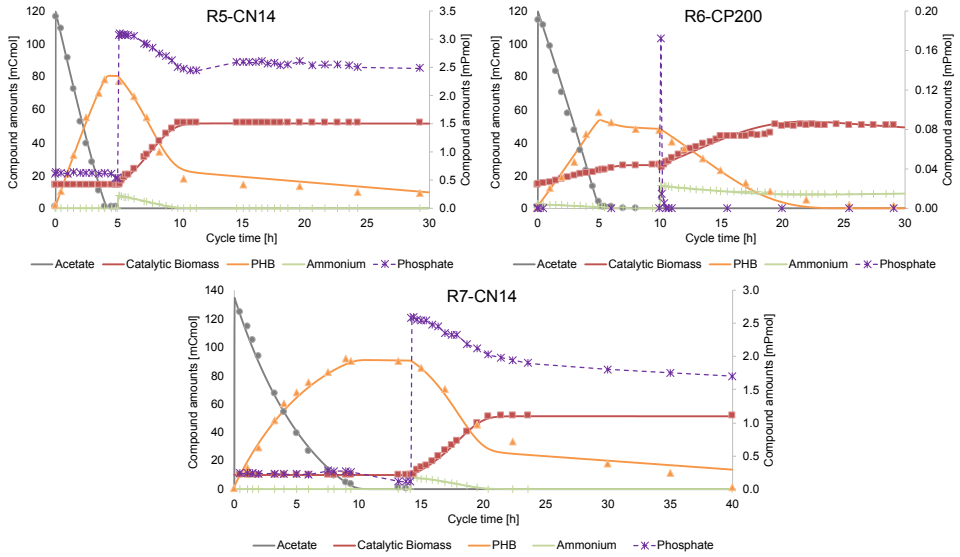

Figure 5.4: Cycle measurements of R5-CN14, R6-CP200, and R7-CN14 during pseudo steady state. Symbols represent the experimental data and continuous lines indicate the kinetic model. Acetate (grey ●), PHA (orange ▲), catalytic biomass (red ■), phosphate (purple ∗), ammonia (green +). The catalytic biomass is based on the organic nitrogen measurements and general biomass composition. Note that the cycle length of these systems is significantly longer than those of R1-R4 (Figure 5.3).

uptake, a direct increase in respiration activity is observed, similar to the response of system R4-CP300 (Figure 5.3).

For R5-CN14 and R6-CP200 a constant substrate uptake rate is observed, independent of the increasing PHA-content after supply of carbon substrate. This indicates that PHA product inhibition plays only a minor role in systems that reach a PHA-content of less than 80% PHA based on dry weight. R7-CN14 showed a decrease in substrate uptake rate after the biomass PHA content exceeded 80 wt%. Despite the reduction in uptake rate at elevated PHA content, the strong selective pressure towards a high PHA storing capacity resulted in a community that every cycle reached a PHA concentration of 89 wt% (gPHA gDW^{-1}), while maintaining a PHA yield on acetate of 0.64 Cmol $Cmol^{-1}$, close to the theoretical maximum (Table 5.2). The biomass enriched at increased exchange ratios showed a clear adaptation to the cyclic high and low PHA contents, as seen through microscopy where microorganisms with well-defined PHA inclusion bodies are observed at the end of the carbon period (Figure 5.5) and almost no PHA is visible at the end of the nutrient period.

Table 5.2: Overview of kinetic and stoichiometric properties of seven enrichments. Measurements from three consecutive cycles, standard deviations are available in Supplementary Materials 5.6.8. A reference column (grey) of a feast-famine (FF) enrichment is included [16].

Bioreactor	(ref.)	R1	R2	R3	R4	R5	R6	R7
Property	FF	CN12	CN20	CP200	CP300	CN14	CP200	CN14
Carbon uptake phase								
Predicted %PHAmax (wt%)	52	60	77	62	75	84	83	89
Maximum %PHA (wt%)	52	60	62	50	46	79	75	89
PHA:X ratio (Cmol Cmol^{-1})	**1.1**	**1.5**	**1.6**	**1.0**	**0.9**	**3.8**	**3.0**	**8.1**
Carbon-uptake length (min)	38	60	120	60	80	240	310	600
Ammonia uptake %		0	0	8.5	14	0	15	0
Gap carbon balance (%)		1	11	6	9	0	6	0
Gap electron balance (%)		1	12	8	12	4	6	5
$Y_{PHB/Ac}$ (Cmol Cmol^{-1})	0.67	0.69	0.64	0.64	0.58	0.66	0.54	0.64
Growth rate (h^{-1})		0.0	0.0	0.16	0.12	0	0.11	0
q_s^{max} (Cmol (Cmol$_X$ h)$^{-1}$)	3.5	2.7	2.2	3.0	2.2	2.3	1.7	2.2
q_{PHA} (Cmol (Cmol$_X$ h)$^{-1}$)	1.74	1.67	1.30	1.73	1.08	1.39	0.93	0.84
Growth phase								
Predicted %PHAres. (wt%)	0	8	50	13	47	24	13	24
Residual %PHA (wt%)	0	7	24	0	4	7	3	2
Nutrient uptake length (min)		400	240	10	5	300	10	380
Ammonia uptake %		100	100	91.5	86	100	85	100
Gap carbon balance (%)		0.2	15	12	9	8	11	13
Gap electron balance (%)		1.2	16	13	11	9	12	14
$Y_{X/PHA}$	0.67	0.63	0.52	0.57	0.65	0.57	0.50	0.57
q_N (molN (Cmol$_X$ h)$^{-1}$)	0.033	0.13	0.24	0.04	0.04	0.11	0.04	0.10
q_P (molP (Cmol$_X$ h)$^{-1}$)	0.002	0.003	0.004	0.19	0.29	0.004	0.34	0.006

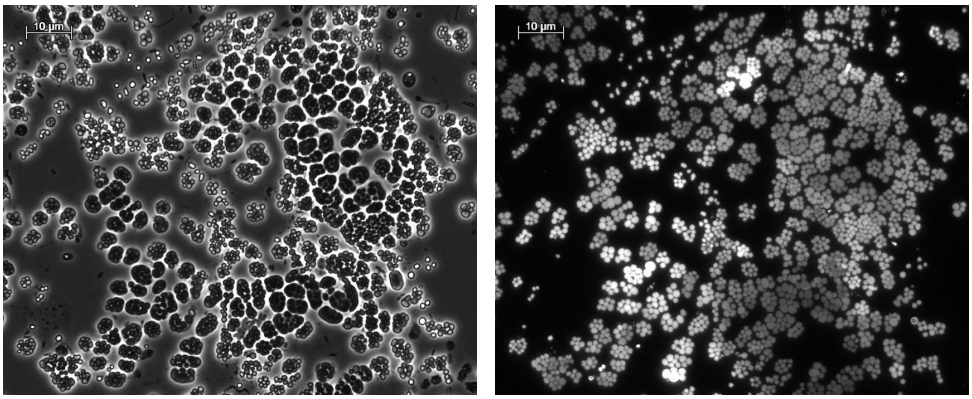

Figure 5.5: Microscopy pictures of biomass sampled at the end of acetate uptake in reactor R7-CN14 operated at 83% exchange ratio with acetate/ammonium uncoupling. PHA granules are clearly visible in intact cells (left). Sample is treated with BODIPY 505/515 to stain PHA under fluorescence light (right). PHA content of total suspended solids is 89 wt% (g g^{-1}). End of cycle pictures are available in Supplementary Materials 5.6.7.

5.4. DISCUSSION

5.4.1. UNCOUPLING AS SUCCESSFUL ENRICHMENT STRATEGY FOR PHA PRODUCTION.

The uncoupling enrichment strategy described in this paper aims to select for microorganisms that produce storage polymers from a carbon substrate stream that lacks either ammonium or phosphate as essential growth nutrient. In all seven systems (Figure 5.3 and Figure 5.4) the pulsed substrate is converted into PHA at a high sustained yield, high biomass specific productivity, and high PHA content, consistently during at least 50 operational cycles (Table 5.2). The produced storage polymers allow microorganisms to grow in a subsequent period when the missing growth nutrients are supplied. The more storage polymers a cell produces, the more catalytic biomass it can form. Therefore, a high PHA production yield and capacity provide microorganisms with a competitive advantage in the alternating presence and absence of carbon substrate and ammonium or phosphate. This strict uncoupling of growth nutrients thereby results in a hard criterion for PHA production. Oliveira *et al.* [17] used uncoupling as a PHA enrichment strategy, but their cheese whey feed was protein-rich, and therefore did not allow for strict uncoupling, resulting in low PHA productivities.

The strict uncoupling strategy is derived from the feast-famine enrichment strategy [3], which can achieve the highest PHA-content with microbial communities to date. In the feast-famine enrichment strategy, the selective pressure predominantly rewards a high substrate uptake rate. Fast growing microorganisms can therefore outcompete storage polymer producing microorganisms when the feast phase lasts long enough for the growers to recuperate the discharged biomass [5]. Therefore, feast-famine enrichments cannot be operated at high exchange ratios as that would lead to longer feast lengths and the competitive advantage of PHA-production over direct growth decreases rapidly. An important consequence of operating at a lower exchange ratio is that a lower maximum PHA content is required. The most successful feast-famine systems operate with a 50% exchange ratio and select for approximately 50 wt% of PHA at the end of the feast phase (Table 5.2: FF). Applying the feast-famine process therefore requires an additional accumulation phase to maximize the cellular PHA content. During the accumulation a carbon rich substrate stream without ammonium is used to feed the biomass, which under certain conditions allows the biomass to reach PHA contents up to 90 wt% [18]. However, one should realize that there is no intrinsic reason for this remarkable phenomenon to succeed at all times since selection is based on the production of up to 50 wt% PHA in the feast-famine cultivation step. Consequently, many feast-famine enrichments can still perform relatively poor (60-80 wt%) in the accumulation step [5, 19–22].

In this study a mixed microbial community was maintained for over 30 cycles, that produced 89±1 wt% of PHA, each cycle. The maximum PHA content in many contemporary enrichment studies varies between 25% and 60% [17, 23–25]. The significance of a difference in PHA content between 25%, 60% and 89% can easily be overlooked due to the non-linear relationship between fractions and PHA yield and PHA content. It is therefore preferred to express these observations as a ratio between storage polymers and catalytic biomass as depicted in Figure 5.6 [26]. This graph demonstrates the relative amount of non-PHA material that needs to be removed by downstream processing

for the recovery of PHA. Additionally, because less catalytic biomass is required, a significant increase in the overall process yield can be achieved at a high PHA content.

The stability of operation and emphasis on PHA yield and capacity make the uncoupled strategy the preferred operational strategy for carbon rich substrate streams, that are limited in nitrogen or phosphorous. Herewith a novel competitive strategy is identified that enables the most effective microbial community based PHA production process to date. This study shows another intriguing example of using microbial ecology based principles for enrichment of specific functional properties as proposed by Mooij *et al.* [6]. Competition and evolution are valuable assets that allow well-designed enrichment systems to show continues improvement. This enrichment strategy is achieved by linking the desired process properties to intrinsic benefits of the microbial community.

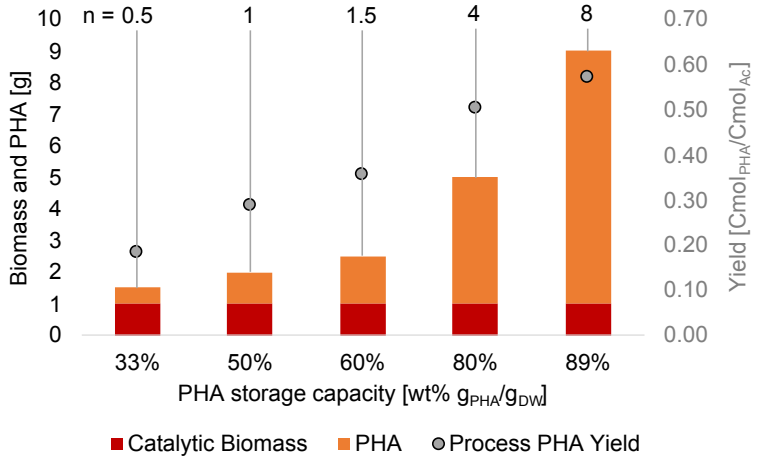

Figure 5.6: Visual representation of the difference in PHA production capacity when expressed as dry weight fraction. For each gram of catalytic biomass that is produced (red), *n* gram of PHA need to be produced (orange) to reach the PHA storage capacity as described on the x-axis. The grey circles denote the overall process yield, expressed as the amount of PHA that is produced from one Cmol of acetate substrate.

5.4.2. THE INFLUENCE OF SECONDARY GROWTH NUTRIENTS, CARBON-NUTRIENT RATIO, AND EXCHANGE RATIO ON PROCESS PERFORMANCE AND COMMUNITY STRUCTURE

The uncoupling strategy resulted in stable, PHA producing enrichments, with either ammonium or phosphate as secondary growth limiting nutrient (Figure 5.3). The nitrogen uncoupled systems follow the predictions from Equation 5.1 well. The phosphate limited cultures performed worse than predicted, because the system was shown to enrich for a microbial community that is capable of lowering the cellular P-content of catalytic biomass as reflected in the lower cellular P/N-ratio. Indirectly, this limits the PHA-content that can be achieved to lower values compared to ammonium limited cultures. Increasing the C:P ratio of the feed pulses even further than was attempted in R4-CP300 may eventually reduce ammonium uptake, but comes at the cost of a strong reduction in the biomass specific uptake rates [2, 4].

The microbial community structure analysis indicates a high relative abundance of well-known PHA producers (Supplementary Materials 5.6.5). *Zoogloea sp.* dominates in phosphate uncoupled cultures, and *Plasiticicumulans sp.* in ammonium uncoupled cultures. Bacteria belonging to the *Mesorhizobium* and *Chryseobacterium* genera also show increased relative abundance in the nitrogen uncoupled systems with excess carbon, R2-CN20, R5-CN14, and R7-CN14. These genera are associated with nitrogen fixation [27, 28] and have the full PHA machinery. Measurement from total organic nitrogen could not determine a difference in dosed and measured organic nitrogen, suggesting that nitrogen fixation contributed little to the absolute abundance. A noteworthy observation was that DNA extraction of samples with high PHA content (> 70 wt%) lead to poor DNA extraction yields, which could influence the observed relative abundances.

Due to the uncoupled supply of C/N and C/P growth nutrients, a new competitive strategy emerges, where microorganisms are now also competing for ammonium or phosphate besides carbon. Therefore, an increased emphasis is placed on biomass specific nitrogen (q_N) and phosphorus (q_P) uptake rates, besides the carbon substrate uptake rate (q_S). When the q_N and q_P values in Table 5.2 are compared, it becomes apparent that the values obtained in ammonium and phosphate limited cultures are respectively 10 to 100 times higher than that of their counterparts. Especially the phosphate uptake rate exceeds the actual growth rate of the microorganisms as reflected in the extended period with elevated oxygen and ammonium uptake rates after phosphate depletion (Figure 5.3: R3-CP200 and R4-CP300), where the highest q_P observed in this work (0.34 ± 0.12 P-mol (C-mol$_X$ h)$^{-1}$) exceeds that of specifically enriched phosphate accumulating organisms [29]. It is remarkable to see in the P-limited system that microorganisms with the capacity to achieve a very high PHA-content, also compete very effectively for extremely high P-uptake rates. This highly effective double hoarding strategy was found to be a prerequisite for survival in this system.

Besides the biomass specific uptake rates, the plasticity of the microbial communities for dealing with a variable intracellular nitrogen and phosphorus content is also rewarded [30]. In the P-limited cultures, the biomass can form proteins from excess carbon and ammonium, but in the N-limited cultures protein synthesis cannot occur without nitrogen fixation. The increased C:N ratio in system R2-CN20 resulted in more PHA production in the carbon phase (Figure 5.3: R2-CN20), but PHA was utilized in the nutrient phase to produce unidentified organic solids. This dilution of catalytic biomass is less pronounced than is the case for phosphate limitation, but still significant. Apparently, the increase in C:N and C:P ratio of the feed is not a hard selector for increasing the maximum PHA content. It facilitated the production of side-products, resulting in undirected resource allocation as also observed by Cavaillé *et al.* [2].

Where an increased carbon to nutrient ratio resulted in undesirable product formation, increasing the exchange ratio in ammonium uncoupled systems resulted in significant increases in maximum PHA content (Figure 5.4). The sustained PHA content of 89 wt% was achieved with a cycle length of 40 hours at an exchange ratio 83.3%. The increased exchange ratio apparently functions as a hard criterion to the strict uncoupling strategy, selecting for microorganisms with a high maximum PHA capacity. In this work the influence of the cycle length was not investigated, therefore it is unknown whether the relatively long periods at the end of the carbon and nutrient phases, with apparent

low biological activity, are instrumental to the uncoupling strategy or whether they allow for process optimization.

5.4.3. ENGINEERING CONSIDERATIONS FOR FULL-SCALE IMPLEMENTATION

Two aspects of the uncoupling enrichment strategy need to be addressed to make it suitable for full-scale implementation. First, the feast-famine and uncoupling strategies use feed pulses, while for full-scale processes more continuous streams are preferred. In an effort to convert the feast-famine enrichment process from a sequential batch to a continuous process, Marang *et al.* [31] demonstrated that the carbon substrate pulses are essential for the selection of biomass with high PHA storage capacity in systems where all other growth nutrients are continuously present. The prolonged carbon phase of 10 hours in R7-CN14 suggests that pulses are not essential requirements in uncoupled systems, and uncoupling could also be accomplished by continuous dosing of carbon substrate during the carbon uptake phase.

The second aspect that needs to be overcome is the low biomass concentration at the start of the carbon feed period. For the enrichments, a fixed amount of carbon is dosed and a low initial biomass concentration is required to achieve a high PHA fraction. Ideally, the biomass concentration in the full-scale bioreactor would make maximum use of the limiting process characteristic, which for aerobic bioreactors is often the oxygen transfer rate. Biomass retention in the carbon phase, through a membrane or settling, would allow for higher biomass concentrations, thereby maximizing the utilization of the oxygen transfer capacity of the bioreactor. This effect is even more pronounced if low substrate concentration wastewater (1-3 g_{COD} L^{-1}) is used as feedstock, as the dissolved organics are converted to, and concentrated as, solids.

By implementing continuous feeding and biomass retention, it could be possible to employ a continuous carbon uptake bioreactor that is able to convert a typical heterogeneous feedstock of 2 g_{COD} L^{-1} into PHA rich biomass, given that a strong limitation of secondary growth nutrients is present in the influent. A process design of a semi-continuous adaptation of R7-CN14 is included in Supplementary Materials 5.6.9, and ongoing efforts for the implementation of the uncoupling strategy in two linked continuous bioreactors [32] could result in a continuous process with the high PHA productivity characteristics of the uncoupled system.

5.5. CONCLUSIONS

By uncoupling the supply of carbon and a secondary growth nutrient we were able to maintain a stable microbial community with an unprecedented combination of PHA storing capacity, productivity, product yield, and general applicability for feed streams without nitrogen or phosphate. The strict uncoupling of carbon and ammonium resulted in the best performing systems, which were able to cyclically reach a PHA content of 89 dw%. Phosphate uncoupled systems showed comparable characteristics, although the plasticity of intracellular phosphate content allowed the biomass to keep assimilating ammonium, reducing the maximum PHA content achieved. The use of ecological-based selective environments for microbial community engineering could and should be exploited further for biological processes that rely on enriched microbial communities.

ACKNOWLEDGEMENTS

We gratefully acknowledge financial support from the Netherlands Organisation for Scientific Research (NWO) funded projects: UNLOCK (NRGWI.obrug.2018.005), and the Paques Partnership Program (13002).

5.6. SUPPLEMENTARY MATERIALS

5.6.1. STOICHIOMETRIC AND KINETIC MODEL FOR STRICT UNCOUPLED SEQUENCING BATCH BIOREACTORS

A metabolic model was designed to determine kinetic properties of the enriched cultures. This model adds uncoupling of carbon and N/P supply to previous work by Johnson *et al.* [11], Tamis *et al.* [12], and Korkakaki *et al.* [4]. This extension allows both feast-famine and uncoupled systems to be modeled by a single set of equations. The model allows for parameter fitting through a least-squares minimization. An excellent fit can be achieved for the acetate, ammonium, PHA, and phosphate concentrations for the nitrogen uncoupled systems without any additional variables. In the phosphate uncoupled systems, the fast phosphate uptake observed and the immediate increase in conversion rates imply that integration of phosphate into active biomass is rather fast. This response could be modeled by allowing the phosphate taken up to form poly-phosphate (polyP). Biomass specific rates are defined per carbon-mole of catalytic biomass, with structure formula ($CH_{1.8}O_{0.5}N_{0.2}P_{0.0125}$). Ammonium uptake in absence of phosphate therefore does not result in increased biomass rates. Previous models implemented switch-like functions to discern between the feast and famine periods, here we use a single set of expressions that describe the behavior of all enrichment cultures, for both ammonium and phosphate limitations. Importantly, all systems could be described based on 4 biomass specific variables (Table 5.3). The python3 code is available online at GitHub: `https://github.com/GRS-TUD/uncoupled-model`

Table 5.3: Overview of biomass specific parameters for the kinetic model, with the primary fitting parameters highlighted in dark, and specific phosphate uncoupled fitting parameters in light.

Description	Symbol	(typical) Value	Unit
Maximum biomass growth rate	μ^{max}	0.15	$Cmol_X/Cmol_X/h$
Maximum Acetate uptake rate	q_{Ac}^{max}	3.00	$Cmol_{Ac}/Cmol_X/h$
Maximum phosphate uptake rate	q_{PO4}^{max}	$\mu^{max}/C:P_X$	$Pmol_P/Cmol_X/h$
Poly-Phosphate production	pP	0	$Pmol_{pP}/Pmol_X$

The mechanistic model might not represent the actual biological mechanisms that govern uncoupled cultivated cultures, but the model proposed here emulates the observed compound profiles with as few variables as possible, thereby it minimizes the risk of predictive power bias [33]. A series of affinity constants, stoichiometric values and fitting parameters were used from previous models, but were kept constant for all model fits (Table 5.4). The most notable values are for maintenance, derived from the ASM3 aerobic model and adjusted for 30°C [34], and the PHA degradation rate constant (κ), which is made proportional to the maximum biomass specific growth rate.

Table 5.4: Overview of kinetic constants, stoichiometric values, and parameters used in the model. These values were kept constant for all model fits.

Description	Symbol	(typical) Value	Unit
Maintenance/decay/lysis at 30°C	m	0.013	$Cmol_X/Cmol_X/h$
PHA yield on Acetate	$Y_{PHA/Ac}$	2/3	$Cmol_{PHA}/Cmol_{Ac}$
Biomass yield on PHA	$Y_{X/PHA}$	2/3	$Cmol_X/Cmol_{PHA}$
Biomass yield on Acetate (direct growth)	$Y_{X/Ac}$	0.5	$Cmol_X/Cmol_{Ac}$
Carbon to nitrogen ratio of biomass	$C:N_X$	5	$Cmol_X/Nmol_X$
Carbon to phosphate ratio of biomass	$C:P_X$	80	$Cmol_X/Pmol_X$
Acetate affinity	K_{Ac}	10^{-3}	mol_{Ac}/L
Ammonium affinity	K_{NH4}	10^{-4}	mol_N/L
Phosphate affinity	K_{PO4}	10^{-4}	mol_P/L
PHA inhibition term	α	2	-
Maximum PHA fraction in a cell	f_{PHA}^{max}	10	$Cmol_{PHA}/Cmol_X$
PHA degradation rate constant	κ	$\mu^{max}/Y_{X/PHA}$	~

MODELLING A SEQUENCING BATCH BIOREACTOR

A generalized sequencing batch bioreactor operation is mimicked by allowing the configuration of the influent amounts and timing of acetate, ammonium, and phosphate, the effluent ratio, the working volume, and cycle length. Furthermore, the concentrations (or amounts) of biomass, PHA, acetate, ammonium, and phosphate at the initial moment are required. The model is implemented in such a way that it allows the system to reach a pseudo steady state, for example by mimicking 100 sequential cycles. The pseudo steady state values of the compounds at the start of a new cycle (t=0) are given as M_i in Table 5.5.

Different limitation and inhibition conditions can be encountered in an uncoupled system, the generalized mechanistic model implements three steps to assess specific rates. The sole assumption is that all biomass aims to maximize the growth rate.

Table 5.5: For modelling the sequencing batch bioreactors, the following configurable parameters are required, coming from direct input or measurements of the system.

Description	Symbol	(typical) Value	Unit
Reactor volume	V	1.4	L
Effluent Ratio	ER	0.5	L/L
Cycle length	CL	12	h
Carbon uptake length	τ	2	h
Acetate pulse amount	C_{load}	0.040	Cmol_{Ac}/cycle
Ammonium pulse amount	N_{load}	0.005	Nmol_{NH4}/cycle
Phosphate pulse amount	P_{load}	0.0016	Pmol_{PO4}/cycle
Biomass amount at t=0	$\text{M}_{\text{X,0}}$	0.01	Cmol_{X}
PHA amount at t=0	$\text{M}_{\text{PHA,0}}$	0.00	Cmol_{PHA}
Acetate amount at t=0	$\text{M}_{\text{Ac,0}}$	0	Cmol_{A}
Ammonium amount at t=0	$\text{M}_{\text{NH4,0}}$	0.002	Nmol_{NH4}
Phosphate amount at t=0	$\text{M}_{\text{PO4,0}}$	0.001	Pmol_{PO4}
Phosphate in biomass at t=0	$\text{M}_{\text{PO4x,0}}$	$M_{X,0}/C : P_X$	Pmol_{P}

ACETATE UPTAKE KINETICS AND ALLOCATION BETWEEN BIOMASS AND PHA PRODUCTION

The potential biomass specific substrate uptake rate $q_{\text{Ac}}^{\text{pot}}$ is based on Michaelis-Menten uptake kinetics with acetate limitation. A certain fraction is directed to biomass growth, by taking into account the growth limitation of ammonium.

$$q_{\text{Ac}}^{\text{pot}} = q_{\text{Ac}}^{\text{max}} \cdot \frac{[\text{Ac}]}{K_{\text{Ac}} + [Ac]} \tag{5.2}$$

$$\text{NH4}_{\text{lim}} = \frac{[NH_4^+]}{K_{NH4} + [NH_4^+]} \tag{5.3}$$

$$\mu_{\text{Ac}} = \min\left(q_{\text{Ac}}^{\text{pot}} \cdot Y_{\text{XS}} \cdot NH4_{\text{lim}}, \mu^{\text{max}}\right) \tag{5.4}$$

$$q_{\text{Ac}}^{\mu} = \frac{\mu_{\text{Ac}}}{Y_{\text{XS}}} \tag{5.5}$$

The residual substrate uptake potential can be used to produce PHA, taking into account inhibition due to accumulated intracellular PHA.

$$\text{PH}A_{\text{inh}} = 1 - \left(\frac{\left(\frac{\text{PHA}}{X}\right)}{f_{\text{PHA}}^{\text{max}}}\right)^{\alpha} \tag{5.6}$$

$$q_{\text{Ac}}^{\text{PHA}} = \left(q_{\text{Ac}}^{\text{pot}} - q_{\text{Ac}}^{\mu}\right) \cdot PHA_{\text{inh}} \tag{5.7}$$

$$q_{\mathrm{PHA}}^{\mathrm{prod}} = q_{\mathrm{Ac}}^{\mathrm{PHA}} \cdot Y_{\mathrm{PHA/S}} \tag{5.8}$$

Acetate cannot be used for other processes, and therefore acetate uptake for growth and PHA formation results in the net biomass specific acetate uptake rate.

$$q_{\mathrm{Ac}} = \left(q_{\mathrm{Ac}}^{\mathrm{PHA}} + q_{\mathrm{Ac}}^{\mu}\right) \tag{5.9}$$

PHA PRODUCTION AND DEGRADATION KINETICS

If microbes are not growing at their full growth potential on acetate, while other nutrients are not the limiting factor, they start consuming PHA. This occurs at the end of the feast phase in the feast-famine system, and in all uncoupled systems after the nutrient pulse. The potential PHA consumption rate is determined by a shrinking particle model (Tamis et al. 2014), with a biomass specific PHA degradation constant (κ).

$$q_{\mathrm{PHB}}^{\mathrm{pot}} = \kappa \cdot \left(\frac{[X_0]}{[X]}\right)^{\frac{1}{3}} \cdot \left(\frac{[\mathrm{PHA}]}{[X]}\right)^{\frac{2}{3}} \tag{5.10}$$

In previous models PHA degradation directly resulted in biomass growth, regardless of the maximum growth rate and ammonium limitations. In the new model, the PHA degradation rate cannot exceed the maximum growth rate of the biomass, and follows the limitation for ammonium. Consequently, the model sensitivity to the degradation rate constant becomes less pronounced, as in the previous models it was used to find/set the growth rate in the famine period. By making κ proportional to the maximum biomass specific growth rate, fewer fitting parameters are required.

$$\kappa = \frac{\mu^{\mathrm{max}}}{Y_{\mathrm{X/PHA}}} \tag{5.11}$$

The PHA degradation potential cannot exceed the maximum growth rate, as is described by the following expression.

$$\mu_{\mathrm{PHA}} = \min\left(q_{\mathrm{PHA}}^{\mathrm{pot}} \cdot Y_{\mathrm{X/PHA}} \cdot NH4_{\mathrm{lim}}, \mu^{\mathrm{max}} - \mu_{\mathrm{Ac}}\right) \tag{5.12}$$

The difference between PHA production and consumption for growth is the net PHA rate.

$$q_{\mathrm{PHA}} = q_{\mathrm{PHA}}^{\mathrm{prod}} - \frac{\mu_{\mathrm{PHA}}}{Y_{\mathrm{X/PHA}}} \tag{5.13}$$

The net growth rate includes growth on acetate, growth on PHA, and the combined process of maintenance, decay, and lysis (m).

$$\mu = \mu_{\mathrm{Ac}} + \mu_{\mathrm{PHA}} - m \tag{5.14}$$

PHOSPHATE UPTAKE AND ALLOCATION INTO CATALYTIC BIOMASS AND POLY-PHOSPHATE

The growth rate μ describes the formation of carbon and nitrogen rich biomass, but for the formation of catalytically active biomass also phosphate is required. Therefore, phosphate has to be taken up from the broth. Phosphate can either be directly incorporated into biomass or stored as poly-phosphate, as is the case in phosphate accumulating organisms. Phosphate uptake is inhibited by the phosphate content of the biomass.

$$PO4_{\text{inh}} = 1 - \frac{[P_X]}{[X]} \cdot \left(\frac{C:P_X}{1+pP} \right) \tag{5.15}$$

For example: if the biomass has no poly-phosphate storage capacity (pP=0), and all biomass is catalytically active, then the phosphate content of the biomass $\frac{[P_X]}{[X]}$ is equal to $\frac{1}{C:P_X}$, and therefore the inhibition term will be 0. Meaning that no additional phosphate can be taken up by the biomass. Alternatively, biomass with poly-phosphate accumulating potential, can decrease the inhibitory effects. The actual phosphate uptake rate will also depend on phosphate affinity:

$$q_{PO4} = q_{PO4}^{\max} \cdot \text{PO4}_{\text{inh}} \cdot \frac{[PO4]}{k_{PO4} + [PO4]} \tag{5.16}$$

As was observed by Korkakaki and colleagues (2017), the biomass specific rates could more closely be modeled by looking at the phosphate content (P_X) then looking at the carbon content (C_X) of the biomass. This distinction allows for the definition of catalytic biomass and the proceeding differential equations of the mass balances.

$$X_{\text{cat}} = P_X \cdot C:P_X \tag{5.17}$$

DIFFERENTIAL EQUATIONS

$$\frac{\text{dAc}}{\text{dt}} = -q_{\text{Ac}} \cdot [X_{\text{cat}}] \cdot V \tag{5.18}$$

$$\frac{dNH4}{\text{dt}} = -\frac{\mu}{C:N_X} \cdot [X_{\text{cat}}] \cdot V \tag{5.19}$$

$$\frac{dPO4}{\text{dt}} = -q_{PO4} \cdot [X_{\text{cat}}] \cdot V \tag{5.20}$$

$$\frac{\text{dX}}{\text{dt}} = \mu \cdot [X_{\text{cat}}] \cdot V \tag{5.21}$$

$$\frac{\text{dPHA}}{\text{dt}} = q_{\text{PHA}} \cdot [X_{\text{cat}}] \cdot V \tag{5.22}$$

$$\frac{dP_X}{\text{dt}} = q_{PO4} \cdot [X_{\text{cat}}] \cdot V \tag{5.23}$$

5.6.2. INFLUENCE OF EXCHANGE RATIO AND CARBON TO NUTRIENT RATIO ON PHA ACCUMULATION POTENTIAL

The maximum PHA content that a microbial culture can achieve in a strict uncoupled system can be derived based on the exchange ratio of the culture, and the carbon to nutrient ratio of the feed streams (an analogue derivation can be made for a phosphate limited culture). In the following section the derivation for a direct equation is made with the definitions and variables as described in Supplementary Materials Table 5.3, Table 5.4, and Table 5.5.

Uncoupling is achieved if all growth nutrients are consumed in their respective phase. It is assumed that all carbon is consumed and converted to PHA and CO_2 during the carbon uptake phase, as no new catalytic biomass is formed due to the absence of secondary growth nutrients. During the ammonium or phosphate phase, all ammonium and phosphate can be taken up and stoichiometrically forms new catalytic biomass, as given by the carbon to nitrogen and carbon to phosphate ratios of the biomass ($C:N_X$) and $C:P_X$). The PHA content of biomass (Cmol/Cmol) is given by the following expression, where PHA_0 is the PHA at the beginning of the carbon feed period, and PHA_{new} is the newly formed PHA, and the catalytic biomass at the beginning of the carbon feed period is defined as X_0:

$$\%PHA = \frac{PHA_{new} + PHA_0}{PHA_{new} + PHA_0 + X_0} \tag{5.24}$$

As the derivation of %PHA is for the PHA fraction, the absolute amounts of biomass and PHA are not required, just the ratio of the biomass to PHA. It therefore suffices to use ratios for all parameters. The input is normalized to the limiting substrate, nitrogen in the system is set to 1. Therefore, the amount of biomass (X_0) at the start of the cycle depends on the exchange ratio and the nitrogen content of the biomass.

$$X_0 = (1 - ER) \cdot C : N_X \tag{5.25}$$

Newly formed PHA (PHA_{new}) depends on the amount of substrate that is dosed, and the yield of PHA on substrate ($Y_{PHA/S}$). The dosed amount of substrate depends on the amount of reactor broth that is exchanged (ER) and the molar carbon content of the feed ($C:N_{feed}$), relative to the molar nitrogen content of the feed.

$$PHA_{new} = ER \cdot C : N_{feed} \cdot Y_{PHA/S} \tag{5.26}$$

This initial amount of PHA (PHA_0) in the biomass depends on the total amount of PHA that can be formed from the carbon in the feed minus the total amount of PHA required to form biomass from the limiting nutrient, corrected for the exchange ratio.

$$PHA_0 = \left(C : N_{Feed} \cdot Y_{PHA/S} - C : N_X \cdot Y_{X/PHA}^{-1}\right) \cdot (1 - ER) \tag{5.27}$$

Filling in the definitions for PHA_{new}, PHA_0, and X_0 in Equation 5.24 results in the following equation, with parameters $C:N_{feed}$ and ER.

$$\%PHA\left(ER,\ C:N_{feed}\right) = \frac{C:N_{feed}\cdot Y_{PHA/S} - C:N_X\cdot Y_{X/PHA}^{-1}\cdot(1-ER)}{C:N_{feed}\cdot Y_{PHA/S} + C:N_X\cdot(1-ER)\cdot\left(1-Y_{X/PHA}^{-1}\right)} \tag{5.28}$$

%PHA expressed in Cmol% with $Y_{PHA/S} = 0.67\ \frac{Cmol_{PHA}}{Cmol_S}$, $Y_{X/PHA} = 0.67\ \frac{Cmol_X}{Cmol_{PHA}}$, $C:N_X = 5$

Which can also be written as a function of X_0 (itself a function of ER and $C:N_X$), more clearly demonstrating the relationship between the maximum achievable PHA fraction and the initial biomass amount:

$$\%PHA\left(X_0,\ C:N_{feed}\right) = \frac{C:N_{feed}\cdot Y_{PHA/S} - X_0\cdot Y_{X/PHA}^{-1}}{C:N_{feed}\cdot Y_{PHA/S} - X_0\cdot Y_{X/PHA}^{-1} + X_0} \tag{5.29}$$

5.6.3. INFLUENCE OF EXCHANGE RATIO ON SUBSTRATE UPTAKE LENGTH AND INITIAL τ ESTIMATION

At an increased exchange ratio, the biomass has to make more PHA and therefore take up an increasing amount of substrate per unit of catalytic biomass. As a result, the time period in which extracellular substrate is present increases at an increased exchange ratio, even when biomass specific rates are equal. Furthermore, at elevated PHA-contents the uptake rate decreases [11]. These combined factors result in an increase in the substrate uptake length, requiring a longer time between the carbon and nutrient pulse (τ) and a longer cycle length, which needs to be taken into account for process design. Main text Figure 5.2 shows the estimated maximum PHA content of the biomass and the substrate uptake length as a function of the exchange ratio, at different uncoupled substrate feed ratios of C:N 12, 14, and 20. Below follows the derivation.

An exact mathematical solution of the expected carbon uptake length can be made by assuming that the substrate uptake rate (R_S) is only limited by the PHA product inhibition.

$$R_S^{max} = X_0 \cdot q_s^{max} \tag{5.30}$$

$$PHA_{inh} = 1 - \left(\frac{\left(\frac{PHA}{X_0}\right)}{f_{PHA}^{max}} \right)^{\alpha} \tag{5.31}$$

$$R_{PHA} = R_S^{max} \cdot Y_{PHA/S} \cdot PHA_{inh} \tag{5.32}$$

The change in the total PHA thereby only depends on the PHA content. Leading to an elegant integration for integer values for the PHB inhibition term (e.g. α=2).

$$\frac{dPHA}{dt} = R_s^{max} \cdot Y_{PHA/S} \cdot \left[1 - \left(\frac{\left(\frac{PHA}{X_0}\right)}{f_{PHA}^{max}} \right)^{\alpha} \right] \tag{5.33}$$

$$PHA(t) = \int \frac{dPHA}{dt} = f_{PHA}^{max} \cdot X_0 \cdot \tanh \left[\frac{q_s^{max} \cdot Y_{PHA/S} \cdot t + X_0 \cdot C}{f_{PHA}^{max}} \right] \tag{5.34}$$

The integration constant C can be found by solving equation 4 at t=0, with PHA_0.

$$C = \tanh^{-1} \left[\frac{PHA_0}{f_{PHA}^{max} \cdot X_0} \right] \cdot \frac{f_{PHA}^{max}}{X_0} \tag{5.35}$$

Where PHA_0 is derived before (Equation 5.27). In this simplified uncoupled system, all the pulsed substrate is converted into PHA, and therefore should be equal to the change in total PHA.

$$C : N_{feed} \cdot ER \cdot Y_{PHA/S} = PHA(t) - PHA_0 \tag{5.36}$$

The mathematical estimate of the end of the carbon uptake is then given by:

$$t = \left(\tanh^{-1}\left[\frac{C:N_{feed}\cdot ER\cdot Y_{PHA/S}+PHA_0}{f_{PHA}^{\max}\cdot X_0}\right]\cdot f_{PHA}^{\max}+X_0\cdot C\right)\cdot\frac{1}{q_s^{\max}\cdot Y_{PHA/S}} \tag{5.37}$$

The asymptotic behavior of tanh[1], when the PHA fraction in the biomass gets close to the maximum PHA fraction $\left(f_{\mathrm{PHA}}^{\max}\right)$, means that small deviations in value estimates have a significant influence on the predicted carbon uptake length (Figure 5.7). But the trend fits the general gist that until moderate PHA fractions (< 75% of $f_{\mathrm{PHA}}^{\max}$) the PHA inhibition term is negligible.

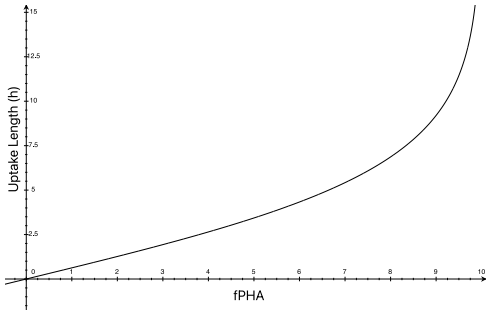

Figure 5.7: Graphical depiction of the inverse hyperbolic tangent function for $f_{PHA}^{\max} = 10$.

5.6.4. PHA ACCUMULATION POTENTIAL OF ENRICHED BIOMASS IN CLASSICAL FED-BATCH EXPERIMENT

Table 5.6: PHA accumulation potential after 7 hours of feed-on-demand acetate dosing in absence of nitrogen in R1 and R2, and phosphate in R3 and R4. After 2 hours R3 and R4 also became nitrogen limited.

System		R1-CN12	R2-CN20	R3-CP200	R4-CP300
Maximum %PHA	gPHA/gTSS	91	82	81	78
$Y_{PHA/Ac}$	Cmol/Cmol	0.69±0.07	0.72±0.07	0.65±0.17	0.73±0.13
Gap carbon balance	%	1	1	18	6
Gap electron balance	%	2	6	20	5

[1] Or in general the Gauss Hypergeometric function ${}_2F_1$ for non-integer values of α.

5.6.5. MICROBIAL COMMUNITY STRUCTURE AND MICROSCOPY

The taxa-based microbial community composition of the enriched cultures was determined by amplicon sequencing of the V3-V4 (341F, 785R) region of the 16S rRNA gene after DNA extraction with the DNeasy PowerSoil Pro kit (Qiagen GmbH, Germany). After sequencing, the paired end reads were quality filtered and analyzed using the NG-Tax 2.0 software [14]. The sequence data are available at NCBI under BioProject accession number PRJNA674007. DNA extraction of samples with high PHA content resulted in a very low DNA yield (100 – 200 times lower) and requires further investigation regarding extraction methodology.

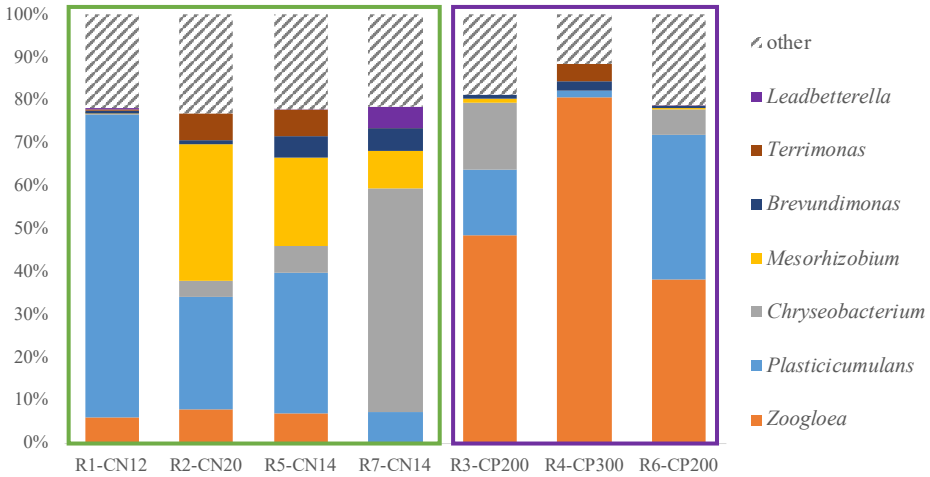

Figure 5.8: Relative abundance of 16S rRNA gene sequence reads with amplicon sequencing of the uncoupled cultures. R1-R4 are sampled after 40 days of operation, and R5-R7 are sampled after 30 days of operation. Samples are grouped in ammonium uncoupled (green), and phosphate uncoupled (purple), where R6-CP200 achieved uncoupling on both ammonium and phosphate. Shown are the highest relative abundant microbial genera, that make up over 5% of the reads in a single sample. For graphing purposes, all other genera are combined under other.

5.6.6. DIFFERENCES IN OXYGEN TRANSFER RATE REQUIREMENTS

In pulse-fed batch operated systems, the oxygen transfer rate (OTR) requirements can vary throughout the cycle. The feast-famine system requires a high OTR for 30 to 60 minutes, followed by a ten-fold lower oxygen requirement for the remaining time (Figure 5.9). The uncoupled system allows for a lower overall carbon substrate uptake rate, and therefore an extended and more balanced oxygen requirement. Even for R7-CN14, where the carbon phase took almost ten hours, a steady oxygen uptake is observed. In all systems, the overall oxygen uptake per carbon mole of substrate remains comparable.

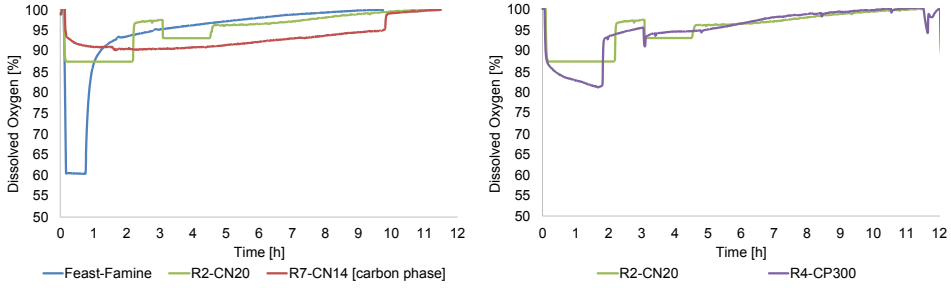

Figure 5.9: Left: Dissolved oxygen concentration measurements of three bioreactors operated as feast-famine (blue), uncoupled with an exchange ratio of 50% (green), and uncoupled with an exchange ratio of 83% (red – only the carbon uptake phase is shown). It is clearly visible that the fast substrate uptake rate in the feast-famine system requires a higher oxygen transfer rate during the carbon uptake period. The dissolved oxygen profiles for R2 and R7 are measured during operational cycles as represented in the main text.
Right: Dissolved oxygen concentration measurements of a nitrogen and phosphate uncoupled bioreactor. The phosphate dosage after 3h leads to a short (minutes) increase in oxygen uptake, and a prolonged smooth decrease in respiration activity. This is significantly different from the block-like response to an ammonium pulse in the ammonium limited system.

5.6.7. END OF CYCLE MICROSCOPY PICTURES

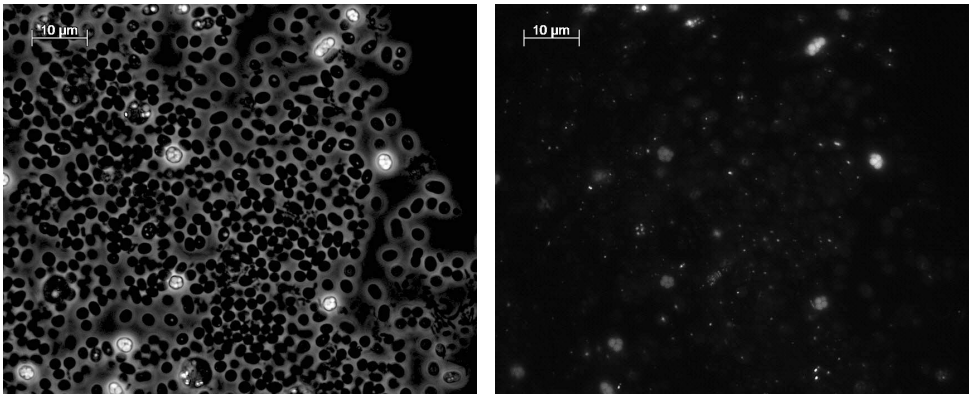

Figure 5.10: Microscopy pictures of biomass sampled at the end of nitrogen uptake phase in reactor R7-CN14 operated at 83% exchange ratio with acetate/ammonium uncoupling. Residual PHA granules are visible in some cells (left). Sample is treated with BODIPY 505/515 to stain PHA under fluorescence light (right). PHA content of total suspended solids is 2 wt% ($g\,g^{-1}$).

5.6.8. KINETIC AND STOICHIOMETRIC PROPERTIES OF UNCOUPLED ENRICHMENT CULTURES

Table 5.7: Overview of kinetic and stoichiometric properties of seven enrichments. Measurements from three consecutive cycles, standard deviations are shown with plus-minus sign. A reference column (grey) of a feast-famine (FF) enrichment is included [16].

Bioreactor	FF	(ref.)	R1	CN12	R2	CN20	R3	CP200	R4	CP300	R5	CN14	R6	CP200	R7	CN14
Carbon uptake phase																
Predicted %PHAmax (wt%)	52		60		77		62		75		84		83		89	
Maximum %PHA (wt%)	52	±1	60	±3	62	±3	50	±5	46	±6	79	±2	75	±2	89	±1
PHA:X ratio (Cmol Cmol^{-1})	**1.1**		**1.5**		**1.6**		**1**		**0.9**		**3.8**		**3**		**8.1**	
Carbon-uptake length (min)	38	±3	60	±5	120	±8	60	±8	80	±7	240	±12	310	±15	600	±20
Ammonia uptake %			0		0		8.5	±2	14	±3	0		15	±4	0	
Gap carbon balance (%)			1	±1	11	±2	6	±2	9	±2	0	±1	6	±2	0	±2
Gap electron balance (%)			1	±1	12	±2	8	±2	12	±3	4	±1	6	±1	5	±1
$Y_{PHA/Ac}$ (Cmol Cmol^{-1})	0.67		0.69	±0.04	0.64	±0.08	0.64	±0.03	0.58	±0.03	0.66	±0.02	0.54	±0.04	0.64	±0.03
Growth rate (h^{-1})			0		0		0.16	±0.08	0.12	±0.04	0		0.11	±0.02	0	
q_s^{max} (Cmol (Cmol$_X$ h)$^{-1}$)	3.5	±0.2	2.7	±0.2	2.2	±0.1	3	±0.3	2.2	±0.2	2.3	±0.2	1.7	±0.2	2.2	±0.2
q_{PHA} (Cmol (Cmol$_X$ h)$^{-1}$)	1.74	±0.05	1.67	±0.1	1.3	±0.1	1.73	±0.2	1.08	±0.1	1.39	±0.1	0.93	±0.05	0.84	±0.05
Growth phase																
Predicted %PHAres. (wt%)	0		8		50		13		47		24		13		24	
Residual %PHA (wt%)	0		7	±3	24	±5	0	±3	4	±4	7	±5	3	±3	2	±3
Nutrient uptake length (min)			400	±20	240	±20	10	±1	4	±1	300	±15	10	±1	380	±30
Ammonia uptake %			100		100		91.5	±2	86	±3	100		85	±4	100	
Gap carbon balance (%)			0.2	±0	15	±3	12	±2	9	±2	8	±1	11	±2	13	±4
Gap electron balance (%)			1.2	±1	16	±3	13	±3	11	±2	9	±1	12	±2	14	±3
$Y_{X/PHA}$	0.67		0.63	±0.05	0.52	±0.08	0.57	±0.08	0.65	±0.04	0.57	±0.07	0.50	±0.03	0.57	±0.04
q_N (molN (Cmol$_X$ h)$^{-1}$)	0.033	±0.003	0.13	±0.02	0.24	±0.03	0.04	±0.005	0.03	±0.01	0.11	±0.03	0.04	±0.01	0.10	±0.02
q_P (molP (Cmol$_X$ h)$^{-1}$)	0.002	±0.002	0.003	±0.002	0.004	±0.002	0.19	±0.03	0.29	±0.05	0.004	±0.002	0.34	±0.09	0.006	±0.003

5.6.9. FULL-SCALE ADAPTATION OF R7-CN14

A potential semi-continuous adaptation of the most productive uncoupled system is shown in Figure 5.11. The first bioreactor (C-reactor) would be fed continuously while exercising biomass retention, allowing a separation of the solid and liquid retention by converting the organic carbon into intracellular PHA with a constant oxygen transfer rate. The PHA titer that can be achieved from the substrate stream will depend on biomass properties, but 25-50 $g_{PHA}\,L^{-1}$ is within scope [35]. After this continuous feeding period the biomass is harvested. Once every three cycles, half of the biomass is transferred to the second bioreactor (N-reactor) where nutrients are dosed for 30 hours. The optimal exchange values require further experimentation, the suggested values result in an exchange ratio of 83% $\left(1-\frac{0.5}{3}\right)$. Meanwhile, the C-reactor is reinoculated with new biomass from the N-reactor, and can be operated for another 10 hours of continuous feeding, thereby minimizing the downtime of the C-reactor. The required residence times in the C and N reactors also requires adjustment and optimization to the process specific conditions. Ongoing efforts for the implementation of the uncoupling strategy in two linked semi-continuous bioreactors where either carbon or nutrients are continuously fed could result in a continuous process with the high PHA productivity characteristics of the uncoupled system.

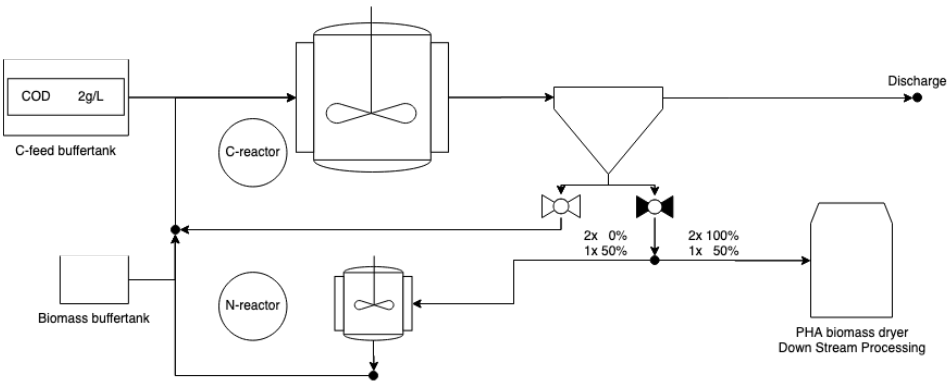

Figure 5.11: Process flow diagram of a semi-continuous adaptation of the uncoupled system as a PHA production process. COD rich influent (volatile fatty acids) is converted in the C-reactor to PHA to discharge level COD concentrations. Biomass is continuously separated in a clarifier or filter and retained in the C-reactor. After 10 hours of feeding, the biomass is fully harvested for downstream processing. The C-reactor is inoculated with biomass from the biomass-buffertank and continuous carbon feeding recommences, resulting in minimal downtime. Every third cycle 50% of the PHA rich harvested biomass is directed to the N-reactor, where over a period of 30 hours new biomass is produced, which is used to refill the biomass-buffertank.

REFERENCES

[1] G. R. Stouten, F. Cecconi, R. J. van Tatenhove-Pel, M. Mulders, P. R. Mooij, H. Dijkman, and R. Kleerebezem, *Uncoupling of nutrient supply for enrichment of polyhydroxyalkanoates accumulating bacteria,* Environmental Science & Technology (2021 under review).

[2] L. Cavaillé, M. Albuquerque, E. Grousseau, A.-S. Lepeuple, J.-L. Uribelarrea, G. Hernandez-Raquet, and E. Paul, *Understanding of polyhydroxybutyrate production under carbon and phosphorus-limited growth conditions in non-axenic continuous culture,* Bioresource Technology **201**, 65 (2016).

[3] K. Johnson, Y. Jiang, R. Kleerebezem, G. Muyzer, and M. C. M. van Loosdrecht, *Enrichment of a Mixed Bacterial Culture with a High Polyhydroxyalkanoate Storage Capacity,* Biomacromolecules **10**, 670 (2009).

[4] E. Korkakaki, M. C. M. van Loosdrecht, and R. Kleerebezem, *Impact of phosphate limitation on PHA production in a feast-famine process,* Water Research **126**, 472 (2017).

[5] G. R. Stouten, C. Hogendoorn, S. Douwenga, E. S. Kilias, G. Muyzer, and R. Kleerebezem, *Temperature as competitive strategy determining factor in pulse-fed aerobic bioreactors,* The ISME Journal (2019), 10.1038/s41396-019-0495-8.

[6] P. R. Mooij, G. R. Stouten, M. C. van Loosdrecht, and R. Kleerebezem, *Ecology-based selective environments as solution to contamination in microalgal cultivation,* Current Opinion in Biotechnology **33**, 46 (2015).

[7] L. Blackall, G. Crocetti, A. Saunders, and P. Bond, *A review and update of the microbiology of enhanced biological phosphorus removal in wastewater treatment plants,* Antonie van Leeuwenhoek, International Journal of General and Molecular Microbiology **81**, 681 (2002).

[8] G. Carvalho, P. C. Lemos, A. Oehmen, and M. A. M. Reis, *Denitrifying phosphorus removal: Linking the process performance with the microbial community structure,* Water Research **41**, 4383 (2007).

[9] P. R. Mooij, G. R. Stouten, J. Tamis, M. C. M. van Loosdrecht, and R. Kleerebezem, *Survival of the fattest,* Energy & Environmental Science **6**, 3404 (2013).

[10] W. V. Vishniac and M. Santer, *The thiobacilli,* Bacteriological reviews **21**, 195 (1957).

[11] K. Johnson, R. Kleerebezem, and M. C. van Loosdrecht, *Model-based data evaluation of polyhydroxybutyrate producing mixed microbial cultures in aerobic sequencing batch and fed-batch reactors,* Biotechnology and Bioengineering **104**, 50 (2009).

[12] J. Tamis, L. Marang, Y. Jiang, M. C. M. van Loosdrecht, and R. Kleerebezem, *Modeling PHA-producing microbial enrichment cultures—towards a generalized model with predictive power,* New Biotechnology Polyhydroxyalkanoate (PHA) by Mixed Microbial Cultures: Fermentation, Control and Downstream Processing, **31**, 324 (2014).

[13] S. Andrews, *FASTQC. A quality control tool for high throughput sequence data.* (2020).

[14] W. Poncheewin, G. D. A. Hermes, J. C. J. van Dam, J. J. Koehorst, H. Smidt, and P. J. Schaap, *NG-Tax 2.0: A Semantic Framework for High-Throughput Amplicon Analysis,* Frontiers in Genetics **10** (2020), 10.3389/fgene.2019.01366.

[15] J. J. Koehorst, *Common Workflow: Amplicon analysis workflow using NG-Tax,* (2020).

[16] Y. Jiang, L. Marang, R. Kleerebezem, G. Muyzer, and M. C. M. van Loosdrecht, *Effect of temperature and cycle length on microbial competition in PHB-producing sequencing batch reactor,* The ISME Journal **5**, 896 (2011).

[17] C. S. Oliveira, C. E. Silva, G. Carvalho, and M. A. Reis, *Strategies for efficiently selecting PHA producing mixed microbial cultures using complex feedstocks: Feast and famine regime and uncoupled carbon and nitrogen availabilities,* New Biotechnology **37**, 69 (2017).

[18] Y. Jiang, L. Marang, R. Kleerebezem, G. Muyzer, and M. C. van Loosdrecht, *Polyhydroxybutyrate production from lactate using a mixed microbial culture,* Biotechnology and Bioengineering **108**, 2022 (2011).

[19] H. Moralejo-Gárate, R. Kleerebezem, A. Mosquera-Corral, and M. C. van Loosdrecht, *Impact of oxygen limitation on glycerol-based biopolymer production by bacterial enrichments,* Water Research **47**, 1209 (2013).

[20] J. Tamis, K. Lužkov, Y. Jiang, M. C. van Loosdrecht, and R. Kleerebezem, *Enrichment of Plasticicumulans acidivorans at pilot-scale for PHA production on industrial wastewater,* Journal of Biotechnology **192**, 161 (2014).

[21] F. Morgan-Sagastume, M. Hjort, D. Cirne, F. Gérardin, S. Lacroix, G. Gaval, L. Karabegovic, T. Alexandersson, P. Johansson, A. Karlsson, S. Bengtsson, M. Arcos-Hernández, P. Magnusson, and A. Werker, *Integrated production of polyhydroxyalkanoates (PHAs) with municipal wastewater and sludge treatment at pilot scale,* Bioresource Technology **181**, 78 (2015).

[22] L. Marang, M. C. van Loosdrecht, and R. Kleerebezem, *Combining the enrichment and accumulation step in non-axenic PHA production: Cultivation of Plasticicumulans acidivorans at high volume exchange ratios,* Journal of Biotechnology **231**, 260 (2016).

[23] D. Sruamsiri, P. Thayanukul, and B. B. Suwannasilp, *In situ identification of polyhydroxyalkanoate (PHA)-accumulating microorganisms in mixed microbial cultures under feast/famine conditions,* Scientific Reports **10**, 3752 (2020).

[24] B. Wu, D. Zheng, Z. Zhou, J.-L. Wang, X.-L. He, Z.-W. Li, H.-N. Yang, H. Qin, M. Zhang, G.-Q. Hu, and M.-X. He, *The Enrichment of Microbial Community for Accumulating Polyhydroxyalkanoates Using Propionate-Rich Waste,* Applied Biochemistry and Biotechnology **182**, 755 (2017).

[25] M. G. E. Albuquerque, G. Carvalho, C. Kragelund, A. F. Silva, M. T. Barreto Crespo, M. A. M. Reis, and P. H. Nielsen, *Link between microbial composition and carbon substrate-uptake preferences in a PHA-storing community,* The ISME Journal **7**, 1 (2013).

[26] L. Marang, *Scale-Up Aspects of PHA Production by Microbial Enrichment Cultures,* Ph.D. thesis, Delft University of Technology (2017).

[27] T. Kaneko, *Complete Genome Structure of the Nitrogen-fixing Symbiotic Bacterium Mesorhizobium loti,* DNA Research **7**, 331 (2000).

[28] S. Gopalakrishnan, V. Srinivas, and S. Samineni, *Nitrogen fixation, plant growth and yield enhancements by diazotrophic growth-promoting bacteria in two cultivars of chickpea (Cicer arietinum L.),* Biocatalysis and Agricultural Biotechnology **11**, 116 (2017).

[29] L. Welles, C. M. Lopez-Vazquez, C. M. Hooijmans, M. C. M. van Loosdrecht, and D. Brdjanovic, *Impact of salinity on the aerobic metabolism of phosphate-accumulating organisms,* Applied Microbiology and Biotechnology **99**, 3659 (2015).

[30] T. Egli, *On multiple-nutrient-limited growth of microorganisms, with special reference to dual limitation by carbon and nitrogen substrates,* Antonie van Leeuwenhoek **60.3-4**, 225 (1991).

[31] L. Marang, M. C. M. van Loosdrecht, and R. Kleerebezem, *Enrichment of PHA-producing bacteria under continuous substrate supply,* New Biotechnology **41**, 55 (2018).

[32] H. Dijkman, *Process for Producing Polyhydroxyalkanoate,* (2017).

[33] D. M. Hawkins, *The Problem of Overfitting,* Journal of Chemical Information and Computer Sciences **44**, 1 (2004).

[34] M. Henze, ed., *Activated Sludge Models ASM1, ASM2, ASM2d and ASM3*, reprinted ed., Scientific and Technical Report / IWA No. 9 (IWA Publ, London, 2007).

[35] J. M. B. T. Cavalheiro, M. C. M. D. de Almeida, C. Grandfils, and M. M. R. da Fonseca, *Poly(3-hydroxybutyrate) production by Cupriavidus necator using waste glycerol,* Process Biochemistry **44**, 509 (2009).

6

UNLOCKING MICROBIAL DIVERSITY FOR SOCIETY – AN OUTLOOK

Gerben Roelandt STOUTEN

Parts of this chapter have been published as Kleerebezem *et al.* [1] and Smidt *et al.* [2].

6.1. EVOLUTION IS THE PROVENANCE OF SCIENCE

Evolution is eerily beautiful; it moves at a pace that generally hides its immense implications. Like a furtively moving tectonic plate, we can suddenly be shaken up, and made aware of its existence in the form of an emerging virus that captivates the world. It is nowadays easy to see how evolution poses a threat to all living things; it is the perpetual power of probability. But with that, evolution also carries safety; it allows life to adapt with nimble resourcefulness.

Just by looking at the world it is difficult to realize that we are not the endpoint of evolution, this is just now. We are a sliver of time, everything led up to this moment, and all that comes, flows through this moment. Everything changes, even evolution itself changed, most notably with the emergence of humans. Humankind brought something new to the table, a novel branch of evolution: science. Science is akin to *evolution with a memory*: it prods at everything, is impartial, combines, and nudges. Evolution and science have many parallels, but maybe the most distinctive one, is that they are curious[1].

Curiosity in evolution is embodied by mutations, it is a persistent phenomenon that yields diversity, from which adaptations and complexity emerge. Curiosity in humans drives science, which, due to its expanding nature leans on the amassed curiosity of centuries. The following passage from John of Salisbury's *Metalogicon* (1159, translation from 2013 [3]) is the scientists adage:

> *"We are like dwarfs sitting on the shoulders of giants. We see more, and things that are more distant, than they did, not because our sight is superior or because we are taller than they were, but because they raise us up, and by their great stature add to ours."*
>
> John of Salisbury, *et alii*[2]

And where much of science could initially be performed by singular scholars, we are coming up in an age where new breakthroughs are of such complexity and scope that they require collaborative efforts. Analogies with early life are easily drawn up, where initially all living organisms could evolve in their own niche, at a certain moment they started to compete and cooperate to form ever more complex and rapid diversifications. Competition of microbes with comparable metabolisms gave rise to symbioses and microbial warfare, a seemingly endless landscape that encourages the evolution of new competitive strategies (section 1.5). And while we are too late to explore the world, and too early to explore the galaxy, we are right in time to explore the myriad of miracles of evolution.

6.1.1. SCIENCE IS EVOLVING

No two scientists think alike, therefore they attempt to align their thoughts through oral and informal discourse, and share their findings in a universal language of communication in the form of scientific articles. Each article represents an idea, a hypothesis, from where new insights can grow. They are living entities that evolve into new articles,

[1] Strange, unusual, but also eager.

[2] Naturally, there is much dispute over which scientist was the first dwarf to acknowledge ancient giants. Scientist can be humble, imperative words: "can be"

become obsolete, or are refuted and redacted. Much in the same way that mutations yield variations, articles yield verities of nature. The success of biological variants materializes when the evolutionary landscape changes or when new properties emerge. In science this convergence and emergence equates to breakthroughs. Breakthroughs are often attributed to a singular scholar, but these scientists are indubitable emblems of their time[3]. In a sense, science proved ready for the next leap, the step-by-step conquering of the *Terra incognita* allowed the dramatic step of new insight. Science requires individuals and collaboration requires individuals. With each new insight, new science is born, uncovering more ground to explore - like Hercules and the Lernaean Hydra. Each slain head resulted in two new challenges. Even in recollecting myths we are lured into the idea that great achievements sprout from the hands of individuals, while Hercules was aided in his task to vanquish the Hydra by his nephew Iolaus.

Figure 6.1: Hercules and the Hydra (1918), Sculpture by Rudolph Tegner, Helsinger, Denmark. Photo from personal archive.

Just as living things grow, so does science, at a bewildering pace. Over the past centuries the total number of peer-reviewed articles has grown steadfast with 3%[4] each year [4, 5], in 2020 an expected 2.5 million new publications have been added to the collective knowledge[5]. It might be just within the scope of a scientist to keep up with his own research field, but what about auxiliary fields? Science has come to the point where there is less and less space for individual development, and the next layer of complexity and insights will come from collaboration and courting between estranged researchers.

[3] Stigler's law of eponymy is beautifully captured by Alfred North Whitehead: "Everything of importance has been said before by somebody who did not discover it."

[4] Depending on maturity of the field of interest this varies between 2.2 and 9.0% per year

[5] The corona pandemic has resulted in a surge in submitted papers, yielding an additional 500.000 articles above previous estimations. "... perhaps because many researchers had to stay at home and focus on writing up papers rather than conducting science."[6]

6.1.2. THE GENERALIST

To facilitate a fruitful form of collaboration a new type of scientist is required that is able to bolster insights, advancements, and opportunities from different fields: "the generalist", as opposed to the specialist. These bridging scientists allow dividing lines to evaporate and bring about new scientific fields[6]. With evolving science come tools by which we can prod deeper into the fabric of life, or maybe it is the tools that allow new scientific fields to emerge and mature[7].

"The challenge we all face is how to maintain the benefits of breadth, diverse experience, interdisciplinary thinking, and delayed concentration in a world that increasingly incentivizes, even demands, hyperspecialization."

David Epstein[11]

CULTIVATION AND CHARACTERIZATION

The setup that is developed in this work (Box 2) is constructed without any individual novelty, but the emulsion of high-tech hardware, custom electronics & software, and cultivation expertise does allow for novel experimentations with microbial communities. Microbial enrichment and cultivation research is significantly limited by the experimental freedom and resources. The uncountable different microbial species will require parallel operated bioreactors, and more control on the cultivation conditions to identify the niches that allow them to thrive while characterizing their behavior. Our setup will allow a more data-driven approach to microbial community cultivation - it brings data and automatization closer to cultivation.

OMICS

A second dimension in microbiology research comes in the form of -omics, which are branches of biology that identify and quantify different groups of biological molecules. Its kin include genomics, proteomics, transcriptomics, and metabolomics. All omics fields develop tremendously ingenious tools and equipment that are able to produce notable amounts of data. At the moment of writing, the NCBI sequence read archive[8] contains 14 peta-byte of sequencing data, and grows at an astounding 55% per year [12]. While the scientific output of biology related fields is only growing with approximately 5% per year [13], this does either mean that the information density of the newly generated data is lower, or that we are missing a tremendous amount of insights.

ECOLOGY

In the lab, it is easy to forget that all living things come from nature. And although cultivation, characterization, and omics are fundamental research tools, they are single dimensions of microbiology research. It is my strong believe that a full-dimensional view of nature arises, when these tools are combined through the application of ecological theory [14, 15].

[6] Examples in biology include: quantum- [7], synthetic- [8], and nano-biology [9]

[7] Did the tool come before the craft? [10]

[8] This public repository stores DNA sequencing data, and is mandated by many journals for publication – most data comes from a single type of measurement: Illumina high-throughput sequencing of rRNA sequences.

6.2. BOX 2 - THE FUTURE OF THE SETUP - CHAPTER 2

The work described in chapter two of this thesis can be regarded as an accretion of tools that together form an operational research platform for mixed microbial culture research. The parallelization of reactor vessels with intricate control and measurement techniques allows studying microbial communities in natural and man-made habitats with increased effort and resolution. Generally, increasing research efforts results in more data, and more work. The smart automatization facilitates long term dynamic cultivations while reducing the laborious medium preparation and reactor maintenance efforts. Additionally, adaptive and meticulous control of the cultivation environment allows for novel and more precise cultivation dynamics. Furthermore, the on-line data processing and analyses tool requires minimal additional effort for additional systems, and facilitates real-time insights in changing microbial activity. These improvements could prove specifically important in cultivating the rare biosphere [16], elucidating microbial interactions [17], and finding the triggers behind the production of new bioactive compounds [18]. The setup hereby delivers opportunities from which all types of bioreactor cultivations can benefit.

REVIEW AND OUTLOOK

Where the reactor automatization aspect was easily embraced by other researchers (Table 6.1), the effective utilization of on-line measurements in (dynamic operated) bioreactor systems is still a source of information that is scarcely used to its full capacity. A comparable faith has befallen the work of Meijer *et al.* [19], Hellinga and Romein [20], van der Heijden *et al.* [21], Le *et al.* [22], whom have also invested considerable efforts in bringing more quantitative tools to the field of microbial cultivation, both in lab and full-scale settings. Possibly, the conceptual distance between cultivation and physics and maths is too abstract, making it more difficult to see the benefits and understanding that they can bring. On-line measurements require a physics, chemical, and mathematical framework to translate the data into information due to the manifestation of physicochemical processes and incomplete and noisy measurements (chapter 2). This intricacy could be the cause of the slow adaptation of data processing tools by researchers that focus on cultivation. Consequentially, insights and research questions are left uncovered, because we only use what we understand or trust, which ultimately hinders experimental design.

The tools developed during this project provide improved cultivation possibilities and on-line characterization of biological conversion rates, but they likely did not succeed in delivering a fit-for-all solution that allows researchers with divergent interests to utilize them easily. It will take another strong effort to develop a platform that truly allows researchers to rethink their experiments and see what treasures of nature they can unravel (preview to Box 4).

6.3. ECOLOGY HARMONIZES CULTIVATION WITH OMICS

To me the beauty of microbiology lies in the tremendous richness of the microbial world left to explore. The term exploring in the title of this thesis "Exploring microbial diversity" is accentuated in two ways in this work. First, by facilitating explorations through improved cultivation tools, and second, the actual exploration, the act of studying microbial communities. As outlined in the introduction, the number of different microbial species is immense, and their survival niches are still very much unknown. Maybe it was a gift to the early biologists that studied the microbial world that this vastness was completely unknown, as its daunting dimensions our enough to humble and deter even the most courageous explorers.

Progress in unraveling the microbial world has generally been made in identifying what metabolic[9] reactions exist in nature. It can be inferred that the presence of a select group of nutrients creates an ecological niche, in which a fraction of the total microbial world can survive. In that same line of reasoning, it also makes sense that a singular species, or microbial team, has evolved to be best suited for any specific niche. Therefore, for any microbial species to be around, and not be outcompeted and gone extinct, there needs to exist a specific niche that allows them to prosper. This is where the reductionist approach leads to some issues. While there are still novel microbial metabolisms being uncovered [23–26], and there are significant permutations in terms of cultivation conditions (e.g.: pH, temperature, redox-potential), we are mathematically running out of niches to fulfill the required diversity.

THE RARE BIOSPHERE AND SYMBIOSES

The microbial richness is most apparent in enrichment studies (cultivation) where highly restrictive conditions are imposed on a system that is inoculated with a natural soil or water sample. Regardless of the cultivation time and care that is taken during these cultivations, community structure analysis (omics) shows that a non-dismissible fraction of the biomass will consist of hundreds to thousands of microbial species at low to moderate abundance [27, 28]. It is possible that this "rare biosphere" is merely a stochastic phenomenon, where the dazzling number of microbial cells is combined with highly competitive species. Odd then, that we do not seem to find many closely related species in these enrichment cultures, but species spanning relatively far in the tree of life. How is it possible that a species is able to outcompete its closest phylogeny, but apparently not a competitor several branches further?

The symbioses that underlay microbial community networks spans from the rare to the abundant biosphere, and could be the most intricate and most idle complex system brought forth by nature. Unraveling this aspect of biology will be accompanied with great breakthroughs and insights in regulation, evolution and co-existence.

[9] Metabolism refers to the means by which microbes harvest energy and obtain their required nutrients.

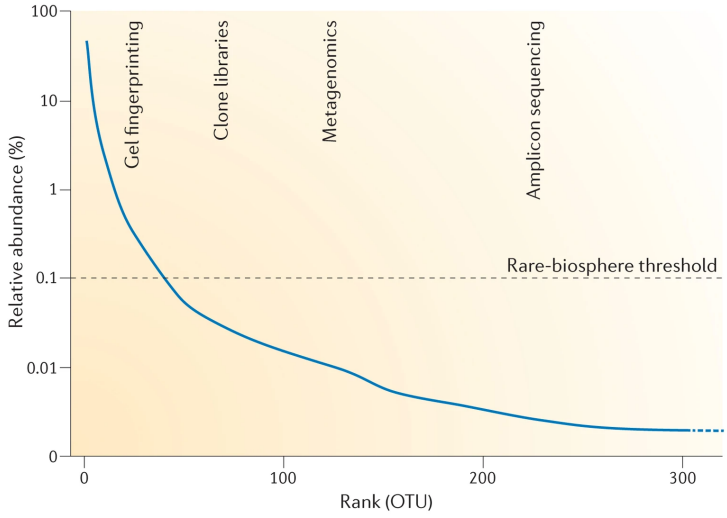

Figure 6.2: The schematic rank–abundance curve shows the measured abundance per "operational taxonomic unit" (OTU: closely related sequences). The long 'tail' corresponds with the rare biosphere, these sequences each make up over less than 0.1% (arbitrary cut-off for rare-biosphere) of the total measurements, but together yield a significant fraction of the genetic material. On the top different experimental techniques are indicated, indicating the progress in coverage depth over time. Figure from Lynch and Neufeld [27]

.

DIFFERENCES RESIDE IN THE OMICS AND EMERGE THROUGH CULTIVATION

Not only the rare biosphere is un-understood, also the abundant biosphere is still full of mystery. One might expect that microorganisms that thrive and dominate in a specific environmental niche (high relative abundance in Figure 6.2), for which we have the full genetic information, also have a specific genetic make-up. Something that clearly stands out. But that is often not so clear. To give an example, related to the work in the thesis; *Plasticicumulans acidivorans* – contender for fattest microbe on Earth, has been fully sequenced [29], but no genetically noteworthy elements have been identified in its 4.2 million basepairs, yet, that could explain its high PHB storing potential, its fast acetate uptake rate, its high respiration rate, or the mechanics behind the fast switching from PHB production to consumption[10]. It seems to be, like any other acetate oxidizing microorganism. Naturally, there is still much information in the genome that we have not uncovered yet, that could explain these characteristics. This puts us in an interesting place; we can select for emerging traits - traits that we cannot lead back to its roots yet.

This is but a single example of a microbial species that demonstrates the richness of nature and the destitute of our understanding. While there are still new metabolic routes to uncover, they will likely contribute little to our true understanding of the biological complexity in the microbial world. The interplay between regulation on cellular level and incipient properties of microbial communities are wholly unknown, and they require a new platform to prosper from. To support a deeper dive, more conjoined research between the ecological cultivation scientists, the omics scientists, and data scientists are required. But this endeavor is not without its hindrances.

[10] Possibly, the mechanics surrounding iron metabolism – explored in chapter 4 – could bring new insights.

6.4. LESSONS LEARNED FROM OUR EXPERIMENTS

Throughout the development of the cultivation set-up a series of experiments is performed (Table 6.1), of which several are published and enclosed in this thesis, others are published by their respective primary researchers, some are in the pre-publication stage, and a couple will solely remain time well spent. All these experiments have in common that they relied on collaborations and combinations of expertise. From the experiences fostered during these collaborations a poignant difference became apparent between the scientific fields, which might explain some difficulty in their integration.

Table 6.1: Overview of long-term enrichments and experiments performed with the parallel bioreactor setup between 2014 and 2019, with their principal researchers.

Researchers	Topic	Status
Setup development		
Sieze Douwenga, Dirk Geerts	Dynamic biological system characterization through automated online data analysis	1
Sten van Brummelen, Daphne van Cuylenburg, Jules Rombouts	Towards long-term axenic cultivations by automatisation of the cleaning process in microbial community experiments	3
Daphne van Cuylenburg, Jasper Koehorst, Sudarshan Shetty	In depth community enrichment analysis – the future of 16S rRNA gene-sequencing	3
Estelle Killias	Assessment of biological and technical replicates in microbial community research	2
Polyhydroxyalkanoates (PHA)		
Carmen Hogendoorn, Estelle Killias	Effect of temperature on the enrichment of PHA storing mixed microbial cultures	1
Galvin Mos	PHA production by thermophiles	4
Francesca Cecconi, Rinke van Tatenhove-Pel, Silvia Cretoiu	Uncoupling of carbon and growth nutrients dosage in time as strategy to enrich for PHA storing organisms	1
Eline van der Knaap Estelle Killias	Influence of pH on feast-famine controlled enrichments	2
Rinke van Tatenhove-Pel	PHA production from ethanol and ethanol acetate mixtures	3
Kelly Hamers Rinke van Tatenhove-Pel	The impact of ions and metal pitting on PHA producing cultures	1
Michel Mulders	Simultaneous growth and PHA accumulation of *P. acidivorans* enrichment cultures	1
Chris Vermeer, Larissa Bons	PHA production from iso-butyrate	2
Estelle Killias	Transcriptomics of *P. acidivorans* during nutrient pulse in feast-famine cultivation	3
Dimitry Sorokin	Isolation of microbial species with high PHA production characteristics, belonging to genera of *Megasphaera, Amaricoccus, Prototheca,* and several novel taxa	3
Non-PHA related enrichments		
Michele Laureni, Aina Soler Jofra, Christopher Lawson	MixAmox - Understanding nitrogen metabolic interactions in mixed anammox-based microbial communities	1
Monica Conthe Calvo	O_2 versus N_2O respiration in a continuous microbial enrichment	1
Laura Valk + Team	*Candidatus* Galacturonibacter soehngenii	1
Mu-En Lu, Roel van de Wijgaart	Comammox - Cyclic conversion in the nitrogen cycle	2
Maximilienne Allaart + Team	*Clostridium* Chain elongation	3
Leonor Guedes da Silva + Team	*Candidatus* Accumulibacter phosphatis	1
Valerie Sels, Lena Depaz, Jure Zlopasa	Anaerobic digestion under haloalkaliphilic conditions	2
Francesc Montserrat	Enhanced weathering of silicate minerals to capture CO_2	4

Status: 1 published, 2 (to be) submitted, 3 writing, 4 not for publication

The different fields are developing on different virtues, where the omics fields are thriving on increased technical advancements and rapidly increasing sequencing and bioinformatics power, cultivation technology is still highly similar to what was possible eighty years ago. The advancements in cultivation research come from the use of dynamic cultivation strategies integrated with high-resolution on-line measurements, and a more profound grasp on ecological differentiation. Where the omics fields aim to quantify and qualify all the building blocks, and make sense out of the generated data, the cultivation field creates the conditions that allow for investigation of the detailed quantitative behavior of microbial species. Cultivation helps to get better insights in microbial communities because we already know the selective pressure. The use of omics data in understanding ecology is still focused too much on abundance and phylogeny and not enough on fluxomics. In chapter 3 we attempted to improve the use of abundance data by linking it to changes in system functionality over time, to ultimately gain better understanding in succession and competition, but regardless of the considerable effort, it still remains a cloudy endeavour.

Figure 6.3: To help paint a picture, the cultivation researcher can grow a forest but only see the tops of the trees and its fringes, omics researchers pull the forest through a shredder and look at the mulch. And if you have ever walked through a dewy forest on a cold autumn morning, you are probably aware that there remains a lot to discover between these two worlds. Photo by Johannes Plenio.

6.4.1. MUCH MICROBIAL FUNCTIONAL BEHAVIOR IS HIDDEN

To take away as much noise from the environment, cultivation researchers aim to reduce the complexity of their cultivations, because constrained cultures give rise to clearer insights. A direct consequence of this approach is that much of the microbial diversity does not reach the lab. This is often referred to as the "great plate count anomaly", where the diversity of what is cultivable in the lab is less than a percent of all microbial diversity. Whether this notion is true or not, it misses a crucial point, and that is that distinct functional behavior is linked to the cultivation conditions, whether in pure or mixed cultures.

The true behavior of microbes and microbial communities only shows itself when it is exposed to certain cultivation conditions, and therefore cultivation involves more than keeping microbes alive. Additionally, as stated in the introduction, by studying isolated cultures, we are limiting our insights in nature's diversity, abilities, and mechanisms. And by studying microbes outside the lab, in their natural habitat, we miss the ability to correlate findings due to the multitude of environmental factors affecting their competitiveness and abundance. The art is to bring the forest, not the tree, to the lab.

6.4.2. CULTIVATIONS HINDER EXPERIMENTAL DESIGN

Reactors demand attention, even the most automated, best monitored systems, set up camp in the vestibule of the brain. This always present exigency debilitates the freedom of thought. Especially enrichment cultivations lead to new observations, new possibilities; they distract and drag the scientist from observation to observation, ever further from hypotheses. I have experienced, and have noticed in others, the difficulty of letting go of a cultivation that you have cared for for months. But a scientist needs time to think, think of what happened, and think of what the next testable idea is. This difficulty is multiplied by the number of distinct microbial worlds that you cultivate in bioreactors. Having multiple systems demands more discipline from the researcher as the cultivation capacity lures one back under the disguise of under-utilization.

A more ideal environment would better support experimental design, would allow for a high intensity experimental phase with more parallel operated bioreactors, with blanks and controls, covering the topic at hand, and it needs closure, where biomass, data, samples, and experimental design are stored. The door to the mind opens, as the door to the lab closes.

ECOLOGY AS EXPERIMENTAL DESIGN TOOL FOR CULTIVATIONS

Outsourcing the cultivation work seems like a good idea, but runs in a particular risk. There is so much undocumentable microbial behavior, specific to each cultivation, that it requires a deep understanding of the system and imposed conditions to distinguish noisy fluctuations from actual response. Cultivations that are not doing what they were *supposed* to be doing therefore allow for three distinct responses. (i) ignorance, the aspect is not recognized, not cared for, or discarded, (ii) biology did something unexpected, or (iii) the researcher did something wrong. The scientist that escapes ignorance is directly attracted to the idea that they are onto something remarkable, leading to many fantastic theories. Alas, in 95% of the cases, it turned out to be the researcher's misdoings.

But let's say that you have invested significant effort in ensuring that your experiment is exactly performed as designed. At a certain point you have to trifle with the idea that you are onto something new. The predominant question that should ring through in that case is: "In what ecological niche would the observed behavior be logical?"[11] The cultivation researcher would do well to spend time on the importance of ecology, as it is both the cause and the outcome.

"Where the cultivation researcher has nothing, but nature,

[11] And in many cases, the answer has to do with competition. Billions of years of evolution is a lot of time to come up with a great many of microbial warfare strategies.

the omics researcher has everything, but nature."

6.4.3. OMICS HINDER EXPERIMENTAL DESIGN

The combination of cultivation and omics research allows investigation of the links between what happens in the cells and the measurable changes in the functional properties of an ecosystem. In order to establish a quantitative understanding of the development of the functional properties of microbial communities to molecular changes within the microbial community, an adequate balance in experimental methods and research objectives needs to be established [1]. The limelight is currently on the omics fields, and with that, the experimental design leans on generating tremendous amounts of data. Hereby, a basic tenet of the scientific method is often overlooked: falsifiability.

Without a proper hypothesis, research becomes a data generation, and tool development, discipline [30]. These are not bad delineations, but the consequence is that truths can be born out of these data and tools that have more shine than sustenance. In the field of microbial community research, possibly the biggest disconcerting trend is the wide spread misuse of relative abundance charts (Figure 6.4). The ease by which these datasets are produced with next generation sequencing data have made them almost mandatory prerequisites for publications. And while almost all researchers are aware that it is incorrect, these bar charts are often interpreted by these same researchers as true depictions of the microbial community composition, while these plots at best represent the relative abundance, and at worst are subject to tremendous biases that affect the apparent abundances by several orders of magnitude (Box 3). Interestingly, when the data do not match the other observations, the biases and relative nature of these measurements are stressed.

It is easy to believe what suits you, but do not be distracted by what you want to be true.

Bertrand Russel

Nurture a will to doubt. We need much doubt, to protect the upcoming omics fields from a comparable faith as that has befallen 16S amplicon metagenomic sequencing (Box 3). Much omics research attempts to describe minute differences, or identify statistical differences between samples, while overlooking the biology that lays at the heart of it. The distance between the omics data scientist and the biological experiment creates a gap that cannot be solved by statistics. Generalist are essential besides specialists to conduct experimental design, data collection and data interpretation.

ECOLOGY AS EXPERIMENTAL DESIGN TOOL FOR OMICS

The ability to measure is so fundamental to science, that the tools by which we measure, and that which we measure, are easily overlooked. The omics related sciences hold the keys to the innards of the microbial world. Because the omics are the golden standard, they are always right, and always wrong. To bring them to fruition they need to be used as comparative tools. This means that experimental design necessitates controls, blanks, or more elegantly: imposed dynamics. By imposing environmental fluctuations (or disturbances) on enriched microbial communities, the response of the cells should

be related to the imposed selective pressure. Work by da Silva *et al.* [31] and Verhagen *et al.* [32] are examples of utilizing these imposed fluctuations to study microbial expression and regulation.

This pull towards fluxomics, whether on protein or metabolite level, with [33] or without radioactive labeling, is strengthened by hypothesising on the ecological aspects of pathways of interest. The already well established enrichments in dynamic conditions, often consisting of accumulating organisms, should be used as a source of low-hanging fruit with respect to the fluxomics fields. They should be used as a stepping stone, because the imposed conditions already give us a profound understanding of the systems. Hereby, the benefit of sequencing batch bioreactors should be taken into account, due to the general (cyclic) homogeneity of expression in these systems the measurable signal will be more distinct.

The next step could be the unraveling of the regulation with respect to carbon storage, cellular growth, and cell division. From this point on, short disturbances or shifts in bioreactor operation (e.g.: change in electron donor/acceptor, trace-nutrients, temperature, pH, redox level) can be used to study regulation on short and long term, allowing for a more quantitative and qualitative understanding of microbial succession and competition.

"If all you have is a hammer, everything looks like a nail."

Abraham H. Maslow

6.5. BOX 3 - THE FALLACY OF SCIENTIFIC HUBRIS

With every new generation of technological tools and measurement equipment, a new boost is given to scientific progress. Thanks to the development of DGGE and its application to separate 16S rRNA gene fragments it became possible to gain insights in the composition of complex microbial communities [34]. This inspired much microbial community research as it was now possible to fingerprint and compare microbial communities. It was paramount to our current understanding that microbial diversity is more extensive than imagined. A decade later, the costs of sequencing started to drop significantly and the fingerprints were replaced by "quantitative" data corresponding to the number of 16S rRNA gene copies that were measured by the Illumina sequencer [35].

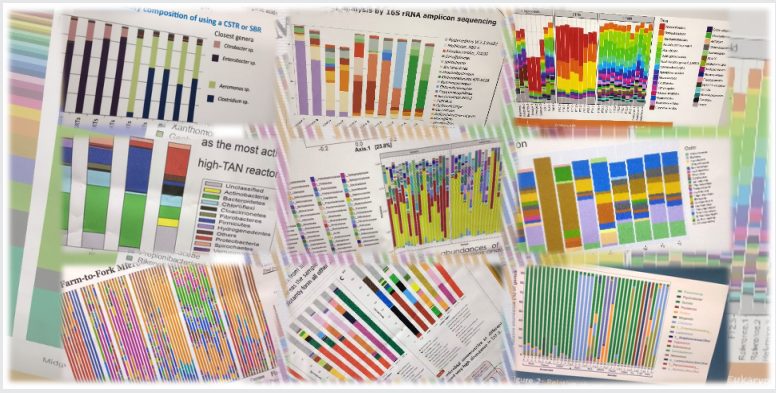

Figure 6.4: Collage of images from FEMS conference posters, with a predominant role for the 16S relative abundance bar chart. Images by Robbert Kleerebezem.

The allure of these numbers and bar-plots was overwhelming, as it now seemed possible to quantify the microbial composition of any community, thereby paving the way to understanding the member contributions, and ability to compare the functionality of distinct communities based on their microbial composition. It transpired that although the measurements were relatively reproducible, they maintained a degree of unreliability due to biases [36]. Improvements were made on the standardization of DNA extraction, primer design, PCR amplification, 16S gene copy number databases, and the sequencing equipment, thereby increasing the reproducibility of the measurements. The ability to compare samples with such a high fidelity contributed to something that can only be described as a collective charade.

THE COLLECTIVE CHARADE

The desire to have true quantitative insights in the microbial community composition trumped the acknowledgement of systematic biases in 16S rRNA gene sequencing. Over a period of several years the biases in quantification due to sample storage, DNA extraction, PCR amplification, and matrix interactions (ranging several orders of magnitude) [37], have become mute points in a large part of the scientific literature. We do a disservice to our scientific legacy by allowing the proliferation of microbial community composition quantification by 16S rRNA gene sequencing.

6.6. FROM EXPLORING TO UNLOCKING MICROBIAL DIVERSITY

Research with microbial communities involves good research questions, advanced cultivation setups, access to omics equipment, and prodigious skill with the generated data. Fruitful research therefore becomes more difficult, and thereby more exclusive. By adding up all aspects, from the misunderstandings between omics and cultivation researchers, to the despairingly high costs to do research, the question arises if it is all worth it. Naturally, everybody working in the field will echo a resounding yes. But there is more than scientific curiosity, there is also necessity.

Humankind is facing tribulations (see Introduction: Back to the basics) with respect to climate change, pollution, and all other aspects of population growth. And everywhere we look we see microorganisms, either emolliating or aggravating the situation. To understand, to explore, this microbial activity is not enough, we have to try to tap in to microbes as resources, unlocking their talents.

Figure 6.5: The parable of the talents (Matthew 25:14-30). A master puts his servants in charge of his talents (one talent equals 36 kg of silver) while he is away on a trip. Upon his return, the master assesses the stewardship of his servants, according to how wise their investments were. He judges two servants as having been "faithful" for using their talents - regardless of outcome - and gives them a positive reward. To the servant who played it safe, by burying his talents, a negative compensation is given. Etch by Jan Luyken (1712)

A collaboration between Wageningen University and Delft University of Technology assessed the possibility of developing a research facility that encompasses all requirements for improved research of microbial communities. Under coordination of Hauke Smidt, Robbert Kleerebezem, Alette Langenhoff and Peter Schaap, the infrastructure proposal for UNLOCK [2] was granted in April 2020 by the Dutch Research Council (NWO). The collective investment of over 24 million euros will be used to set up a state-of-the-art research facility between four research departments in Wageningen and Delft.

The parallel cultivation platform in Delft has a strong foundation in the work performed during this Doctoral research. A key aspect of the facility will be to lower the bar to perform good experiments, and thereby raising the bar of scientific excellence. In Box 4 excerpts from the proposal's abstract are included, and the interested reader can visit `https://m-unlock.nl`.

6.7. BOX 4 - UNLOCKING MICROBIAL DIVERSITY FOR SOCIETY

AN OPEN INFRASTRUCTURE FOR EXPLORING NEW HORIZONS FOR RESEARCH ON MICROBIAL COMMUNITIES

UNLOCK is a unique facility for research on mixed microbial communities, the first of its kind worldwide. *UNLOCK* is an experimental and data platform, enabling breakthrough research and knowledge sharing on natural and synthetic mixtures of microorganisms. Such microbial communities are of key importance at different scales in our society, ranging from individual-based health issues related to microbial communities inhabiting the human body, to global greenhouse gas emissions related to microbial activity. Herewith *UNLOCK* provides the means to analyse and solve some of the major societal challenges we are facing in the coming decades related to food production, health, environmental protection, climate change, and sustainable production of plug-in commodity chemicals.

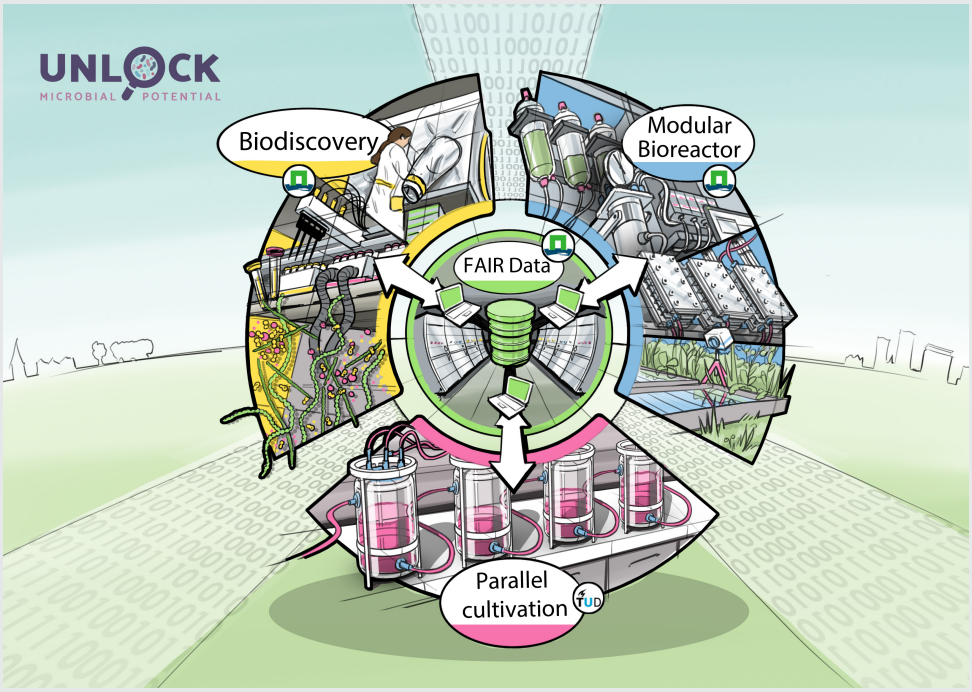

Figure 6.6: Schematic representation of the four research platforms that form the *UNLOCK* experimental research and data infrastructure for investigating microbial communities. Illustration: Haans Industrial Design

With *UNLOCK*, Wageningen University and Delft University of Technology have joined forces to integrate the expertise of the research groups involved in four complementary platforms (Figure 6.6). The first platform is the Biodiscovery platform located in Wageningen for high-throughput discovery and characterization of yet-uncultured microbes, specifically focusing on fastidious anaerobes. The second platform in Wagenin-

gen, the modular bioreactor platform, is specifically suitable for investigating sustainable solutions for environmental challenges, such as degradation of (micro)pollutants, sustainable energy generation, and recovery of resources from complex waste streams. The third platform of *UNLOCK* is located in Delft and facilitates users to conduct dozens of high-resolution cultivation experiments in bioreactors in parallel for comparative analysis of how process variables affect system development. On-line analytical facilities and state-of-the-art liquid handling equipment enable high-resolution analysis of functional system development in time. Finally, the fourth platform, the FAIR-data platform also located in Wageningen, allows for data storage, data extraction and analysis of high-throughput data in a cloud-based infrastructure, the basic framework of which has been implemented in close cooperation with SURFsara. The data generated will be FAIR (Findable, Accessible, Interoperable, Reusable) by design, enabling transparent procedures.

UNLOCK represents a unique infrastructure for exploring new horizons for research on microbial communities. Owing to the smooth access procedure, the experimental hardware available, and the expertise of involved researchers, *UNLOCK* enables research that to date is considered too complex and too expensive for one researcher (or one research group) to conduct. Combining and exploring the fields of expertise of the *UNLOCK* research groups will boost the research community and strengthen the position of Dutch research in the fields of microbiology, microbial ecology, and bioprocess engineering. *UNLOCK* is open to excellence-driven users from Dutch universities, knowledge institutes and industries and beyond, placing them in the unique position to conduct research at unmet speed and resolution.

ON TO GREAT THINGS

The idea behind UNLOCK is to facilitate breakthrough research on microbial communities. Parallels between UNLOCK and the work described within this thesis is that there is again a need for the technical development & integration, and the research itself. Highlights of technical advancements include the ability to bridge cultivations between the discovery platform in Wageningen (microliters) and functionality measurements in Delft (liters). This should facilitate the formation and investigation of defined microbial communities, and the isolation of community members from enrichments. By spanning this gap, it will be possible to improve the investigation of microbial interactions. Furthermore, the intensification of research by parallelization will allow for improved research fidelity by operating cultivations in replicates and at higher granularity. The facility is set up in such a way that upcoming technologies, like micro-fluidics, single cell studies, and lab-on-a-chip, can already make use of the FAIR data platform. And once these technologies have matured and have a strong support network, they can become integral techniques in the UNLOCK platform.

The data standardization efforts by the FAIR data platform in Wageningen opens up a wealth of possibilities by allowing researchers to curate and maintain their results to the best degree possible. Meta-analysis, aggregating of data sets, and data reuse improve the ease of collaboration and allow for documented reproducibility. These are all things that we would like to associate with scientific research, and the UNLOCK facility brings this notion a step closer for microbial community research.

6.8. OUTLOOK

Throughout this final chapter, several short expeditions have been made into the topics on, and manner by which future microbial community research will be conducted. The astute reader will appreciate that the field of microbiology is vast, which, when combined with my interest in all things complex, can result in a diffuse image of what the scientific future has in store for us. Therefore, I will organize this last section to address the different aspects in a proper outlook. We will start with an outlook of scientific ideas that flow from the work performed during my masters and Doctoral research, and in the next section we will work our way to some envisioned breakthroughs that emanated from a larger curiosity.

6.8.1. PHA TO BIOPLASTICS

After following the PHA research closely for the past decade, I am confident that we have good insights and practice in applying microbial community engineering for the production of PHA from the majority of carbon rich waste streams. The bottlenecks for large scale adoption of PHA as bioplastic no longer lay in the domain of microbiology, but have moved into the chemical field, where aspects as extraction, purification, and material properties are addressed. Naturally there will be a feedback loop, where insights in PHA properties and process design are used to design new selection targets for microbial community engineering. For example the implementation of a settling step during the enrichment could prove valuable in the de-watering and extraction process (Figure 5.11).

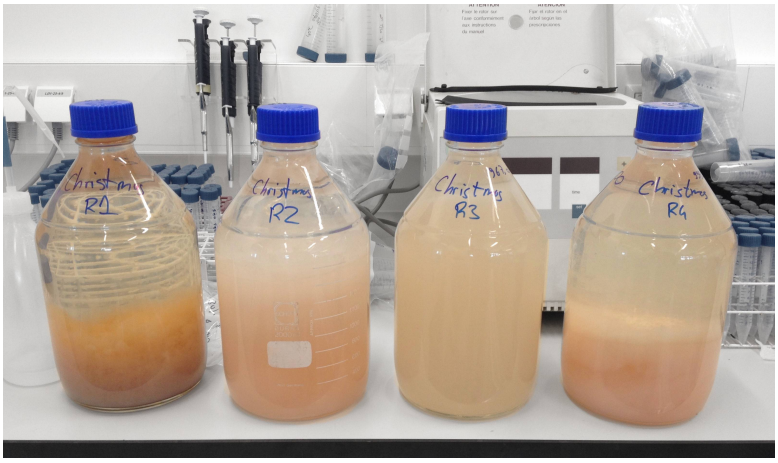

Figure 6.7: Effluent from four different PHA producing enrichment cultures, with distinct settling properties. The PHA content of biomass in the storage bottles is approximately 80 dry weight %. The cultures were not selected for their settling properties. Photo from personal archive.

From a *Terra incognita* point of view, there is still much low-hanging fruit in the field of PHA production by microbial communities. A legion of experiments burst forth from the uncoupling strategy as proposed in chapter 5. For example, whether the uncoupling strategy will be as successful under a wide variety of environmental conditions and sub-

strates remains to be seen. Preliminary research showed highly productive species in uncoupled operated systems that were operated at 40°C (Figure 6.8). This is promising for the general applicability of the uncoupling strategy, as cultures operated at 40°C in the feast-famine operated system did not show PHA production characteristics during normal cycle operation, because fast growing, and decaying, microorganisms outcompeted the PHA producers (chapter 3).

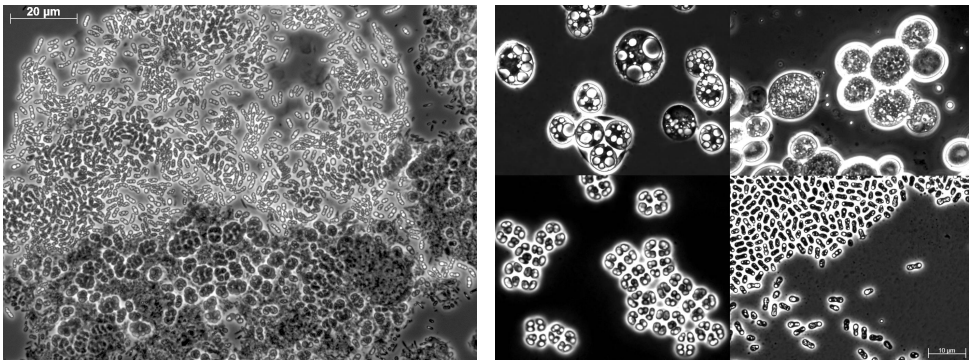

Figure 6.8: Microscopy images of a microbial culture enriched with the uncoupling strategy at 40°C, enrichment culture on the left, and isolates by Dimitry Sorokin on the right. Clearly visible are the PHA inclusion bodies and at least three morphologically different species. Where feast-famine enrichments have a strong tendency to select for a single dominant species, in many uncoupled systems we encountered several PHA producing species at moderate to high abundance. This could signify that more competitive species emerge under these conditions and that more stringent selective pressures can be adopted.

The bulbous microorganism (top right) is a member of the *Prototheca* genus. This genus is generally classified as a pathogenic, green algae that lost its chlorophyll pigment. But our species was able to facultatively produce chlorophyll. When the colourless, PHA-rich, microorganisms were cultivated at a lower temperature – in oxygen poor conditions, they started to produce chlorophyll. Together with its ability to thrive at 40°C, this might be an interesting target to investigate whether PHA can be produced phototrophically.

At the same time, applying the uncoupling strategy with more exotic carbon sources, like iso-butyric acid, does worse than the feast-famine strategy for the enrichment of PHA producing cultures [38, preliminary data]. This, to me, is exceptionally surprising, as the uncoupling strategy should perform at least as well. When, after more rigorous attempts to implement the uncoupling strategy, it still fails to result in the selection for storage polymers, a deeper investigation in the protein expressions, metabolites, and pathways for iso-butyric acid metabolism is warranted. Especially, because it would be a negative control which could give more insights in the regulation of carbon resources.

And lastly, the adaption of the uncoupling strategy from the sequencing batch to a continuous system will require more in depth investigation on the biological processes that occur between the substrate pulses. Previous attempts to convert the feast-famine sequential batch to a continuous process resulted in a loss of selective pressure for PHA producers [39], suggesting that regulation and homogeneous cycles could play a role in these selection strategies. Proteomics and metabolomics analysis throughout a cycle could elucidate which cellular growth processes take place when, and how the biology responds to the short availability of limiting substrates, and rhythmic disturbances in substrate availability.

6.8.2. ALGAE TO SUGAR AND OIL

Their ability to produce sugars and oils directly from CO_2 and light has resulted in an inflated enthusiasm in *Green Oil* in the early 70s, followed by a long hiatus, on again in the 90s, and after a short lull, again after the turn of the millennium. And these green miracles are also what moved me into the world of environmental biotechnology. The elegance of algae as direct converters of sunlight to oil and food is undeniable, but it also attracts some fantastic charlatans from industry and science. It is an ever repeating story where people ultimately discover that the production of commodities in high-tech phototrophic bioreactors with pure cultures will not be cost-effective.

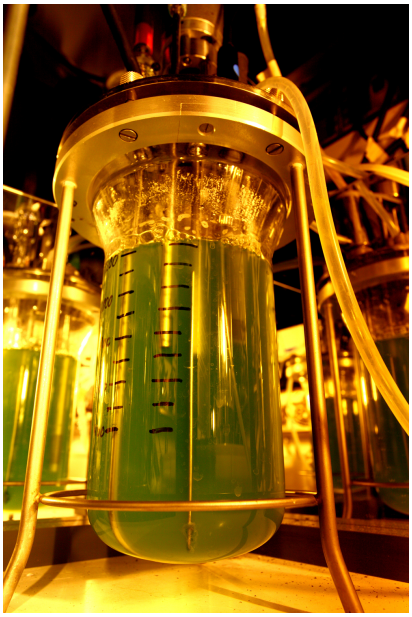

Figure 6.9: Phototrophic bioreactor setup used during my master research, as part of the "Survival of the fattest" research [40]. These bioreactors were operated in an 'open' fashion, contrary to the closed systems that were generally used to study algae. By imposing a strong uncoupled selection strategy we were able to enrich for very fat algae, from environmental samples from all over the world. The selection strategy also proved successful outside the lab. Photo by Renco Beunis (2012).

Peter Mooij took a different approach by implementing an uncoupling strategy in algae [40, 41]. The success of his work warrants significant more investigations into the application of algae in large-scale open systems. The key metabolic switch that needs to be found is steering the allocation of carbon towards either oils or sugars. An avenue worth exploring is the use of CO_2 limited conditions (either in pulses or continuously low), rewarding the algae that conserve the most energy per carbon. Furthermore, it will be rewarding to investigate what specific metabolic pathways are employed when prolonged light phases are used, as this is a "substrate" that is difficult to reject for the unwilling algae. At a certain point no additional internal storage polymers can be produced, will the algae produce external carbon compounds, reduce existing compounds (sugar to oil), or decrease photosynthetic activity by some defensive mechanism?

6.8.3. EXTRACELLULAR POLYMERIC SUBSTANCES TO COMPOSITES

A different group of biological polymers that is gaining significant interest, is that of extracellular polymeric substances (EPS). Granular sludge consists of microbes in a matrix of excreted polymers. These polymers are more complex in their make-up, and therefore could range a wider field of application [42, 43]. There is a strong pull to valorizing this EPS, as it is produced in bulk as a biological waste product in large-scale granular sludge reactors. The make-up and properties of these polymers is likely related to the environmental conditions that the microbes are exposed to. Research into the relationship between EPS components and ecological niche in which they are found [44] would benefit from the combined omics and cultivation expertise of the UNLOCK facility.

Figure 6.10: Section of a bubble column reactor, containing enriched granular biomass. Several different applications of granular biomass are under investigation. Possibly the simplest system to start exploring omics tools with is anaerobic VFA production from glucose [45]. Photo from personal archive.

The significant challenges, with respect to the use of omics, in these systems are that the biomass has a relatively long residence time in the bioreactors, and that some form of substrate and product gradient can arise along the radius of the granule. Along these spatial gradients selection for specific microorganisms occurs. The old biomass and stratification blur out a significant fraction of the omics measurements, because only whole or chunks of granules can be processed. Omics data on granules will therefore be of a heterogeneous population, in heterogeneous conditions.

Experimental work on the solids retention time has already shown that the type of EPS that is produced seems strongly correlated with the age of the biomass [45]. By continuing the granular research with exceptional short retention times should allow for more clear omics results and could therefore be a good stepping stone in applying the full omics suite in granular research, while also contributing to the EPS composition steering research.

6.9. BREAKTHROUGH SCIENCE

6.9.1. UNLOCK - MICROBIAL COMMUNITIES FOR SOCIETY

To gain a feeling for the breakthroughs that can arise from UNLOCK, we have to appreciate that the microbial world supplies the machinery on which all elemental cycles rely, and thereby they sustain all multicellular life. Microbes sustain us from within, and contribute to the world around us. Currently, humankind is pushing the circular nature of life by increasing the rate by which resources are depleted and waste is produced, this behavior changes the environment so quickly that a breaking point is foreseeable where nature is not able to sustain our endeavors anymore. A deep understanding and control over microbial communities allows us to direct and accelerate the natural cycles, thereby rebalancing human impact on the environment, and consequently support a sustainable future for humankind.

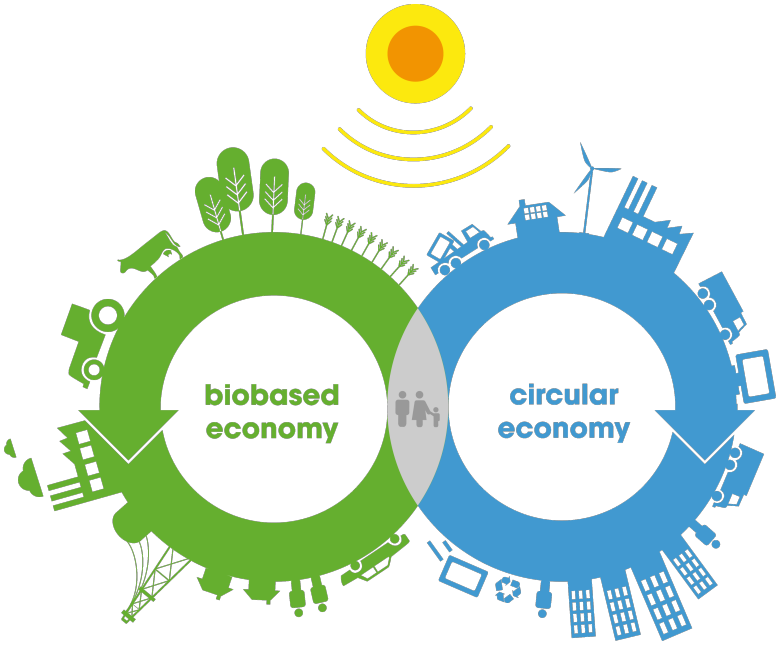

Figure 6.11: In the biobased economy the production of resources predominantly takes place by biological processes. Converting waste products into new resources requires energy, which in the biobased economy comes from the sun. If all gears fall in place, the pace by which resources are consumed is only limited by the rate of conversion. This applies to all elemental cycles, ranging van carbon, nitrogen, and phosphorous from our food and transportation requirements, to metals and gasses for industrial applications. Image adapted from Partners for Innovation.

A more profound outcome for Unlock than *time* is difficult to imagine, but it is also esoteric, therefore here follows a non-exhaustive overview of tangible progress that can be made with the Unlock infrastructure and the research topics where those will make the biggest impact.

6.9.2. EXPERIMENTAL BREAKTHROUGHS

THE CONSTRUCTION AND DECONSTRUCTION OF MICROBIAL COMMUNITIES

The bio-discovery platform in Wageningen will allow for an automated method to physically isolate community members from interesting microbial communities (Figure 6.12). The (anaerobic) Fluorescence-activated Cell Sorter combined with the micro-cultivation setup allows for the creation of a community library. Investigators can then attempt to cultivate sorted/isolated cells either as pure cultures, or as defined co-cultures. This control on community complexity will allow for a systematic approach to understanding the relative contribution of community members.

By combining the bio-discovery platform with the parallel cultivation platform in Delft, it will become possible to characterize isolates, defined co-cultures, and enrichment cultures. Hereby we can start to unravel aspects of microbial symbioses. And inversely, promising microbial enrichments can be deconstructed to identify interesting community members with new or different pathways and expression patterns.

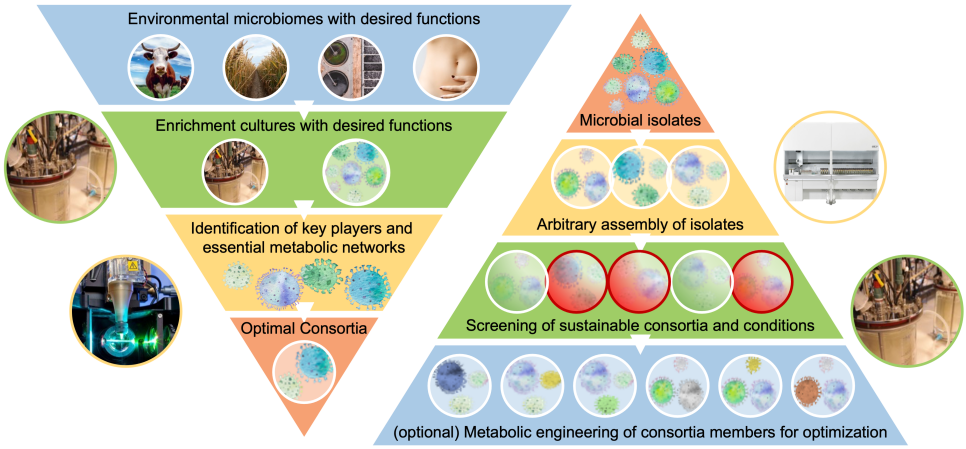

Figure 6.12: Schematic representation of the deconstruction (left) and construction (right) of microbial communities, by making use of cultivation, bio-discovery, and omics tools. Image adapted from Che and Men [46].

DYNAMIC CULTIVATION, ONLINE CHARACTERIZATION, AND DISTURBANCES

The ability to run (defined) enrichment cultures axenically by linking sterile systems and utilizing cleaning in place methods [47] long term studies can be performed that investigate adaptation and evolutionary processes. It will also allow the fastidious selection of very sensitive or slow growing organisms, as interventions are minimized, while the selective conditions are maintained (e.g.: by removal of, or selection for, biofilm formation Figure 6.13).

The online characterization of (dynamic) cultivations (chapter 2) allows for automated and reproducible experimental design. By robotizing the substrate supply it will become possible to monitor the response of a microbial community to changes in the milieu. When employed in systems where cultivation broth from a “mother” reactor is

axenically transported to parallel operated systems, the comparative and automated online experimental design can be used to examine the response to the new conditions.

Heterogeneity in microbial cultures, and the influence of invading species are aspects that can be investigated with great ambition and precision. Furthermore, changes in functional performance of micro-organisms resulting from variations in cultivation conditions and medium compositions could unravel tremendous hidden functional performance (chapter 4).

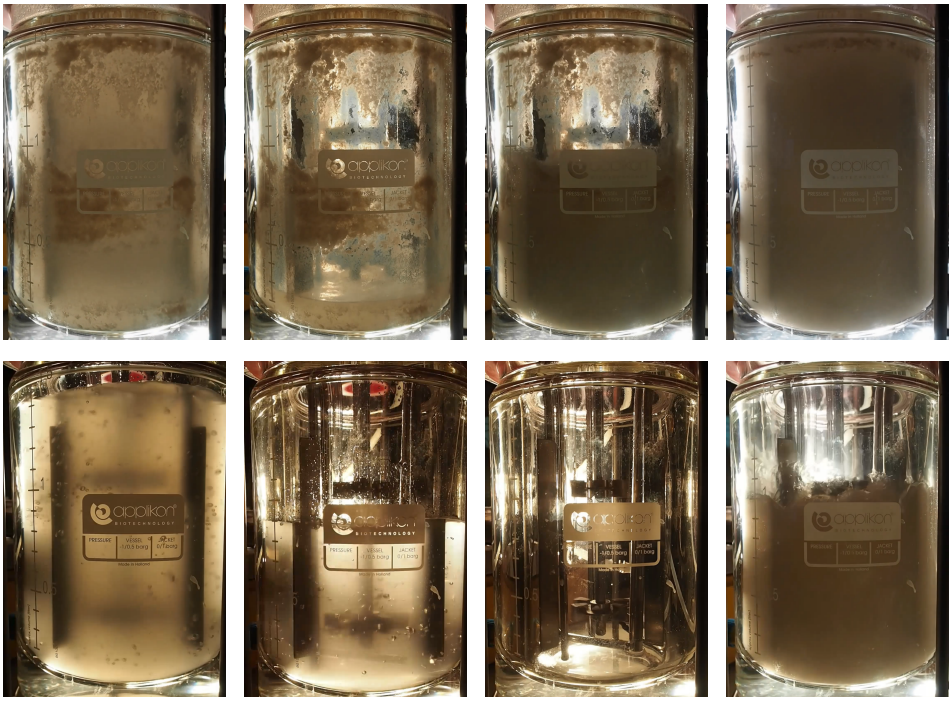

Figure 6.13: Automatic, anaerobic, and axenic in place cleaning of long term cultivations. In the direction of the clock: (1 top left) a suspended culture enrichment is impeded by biofilm forming cultures, (2) the suspended culture is pumped to a parallel operated biorector, (3) caustic cleaning solution is added, (4) strong agitation and high pH detach biofilm from glass and metal surfaces, (5 bottom right) the cleaning solution is discharged, (6) the reactor is rinsed with water, (7) new medium is added to the bioreactor, (8) biomass from the second reactor is used as reinoculation biomass. Pictures are captured from van Brummelen *et al.* [47]

INTEGRATION OF OMICS AND CULTIVATION & GENOME MINING

By reducing the analysis time of omics, it will become possible to use the results from omics measurements as input for enrichment strategies. Currently the cultivation experiments are concluded before the results from omics measurements become available. A quick feedback allows for piecemeal identification of best selection strategies, which could contribute to the tightening of the cultivation conditions and increasing our ability to cultivate the uncultivable microorganisms.

Furthermore, for all cultivation conditions we want to be able to create as clear as possible differences in the microbial expression patterns to allow us to identify pathways

and mechanisms that contribute to the exhibited functionality. The stricter control on the cultivation conditions, the parallel cultivation of controls, and the ability to perform automated disturbances create the perfect conditions for proper omics studies.

Genome sequencing has revealed a wealth of untapped potential for the production of bioactive compounds by microorganisms, under which antibiotics and terpenoids[12] [48]. Many of these products are associated with gene clusters that are poorly expressed under standard laboratory cultivation conditions. To harness their full potential we need to combine high resolution omics with dynamic cultivation conditions, which might give us the chemical-ecological cues by which their expression is controlled.

As most microorganisms typically grow in consortia, they can also collaborate in their reactions to external stressors. Recent explorations have shown that novel antibiotics are only produced by microbial co-cultures, and not by the individual fungi strains [49]. Because of the current dominating focus on monocultures, the potential of microbial consortia is only minimally explored, and actually wholly unknown [50].

6.9.3. BREAKTHROUGH RESEARCH AREAS

MICROBIOME AUGMENTATION FOR PERSONALIZED HEALTH, VEGETATION, AND CROPS

The expertise from Wageningen combined with Unlock allows us to focus on personalized medicine through the gut microbiome, contributing to individual health of humans and animals [51]. The gut is regarded as the second brain of the body with delicate interactions with the microbiome that resides within it, and a growing number of diseases and illnesses are strongly associated with the gut-brain neural circuit [52–56]. The unraveling of host-microbe interactions will transform our health-care system by introducing a strong personal health aspect to the tools of medicine. Progress will be made by designing bioreactors that mimic the human intestines, mouse models [57], and unprecedented microbial community disassembly and assembly (Figure 6.12).

Also the health and properties of soil are largely dominated by the microbiome in the rhizosphere. The cycling of carbon, nitrogen and phosphorous in soil determines its capacity to sustain new crop cycles. The matrix becomes more complex, by taking into account all minerals and oxidation states of compounds that influence the interactions of the microbes and the roots of plants [58]. Profound understanding will allow improved food production, the reversal of desertification, and reduction in methane production by the reclining permafrost.

These research topics themselves are not new, but they are all struggling with the tremendous complexity and difficulty associated with microbial community cultivation, characterization, and methodological research design. The Unlock facility supports collaboration, centralization of expertise, and involvement of generalists to address the research topics that will contribute to a new biotechnological revolution.

ORIGIN OF LIFE, EVOLUTION, REGULATION, SYMBIOSES, AND ARTIFICIAL INTELLIGENCE

I have addressed breakthroughs with applied and practical implications. What will follow are more fundamental questions and research lines, which might transform our view on and off biology.

[12] About half of all known natural products are terpenoids, they include taste, flavor, pigments, but also hormones like steroids and sterols, and are used as precursors in many contemporary drugs.

Quantifying evolution and seeing it take place is possible with frequent genomic analysis. Recently we have come to the realization that the rate of mutation can be regulated by living cells [59]. I pose that this ability to regulate and adapt to the unknown through the mechanics of probability could be interpreted as a form of conscience. Experiments can be designed in which a defined culture is divided and exposed to stringent, dynamic, or relaxed conditions. The difference in mutation rates, and adaptation to new triggers, could give us insights in the brains of microbial communities.

An important driving force in evolution is viruses [60, 61], and they abide by the same logic of chance as all other living things [62]. But at the same time they are largely ignored in the field of microbial biotechnology. For us to gain a full picture of biology, evolution, and life, the interaction of viruses and microorganisms needs to be considered. The Unlock facilities are well equipped to investigate how microbial communities use their genetic arsenal to defend themselves, how they respond to infections, how viruses evolve, and how viruses can alter the behavior of a community.

The field of astrobiology involves the origins, evolution, and distribution of life in the universe. It does not take a large leap of faith to appreciate the possibility that microbial life exists elsewhere in the universe. Neither does the option that microscopic life is being distributed through the universe by means of meteors and asteroids [63]. It is well known that rocky material is exchanged between nearby planets (e.g.: Mars, Venus and Earth) by high impact meteorites, and it is hypothesised that actually the Galaxy is saturated with life-bearing objects [64]. Recent findings of phosphine in the atmosphere of Venus [65][13], and methane and water deposits on Mars allow for rather elegant experiments in which enrichments are combined with mimicking of (ancient) planetary conditions in the extreme condition setup in Wageningen, in search for niche survivors.

Figure 6.14: Venus shines bright over Mt French, Quaterdeck, New Zealand. Photo by Aleks Dahlberg.

[13] The claim is still disputed but the implications are profound: The presence of PH_3 is unexplained after exhaustive study of steady-state chemistry and photochemical pathways, with no currently known abiotic production routes in Venus's atmosphere, clouds, surface and subsurface, or from lightning, volcanic or meteoritic delivery. PH_3 could originate from unknown photochemistry or geochemistry, or, by analogy with biological production of PH_3 on Earth, from the presence of life.

The last research effort I will touch upon involves trying to bridge a gap between the natural and artificial world. A micro-organism has its instruction set embedded in its (epi-)genetics. By approaching the culture (or single micro-organism) as a black box, it could be possible to measure the output of the black box to certain stimuli. From that idea, it is feasible that an automated process can be designed in, meticulously controllable environments, that explores the responses of the black box to a myriad of input combinations, in an unsupervised machine learning approach. Essentially, this signal-response duet would result in an *in-silico* representation of the culture, where cellular regulation is captured as an artificial neural network.

We will not go further into the philosophical implications of studying life, and the wealth of possibilities that come along with improved cultivation tools, but we will leave the reader with all their questions on how a project investigating the production of biopolymers resulted in this outlook.

REFERENCES

[1] R. Kleerebezem, G. R. Stouten, J. J. Koehorst, A. Langenhoff, P. Schaap, and H. Smidt, *Experimental infrastructure requirements for quantitative research on microbial communities,* Current Opinion in Biotechnology **67**, 158 (2021).

[2] H. Smidt, R. Kleerebezem, A. Langenhoff, P. Schaap, J. Koehorst, and G. R. Stouten, *UNLOCK - UNLOCKing Microbial Diversity for Society,* (2019).

[3] J. of Salisbury, *Metalogicon*, edited by J. Hall, Corpus Christianorum in Translation, Vol. 12 (Brepols Publishers, Turnhout, 2013).

[4] A. E. Jinha, *Article 50 million: An estimate of the number of scholarly articles in existence,* Learned Publishing **23**, 258 (2010).

[5] K. White, *Publications Output: U.S. Trends and International Comparisons*, Tech. Rep. (National Science Board-Science and Engineering Indicators, 2019).

[6] H. Else, *How a torrent of COVID science changed research publishing — in seven charts,* Nature **588**, 553 (2020).

[7] A. Marais, B. Adams, A. K. Ringsmuth, M. Ferretti, J. M. Gruber, R. Hendrikx, M. Schuld, S. L. Smith, I. Sinayskiy, T. P. J. Krüger, F. Petruccione, and R. van Grondelle, *The future of quantum biology,* Journal of The Royal Society Interface **15**, 20180640 (2018).

[8] M. El Karoui, M. Hoyos-Flight, and L. Fletcher, *Future Trends in Synthetic Biology—A Report,* Frontiers in Bioengineering and Biotechnology **7** (2019), 10.3389/fbioe.2019.00175.

[9] A. T. Blanchard and K. Salaita, *Emerging uses of DNA mechanical devices,* Science **365**, 1080 (2019).

[10] G. R. Scott and L. Gibert, *The oldest hand-axes in Europe,* Nature **461**, 82 (2009).

[11] D. J. Epstein, *Range: Why Generalists Triumph in a Specialized World* (Riverhead Books, New York, 2019).

[12] *NCBI - SRA growth statistics,* https://www.ncbi.nlm.nih.gov/sra/docs/sragrowth/ (2020).

[13] M. Pautasso, *Publication Growth in Biological Sub-Fields: Patterns, Predictability and Sustainability,* Sustainability **4**, 3234 (2012).

[14] S. M. Scheiner and M. R. Willig, eds., *The Theory of Ecology* (The University of Chicago Press, Chicago ; London, 2011).

[15] S. P. Hubbell, *The Unified Neutral Theory of Biodiversity and Biogeography (MPB-32).* (Princeton University Press, Princeton, 2011).

[16] C. Pedrós-Alió, *Rare Biosphere,* in *Reference Module in Life Sciences* (Elsevier, 2017) p. B9780128096338022834.

[17] K. Faust and J. Raes, *Microbial interactions: From networks to models,* Nature Reviews Microbiology **10**, 538 (2012).

[18] H. Gross, *Genomic mining–a concept for the discovery of new bioactive natural products,* Current Opinion in Drug Discovery & Development **12**, 207 (2009).

[19] J. J. Meijer, B. Romein, J. P. van Dijken, and K. C. A. M. Luyben, *Steady-state analysis of hybridomas in chemostat culture,* in *Animal Cell Technology*, edited by R. E. Spier, J. B. Griffiths, and W. Berthold (Butterworth-Heinemann, 1994) pp. 539–541.

[20] C. Hellinga and B. Romein, *MACROBAL: A Program for Robust Data Reconciliation and Gross Error Detection,* IFAC Proceedings Volumes **25**, 459 (1992).

[21] R. T. J. M. van der Heijden, J. J. Heijnen, C. Hellinga, B. Romein, and K. C. A. M. Luyben, *Linear constraint relations in biochemical reaction systems: I. Classification of the calculability and the balanceability of conversion rates,* Biotechnology and Bioengineering **43**, 3 (1994).

[22] Q. H. Le, P. J. T. Verheijen, M. C. M. van Loosdrecht, and E. I. P. Volcke, *Experimental design for evaluating WWTP data by linear mass balances,* Water Research **142**, 415 (2018).

[23] H. Daims, E. V. Lebedeva, P. Pjevac, P. Han, C. Herbold, M. Albertsen, N. Jehmlich, M. Palatinszky, J. Vierheilig, A. Bulaev, R. H. Kirkegaard, M. von Bergen, T. Rattei, B. Bendinger, P. H. Nielsen, and M. Wagner, *Complete nitrification by Nitrospira bacteria,* Nature **528**, 504 (2015).

[24] M. A. H. J. van Kessel, D. R. Speth, M. Albertsen, P. H. Nielsen, H. J. M. Op den Camp, B. Kartal, M. S. M. Jetten, and S. Lücker, *Complete nitrification by a single microorganism,* Nature **528**, 555 (2015).

[25] L. Chistoserdova, *New pieces to the lanthanide puzzle,* Molecular Microbiology **111**, 1127 (2019).

[26] U. Johnsen, J.-M. Sutter, A. Reinhardt, A. Pickl, R. Wang, H. Xiang, and P. Schönheit, *D-Ribose Catabolism in Archaea: Discovery of a Novel Oxidative Pathway in Haloarcula Species,* Journal of Bacteriology **202** (2020), 10.1128/JB.00608-19.

[27] M. D. J. Lynch and J. D. Neufeld, *Ecology and exploration of the rare biosphere,* Nature Reviews Microbiology **13**, 217 (2015).

[28] M. Y. Skopina, A. A. Vasileva, E. V. Pershina, and A. V. Pinevich, *Diversity at low abundance: The phenomenon of the rare bacterial biosphere,* Microbiology **85**, 272 (2016).

[29] *Plasticicumulans acidivorans (ID 69584) - Genome - NCBI,* https://www.ncbi.nlm.nih.gov/genome/?term=txid886464[Organism:noexp].

[30] J. I. Prosser, *Putting science back into microbial ecology: A question of approach,* Philosophical Transactions of the Royal Society B: Biological Sciences **375**, 20190240 (2020).

[31] L. G. da Silva, K. O. Gamez, J. C. Gomes, K. Akkermans, L. Welles, B. Abbas, M. C. M. van Loosdrecht, and S. A. Wahl, *Revealing the Metabolic Flexibility of "Candidatus Accumulibacter phosphatis" through Redox Cofactor Analysis and Metabolic Network Modeling,* Applied and Environmental Microbiology **86** (2020), 10.1128/AEM.00808-20.

[32] K. J. Verhagen, W. M. van Gulik, and S. A. Wahl, *Dynamics in redox metabolism, from stoichiometry towards kinetics,* Current Opinion in Biotechnology Analytical Biotechnology, **64**, 116 (2020).

[33] L. C. Valk, M. Diender, G. R. Stouten, J. F. Petersen, P. H. Nielsen, M. S. Dueholm, J. T. Pronk, and M. C. M. van Loosdrecht, *"Candidatus Galacturonibacter soehngenii" Shows Acetogenic Catabolism of Galacturonic Acid but Lacks a Canonical Carbon Monoxide Dehydrogenase/Acetyl-CoA Synthase Complex,* Frontiers in Microbiology **11** (2020), 10.3389/fmicb.2020.00063.

[34] G. Muyzer, E. C. de Waal, and A. G. Uitterlinden, *Profiling of complex microbial populations by denaturing gradient gel electrophoresis analysis of polymerase chain reaction-amplified genes coding for 16S rRNA.* Applied and Environmental Microbiology **59**, 695 (1993).

[35] S. G. Tringe and P. Hugenholtz, *A renaissance for the pioneering 16S rRNA gene,* Current Opinion in Microbiology Antimicrobials/Genomics, **11**, 442 (2008).

[36] M. F. Polz and C. M. Cavanaugh, *Bias in Template-to-Product Ratios in Multitemplate PCR,* Applied and Environmental Microbiology **64**, 3724 (1998).

[37] J. P. Brooks, D. J. Edwards, M. D. Harwich, M. C. Rivera, J. M. Fettweis, M. G. Serrano, R. A. Reris, N. U. Sheth, B. Huang, P. Girerd, J. F. Strauss, K. K. Jefferson, and G. A. Buck, *The truth about metagenomics: Quantifying and counteracting bias in 16S rRNA studies,* BMC Microbiology **15** (2015), 10.1186/s12866-015-0351-6.

[38] L. Bons and C. Vermeer, *Survival of the Fattest: The Bacterial Synthesis of Polyhydroxyalkanoates with Isobutyrate as Sole Carbon Source*, Master Thesis (Delft University of Technology, 2019).

[39] L. Marang, M. C. M. van Loosdrecht, and R. Kleerebezem, *Enrichment of PHA-producing bacteria under continuous substrate supply,* New Biotechnology **41**, 55 (2018).

[40] P. R. Mooij, G. R. Stouten, J. Tamis, M. C. M. van Loosdrecht, and R. Kleerebezem, *Survival of the fattest,* Energy & Environmental Science **6**, 3404 (2013).

[41] P. Mooij, *On the Use of Selective Environments in Microalgal Cultivation*, Ph.D. thesis, Delft University of Technology (2016).

[42] P. R. Mooij, J. Zlopasa, and Loosdrecht, Mark C. M. van, *WASCOM - Converting Wastewater in Composites - Projectnumber TEBE117002,* TopSector Energie (2017).

[43] P. R. Mooij, J. Zlopasa, and Loosdrecht, Mark C. M. van, *COMPRO - From Composite to Product - Project number TBBE119001,* TopSector Energie (2019).

[44] J. Zlopasa, G. R. Stouten, R. Kleerebezem, D. Vasquez-Cardenas, F. J. Meysman, M. C. M. Van Loosdrecht, S. J. Picken, and G. J. Koper, *Elevated fixed charge densities in biofilms reduce osmotic stress,* submitted (2020).

[45] M. Mulders, A. Estevez-Alonso, G. R. Stouten, J. Tamis, M. Pronk, and R. Kleerebezem, *Volatile Fatty Acid Product Spectrum as a Function of the Solids Retention Time in an Anaerobic Granular Sludge Process,* Journal of Environmental Engineering **146**, 04020091 (2020).

[46] S. Che and Y. Men, *Synthetic microbial consortia for biosynthesis and biodegradation: Promises and challenges,* Journal of Industrial Microbiology and Biotechnology **46**, 1343 (2019).

[47] S. van Brummelen, G. R. Stouten, D. van Cuylenburg, and R. Kleerebezem, *Towards Long-Term Axenic Cultivations by Automatisation of the Cleaning Process in Microbial Community Experiments*, Bachelor Thesis (Delft University of Technology, 2019).

[48] N. Ziemert, M. Alanjary, and T. Weber, *The evolution of genome mining in microbes – a review,* Natural Product Reports **33**, 988 (2016).

[49] A. A. Stierle, D. B. Stierle, D. Decato, N. D. Priestley, J. B. Alverson, J. Hoody, K. McGrath, and D. Klepacki, *The Berkeleylactones, Antibiotic Macrolides from Fungal Coculture,* Journal of Natural Products **80**, 1150 (2017).

[50] A. J. J. Straathof, S. A. Wahl, K. R. Benjamin, R. Takors, N. Wierckx, and H. J. Noorman, *Grand Research Challenges for Sustainable Industrial Biotechnology,* Trends in Biotechnology **37**, 1042 (2019).

[51] J. R. Marchesi, D. H. Adams, F. Fava, G. D. A. Hermes, G. M. Hirschfield, G. Hold, M. N. Quraishi, J. Kinross, H. Smidt, K. M. Tuohy, L. V. Thomas, E. G. Zoetendal, and A. Hart, *The gut microbiota and host health: A new clinical frontier,* Gut **65**, 330 (2016).

[52] V. Ridaura and Y. Belkaid, *Gut Microbiota: The Link to Your Second Brain,* Cell **161**, 193 (2015).

[53] E. M. M. Quigley, *Microbiota-Brain-Gut Axis and Neurodegenerative Diseases,* Current Neurology and Neuroscience Reports **17**, 94 (2017).

[54] R. Nagpal, R. Mainali, S. Ahmadi, S. Wang, R. Singh, K. Kavanagh, D. W. Kitzman, A. Kushugulova, F. Marotta, and H. Yadav, *Gut microbiome and aging: Physiological and mechanistic insights,* Nutrition and Healthy Aging **4**, 267 (2018).

[55] S. Westfall, N. Lomis, I. Kahouli, S. Y. Dia, S. P. Singh, and S. Prakash, *Microbiome, probiotics and neurodegenerative diseases: Deciphering the gut brain axis,* Cellular and Molecular Life Sciences **74**, 3769 (2017).

[56] W. Zhou, Y. Chen, T. Roh, Y. Lin, S. Ling, S. Zhao, J. D. Lin, N. Khalil, D. M. Cairns, E. Manousiouthakis, M. Tse, and D. L. Kaplan, *Multifunctional Bioreactor System for Human Intestine Tissues,* ACS Biomaterials Science & Engineering **4**, 231 (2018).

[57] Z. Li, C.-X. Yi, S. Katiraei, S. Kooijman, E. Zhou, C. K. Chung, Y. Gao, J. K. van den Heuvel, O. C. Meijer, J. F. P. Berbée, M. Heijink, M. Giera, K. W. van Dijk, A. K. Groen, P. C. N. Rensen, and Y. Wang, *Butyrate reduces appetite and activates brown adipose tissue via the gut-brain neural circuit,* Gut **67**, 1269 (2018).

[58] L. Philippot, J. M. Raaijmakers, P. Lemanceau, and W. H. van der Putten, *Going back to the roots: The microbial ecology of the rhizosphere,* Nature Reviews Microbiology **11**, 789 (2013).

[59] E. Denamur and I. Matic, *Evolution of mutation rates in bacteria,* Molecular Microbiology **60**, 820 (2006).

[60] S. Chibani-Chennoufi, A. Bruttin, M.-L. Dillmann, and H. Brüssow, *Phage-Host Interaction: An Ecological Perspective,* Journal of Bacteriology **186**, 3677 (2004).

[61] D. Paez-Espino, E. A. Eloe-Fadrosh, G. A. Pavlopoulos, A. D. Thomas, M. Huntemann, N. Mikhailova, E. Rubin, N. N. Ivanova, and N. C. Kyrpides, *Uncovering Earth's virome,* Nature **536**, 425 (2016).

[62] E. V. Koonin, *The Logic of Chance: The Nature and Origin of Biological Evolution* (FT Press, 2011).

[63] P. H. Rampelotto, *Panspermia: A Promising Field of Research,* **1538**, 5224 (2010).

[64] I. Ginsburg, M. Lingam, and A. Loeb, *Galactic Panspermia,* The Astrophysical Journal **868**, L12 (2018).

[65] J. S. Greaves, A. M. S. Richards, W. Bains, P. B. Rimmer, H. Sagawa, D. L. Clements, S. Seager, J. J. Petkowski, C. Sousa-Silva, S. Ranjan, E. Drabek-Maunder, H. J. Fraser, A. Cartwright, I. Mueller-Wodarg, Z. Zhan, P. Friberg, I. Coulson, E. Lee, and J. Hoge, *Phosphine gas in the cloud decks of Venus,* Nature Astronomy , 1 (2020).

All that ends well, is well

The end

well

EPILOGUE: EMERGENT PROPERTIES

I lack the eloquence and understanding to do justice to the magic behind emergent properties; how listless chemical molecules can combine to form organic structures. How some of these structures gain catalytic properties, from which reactions follow that slow down energy decay, and hasten chaos production. This results in organized structures that develop a sense for the same elements from which they are made. Cells follow; they withstand time and everlastingly pass on life, allowing and restricting variations to their core. And due to their own success, variants are driven into niches, giving birth to the fantasies of symbioses and specialization. Collaboration of specialties unites in multicellular structures, and somewhere along our timeline a precipice is crossed that breathed soul into life. And possibly, a fragment of that soul is already present in the smallest inhabitants of our planet.

> *"It is probably not accidental that, of all sciences, biology is the only one that is unable to define its object: we have no scientific definition of life. The most exact studies are, in fact, performed on dead cells and tissues. I say it with all due diffidence, but it is not impossible that we are encountering here a form of an exclusion principle: our inability to comprehend life in its reality is due to the very fact that we are alive. If this were so, only the dead could understand life; but they publish in other journals."*
>
> Erwin Chargaff (1978) [1]

It is a privilege made possible by a mondial curiosity that allows scientists to oscillate between the brightness of reality and the darkness of the unknown. It is an art of truths that is in a continuous clash with humankind's desire for progress, results, and appraisal. Where artistry is the product of imagination, freedom, and individuality, academia is leading young, artful, scientists more and more astray. The principles of philosophy and 'Erkenntnisinteresse', are substituted by quantifiable metrics of artifice and output. What are we really doing? The difference between a painter and those who apply paint can be as big as the difference between a scientist and those who apply the scientific method. It is impossible to emerge when we all grow in the same mold.

REFERENCES

[1] E. Chargaff, *Heraclitean Fire: Sketches from a Life before Nature* (Rockefeller University Press, New York, 1978).

Notes from the author

Pling. Plong.

ACKNOWLEDGEMENTS

The benefit of lingering is that you get to meet so many people. The downside of many people is that it becomes difficult to appropriately thank and acknowledge their contributions in shaping you. I like to think that all people that read these words are imbibed in my growth, you have been my nutrients, light, warmth, and patience - and I thank you all with great affection for sharing your time with me.

Terry Pratchett writes of *small gods*, referring to deities whose power is proportional to the number and quality of their followers. I am that follower and any qualities that I posses can be attributed to my reluctance to follow and to my infatuation with paradoxes. You are the small gods and goddesses, forming the pantheon of my Emanationism. The beauty of real gods is that they are imperfect, just like the gods from ancient times, just like you. This thesis is truly a by-product of a tremendous enjoyable occupation, made possible by an imperfect collective of small gods. This is to you.

SMALL GODS

Peter - you are the Alfa and Omega of my journey. You introduced me to the world of microbial ecology, to the world of Baas Becking. A scientific world that drew me in and played om my heartstrings. We explored the world of our beloved algae, and co-habited the Monkey&Typewriters' office together with Jelmer. I have you to thank for stopping me along the road of everlasting discovery and herald in me the interest to finalize this thesis. Thank you, my colleague, editor, guide, and my dear friend.

Robbert - you personify Ponos, the deliberate choice of a hard life. You are a locomotive that has relentless stamina and force, *but* you need time to get going. You thrive when you cycle the world, take on a new teaching course, chop a forest to mulch, work on ambitious scientific projects, and when you digest my work. You need some suffering, maybe that is why menial and administrative tasks accumulate until you suffer. This suffering is what drew us together and what allowed me to invest deeply in the scientific endeavour of setting up a lab - I have never doubted your confidence in the project and have always experienced tremendous support. Thank you, for allowing me to explore my science, for being receptive to my mind, and for your precious patience.

Mark - Zeus Xenios as the patron of hospitality. Your ability to maintain an open research department for a truly wide variety of strange scientists and microbes falls beyond comparison. As the paterfamilias you are at the helm of the research group that took me in and has supplied me with more joy and challenges than I could have dreamt of. You have a vision on science, scientists, and academic development that is gracefully poised and which allowed me to prosper. My struggles were not with science, nor with me as a scientist; only very late I started to appreciate the value in a guide for academic development. Thankfully you are a highly efficient communicator; time will tell whether I was in time to realise this divine opportunity.

Jure and Morez - Themis and Nabu, the forces of justice and literacy. Getting to know you guys was possible due to my ingrained disregard for finishing my thesis in time. You are more valuable to me than any hypothetical lost time. You are the true gifts of my PhD. Talent & reward. You have fed my mind with exaltations. From our benign mutterings at lunch regarding Stalin, Camus, or world politics, to the profound discourse on morality, personality, and life. You are my compass for true North.

Michel and Marissa - Janus and Athena, gods of change, war and strategy. We shared my second office, a *survive*rs stronghold reigned by MP5arissa. Your calming presence in the office, your boisterous presence at late night events. A lady with true range, and a highly enjoyable personality. I look forward to loosing any game of your choosing. De Spin, 'Ajeto, buur!', you are possibly the most pragmatic person I know that is still a highly enjoyable person to be around. A man that - when he puts his mind to it - can do anything. I have seen you transform while staying the same. Some of that pragmatism has rubbed off on me, for which I am deeply thankful. You beautiful Brabander, I am happy to call you my friend.

Jelmer - Ormuzd and Ahriman, one man and the impossible union of two deities of Dystheism. You have been there from my first day, and we have shared every office of significance since. I have seen you create beautiful ideas, sentences, science, life, and I have witnessed you ravage all and more. You live life with exceptional amplitude and supply the teeth that sharpen the mind. You supply me with freedom, freedom of mind. My cherished comrade, I trust us to always clash and always grow. With you there is always the risk of excitement.

Dirk - Hephaestus, god of craftsman. You are the conductor of all equipment, the smith of smithing, and by your hands science flows freely in the whole department. Through your always open door, you give advice and skills to mortal scientific artists. You are the most frictionless character and a joy to work with. I thank you for sharing with me your vision and expertise while we were building the lab - and I majorly look forward to join hands again in the Unlock project.

Udo and Mario - Annapurna and Hermes, deities of food and sports. If our department has a spirit, it is you guys. A love for things outside science, the grapple with finding a balance between work and life. A lunch professor, and a humble professor, skirmishing for fully suspended analog and digital bikes, while also delivering insightful science. Beautiful stories and exceptionally warm colleagues that form the glue that I strive to be.

Diana and Francesc - Aletheia and Vé, spirits of truth and language. Two late additions to the pantheon, living a life of assuaging grandeur. A life to be coveted. Francesc, with so much joy for life that I wonder whether you became a polyglot just to express your infectious enthusiasm. I love your passion for ~~rocks~~/~~gravel~~/minerals. Diana, with a mind so open, that you have to close it a bit to perform science. You see through the facade of academia into the soul of science. Likewise with people. I adhere to your open-minded wholistic vision for research, academia, and life, which I love to see materialize. If we slide out of academia, then we will see each-other in space. I cannot imagine a more tranquil and sensational companion for the journey to Mars.

Martijn - Dionysus, the god of 'letting go'. All this time, you have been with me as a golden statue, while your value is in all but gold. Now, is when I need to let go; the statue is free and the memory of you can move again. Till we meet again, my old friend.

BAND OF GODS

Paques boys - the Giants, in contrast to the Gigantomachy these industrial Giants have been a tremendous driving force behind a great number of research projects involving biopolymers and the circular society. With time I start to fully appreciate the almost altruistic drive of Paques and Paques biomaterials that allowed my research to take place. René, I thank you for reprimanding me when I was blind to the different interests of stake holders. It was a wake-up call that science is truly connected to the real world. Henk, I thank you for sharing your expertise and the discussions regarding the intricate aspects of fat bacteria. I think we could, and maybe should, have continued our talks for days. João, you brought a gentle youthfulness to the team, with a keen eye for the project and its status. Joost and Jos, your interest and excitement when we met in the lab in Delft is contagious - it cannot be overstated that all that happened in that lab was made possible by you, and for that I am deeply grateful.

The Amsterdam squad - Thoth and Seshat, the deities of numbers. We set out to merge the world of mixed microbial cultivations with that of genomics. This brought with itself a significant challenge as we were seeing different sides of the same coin. Cultivations that took months resulted in a crescendo of sequencing data. This required flexibility from either end of the scientific landscape. And you, Estelle, have been greatly involved and appreciated the difficulty and ambition of the project. Now I see that we set our initial benchmark too high and as a result toiled a monstrous behemoth into the publication literature. But at least we were joyful partners in that crime. Silvia, you took over from Estelle, after the first unification battle. Something I never fully recovered from, but regardless, you persisted and were able to see deeply into the data. I thank you for your grit and perseverance. And Gerard, the co-instigator with Robbert of this project, you have been a cheerful and supportive satellite supervisor. I wish that I would have taken more breathing room in the early phase of the project to better understand the different ambitions of the respective scientific fields, as that would have been illuminating. I thank you for allowing me to roam around in your neck of the scientific woods.

Acid Heads - the Agathodaemons, you were the closest to companion spirits that I had during my PhD. You invited me into your meetings, where we shared frolics and sincere discussions. Thank you Leonor for pushing me to reduce the complexity of my stories. Thank you Jules for the beautiful energy and passion that you possess for our beloved research. And Laura, I am humbled by your odyssey, you have been an exceptional inspiration and I firmly hope that our scientific paths will cross in the future. I thank you three for journeying with me.

My students, c.q. sparring partners, fountains of wisdom, and bottomless wells thirsting for adventure - you are my Kharites, gods and goddesses of joy and mirth. That is what you brought me, by being focal points to breathe science into. You had such varying desires and interest that allowed me to explore and expose my full gamut of interest. I hope to have been able to cater to yours, while still challenging you into unknown territories. You were a joy, as you allowed me to entice you to step outside your comfort zone, where we were confronted with your and my limitations. I admire the honesty and trust that you confided in me - that led to moments that are of exceptional value to me - for which I thank you more dearly than for all scientific insights combined. You have all instilled in me everlasting memories of such profound beauty that it feels like

an enchanted reverie. Thank you, Galvin, Carmen, Sieze, Rinke, Eline, Kelly, Francesca, Maximilienne, Valerie, Lena, Daphne, Sten, and Mu-En.

There are so many more students and colleagues with unforgettable names and stories - the Mnemosyne, you have walked the hallways of the old Kluyver lab or are still leaving footprints in the new building. Ahmed, Aina, Alan, Alberte, Ali, Andrea, Angel, Anka, Apilena, Astrid, Bart, Ben, Britt, Carol, Cees, Chris, Christian, Christopher, Claudia, Cor, Danny, David, David, Dimitry, Duncan, Edward, Elena, Emma, Emmanuelle, Erwin, Esengül, Eveline, Felipe, Francesc, Fred, Geert-Jan, Gijs, Guido, Guus, Hans, Helena, Hugo, Ingrid, Isabel, Jack, Jannie, Jenifer, Johan, Jonas, Jos, Julio, Kawieta, Kees, Leonie, Lesley, Luuk, Maaike, Maarten, Maita, Marcel, Marco, Maria, Marta, Martin, Mathijs, Matthijs, Max, Merle, Michele, Michelle, Mieke, Miranda, Mirjam, Mitchell, Monica, Nayyar, Nina, Patricia, Philipp, Pilar, Rebeca, Rob, Robert, Roel, Richard, Ruizhe, Sam, Sef, Sergio, Sjaak, Shiva, Simon, Sirous, Song, Stef, Stefan, Tim, Timmy, Tommaso, Victor, Viktor, Vincent, Walter, Winnifred, Yang, Yuemei, Zita, to name a few. Together with the countless students in the lecture rooms, the co-supervised students with my colleagues, colleagues from other departments, guest researchers, you all were essential actors to the joys and woes of this adventure.

REAL WORLD GODS

There exists a world outside of academia, a world filled with treasures of inescapable beauty. Here lie the source of my character, and the objects of my devotion. This text is not the place to expand on your value to me, but it is the place to thank you for all the nature and nurture you have brought me.

My Budo buddies - Kwatee, the cheerful gods of transformation and improvement. “It is not about being better than the other. It is about being better than you were yesterday.” There are few places where I feel as much at home and welcome as with you in the dojo. You have seen me grow up and helped shape me into the man I am today, from Aikido, through Katori, and into Karate - on to explore the world. At the end of my restless travels around the globe, I know that I will always find my way home to the tatami, and can join the mokuso to find that place of rest. Osu.

My fantastic friends - Aje, the apotheosis of wealth. You are the fire in my life. Among you are colleagues, kitesurfers, martial artists, mountaineers, snowboarders, fact consumers, family, scientists, artists, entrepreneurs, board&card-gamers, chess-players, programmers, readers, writers, teachers, travelers, and philosophers. You bear colorful richness and are the embodiment of my principle truths. I am eternally indebted to you, for the time we share and the myriad of life’s colors that you display.

My family, parents, fathers, mothers, brothers, sisters, and progeny - you are my Hestia, at the same time the oldest and the youngest, gods and goddesses of hearth and home. In you I see the world.

With great warmth,
Gerben

CURRICULUM VITÆ

GERBEN ROELANDT STOUTEN

G.R.Stouten@tudelft.nl | ResearchGate

I am born in January 1985; a thick blanket of snow covered the Netherlands. Snow that I have loved ever since. Pristine; composed of trillions of unique snowflakes, together forming one uniform scenery. I am enchanted by the relationship between complexity and simplicity and try to explore it in education, research, work and sports.

EXPERIENCE

Technical Manager UNLOCK (2021)
Delft University of Technology
Responsible for the realization of the UNLOCK infrastructure at the Delft University of Technology, and its integration in the overall UNLOCK project.

PhD. Environmental Biotechnology (2013-2021)
Delft University of Technology

Thesis:	Exploring microbial diversity - Extending the boundaries of biopolymer production using parallel cultivation
Promotors:	Dr. R. Kleerebezem Prof.dr.dr.h.c.ir. M.C.M. van Loosdrecht

PostDoc UNLOCK (2018-2020)
Delft University of Technology & Wageningen University & Research
Co-author of the Unlock research proposal for an improved infrastructure in microbial community research. This proposal is a collaboration between Delft and Wageningen universities and was collectively granted 24.5 M€ by NWO and the universities (2020).

Scientist-Entrepreneur
I love exploring the connection between the real world and science and I push for the adaptation of the inexhaustible capabilities of the natural world.

2017:	AmbixBio
2014:	Monkey's and Typewriters
2013:	OPE-Group
1989:	Wespmachine

List of Publications

16. Stouten, Gerben Roelandt, Francesca Cecconi, Rinke Johanna van Tatenhove-Pel, Michel Mulders, Peter Rudolf Mooij, Henk Dijkman, and Robbert Kleerebezem. *Uncoupling of Nutrient Supply for Enrichment of Polyhydroxyalkanoates Accumulating Bacteria.* under review 2021.

15. Allaart, Maximilienne Toetie, Gerben Roelandt Stouten, Diana Z. Sousa, and Robbert Kleerebezem. *Product Inhibition and pH Affect Stoichiometry and Kinetics of Chain Elongating Microbial Communities in Sequencing Batch Bioreactors.* Frontiers in Bioengineering and Biotechnology 9 (June 2021).

14. Stouten, Gerben Roelandt, Kelly Hamers, Rinke Johanna van Tatenhove-Pel, Eline van der Knaap, and Robbert Kleerebezem. *Seemingly Trivial Secondary Factors May Determine Microbial Competition: A Cautionary Tale on the Impact of Iron Supplementation through Corrosion.* FEMS Microbiology Ecology 97, (February 2021).

13. Kleerebezem, Robbert, Gerben Roelandt Stouten, Jasper J. Koehorst, Alette Langenhoff, Peter Schaap, and Hauke Smidt. *Experimental Infrastructure Requirements for Quantitative Research on Microbial Communities.* Current Opinion in Biotechnology 67 (February 2021).

12. Stouten, Gerben Roelandt, Sieze Douwenga, Carmen Hogendoorn, and Robbert Kleerebezem. *System Characterization of Dynamic Biological Systems through Improved Data Analysis.* BioRxiv (2021).

11. Mulders, Michel, Angel Estevez-Alonso, Gerben Roelandt Stouten, Jelmer Tamis, Mario Pronk, and Robbert Kleerebezem. *Volatile Fatty Acid Product Spectrum as a Function of the Solids Retention Time in an Anaerobic Granular Sludge Process.* Journal of Environmental Engineering 146, no. 8 (August 2020).

10. Allaart, Maximilienne Toetie, Robbert Kleerebezem, Julius Laurens Rombouts, Gerben Roelandt Stouten, Marinus (Mark) Cornelius Maria van Loosdrecht, and David Gregory Weissbrodt. *High Yield Lactic Acid Production Using Mixed Cultures.* WO2020229370A2, filed May 8, 2020, and issued November 19, 2020.

9. Valk, Laura C., Martijn Diender, Gerben Roelandt Stouten, Jette F. Petersen, Per H. Nielsen, Morten S. Dueholm, Jack T. Pronk, and Mark C. M. van Loosdrecht. *'Candidatus Galacturonibacter Soehngenii' Shows Acetogenic Catabolism of Galacturonic Acid but Lacks a Canonical Carbon Monoxide Dehydrogenase/Acetyl-CoA Synthase Complex.* Frontiers in Microbiology 11 (2020).

8. Mulders, Michel, Jelmer Tamis, Gerben Roelandt Stouten, and Robbert Kleerebezem. *Simultaneous Growth and Poly(3-Hydroxybutyrate) (PHB) Accumulation in a Plasticicumulans Acidivorans Dominated Enrichment Culture.* Journal of Biotechnology: X 8 (December 2020).

7. Zlopasa, Jure, Gerben Roelandt Stouten, Robbert Kleerebezem, Diana Vasquez-Cardenas, Filip J.R. Meysman, Mark C. M. Van Loosdrecht, Stephen J. Picken, and Ger J.M. Koper. *Elevated Fixed Charge Densities in Biofilms Reduce Osmotic Stress.* Under review, 2020.

6. Stouten, Gerben Roelandt, Carmen Hogendoorn, Sieze Douwenga, Estelle Silvia Kilias, Gerard Muyzer, and Robbert Kleerebezem. *Temperature as Competitive Strategy Determining Factor in Pulse-Fed Aerobic Bioreactors.* The ISME Journal 13 (September 2019).

5. Smidt, Hauke, Robbert Kleerebezem, Alette Langenhoff, Peter Schaap, Jasper Koehorst, and Gerben Roelandt Stouten. *UNLOCK - UNLOCKing Microbial Diversity for Society.* NWO (June 2019).

4. Conthe, Monica, Camiel Parchen, Gerben Roelandt Stouten, Robbert Kleerebezem, and Mark C. M. van Loosdrecht. *O2 versus N2O Respiration in a Continuous Microbial Enrichment.* Applied Microbiology and Biotechnology 102, no. 20 (October 2018).

3. Stouten, Gerben Roelandt, Carmen Hogendoorn, Sieze Douwenga. *ExploDiv - Temperature Dataset (200 Cycles, 8 Reactors).* 4TU.ResearchData (April 2018).

2. Mooij, Peter Rudolf, Gerben Roelandt Stouten, Mark C. M. van Loosdrecht, and Robbert Kleerebezem. *Ecology-Based Selective Environments as Solution to Contamination in Microalgal Cultivation.* Current Opinion in Biotechnology 33 (June 2015).

1. Mooij, Peter Rudolf, Gerben Roelandt Stouten, Jelmer Tamis, Mark C. M. van Loosdrecht, and Robbert Kleerebezem. *Survival of the Fattest.* Energy & Environmental Science 6, no. 12 (2013).